NASA TECHNICAL TRANSLATION

NASA TT F-620

c. 1



NASA TT F-620

# NATURAL CONVECTION HEAT TRANSFER IN BOILING OF METALS

*by V. I. Subbotin, D. N. Sorokin, D. M. Ovechkin, and A. P. Kudryavtsev*

*"Nauka" Press, Moscow,* 1969

NATIONAL AERONAUTICS AND SPACE ADMINISTRATION • WASHINGTON, D. C. • JUNE 1971

# NATURAL CONVECTION HEAT TRANSFER IN BOILING OF METALS

By V. N. Subbotin, D. N. Sorokin, D. M. Ovechkin, and A. P. Kudryavtsev

Translation of "Teploobmen pri kipenii metallov v usloviyakh yestestvennoy konvektsii." "Nauka" Press, Moscow, 1969.

NATIONAL AERONAUTICS AND SPACE ADMINISTRATION

For sale by the National Technical Information Service, Springfield, Virginia 22151
price $3.00

TABLE OF CONTENTS

## SYMBOLS

| | |
|---|---|
| $\alpha$ | heat transfer coefficient, kcal/m$^2$hr°C |
| $\alpha_b$ | heat transfer coefficient at phase separation boundary, kcal/m$^2$hr°C |
| q | specific heat flow, kcal/m$^2$hr |
| $q_{cr}$ | critical heat flow, kcal/m$^2$hr |
| t | temperature, °C |
| T | Temperature, °K |
| $T_{cr}$ | critical temperature, °K |
| $\Delta t$ | temperature difference, °C |
| $\Delta t_\alpha$ | temperature difference between heating surface and liquid, °C |
| $\Delta t_s$ | difference between temperature on heating surface and saturation temperature, °C |
| P | pressure, atm. abs. |
| $P_{cr}$ | critical pressure, atm. abs. |
| r | heat of vaporization, kcal/kg |
| $C_p$ | specific heat capacity, kcal/kg°C |
| $\lambda$ | heat conductivity coefficient, kcal/mhr°C |
| $\gamma$ | specific gravity of liquid, kg/m$^3$ |
| $\gamma''$ | specific gravity of vapor, kg/m$^3$ |
| $\sigma$ | coefficient of surface tension, kg/m |
| $\nu$ | coefficient of kinematic viscosity, m$^2$/hr |
| a | coefficient of temperature conductivity, m$^2$/hr |
| $\mu$ | coefficient of dynamic viscosity, kg·sec/m$^2$ |
| $\beta_k$ | coefficient of volumetric expansion, 1/°C |
| $\theta$ | contact wetting angle, deg |
| $\rho^*$ | vapor seed radius, m |
| R | vapor bubble radius, m |
| f | frequency of separation of vapor bubbles, 1/sec |
| $d_0$ | diameter of separating vapor bubbles, m |
| F | surface area, m$^2$ |
| d | diameter, m |
| $\ell$ | length, m |

$\tau$ time, hr

x, y coordinates

g acceleration of force of gravity (9.81 $m/sec^2$)

A thermal equivalent of work (1/427 kcal/kg·m)

$B_g$ universal gas constant

K Boltzman's constant ($1.38 \cdot 10^{-16}$ erg/°K)

e* electron charge

M molecular weight;

$Nu = \alpha d/\lambda$ Nusselt number

$Pr = \nu/a$ Prandtl number

$Gr = \beta_k \frac{gd^3}{\nu^2} \Delta t$ Grashoff number

## SUBSCRIPTS

s saturation

w wall

$\ell$ liquid

v vapor

# INTRODUCTION

The investigation of heat exchange during the boiling of metals began with mercury at the end of the 1920's in connection with the attempts to create binary power supplies. In the Soviet Union during the period before the war, experiments with boiling mercury were performed at the Central Boiler-Turbine Institute by M. A. Styrikovich et al [1, 2], A. I. Lozhkin and A. A. Kanayev [3, 4]. The principal results of the investigations during this period, both domestic and foreign, are presented in [4]. In the first years after the war in the USSR, only a few individual experiments were continued with the boiling mercury [5], since binary power supplies had not become widespread. In the 1950's, M. I. Korneyev [6-8] performed investigations into heat exchange during the boiling of pure mercury and amalgam under conditions of free convection and with forced movement. Up to the present time, several more experimental works on heat exchange during the boiling of mercury and amalgam have been published [9-13]. These works have revealed certain individual factors (heating surface materials, addition of surface-active materials, etc.) influencing the heat exchange during the boiling of mercury. However, in order to provide reliable heat removal by boiling mercury (particularly for great thermal flows, approximately $10^6$ kcal/m$^2$ hr and higher) a number of problems remained to be solved.

The first data on heat transfer during the boiling of alkali metals (sodium and sodium-potassium alloy) were published by Lyon et al [9] in 1955. In recent years, a number of experimental works have been published on heat exchange during boiling of alkali metals. Heat transfer has been investigated during the boiling of sodium [14-19, 35], potassium [16, 20], cesium [21] and an alloy of sodium-potassium [22] under conditions of free convection, and potassium [23-30, 34], rubidium [31, 32], cesium [32] and sodium [28, 33] with forced circulation.

Data on the critical heat flows with free convection have been published for sodium [14, 18, 33, 36, 37], cesium [38], potassium [37, 39] and rubidium [37]. Data have been produced on critical heat flows with forced circulation for potassium [23, 26, 34] and sodium [33].

The interest in the investigation of heat exchange during boiling of metals results from the following principal factors.

1. Some metals can be used as working media in power plants with vapor turbines [40, 41].

2. The vapors of alkali metals can be used for the acceleration of liquid metal in MHD-generators [42, 43].

3. In certain high energy installations, for example in atomic reactors with sodium as a heat transfer medium, local boiling of the heat transfer medium may occur in emergency situations [44].

4. The boiling of metals can also be used to carry heat away from the anodes of powerful generator tubes, from crystallizers, in the melting of refractory metals and in a number of other cases when large heat flows must be carried away at a high temperature level.

5. Heat exchange by evaporation is important in the operation of a heat pipe, which in many cases uses metals as the working medium [45].

6. The study of the boiling of metals is of doubtless interest for an understanding of the problem of boiling in general, since many properties of metals differ strongly from properties of non-metallic heat transfer media.

The differences in the properties of these groups of heat transfer media lead to differences in such important characteristics for heat exchange during boiling as the speed and frequency of separation of vapor bubbles, the dimensions of vapor nuclei, the wettability of the heating surface, the stability of operation of vapor formation centers, the relationship between the quantity of heat transfer through the boundary layer by the vapor and the liquid and others, although the fundamental rules which determine the heat exchange during boiling are common for metals and non-metallic liquids.

The same modes of heat removal have been produced in metals under conditions of free convection (heat removal by convection with subsequent heat transfer by evaporation from the free surface, heat removal with developed, unstable and film boiling) as have been produced with other liquids. For example, with developed boiling, the dependence of the heat transfer coefficient on the heat flow for metals is approximately the same as for non-metallic liquids, while the value of critical heat flow increases with increasing pressure. However, the data available at the present time indicate (along with their common features) some differences in heat exchange during the boiling of metals and non-metallic liquids, resulting from the difference in properties of these heat transfer media. For example, alkali metals have a characteristic high (frequently exceeding 100°C) superheating of the liquid on the heat transfer surface, which is necessary for boiling; unstable boiling over a rather broad range of pressures and heat flows (right up to the critical levels) is also characteristic. The dependence of the critical heat flow on pressure with metals with the same corrected pressures (within the pressure range investigated) is significantly weaker than for non-metallic liquids, etc.

Metals may interact actively with the heat liberating surface, the state of which, as we know, determines to a significant extent the heat exchange during boiling. In particular, depending on the material and temperature, the wall itself may reduce oxides in the metal or the metal may reduce oxides on the wall. Depending on this, the wettability of the heating wall, which is important in heat exchange during boiling, may change. Corrosion also depends on the wall material, temperature level and content of impurities in the metal being boiled [46].

At the present time, reliable data on heat exchange during boiling of metals can be produced only experimentally. However, experiments with boiling metals and particularly with alkali metals, are more difficult and cumbersome than similar experiments with ordinary liquids. The difficulty of experimental investigation of heat exchange during boiling of metals is related primarily to their high boiling points. At these high temperatures, construction materials have limited strength and frequently limited resistance to the liquid metals. Measurement of temperatures and particularly the temperature of the heating wall is difficult, since the service lives of thermocouples are limited. Furthermore, their characteristics may change, and high temperature insulation is required. The danger to experimenters in case of an accident is increased.

The good electrical conductivity of metals creates difficulties, and in many cases makes it impossible to perform direct heating of working sectors by passage of electrical current, which is ordinarily used in experiments with water and organic liquids and makes it possible to produce high heat flows, which are required for studies of heat exchange during boiling.

Also, operation with boiling metals requires high temperature heaters and special equipment (fittings, etc.) which are not always reliable in operation.

This book presents an analysis of methods of experimental investigation and experimental techniques as applicable to studies of heat exchange in the boiling of metals under conditions of free convection.

The results are presented from experimental works on heat transfer and critical heat flows during the boiling of metals under conditions of free condition, performed by Soviet and foreign investigators, and an analysis of these works. Work on investigation of heat exchange during boiling of metals, whose results are published in this book, was begun by the authors at the Physics and Energy Institute in 1957.

The data on heat exchange during boiling under free convection conditions are of independent interest and will provide a better understanding of a number of regularities of boiling under conditions of forced circulation.

# NATURAL CONVECTION HEAT TRANSFER IN BOILING OF METALS

V. N. Subbotin, D. N. Sorokin, D. M. Ovechkin and
A. P. Kudryavtsev

ABSTRACT. This book presents original data produced by the authors at the Physics and Energy Institute, plus analyses of publications on heat transfer and critical heat flow during the boiling of alkali metals and mercury under conditions of free convection. For a better understanding of the mechanism of boiling in general, a comparison is performed of the processes of boiling of metals and non-metallic liquids. In their investigation of heat transfer in the boiling of metals, the authors used electronic heating, making it possible to produce practically unlimited specific heat flows; x-ray irradiation (for visual observation of the boiling process); microthermocouples (for measurement of the temperature of the heat liberating wall, fluid and vapor) and high-speed secondary devices (for investigation of changes in temperature with time).

## CHAPTER 1

/13*

## METHODS OF INVESTIGATION OF HEAT EXCHANGE DURING BOILING OF METALS AND EXPERIMENTAL APPARATUS

### Methods of Heating the Test Section

In experiments on heat exchange during boiling, one must be able to produce high heat flows (on the order of $10^6$ kcal/$m^2$hr) both for the investigation of critical heat flows and for the investigation of the dependence of heat transfer on heat flow.

For conditions involving large volumes, heating by direct passage of current through the working sector, widely used in experiments with water and organic liquids, is not usable due to the electrical conductivity of the metal heat transfer media. Investigations of heat exchange during boiling of metals can use the following methods of heating the working sector:

*Numbers in the margin indicate pagination in the foreign text.

radiation heating, the heat exchanger method (in particular if the saturated vapor is used as a heating medium), heating by passage of current through an insulated conductor, the thermal wedge, electronic heating and the heat pipe. Let us analyze these methods of heating.

Radiation Heating

The quantity of heat transmitted by radiation from one plate at temperature $T_1$ to another parallel plate at temperature $T_2$ (the dimensions of the plate being rather great in comparison to the distance between them) can be evaluated using the formula

$$q = 4.9 \cdot \varepsilon_c \left[\left(\frac{T_1}{100}\right)^4 - \left(\frac{T_2}{100}\right)^4\right], \qquad (I.1)$$

where $\varepsilon_c$ is the derived black body emittance.

If the most refractory metal available - tungsten (the melting point of tungsten according to data from [47] is 3,410 ± 20°C) is used as the heater, for which the emittance does not exceed approximately 0.3, and if the material of the surface to be heated is selected with high blackness factor (about 0.8), the value $\varepsilon_c$ will be approxiamately 0.20-0.25. For this type of radiation heater, at a temperature of 2,500°C heat flows of approximately (600-800) $\cdot 10^3$ kcal/m$^2$·hr can be achieved, or at 3,000°C - approximately (1.1-1.4) $\cdot 10^6$ kcal/m$^2$·hr. At high temperatures, the strength of the heater is significantly reduced and the rate of evaporation is increased [47]. For example, for tungsten the rate of evaporation changes from $1.1 \cdot 10^{-7}$ g/cm$^2$sec to $1.5 \cdot 10^{-5}$ g/cm$^2$ sec as the temperature changes from 2,800 to 3,300°K [48]. In actual designs with the heater temperatures mentioned above, the heat flows will be less both due to the irradiation factor and due to the derived black body emittance. /14 /15

Figure 1 shows a radiation heater used by Marto and Rohsenow [19] in experiments on heat transfer during boiling of sodium. It is made of three sections, consisting of corrugated strips (101.6 mm long) of an alloy of tantalum and tungsten (10% tungsten) with a melting point of approximately 2,930°C. The width of each corrugated strip was 25.4 mm. Each heater section is made of a sheet 2.54 mm thick and 76.2 mm wide. The angle of inclination of the corrugation to the plane in which the heater lies is 30°. The corrugated surface was used in order to increase the specific power of the heater. The operating temperature of the heater reached approximately 2,200°C. Their experiments produced heat flows up to $640 \cdot 10^3$ kcal/m$^2$·hr with a sodium temperature of up to 815°C.

With series connection of the sections, the heater was supplied with power by a current source with adjustable voltage (up to 15 V) with current up to 1,000 A.

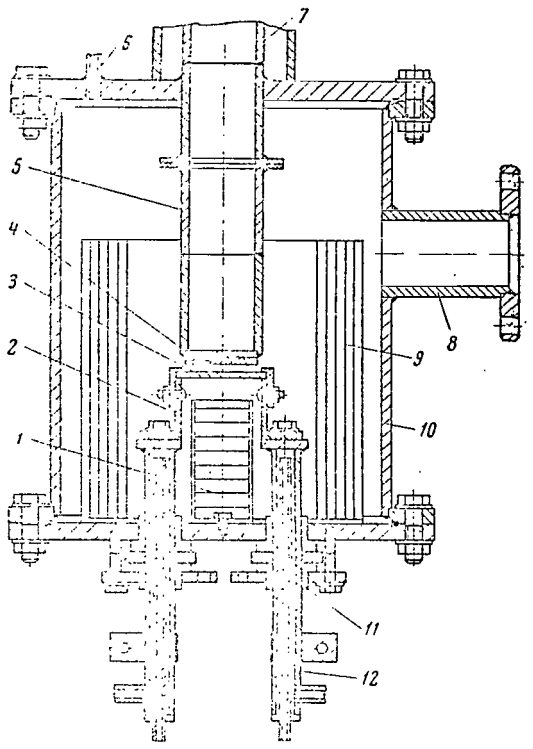


Figure 1. Radiation Heater Used By Marto and Rohsenow [19].
1, 9, Heat screens; 2, Molybdenum current conductor; 3, Heating element (tantalum + 10% tungsten); 4, Working sector; 5, Boiling tank; 6, Tube for thermocouples; 7, Vapor condenser; 8, Tube for connection to vacuum system; 10, Vacuum chamber; 11, Teflon insulators; 12, Water cooled conductors.

Heating by Heat Exchanger Method

With this method of heating, a loop must be used with a heat transfer medium whose temperature is higher than the temperature of the heat transfer medium being studied. For example, if stainless steel 2 mm thick is used as the separating wall (it is difficult to place thermocouples for measurement of high temperatures in thinner walls) and if we consider that the heat transfer coefficients of both heat transfer media are $10^4$ kcal/m$^2$·hr°C, in order to produce a heat flow of $10^6$ kcal/m$^2$·hr, the temperature difference between heat transfer media must be approximately 300°C. For alkali metals, which have high boiling points, the usage of this heating method for large volumes is difficult, since it requires the creation of a reliably operating high temperature (up to 1,000°C and higher) liquid metal loop, which is a difficult task in itself. When heating is performed by the heat exchanger method, it must be kept in mind that the heat flow of heating surface will not be even due to changes in the temperature head resulting from cooling of the heat transfer medium. In order to decrease the unevenness of the heat flow, high flow rates of the heat transfer medium should be used.

It is convenient to use saturated metal vapors as a heating medium. When this is done, first of all it is possible to achieve good evenness of the heat flow, and secondly, since we know the quantity of vapor condensed and its temperature, we can determine the heat flow over the working sector and the heat transfer coefficient of the heat transfer medium being investigated with good accuracy, since the heat transfer coefficients involved in the condensation of pure metal vapors at high temperatures are great [49, 50]. In this case, the heat flows calculated using the formula

/16

$$q = \frac{rG + GC_p\Delta t_к - Q_у}{F}. \qquad (I.2)$$

The temperature head between the heating surface and the heat transfer medium being investigated, in addition to measurements of the wall temperature, can be determined from the formula

$$\Delta t_{\alpha} = t_{v} - \Delta t_{v} - \Delta t_{w} - t_{l} \qquad \text{(I.3)}$$

In formulas (I.2) and (I.3) G is the flow rate of the heating vapor, kg/hr; $\Delta t_k$ is the super cooling of the condensate, °C (which may be small, and $\Delta t_k$ will approach 0); $Q_v$ is the heat loss in the working sector, kcal/hr, estimated for each concrete design; F is the area of the working surface of the sector, $m^2$; $\Delta t_v$ is the temperature head between the wall and the condensing vapor, °C.

The value of $\Delta t_v$ is determined from the formula

$$\Delta t_{v} = \frac{q}{\alpha_{v}} . \qquad \text{(I.4)}$$

With film condensation, which is characteristic for alkali metal vapors, the intensity of heat exchange is determined by diffusion resistance in the vapor, resistance to the phase transition and the thermal resistance of the condensate film. For pure materials, the diffusion resistance is zero, and the heat transfer coefficient for the phase transition can be calculated using the formula

$$\alpha_{ph} = \left( 2 \frac{r^4 p_s^2 M^3}{2\pi g B_g^3 T_s^5} \right)^{1/2} . \qquad \text{(I.5)}$$

The heat transfer coefficient resulting from thermal resistance of the condensate film can be calculated, for example, for a vertical wall with q = const using the Nusselt formula

$$\alpha_x = \left( \frac{\lambda^3 \gamma'' r}{3 \cdot \mu x q} \right), \qquad \text{(I.6)}$$

where x is the distance from the upper edge of the wall.

The effective heat transfer coefficient is defined as

$$\alpha_{v} = \frac{\alpha_{ph} \alpha_{x}}{\alpha_{ph} + \alpha_{x}} . \qquad \text{(I.7)}$$

When alkali metal vapors condense at pressures of some tenths of an atmosphere, the values of heat transfer coefficients amount to hundreds of thousands of kcal/m$^2$·hr°C. However, it should be particularly emphasized /17
that high values of $\alpha_v$ can be produced only with careful removal of non-condensing gases from the vapor space [49, 50].

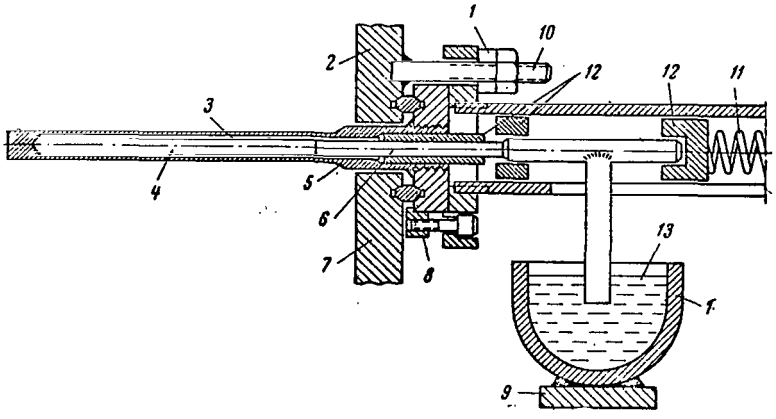


Figure 2. Heater With Insulated Conductor Used by Noyes [18]. 1, Spring disc; 2, Boiling tank wall; 3, Boron nitride bushing; 4, Heating element (graphite rod); 5, Heater collar; 6, Molybdenum electrode; 7, Nickel sealing ring; 8, Stopping ring; 9, Copper plate; 10, Bolt; 11, Spring; 12, Insulators; 13, Melt; 14, Wall of bath.

Heating by Passing a Current Through Insulated Conductor

As practice has shown, ordinary insulated resistance heaters (spirals contained in porcelain tubes, wire heaters in beads, strip or band heaters wound on mica) do not allow heat flows greater than about (100-200)·10$^3$ kcal/m$^2$hr to be achieved even at low (down to 100°C) temperatures of the heat transfer medium.

The development of special heaters is required to produce high heat flows with high temperatures of the heat transfer medium.

Noyes [18], in his experiments on heat exchange during boiling of sodium, used a heater specially developed for this purpose. It is shown on Figure 2. The heater consists of an internal heating element made of graphite, a layer of electrical insulation consisting of a boron nitride bushing and a metal tube, with boiling occurring on the external surface of the tube. The electrical current is applied to the graphite heater by a /18

molybdenum electrode, tightly pressed against the graphite heater with a spring. Good thermal contact between the surfaces of the insulator, heater and external tube is provided by tight mechanical seating.

The length of the heater was 76 mm, the external diameter 9.5 mm. The heater was supplied with electric power by a power supply with adjustable voltage (up to 32 V) with a current of up to 1,200 A. This heater, in experiments with sodium (with sodium temperatures up to about 850°C) achieved heat fluxes up to $2.5 \cdot 10^6$ kcal/m$^2$hr.

In [39], using a similar heater, critical heat flows were investigated during the boiling of potassium under conditions of free convection at pressures up to 1.5 atm.abs. Heat flows up to $1.8 \cdot 10^6$ kcal/m$^2$·hr were produced with potassium temperatures up to 800°C.

One type of heater with an insulated conductor is the heater shown on Figure 3. Its difference from the heater shown on Figure 2 is that, first of all, the clearance between heating element and external tube is filled with metal, thus assuring good thermal contact; secondly, the insulating layer can be rather thin (a few tenths of a micron, applied by sputtering) thus providing low heat resistance; third, the clearance can contain thermocouples (with or without covers) which, if the metal used for filling has good heat conductivity provides minimal error in determining the wall temperature.

The material used for the heating elements can be such refractory metals as molybdenum, niobium, tantalum, tungsten, while the insulators can be made of the oxides of aluminum and zirconium, which have relatively high heat conductivity and high operating temperatures. If an insulating layer of these materials is applied using a plasmatron, good strength and satisfactory density of the covering will be achieved. The space between heating element and external tube should be filled using metals with high heat conductivity such as silver or copper.

One such heater was developed by the authors. Its external shell consisted of a tube 2.5 × 0.2 mm, the heating element was a niobium capillary 0.8 × 0.15 mm, covered with Alundum. The space between the heating element and the external tube was filled with copper by zone melting. This heater was used to achieve heat flows of up to $1.5 \cdot 10^6$ kcal/m$^2$·hr.

Figure 4 shows a diagram of an installation created for filling of the heater with copper. The ring shaped gap between the insulated heater and the external tube is filled with copper. A fine molybdenum wire passes through slots (or gaps) in the copper. At the bottom, the wire is connected to a molybdenum ring. The sector to be filled with copper is suspended on a wire in a furnace so that melting of the copper begins at the bottom. The furnace is a tube which is evacuated by a vacuum pump. The outside of the tube is heated by a silit resistance furnace. /20

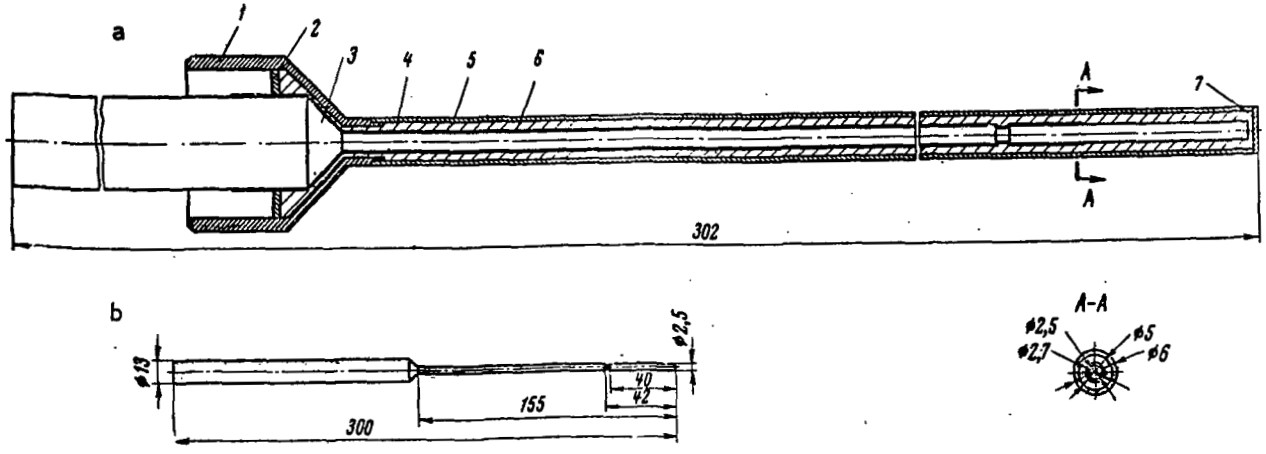


Figure 3. Heater With Insulated Conductor Filled With Copper (a, Overall View of Filled Sector; b, Heating Element). 1, Cone; 2, Supporting disc; 3, Molybdenum heating element; 4, Copper; 5, Cover of 1Kh18N9T steel (tube 6 × 0.5 mm); 6, Electrical insulation (aluminum oxide); 7, Cap.

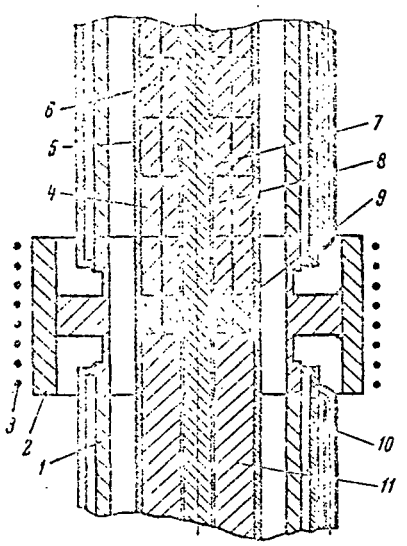


Figure 4. Diagram of Installation for Filling of Heater With Copper By Zone Melting.
1, Body; 2, Ring; 3, Electrical furnace; 4, Unmelted copper; 5, 1Kh18N9T steel tube; 6, Pole wires; 7, Heating element; 8, Electrical insulation (Alundum); 9, Guide; 10, Cooling chamber; 11, Solidified copper.

A ring is welded to the tube for local heating and melting of the copper. Local heating assures brief contact time between the liquid copper and the envelope. At the top and bottom of the ring are jackets cooled with air. The air is supplied by a compressor. As the copper melts, the assembly drops under its own weight and the weight of the additional load, thereby providing directed crystallization. The progress of the melting can be judged from the descent of the load through a glass tube placed in the cold zone.

The filling of the gap can be performed by other methods, for example under pressure. However in all cases, directed crystallization must be achieved in order to avoid shrinkage cracks and relatively short (preferably not over 1 minute) contact time of the envelope of the heater, if it is made of such materials as stainless steel, iron, nickel, etc. with the liquid copper, since liquid copper dissolves these metals intensively.

The heat flow in heaters with insulated conductor and filled gap will be limited either by melting of the filling metal or by melting of the heating element, or by the maximum possible operating temperature of the insulation.

The maximum heat flow $q_{max}$ for this type of heater can be determined from the formulas /21

$$q'_{max} = \frac{t'_m - t_l}{d_1\left(\frac{1}{\alpha d_1} + \frac{1}{2\lambda_1}\ln\frac{d_1}{d_2} + \frac{1}{2\lambda_2}\ln\frac{d_2}{d_3}\right)}, \qquad (I.8)$$

$$q''_{max} = \frac{t_{per} - t_l}{d_1\left(\frac{1}{\alpha d_1} + \frac{1}{2\lambda_1}\ln\frac{d_1}{d_2} + \frac{1}{2\lambda_2}\ln\frac{d_2}{d_3} + \frac{1}{2\lambda_3}\ln\frac{d_3}{d_4}\right)}, \qquad (I.9)$$

$$q'''_{max} = \frac{t''_m - t_l}{d_1\left(\frac{1}{\alpha d_1} + \frac{1}{2\lambda_1}\ln\frac{d_1}{d_2} + \frac{1}{2\lambda_2}\ln\frac{d_2}{d_3} + \frac{1}{2\lambda_3}\ln\frac{d_3}{d_4} + \frac{1}{4\lambda_4}\right)}. \qquad (I.10)$$

where $t'_m$, $t''_m$ are the melting temperatures of the filling metal and heater respectively, °C; $t_{per}$ is the permissible operating temperature of the insulation, °C; $d_1$, $d_2$ are the external and internal diameters of the outer tube of the heater respectively, m; $d_3$, $d_4$ are the external and internal (equal to the diameter of the heater) diameters of the insulating layer respectively, m; $\lambda_1$,$\lambda_2$, $\lambda_3$, $\lambda_4$ are the heat conductivity of the external tube, filler, insulation and heater respectively, kcal/m·hr °C.

The maximum permissible heat flow will be the least of those calculated using formulas (I.8) - (I.10).

Let us estimate as an example the value of $q_{max}$ for a heater with an external diameter $d_1$ = 10 mm, the external shell of which is 0.5 mm thick ($d_2$ = 9 mm) made of stainless steel ($\lambda_1$ approximately 20 kcal/m·hr °C).

The clearance between the heating element and the shell is 1.5 mm ($d_3$ = 6 mm), filled with copper ($\lambda_2$ approximately 270 kcal/m·hr°C at a temperature near the melting point), and the heating element ($d_4$ = 5.7 mm) is made of molybdenum ($\lambda_4$ approximately 60 kcal/m·hr°C), covered with a dense layer of Alundum ($\lambda_3$ approximately 4.5 kcal/m·hr°C) 0.15 mm thick. The melting points of copper and molybdenum are 1,080 and 2,600°C respectively [51]; the permissible operating temperature of Alundum products is 1,700°C [51]. The value of $q_{max}$, calculated from formulas (I.8) - (I.10) with these values of the quantities and with heat transfer coefficient $\alpha = 50 \cdot 10^3$ kcal/m$^2$·hr°C for a liquid temperature of 800 and 900°C are presented below:

| $t_l$, °C | $q'_{max}$, kcal/m$^2$·hr | $q''_{max}$, kcal/m$^2$·hr | $q'''_{max}$, kcal/m$^2$·hr |
|---|---|---|---|
| 800 | $5.2 \cdot 10^6$ | $8.0 \cdot 10^6$ | $11.6 \cdot 10^6$ |
| 900 | $3.3 \cdot 10^6$ | $7.1 \cdot 10^6$ | $11.0 \cdot 10^6$ |

Consequently, for this example, the maximum heat flow will be limited by the melting of the copper interlayer.

Thermal Wedge /22

The essence of this method is that the heat is transmitted directly from the heater to a surface, whose area is greater than the working surface. The heat is transmitted to the working surface by heat conductivity. The heat flow on the working surface will be approximately equal to

$$q = q_{heat} \frac{F_{heat}}{F_{work}}, \qquad (I.11)$$

where $q_{heat}$ is the heat flow on the heated surface; $F_{heat}$ is the area of the heated surface; $F_{work}$ is the area of the working surface.

Figure 5 shows schematically a heater based on the thermal wedge method. Heating of the body of the working sector is by radiation from heaters located within and without.

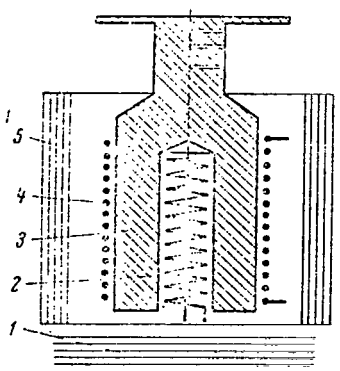


Figure 5. Heater Operating According to Principle of Thermal Wedge.
1, 5, Screen; 2, 4, Internal and external heaters; 3, Heat transmitting wall.

The works of Bonilla [10, 20, 22] made use of a heater as shown on Figure 6. In this heater, vertical ribs were welded or soldered to the body of the working sector. Wire resistance heaters were wound around the ribs (over mica). Using a heater of this design in experiments with mercury, heat flows of up to about $5.5 \cdot 10^5$ kcal/m$^2$·hr were achieved (with mercury temperatures of up to 360°C); and in experiments with potassium, heat flows of up to $0.3 \cdot 10^6$ kcal/m$^2$·hr were produced (with potassium temperature 830°C).

The heat flow on the heating surface of the working sectors shown on Figures 5 and 6 can be determined by measuring the difference in temperature $\Delta t$ through the height of the sector

$$q = \Delta t \frac{\lambda_w}{\delta_w}, \qquad (I.12)$$

where $\delta_w$ is the distance between the centers of the thermocouple junction; $\lambda_w$ is the heat conductivity of the material in the working sector. For more precise determination of q, it is best to have several thermocouples in each cross section, since in this case errors in determining the distance between junctions of thermo couples are averted. /23

For each individual design, one should also estimate the radial leakage of heat and the related distribution of heat flow over the working surface.

## Electronic Heating

Electronic heating for investigations of heat exchange in boiling water was first used by P. I. Povarnin and I. G. Kulakov [52]. The usage of the electronic method of heating for investigation of heat exchange in boiling of metals is quite promising, although as yet this method has not been widely used in practice. Therefore, let us analyze it in greater detail.

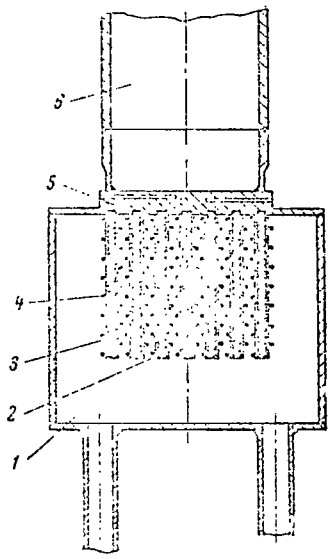


Figure 6. Heater Operating According to Thermal Wedge Principle Used by Bonilla [10, 20]. 1, Vacuum chamber; 2, Molybdenum plates; 3, Mica insulator; 4, Heater; 5, Working sector; 6, Working tank.

Electronic heating is performed by bombarding the heating wall with electrons emitted by a cathode and accelerated under the influence of an anode voltage. When the electrons collide with the anode, the kinetic energy of the electrons is converted to thermal energy, thus creating a heat flow on the surface, since with an anode voltage of even 10 kv deceleration of the electrons occurs in a thin (on the order of one micron) surface layer.

For one electron, the kinetic energy is

$$\frac{m_e W_e^2}{2} = e^* U_a, \qquad \text{(I.13)}$$

where $m_e$ is the mass of an electron; $W_e$ is the velocity of the electron at the moment of collision with the anode; $U_a$ is the potential difference between the cathode and anode (anode voltage).

The power liberated at the anode $Q_a$ is calculated using the anode current $I_a$ and the anode voltage $U_a$, since

$$Q_a = \sum \frac{m_e W_e^2}{2} = U_a \sum e^* = U_a I_a. \qquad \text{(I.14)}$$

This formula does not consider energy losses due to X-ray radiation and secondary electrons. The error in determination of the anode power due to these faults with voltages ordinarily used (up to about 10 kv) will be less than 1%.

The usage of voltages over 10 kv is not desirable. First of all, with high voltages in order to avoid gas discharge (breakdown) in the electron heater, a deeper vacuum is required; secondly, special biological protection from X-rays may be required. /24

In addition to electron bombardment, the heating wall will be heated by radiation from the cathode. The thermal flow due to radiation from the cathode depends on the design of the installation. However, with high thermal flows (about $10^6$ kcal/m$^2$·hr) in all cases the principal contribution will be that of the anode component.

With electron heating, the energy is transmitted to the heating wall without contact and at a high potential (up to several kilovolts) making it possible to apply significant energy levels to a relatively small surface area and thereby produce high heat flows. For example, in powerful generator tubes, the heat fluxes reach $86 \cdot 10^6$ kcal/m$^2$·hr [53]. With electron heating the surface of the heating wall turned toward the cathode is not oxidized or corroded even at high temperatures, since it is under a vacuum on the order of $10^{-5}$- $10^{-6}$ mm Hg.

Standard equipment can be used to make the high voltage and high vacuum apparatus required when this method is used.

One of the principal elements of any electron tube is the cathode. At the present time, pure metal, film and semiconductor cathodes are used. According to the type of heating, directly and indirectly heated cathodes are distinguished. In an electronic heater for investigation of heat exchange, the cathode operates under more difficult conditions than the conditions of operation of a cathode in an electron tube. In the heater, the cathode must rapidly recover its emission properties after ion bombardment and contact with air, must operate under relatively low vacuum conditions (about $10^{-4}$ mm Hg) and must have high specific emission. Heaters designed for operation with boiling alkali metals require that the operating temperature of the cathode be above the surface temperature of the heating wall turned toward the cathode, which may exceed 1,300-1,500°C. These conditions are best satisfied by a tungsten cathode [48].

The electronic emission is described by the Richardson-Dushman equation

$$j = A_j T^2 e^{-\frac{e\varphi}{kT}} \qquad \text{(I.15)}$$

where j is the saturation current, A/cm$^2$; $A_j$ is the emission constant, A/cm$^2$deg$^2$; $\phi$ is the work function of the electron.

The dependence of specific emission j of tungsten on temperature, according to data presented in [48], is constructed on Figure 7. We can see that up to 2,300°K, it is near zero. Then, it grows rapidly as temperature increases. In electron tubes, the operating temperatures of tungsten cathodes lie between 2,450 and 2,650°K [48]. /25

Electron tubes can operate in two modes: the saturation mode and the space charge mode. The saturation mode occurs when the anode current is limited by the emission capability of the cathode. When the emission capability of the cathode exceeds the anode current, the reason for limitation of the anode current is the space charge between the cathode and the anode. In the space charge mode, the dependence for anode current $I_a$ is as follows [48]:

$$I_a = 2.33 \cdot 10^{-6} F_a \frac{U_a^{3/2}}{h_к^2} \varkappa, \qquad (I.16)$$

where $F_a$ is the area of the surface of the anode subjected to electron bombardment, $m^2$; $h_k$ is the distance between cathode and anode, m; $\kappa$ is a factor dependent on the geometry and mutual placement of the cathode and anode ($\kappa \leqslant 1$); $U_a$ is the anode voltage, v. For a flat system of electrodes, when the area of the cathode surface is equal to the area of the anode surface, $\kappa = 1$. The specific heat flow produced due to electron bombardment is calculated using the formula

$$q_a = 0.86 \frac{I_a U_a}{F}. \qquad (I.17)$$

Therefore, in the space charge mode $q_a \sim U_a^{5/2}$.

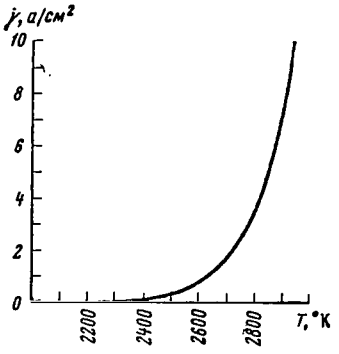


Figure 7. Dependence of Specific Emission of Tungsten on Temperature.

Figures 8 and 9 reflect the qualitative nature of the dependence of anode current and thermal load during operation of a tube in the space charge and saturation modes (branches $T_1$; $T_2$; $T_3$). The dependences shown on Figures 8 and 9 can be conveniently used in analyzing methods of regulation of tube powers. For each concrete case, these can be calculated. The heat liberation at the surface subjected to electron bombardment may be uneven. The unevenness may result from the design of the installation (geometry of cathode, anode and their mutual placement). When operating in the saturation mode, the unevenness of heat liberation arises due to uneven distribution of temperature over the cathode and differences in the work functions of electrons, related for example to nonhomogeneity of the material of the cathode. In the space charge mode, unevenness of heat liberation arises due to differences in the distances from the anode ($h_k$) to individual sectors of the cathode. The unevenness of heat liberation on the heat liberating surface will be smoothed by heat conductivity to some extent. Therefore, for each concrete installation, an estimate should be made of the evenness of heat liberation on the heating surface. /26

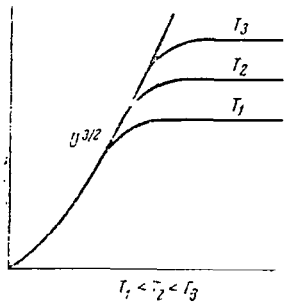


Figure 8. Qualitative Dependence of Anode Current on Anode Voltage For Space Charge Mode ($I_a \sim U_a^{3/2}$) and Saturation Mode (With Various Temperatures $T_1 < T_2 < T_3$.

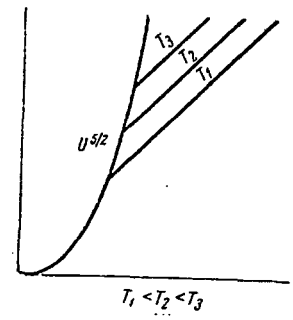


Figure 9. Qualitative Dependence of Heat Flow on Anode Voltage for Space Charge Mode ($q_a \sim U_a^{5/2}$) and Saturation Mode ($T_1 < T_2 < T_3$).

Figure 10, a and b shows a working sector with electron heating used by the authors for the investigation of heat exchange during boiling of metals [14, 15, 21, 36, 38, 54]. Subsequently, this sector will be referred to as the tube, since it is a diode. The body of the tube (anode) is grounded, and an adjustable voltage is fed to the cathode.

A removable cup is fastened to the upper portion of the body. The central portion of the end of the cup is the working area. Subsequently, the working area of the cup will be called the plate. The internal surface of the plate is subjected to electron bombardment and radiation heating from the cathode.

The cathode is made of tungsten wire 1 mm in diameter in the form of an Archimedes spiral with a mean external diameter of 38 mm and a distance between centers of turns of 3 mm. The blades of the cathode are fastened to two molybdenum holders by a molybdenum wire 0.3 mm in diameter, tightly wound over a length of 15 mm. This type of connection provides good electrical contact in a vacuum. The holders are fastened in copper current conductors. The design of the current conductors allows the cathode to be centered and allows its position to be adjusted in height as well. In order to avoid sagging of the cathode, it is supported from beneath by six supports made of thin (0.15 mm) sheet tantalum. In order to provide for focusing of /28
the electrons moving from the cathode to the plate of the cup, the cathode is surrounded with a tantalum screen carrying the same potential as the cathode. The internal diameter of this screen is 39 mm. The cathode is set at a distance of 15-20 mm from the plate, and the screen is 10-15 mm higher than the plane of the cathode.

/27

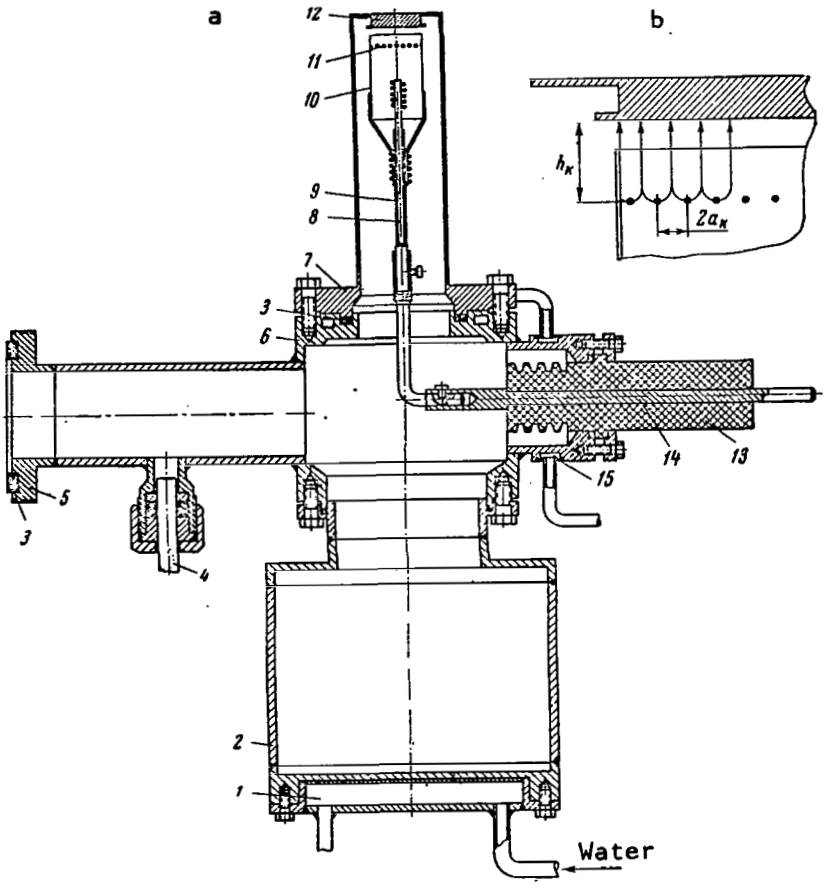


Figure 10. Electron Heater Developed by the Authors
a, General view; b, Section of cathode and anode.
1, 15, Water cooling; 2, Collecting tank; 3, Rubber inserts;
4, Device for sealing pressure pickups; 5, Tube for connection
to vacuum system; 6, Body; 7, Cup; 8, Molybdenum holder;
9, Porcelain insulator; 10, Tantalum screen; 11, Cathode;
12, Working sector (plate); 13, Insulator made of "K-153";
14, Current conducting leads.

Input of power to the tube is performed through the current conductors, /29
which are hermetically sealed in an insulator made of "K-153" compound. The current conductors were filled with the compound during the process of manufacture of the insulator. This insulator can operate without special cooling, since "K-153" compound withstands temperatures up to 150°C.

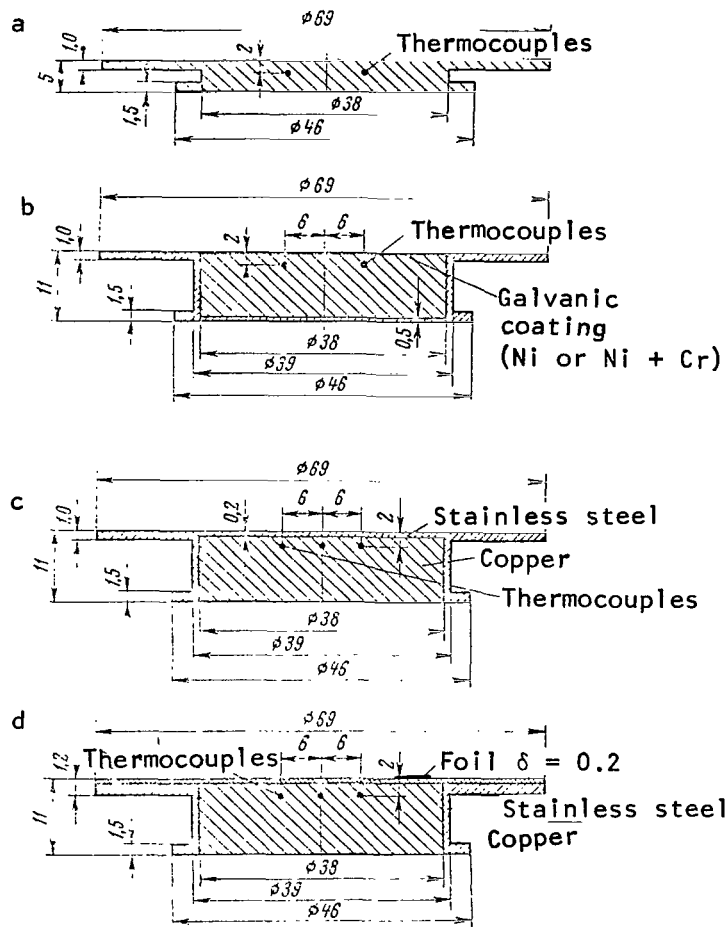


Figure 11. Types of Heating Surfaces (Plates) Used by the Authors In Boiling Experiments.
a, One piece turned; b, Copper-filled. Working surface covered with galvanic nickel or chrome; c, Unit wall, copper-filled; d, Copper-filled (with working surface side made of foil of various materials: stainless steel, molybdenum, tantalum, etc.

The lower portion of the tube body is fastened to a removable tank for collection of metal in case the plate fails during the process of operation. At the points of vacuum seals subjected to heating, water cooling is provided.

Various plates may be welded to the cup. The types of plates used by the authors in the experiments on heat exchange in the boiling of metals are shown on Figure 11.

For the geometry of this tube ($a_k$ and $h_k$; see Figure 10, b) the value of $\kappa$ in formula (I.16) is near 1 [48]. This means that heat liberation due to electron bombardment on the surface of the plate turned toward the cathode in the space charge mode should be nearly even. The slight unevenness of heat liberation, if any exists, will be smoothed out on the heat exchange surface by heat conductivity. Let us show this with an example.

Let us assume, as an extreme case, that the heat flow on the internal surface of the plate is distributed in a spiral, the dimensions of which are equal to the dimensions of the spiral of the cathode. Let us make the following assumptions.

1. The plate is looked upon as an infinite plate and the spiral distribution of heat flow is replaced with a stepped distribution. The step of the distribution ($2a_k$) is equal to the step of the spiral of the cathode, the width of the step ($b_k$) is equal to the diameter of the cathode wire (Figure 10, 12).

2. The heat conductivity of the plate and the heat transfer coefficient from plate to liquid are considered constant.

The process of heat transfer in the plate is described by the equation

$$\frac{\partial^2 t}{\partial x^2} + \frac{\partial^2 t}{\partial y^2} = 0 \tag{I.18}$$

with the following boundary conditions:

$$\left(\frac{\partial t}{\partial x}\right)_{x=0} = 0, \tag{I.19}$$

$$\left(\frac{\partial t}{\partial y}\right)_{y=0} = -\frac{q(x)}{\lambda}, \tag{I.20}$$

$$\left(\frac{\partial t}{\partial y}\right)_{y=\delta_w} = -\frac{\alpha t}{\lambda}. \tag{I.21}$$

Solving equation (I.18) by separation of variables, we produce an expression for the heat flow on the heating surface

$$q = \frac{q_0 b_k}{2a_k} - \lambda \sum_{i=1}^{\infty} \frac{\pi n_i}{a_k} \left(A_n e^{\frac{\pi n_i}{a_k} y} - B_n e^{-\frac{\pi n_i}{a_k} y}\right) \cos \frac{\pi n_i}{a_k} x. \tag{I.22}$$

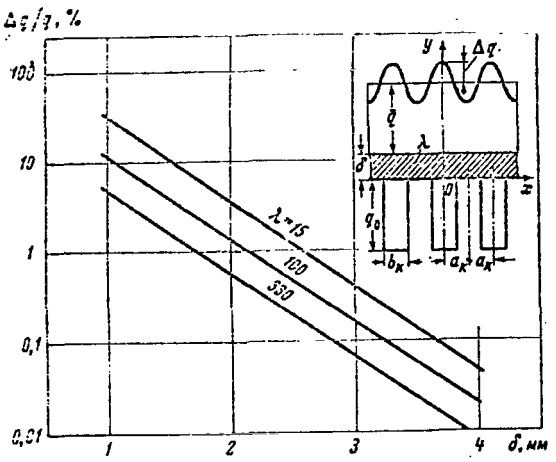


Figure 12. Dependence of Unevenness of Heat Flow on Heat Transfer Surface of Plate on Its Thickness With Various Values of Heat Conductivity, Calculated According to Formula (I.22).

The values of coefficients are found from the equations /30

$$A_n - B_n = -\frac{2 \cdot q_0 \cdot a_к}{\lambda \pi^2 \cdot n_i^2} \cdot \sin \frac{\pi n_i}{2a_к} b_к, \quad \text{(I.23)}$$

$$A_n e^{\frac{\pi n_i}{a_к} \delta_w} \left(1 + \frac{\alpha \cdot a_к}{\lambda \pi n_i}\right) = B_n e^{\frac{\pi n_i}{a_к} \delta_{ст}} \left(1 - \frac{\alpha a_к}{\pi n_i \lambda}\right), \quad \text{(I.24)}$$

and the value of $q_0$ is determined from the formula

$$q_0 = \frac{q_a \cdot 2a_к}{b_к}. \quad \text{(I.25)}$$

Figure 12 shows the dependence of the relative unevenness of heat flux on the heating surface of the plate on the thickness of the plate with various values of heat conductivity for a value of heat transfer coefficient of $10^5$ kcal/m$^2$·hr°C. For the lowest values of heat transfer coefficients, the unevenness is least. We /31 can see from Figure 12 that even in this hypothetical case, the plates used (see Figure 11) would provide unevenness of heat flow on the heating surface resulting from cathode geometry of less than 0.1%.

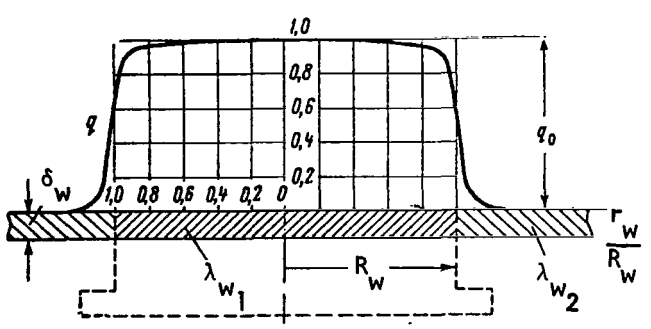


Figure 13. Distribution of Heat Flow On Heating Surface of Plate, Working Portion of Which is Made of Copper (see Table 1.1): $\delta_w$ = 1 mm; $\alpha = 40 \cdot 10^3$ kcal/m$^2$hr°C; $\lambda_{w1}$ = 300 kcal/m·hr°C; $\lambda_{w2}$ = 15 = kcal/m·hr°C.

The heat flow on the surface turned toward the heat transfer medium will not be even, due to radial leakage of heat from the working portion of the plate. In this case, the process of heat transfer is described by the equation

$$\frac{\partial^2 t}{\partial r_w^2} + \frac{1}{r_w} \frac{\partial t}{\partial r_w} + \frac{\partial^2 t}{\partial y^2} = 0 \quad \text{(I.26)}$$

with the following boundary conditions:

$$\left(\frac{\partial t}{\partial y}\right)_{y=0} = -\frac{q_{(r_w)}}{\lambda_w}, \quad \text{(I.27)}$$

$$\left(\frac{\partial t}{\partial y}\right)_{y=\delta_w} = -\frac{\alpha t}{\lambda_w}. \qquad (I.28)$$

For plates filled with copper, we must add to boundary conditions (I.27), (I.28) the additional "seam" condition where $r_w = R_w$ (see Figure 13)

$$t_{r_w} = R_w - 0 = t_{rw} = R_w + 0, \qquad (I.29)$$

$$\lambda_{w_1} \left(\frac{\partial t}{\partial r_w}\right)_{r_w=R_w-0} = \lambda_{w_2} \left(\frac{\partial t}{\partial r_w}\right)_{r_w=R_w+0} \qquad (I.30)$$

Equation (I.26) with conditions (I.27)-(I.30) and the assumption of the heat transfer coefficient and heat conductivity are constant, has been solved numerically by N. I. Buleyev and V. A. Mosolova for various combinations of $\alpha$, $\lambda_w$ and $\delta_w$. The results of this calculation are presented in Tables I.1-I.4.

TABLE I.1

| $r_w/R_w$ | For plate made of homogeneous material: $R_w$ = 18 mm, $q/q_0$ | | | | | | | | | |
|---|---|---|---|---|---|---|---|---|---|---|
| 0,224 | 1,00 | 1,00 | 1,00 | 1,00 | — | — | — | — | — | — |
| 0,316 | — | — | — | — | 0,997 | 0,981 | 0,997 | 0,999 | 0,989 | 1,00 |
| 0,387 | 1,00 | 1,00 | 1,00 | 1,00 | — | — | — | — | — | — |
| 0,500 | 0,995 | 0,994 | 1,00 | 0,998 | — | — | — | — | — | — |
| 0,548 | — | — | — | — | 0,988 | 0,952 | 0,997 | 0,995 | 0,954 | 0,999 |
| 0,592 | 0,995 | 0,985 | 0,999 | 0,998 | — | — | — | — | — | — |
| 0,671 | 0,995 | 0,975 | 0,999 | 0,998 | — | — | — | — | — | — |
| 0,707 | — | — | — | — | 0,980 | 0,907 | 0,997 | 0,991 | 0,892 | 0,982 |
| 0,742 | 0,995 | 0,954 | 0,999 | 0,998 | — | — | — | — | — | — |
| 0,806 | 0,981 | 0,919 | 0,999 | 0,994 | — | — | — | — | — | — |
| 0,837 | — | — | — | — | 0,914 | 0,801 | 0,982 | 0,949 | 0,779 | 0,918 |
| 0,886 | 0,951 | 0,859 | 0,998 | 0,981 | — | — | — | — | — | — |
| 0,922 | 0,877 | 0,758 | 0,980 | 0,927 | — | — | — | — | — | — |
| 0,950 | — | — | — | — | 0,718 | 0,613 | 0,854 | 0,774 | 0,588 | 0,709 |
| 0,975 | 0,705 | 0,603 | 0,870 | 0,766 | — | — | — | — | — | — |
| 1,05 | 0,172 | 0,260 | 0,060 | 0,123 | 0,231 | 0,303 | 0,118 | 0,187 | 0,322 | 0,238 |
| 1,2 | 0,018 | 0,068 | 0,001 | 0,0078 | 0,045 | 0,110 | 0,008 | 0,024 | 0,126 | 0,043 |
| 1,4 | — | 0,001 | 0,007 | — | 0,004 | 0,023 | — | 0,0014 | 0,030 | 0,0035 |
| 1,83 | — | — | — | — | — | 0,0016 | — | — | 0,002 | — |

/32

Commas indicate Decimal points.

TABLE I.2

Calculated data for table 1.1

| $\delta_w$, mm | 0,5 | 0,5 | 0,5 | 0,5 | 1 | 1 | 1 | 1 | 2 | 2 |
|---|---|---|---|---|---|---|---|---|---|---|
| $\alpha$, $\frac{kcal}{m^2 \cdot hr^\circ C}$ | $5 \cdot 10^4$ | $5 \cdot 10^4$ | $1 \cdot 10^5$ | $1 \cdot 10^5$ | $5 \cdot 10^4$ | $5 \cdot 10^4$ | $1 \cdot 10^5$ | $1 \cdot 10^5$ | $5 \cdot 10^4$ | $1 \cdot 10^5$ |
| $\lambda_w$ $\frac{kcal}{m \cdot hr^\circ C}$ | 100 | 330 | 20 | 100 | 100 | 330 | 20 | 100 | 100 | 20 |
| $\Omega = \frac{\alpha \cdot R_w}{\lambda_w}$ | 9,00 | 2,73 | 90,0 | 18,0 | 9,00 | 2,73 | 90,0 | 18,0 | 5,40 | 90,0 |

Commas indicate decimal points.

TABLE I.3

/33

| $r_w/R_w$ | For plate made of heterogeneous materials: $\lambda_{w_1} = 300 \frac{kcal}{m \cdot hr^\circ C}$ $\lambda_{w_2} = 15 \frac{kcal}{m \cdot hr^\circ C}$ | | |
|---|---|---|---|
| | q/q₀ | | |
| 0,316 | 0,988 | 1,00 | 1,00 |
| 0,548 | 0,975 | 0,99[illegible] | 0,970 |
| 0,707 | 0,969 | 0,[illegible]5 | 0,950 |
| 0,837 | 0,937 | 0,968 | 0,940 |
| 0,919 | 0,888 | 0,918 | 0,900 |
| 1,02 | 0,337 | 0,256 | 0,210 |
| 1,05 | 0,149 | 0,090 | 0,110 |
| 1,09 | 0,065 | 0,024 | 0,[illegible]2 |
| 1,13 | 0,027 | 0,006 | 0,025 |
| 1,18 | 0,010 | 0,0014 | 0,012 |
| 1,23 | 0,003 | — | 0,005 |
| 1,30 | 0,001 | — | — |

Commas indicate decimal points.

TABLE I.4

Calculated data for table 1.3

| | | | |
|---|---|---|---|
| $\delta_w$, mm | 1 | 1 | 1,5 |
| $R_w$, mm | 18 | 28 | 18 |
| $\alpha$, $\frac{kcal}{m^2 hr°C}$ | $40 \cdot 10^3$ | $40 \cdot 10^3$ | $80 \cdot 10^3$ |
| $\Omega = \frac{\alpha \cdot R_w}{\lambda_w}$ | 2,18 | 3,39 | 4,36 |

Commas indicate decimal points.

On Figure 13 as an example we show the distribution of heat flow over the heating surface of a floor, the working portion of which is made of copper. The dimension of the cathode is selected in correspondence with the dimension of the working portion of the floor (38 mm). Calculation of the heating current and voltage of the cathode is performed as follows.

The area of the surface of the spiral portion of the cathode is

$$F_к = \pi d_к l_к = \pi d_к \pi D_{av} n_к, \tag{I.31}$$

where $d_k$ is the diameter of the wire of which the cathode is made; $l_k$ is the length of the working portion (spiral) of the cathode; $D_{av}$ is the mean diameter of the spiral; $n_k$ is the number of turns of the spiral.

Knowing the working surface area of the cathode $F_k$ and the nominal rectifier current $I_a$, we can find the necessary emission current density /34

$$j = \frac{I_a}{F_к}. \tag{I.32}$$

After determining j, using the dependence of specific emission on temperature, we can find the operating temperature of the cathode. Once we know the operating temperature and the dimensions of the cathode, we can find the heating power required

$$N_к = \eta \pi d_к l'_к, \tag{I.33}$$

where $l_k'$ is the length of the cathode, and $\eta$ is the specific radiation power from the cathode at the operating temperature. The value of $\eta$ for tungsten and a number of other metals can be found in [48]. After determining the heating temperature and knowing the specific resistance of the cathode at the operating temperature, we can easily calculate the current and voltage required for heating. For example, for the tube design shown on Figure 10, the heating power is approximately 1.0 kw, the current and voltage for heating are 50 A and 20 V respectively. On the basis of these data, the parameters of the filament transformer can be selected.

The electron tube is supplied from a rectifier device. A circuit of the rectifier device used by the authors is illustrated on Figure 14. The rectifier, made of thyratrons, was supplied by an anode transformer, the voltage at the input of which was adjusted by an autotransformer.

The heating supply for the cathode of the lamp was from a filament transformer, whose circuit contained an autotransformer and voltage stabilizer.

The anode voltage was measured using a voltage divider with a multiple range volt meter. The anode current was measured with a multi-range ammeter. The ammeter and volt meter, the indications of which determine the filament power, were connected at the input of the filament transformer, due to which these devices did not carry the anode voltage. The filament circuit of the tube included vacuum blocking in the tube. The anode circuit was blocked with respect to the filament of the tube and the temperature of the floor, as well as a number of protective blocking arrangements.

The nominal anode power was 20 kw; the nominal anode current was 2 A; the anode voltage was adjusted between approximately 0 and 10 kV.

The heat flow on the heating surface for the tube design shown on Figure 10 can be calculated using the formula

$$q = q_a + q_s - q_{rad}. \tag{I.34}$$

The anode component of the heat flow $q_a$ is determined from formula (I.17).

The heat flow due to radiation from the cathode can be calculated using the formula /35

$$q_s = KK_1 \frac{0.86\, U_s I_s}{F_a} \varepsilon, \tag{I.35}$$

and due to radiation from the internal surface of the base

$$q_{rad} = 4.9 \cdot \varepsilon \frac{F_{rad}}{F_a} \left( \frac{T_{rad}}{100} \right)^4, \qquad (I.36)$$

where $F_a$ and $F_{rad}$ are determined by the diameters of 38 and 46 mm respectively (see Figure 11); $\varepsilon$ is the blackness of the plate surface. In formula (I.35), coefficient K considers power losses in the filament transformer and can be determined experimentally in each concrete case.

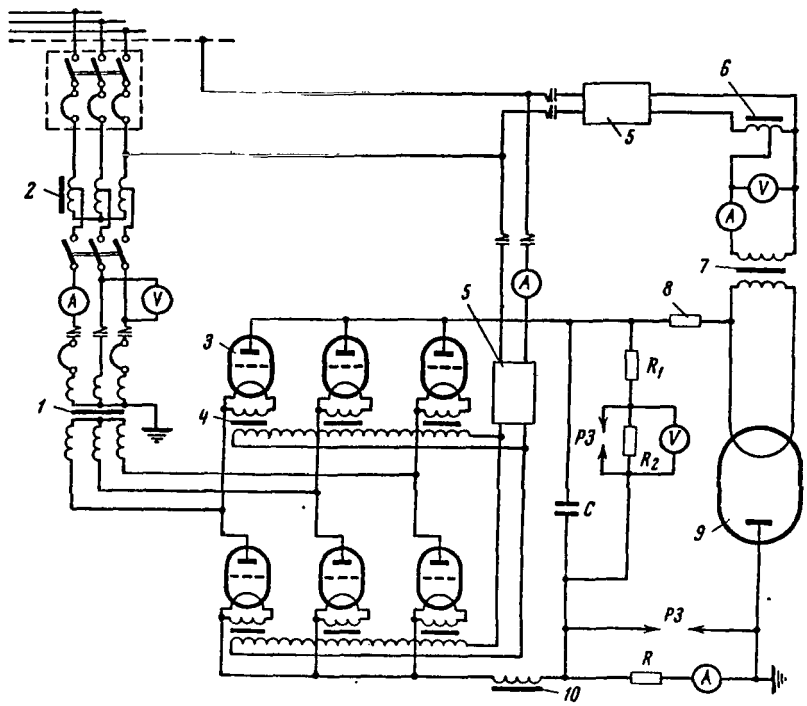


Figure 14. Diagram of Electronic Heater Power Supply.
1, Step-up transformer; 2, Regulating transformer;
3, Thyratrons; 4, Thyratron filament transformer;
5, Voltage stabilizer; 6, Adjusting transformer;
7, Dividing transformer; 8, Fuse 9, Electron tube;
10, Choke; SG, Spark gaps.

Coefficient $K_1$ considers the share of the power consumed on the cathode, /36 which is transmitted to the plate by radiation. The value of $K_1$ is also estimated for each concrete case. The value of the product $K_1 \cdot \varepsilon$ can be

determined experimentally from the temperature difference measured by thermocouples located in two or several different cross sections of the plate. It is desirable in this case to have reliable data on heat conductivity of the plate material. The heat flow related to radiation from the internal surface of the plate makes a contribution to the total heat flow only at high temperatures in experiments on metals. The value of $T_{rad}$ is found from the indications of thermocouples placed in the plate, considering the temperature drop. For the tube design which we have analyzed, the value of $(q_{fil} - q_{rad})$ does not exceed $0.2 \cdot 10^6$ kcal/m$^2$·hr. Therefore, with high heat flows (about $10^6$ kcal/m$^2$·hr) the principal contribution to the total heat flow is that of the anode component of heat flow, which is determined more precisely (with an accuracy of 2-3%) than $q_{fil}$ and $q_{rad}$.

The possibility of producing high heat flows was tested with the plate cooled by a cold air current moving at high speed through a slit made between the plate and a special cover. This tube (with the cooling equipment) achieved a heat flow of $20 \cdot 10^6$ kcal/m$^2$·hr, which was maintained for a long period of time. The maximum heat flow achieved was $36 \cdot 10^6$ kcal/m$^2$·hr. However, this flow could be maintained only for a few minutes, due to overloading of the anode transformer.

With electronic heating, the maximum heat flow is principally limited by the strength (mechanical or melting) of the heated surface, in which the temperature gradients are high with high heat flows.

In [17], a cylindrical working sector was used with electronic heating, as shown on Figure 15. The cathode is made of tungsten wire 1 mm in diameter in the form of a bifilar spiral 8 mm in diameter and 60 mm long. In order to equalize the temperature field through the length of the cathode and decrease heat losses by radiation, the ends of the cathode were covered with molybdenum screens. The working length of the cathode is equal to the distance between the screens. The cathode is fastened to two molybdenum rods 2 mm in diameter, set in the copper current conductors. The conductors are soldered to kovar-glass-kovar connectors. The cathode is also supported by a molybdenum rod 2 mm in diameter, which is centered by Alundum inserts.

The heating wall consists of two coaxially located thin walled (29.6 × 0.35 and 21 × 0.5 mm) stainless steel tubes. Copper is poured into the space between the tubes, in which thermocouples in stainless steel covers (1.5 × 0.25) are also placed.

This working sector was used in an investigation of heat transfer in boiling sodium at temperatures up to 850°C with heat flows up to $1.5 \cdot 10^6$ kcal/m$^2$·hr. /37

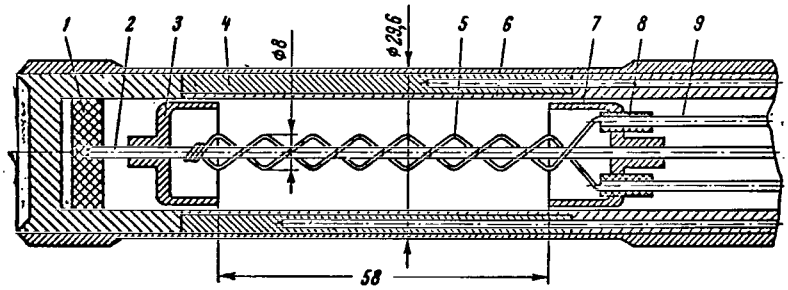


Figure 15. Electronic Heater Used in [17].
1, Alundum spacer; 2, Molybdenum rod; 3, 7, Molybdenum screens; 4, Copper filler; 5, Tungsten wire cathode, 1 mm diameter; 6, 1Kh18N9T steel tube; 8, Alundum insulators; 9, Current conductors.

## Heat Pipe

In experiments on heat exchange during boiling of metals conducted at high temperatures with high heat flow densities, the heat pipe can be used both for input of heat to the working sector and for carrying heat away from the condenser.

A heat pipe is shown schematically on Figure 16. The heat transfer in the heat pipe is achieved by vapor, which is generated by input of heat to the evaporation zone and moves through the vapor channel to the condensation zone. The condensate is returned to the evaporation zone by capillary forces. The capillary devices may be wire wicks, channels scratched on the internal side of the tube, etc. For stable operation of the heat pipe it is necessary that the vapor flow correspond to the flow of condensate through the capillary device.

For a laminar flow mode, [55] produced an equation for the quantity of heat transferred along the tube

$$Q = \frac{r\gamma''}{32 \cdot T\left[\frac{\nu''}{F_v d_v^2} + \frac{\gamma''}{\gamma}\frac{\nu}{F_l d_l^2}\right]}\frac{\Delta T}{l_T}, \qquad (I.37)$$

where $F_v$, $F_l$ are the cross sections of vapor and condensate flow respectively, $d_v$, $d_l$ are the hydraulic diameters of the vapor channel and capillary device respectively; $l_T$ is the length of the heat pipe; $\Delta T$ is the vapor temperature difference at the ends of the heat pipe. Formula (I.37) was produced on the /38

following assumptions: the temperature and pressure change linearly over the length of the pipe; the physical properties of the liquid and vapor are constant and gravitation is absent.

The maximum temperature difference in expression (I.37) can be determined from the following formula:

$$\Delta T_{max} = \frac{4AT\sigma}{d_{\ell} r \gamma''} \left[ \frac{1}{1 + \frac{\nu}{\nu''} \frac{F_v d_v^2}{F_{\ell} d_{\ell}^2}} + \frac{\gamma''}{\gamma} \right], \tag{I.38}$$

while the maximum power, corresponding to $\Delta T_{max}$, can be determined from the formula

$$Q_{max} = \frac{r\sigma}{8\zeta_T d_{\ell} \left( \frac{\nu''}{F_v d_v^2} + \frac{\nu}{F_{\ell} d_{\ell}^2} \right)}. \tag{I.39}$$

We can see from (I.39) that the power transmitted by a heat pipe depends both on its design and on the properties of the working fluid. For any given design, the quantity of heat transferred is greater when working fluids with higher latent heat of evaporation (r), surface tension ($\sigma$), vapor density ($\gamma''$) and liquid density ($\gamma$) are greater. Another important condition is the wettability of the working surface of the material of which the capillary device is made. The less the boundary wetting angle the better the capillary device will work.

The working media used in high temperature heat pipes may be lithium, sodium, lead, bismuth, silver or certain other metals. The selection of the structural material is very important for successful operation of a heat pipe. It should be resistant to the working medium and sufficiently strong at the operating temperatures. During the process of operation of the heat pipe, continuous distillation of the fluid occurs. If the fluid dissolves the construction material, the products of solution will precipitate in the evaporation zone, which can lead to over heating and failure of the entire heat pipe.

The structural materials used for high temperature heat pipes are the refractory metals (niobium, molybdenum, tantalum) and their alloys. /39

Table I.5, borrowed from [45], shows information on working media, temperature levels and structural materials for heat pipes.

In [45], experiments were performed with a tube 600 mm in length, external diameter 14 mm with wall thickness 1 mm. The capillary device

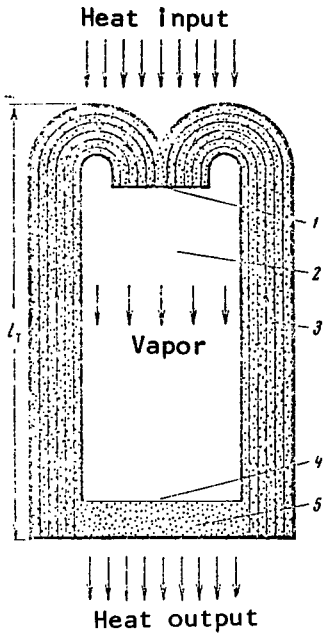


Figure 16. Diagram of Heat Pipe. 1, Evaporation zone; 2, Vapor channel; 3, Capillary device; 4, Condensation zone; 5, Working fluid (heat transfer medium).

was a three section wick of 0.22 mm diameter wire with an open cell diameter of 0.43 mm. The outer tube and wire wick were made of chrome-nickel steel.

The heating zone was 90 mm, the condensation zone - 510 mm. On the internal surface of the tube, the heat flux in the heating zone was about $190 \cdot 10^3$ kcal/m$^2$·hr, and in the condensation zone - about $32 \cdot 10^3$ kcal/m$^2$·hr. In the heating zone, the heat flow briefly reached $(500\text{-}600) \cdot 10^3$ kcal/m$^2$·hr. The heat flow, related to the free cross section of the tube, reached $5.6 \cdot 10^6$ kcal/m$^2$·hr. This heat pipe had an apparent heat conductivity of about $860 \cdot 10^3$ kcal/m·hr °C, that is exceeded the heat conductivity of the wall material by approximately $40 \cdot 10^3$ times.

The transport medium in the pipe was sodium, 17.3 grams. The vapor pressure of sodium during operation was about 0.15 atm. abs. The vapor velocity in the heating zone was 65 m/sec. The calculated pressure drop in the vapor space was about $1.8 \cdot 10^{-3}$ atm.abs., and the calculated temperature drop was about 0.72°C. /40

For purposes of cleaning and to assure good wetting, the tube and wick were heated in a vacuum for several hours at 1200°K.

TABLE 1.5

| Operating temperature | Material transported | Structural material | Operating life |
|---|---|---|---|
| 300-540 | Water | Chrome-nickel steel | Over 7500 hrs. at 360°K |
| 640-1000 | Cesium | Titanium | Over 2000 hrs. at 650°K |
| 650-1100 | Potassium | Chrome-nickel steel | --- |
| 750-1200 | Sodium | " | Over 500 hrs. at 1050°K |
| 1150-1600 | Lithium | Niobium-zirconium alloy | 4300 hrs. at 1350°K |
| 1450-1900 | Barium | Tantelum | 280 hrs. at 1850°K |
| 1600-2100 | Lead | " | 280 hrs. at 1850°K |
| 1750-2300 | Indium | Tungsten | 75 hrs. at 2150°K |
| 1850-2500 | Silver | " | 335 hrs. at 2150°K |

The heating is also necessary for removal of non-condensing gases from the system, since the presence of even small quantities of these gases creates considerable thermal resistance in the condensation zone, resulting in sharply decreased effectiveness of operation of the pipe.

On the basis of analysis of various methods of heating, we can conclude that the broadest possibilities for investigation of heat exchange during boiling of metals under conditions of free convection are provided by the method of electronic heating of the heating wall. The usage of refractory materials (molybdenum, niobium, tantalum and alloys based on these metals) in combination with electronic heating makes it possible to investigate heat transfer and critical heat flows in the boiling of metals at temperatures over 1,000°C.

In some cases, plasma heating and radiation heating with focused beams can be used for the creation of high heat flows, in addition to the methods we have mentioned. For example, in the latter case a system consisting of an electrical arc and mirrors placed in a vacuum chamber can be used.

## Temperature Measurement

Experimental investigation of heat transfer must include determination of the temperature of the heating surface. In experiments on heat transfer and boiling (and boiling of metals in particular), determination of the temperature of the heating surface requires particular care, since in this case the heat transfer coefficients have high values.

In experiments on heat transfer in boiling of non-metallic liquids in tubes heated by the passage of electric current, the temperature of the heating surface can be determined rather precisely from measurements of temperatures by thermocouples or a resistance thermometer located within the tube, considering the temperature drop in the surface.

When the heating methods analyzed above, suitable for investigation of heat exchange in boiling of metals, are used, the principal method of determining the temperature of the heating surface is measurement of the temperature with thermocouples placed in the wall. In determining the /41
temperature of the heating wall, serious attention must be given to such problems as:

1) correction for the temperature drop in the heating wall and distortion of the temperature field at the point of placement of the thermocouple; 2) changes in the temperature of the fluid and heating wall with time; 3) changes in the characteristics of the thermocouple during the process of operations. Let us analyze these problems in more detail.

### Correction for Temperature Drop in Heating Wall and Distortion of Temperature Field at Point of Installation of Thermocouple

With high heat flows, the temperature gradients in the heating surface (particularly in a wall with low heat conductivity) are great. The

temperature drops over a distance equal to the diameter of a thermocouple may be comparable to the temperature head between the wall and the liquid. For example, with a heat flow of $10^6$ kcal/m$^2$·hr in a wall of stainless steel, the temperature drop over 1mm is approximately 50°C, while $\Delta t_\alpha$ in the boiling of metals may be 20-30°C.

Distortions of the temperature field in the heat transmitting wall by a thermocouple well may lead to significant errors in the determination of the surface temperature [56, 57]. Figure 17 shows the qualitative distribution of temperature in a wall with an aperture and a rectangular slot for which the heat conductivity $\lambda_1$ is less than the heat conductivity of the wall material $\lambda_2$, which is usually the case in practice. The heat flow moves around the slot, as a result of which the temperature field in this region is distorted. For example, if the thermocouple junction is located at point K, the thermocouple will measure temperature $t_2$, not $t_1$, which corresponds to the temperature in this cross section away from the well. The error rising in this case depends on the amount of displacement of isotherm $t_2$ relative to isotherm $t_1$.

The distortion of the temperature field in the area of the thermocouple well for various well geometries and various well locations in the surface for the boundary conditions at the surface $t_w$ = const and $\alpha$ = const has been investigated analytically and using electric modeling in [56] under the condition $\lambda_1 = 0$ (see Figure 17). The calculation of the difference between temperatures $t_1$, $t_2$ and $t_3$ can be performed using the formulas

$$t_1 - t_2 = \frac{q_0 \varepsilon_T}{\lambda_2}, \tag{I.40}$$

$$t_1 - t_3 = \frac{q_0 \eta_T}{\lambda_2}. \tag{I.41}$$

The values of $\varepsilon_T$ and $\eta_T$ are presented in Tables in [56]. In particular, for /42
a circular well, sufficiently remote from the heat exchange surface, $\varepsilon_T$ is equal to its radius $r_T$.

V. N. Popov [57] produced an analytic solution for the temperature field in a semi-limited mass having an inclusion in the form of an infinitely long cylinder with arbitrary heat conductivity $\lambda_1$ (see Figure 17, a) with the boundary condition $t_w$ = const. Area 1 can be looked upon as the cross section of the cylindrical thermocouple junction or as the cross section of the cylindrical aperture for placement of the thermocouple, at one point of which the point junction of the thermocouple is located. The temperature is sought

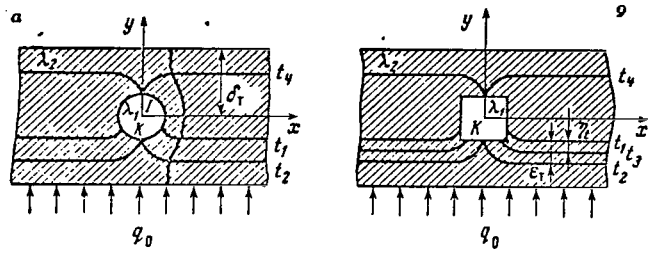


Figure 17. Distribution of Temperature in Plate With Circular Aperture (a) and Rectangular Well (b).
$\lambda_1$ and $\lambda_2$, Heat conductivity of well material and wall respectively; $t_2$ and $t_4$, Isotherms passing through center of lower (point K) and upper planes of well respectively; $t_1$, Isotherm corresponding to temperature in cross section of point K far from well; $\varepsilon_T$ and $\eta_T$, Displacement of isotherms $t_1$ and $t_3$ respectively relative to isotherm $t_1$; $\delta_T$, Distance from wall center to wall surface.

in dimensionless form

$$T_T = \frac{t - t_w}{\frac{\lambda_2}{q_0 r_T}} = T_T^* + T_T^{**}, \qquad (I.42)$$

where $T_T^*$ is the known solution of the La Place equation

$$\nabla^2 T_T = 0, \qquad (I.43)$$

and $T_T^{**}$ is the correction for temperature field distortion at this point.

For example, for $\delta_T/r_T > 5$, the value of $T_T^{**}$ at the center (x = 0; y = 0) can be calculated with good accuracy (1-2%) using the formula

$$T_T^{**} = \frac{r_T(\lambda_2 - \lambda_1)}{2\delta_T(\lambda_2 + \lambda_1)}. \qquad (I.44)$$

In measuring the temperature of the heat giving surface, it is expedient to select a thermocouple well design which can be easily analyzed from the point of view of measurement error. When the position of the thermocouple junction in the well is not known, which is frequently the case in practice, /43 the maximum uncertainty in temperature measurement may be $\Delta t = t_2 - t_4$, that

is quite great. The value of difference $t_2 - t_4$ can be reduced by decreasing the dimensions of the thermocouple and correspondingly the dimensions of thermocouple well and by increasing the heat conductivity of the surface material $\lambda_2$. At the present time, the dimensions of thermocouples in covers used in experiments on heat exchange in the boiling of metals are between 0.3 and 0.8 mm. It is difficult to anticipate any essential decrease in the dimensions of thermocouples designed for these purposes in the near future. More promising is the usage of materials with high heat conductivity in the area of placement of the thermocouples. With this purpose in mind, the authors have developed a special method of manufacture of working sectors, [58].

Figure 18 shows a diagram of an installation for manufacture of working sectors with a copper interlayer (plate) for the heater design used by the authors. Melting of the copper occurs in a stainless steel tube evacuated by a diffusion pump, which is heated on the outside by a silit heater. At the bottom, at the end of the pipe, there is a slit chamber, through which air can be pumped by a compressor. A pipe is welded to the copper-filled plate to draw away the shrinkage cavity. A molybdenum crucible filled with copper is fastened above the pipe. The temperature of the plate during the process of manufacture is checked by thermocouples in capillaries. Usually, capillaries 0.8 × 0.15 mm made of stainless steel or VN-2 alloy are used. The indications of the thermocouples are recorded on type EPP-09 recording potentiometers. The beginning of melting of the copper is precisely indicated by the thermocouples. A few minutes after the beginning of melting, air cooling is turned on, in order to assure directed crystallization of the copper in the plate.

After the plate is filled, it is worked on a lathe. With copper filling, the heat transmitting surface may be any one of several metals. It is convenient to use a foil sheet of the metal, with the remaining portion of the floor made of stainless steel.

Metallographic investigations have indicated that good diffusion bonding occurs between the copper and the material of the heat transmitting surface, while the area of interpenetration of the metals into each other (for which the value of heat conductivity is not known) does not exceed some hundredths of a millimeter. Therefore, the thermal contact between the copper and steel can be considered ideal with a good degree of accuracy. Figure 19 shows a micro-section of the junction of copper with stainless steel produced during pouring.

In the sectors filled with copper the area in determining the temperature difference is considerably less than in the remaining sectors due to the lower temperature gradients in the copper. With identical heat flows and dimensions of thermocouple wells, the temperature difference $t_2 - t_4$ (see Figure 17) for copper will be 15-20 times less than for stainless steel. Furthermore, when filling is used the temperature difference can be reduced

/45

by decreasing the dimensions of the well (radius $r_T$) in comparison with a well made mechanically. For example, the temperature electrodes in the temperature measurement zone can be covered with copper without a protective cap, with the electrodes covered only by alundum. With high heat flows (about $10^6$ kcal/m$^2$·hr), the copper-covered sectors can operate at approximately the same temperatures of heat transfer medium metal as the steel sectors.

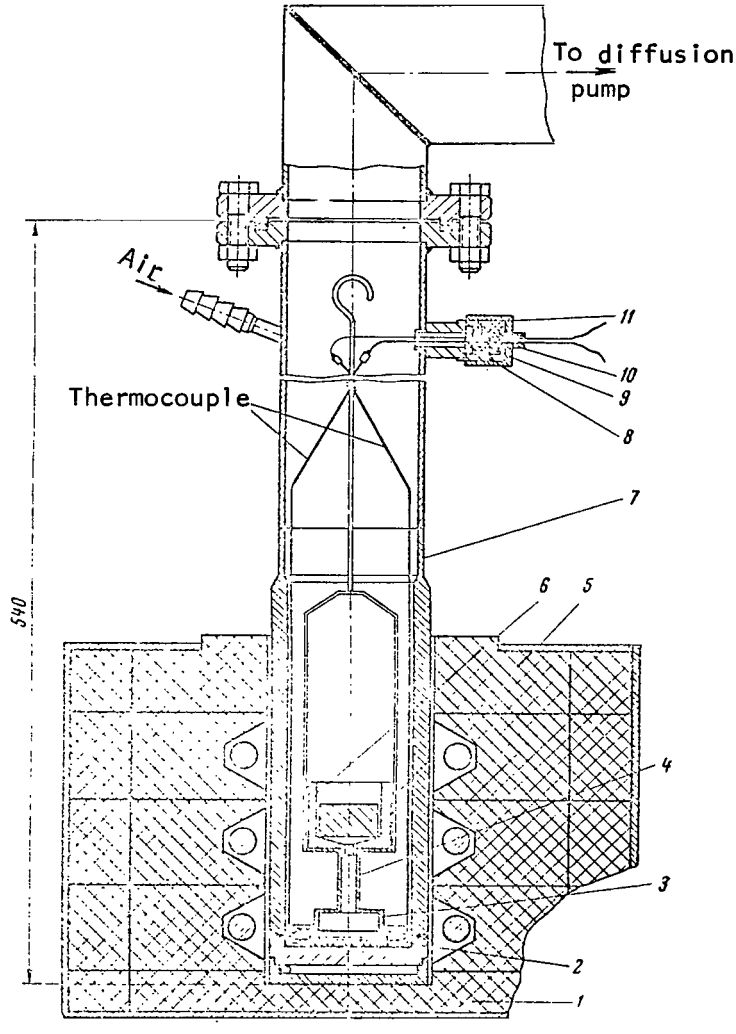


Figure 18. Diagram of Installation for Copper Filling of Working Sectors. 1, Electric furnace; 2, Molybdenum sublayer; 3, Plate; 4, Casting pipe; 5, Copper piece; 6, Molybdenum crucible; 7, Body; 8, Inset; 9, Siloxane resin and Teflon seal; 10, Bushing; 11, Tension screw.

Thus, working sectors with varying geometry can be manufactured.

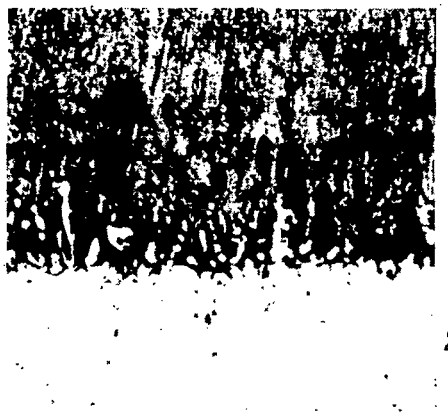


Figure 19. Micro-section of Interface Between Copper (1) and 1Kh18N9T Steel (2) Produced by Pouring Copper. (Magnified 200 Times).

## Change of Temperature of Liquid and Heating Wall with Time

In certain works, in order to determine the temperature head between wall and liquid, the temperature of the wall and the temperature of the liquid are measured individually. In other words, the temperature difference between wall and liquid is measured directly. Measurement of the temperature difference, in our opinion, is preferable, since experience has shown that during the boiling process certain changes in the liquid temperature are possible, so that in order to determine the temperature head on the basis of wall and liquid temperatures measured separately, precise synchronization of measurements is required. The metal temperature in volume may change due to insufficiently balanced heat input and output in the installation. This is particularly true with unstable boiling and alternation between heat removal by convection and heat removal by boiling.

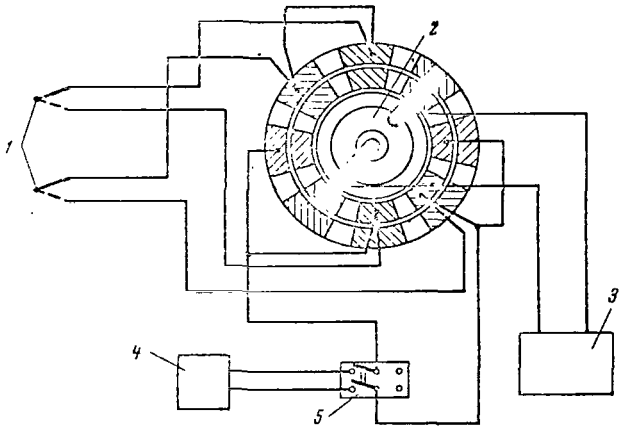


Figure 20. Diagram of Measurement of Temperatures. 1, Thermocouples; 2, Switch; 3, Semi-automatic potentiometer, P 2/1; 4, Automatic EPP-09 potentiometer; 5, Breaker switch.

As experiments have shown [14, 15, 17, 19], when metals boil, significant pulsations of the temperature of the heating wall may occur. In this case, both the nature of the change of the wall temperature and the average temperature heads can be determined by recording only the indications of the thermocouples. Figure 20 shows a diagram for measurement of temperatures used by the authors which allows an automatic potentiometer and periodic measurements with a portable potentiometer to be used for measurements both of the wall-liquid temperature difference and of the absolute temperatures in wall and liquid. /46

The temperatures were recorded using a multi-range (scales 0-0.5, 0-1, 0-2, 0-5, 0-10 and 0-20 mV) potentiometer, remade from a

standard single scale potentiometer type EPP-09, with a pen full scale travel time of 1 sec for all scales. Investigation of the frequency characteristics of the EPP-09 one second potentiometer were performed at the Physics and Energy Institute by M. Kh. Ibragimov, who showed that the device cannot record frequencies over 30 Hz. However, at frequencies of 10-30 Hz, the amplitude is essentially decreased. At frequencies of 2-3 Hz, the EPP-09 can record oscillations with amplitudes not over 10-20% of the maximum scale limit without distortion. Figure 21 shows the frequency characteristic of the EPP-09 potentiometer with full scale pen travel time 1 sec. Thus, in order to record large scale pulsations of temperature during boiling of metals, the EPP-09 multi-range 1 second potentiometer can be used, since the frequency of these pulsations does not exceed a few Hz. When temperature pulsations at frequencies over 10 Hz must be recorded, an oscillograph should be used.

/47

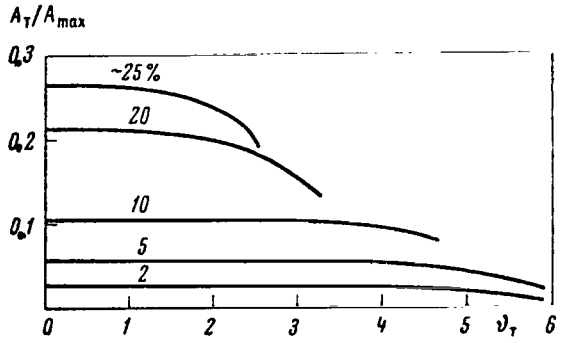


Figure 21. Frequency Characteristic Of EPP-09 Potentiometer With Full Scale Pen Travel Time of 1 sec. $\nu_T$, Frequency; $A_T$, Oscillation amplitude; $A_{max}$, Upper limit of scale of device.

## Change in Characteristics of Thermocouple During Process of Operation

The correct measurement of temperatures may be essentially influenced by a change in thermal e.m.f. during the operating process, by heterogeneity of the material of thermal electrodes, and by the resistance of the insulation [59].

A change in thermal e.m.f. may be caused by aging of thermal electrodes, diffusion of foreign materials, restructuring of the crystalline lattice under the influence of temperature, etc. Changes in the thermoelectric properties of most thermal electrode materials are strongly influenced by diffusion of such metals as iron and copper, for example.

All materials, including those of thermal electrodes, are characterized by a certain degree of heterogeneity. As the diameter of the thermal electrodes decreases, the heterogeneity and its influence may increase. The influence of heterogeneity of the thermal electrode material on indications of thermocouples appears when there is a temperature gradient. In individual sectors of installations, particularly high temperature sectors, significant temperature gradients are possible. If it is impossible to avoid areas with high temperature gradients in placing thermocouples, measures should be taken to decrease the gradients at the point of installation of the thermocouples. The manufacture of thermal electrodes should be performed using sections of

wire with minimal heterogeneities. The degree of homogeneity of thermal electrode wire can be easily tested by heating the wire in individual sections in the flame of an alcohol burner and measuring the air e.m.f. produced. Local heterogeneity of the thermal electrode wire can be decreased by annealing. For example, annealing of chromel and alumel for this purpose /48 is recommended at 800°C for one hour by [59].

At high temperatures, the resistance of insulation may be noticeably decreased. The voltage at the terminals of a thermocouple $U_k$, considering resistance of insulation $R_{ins}$, can be determined using the following formula [59]

$$U_k = \frac{U_T}{1 + \frac{R_T}{R_{ins}}}, \qquad (I.45)$$

where $U_T$ is the e.m.f. of the thermocouple; $R_T$ is the resistance of the thermocouple. In measuring high temperatures by thermocouples, in order to avoid errors, attention should be turned to these effects.

In measuring the wall-liquid temperature difference, it is necessary to know the differences in graduation curves of thermocouples at the moment of measurement (for example, on Figure 22 at temperature $t_1$, the difference in graduation $\Delta E_0$) in order to determine the temperature difference between the heat transmitting surface and the liquid ($\Delta t$) from the measured difference in e.m.f. $\Delta E_1$.

In order to determine $\Delta t$ from $\Delta E = \Delta E_1 - \Delta E_0$, a standard calibration can be used for the type of thermocouple in question. This will not result in great error, since the tangent of the angle of inclination of individual curves (considering their sectors linear) is near the tangent of the angle of /49 inclination of the standard calibration curve. As experience has shown, for example for a chromel-alumel thermocouple, widely used in experimental practice, the calibration curves usually do not differ from the standard curves by more than 10-15°C even at temperatures of 800-900°C. Therefore, the error in determination of $\Delta t$ resulting from usage of a standard calibration curve will not exceed 1-1.5%. At the same time, failure to consider differences in calibration curves of thermocouples ($\Delta t$) may lead to essential errors (about $\Delta t_0/\Delta t \cdot 100\%$) in the determination of $\Delta t$. For example, if the temperature difference $\Delta t$ measured is 30°C, and the difference in calibration curves of the thermocouple $\Delta t_0$ is 15°C, if the difference in calibration is not considered the error in determination of $\Delta t$ will be 50%. In the measurement of smaller temperature differences, the error will be even greater.

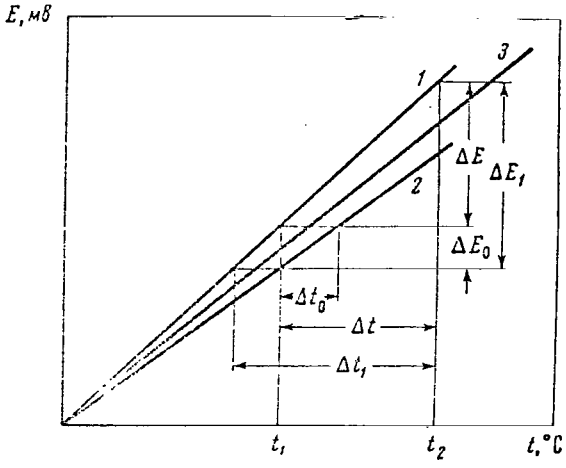


Figure 22. Thermal e.m.f. of Thermocouples As A Function of Temperature. 1, For thermocouple measuring surface temperature; 2, For thermocouple measuring liquid temperature; 3, Standard calibration line.

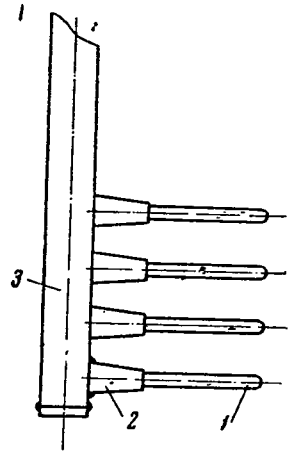


Figure 23. Thermocouple Grid For Measurement of Temperature Distribution by Height. 1, Capillary containing thermocouple; 2, Connecting piece; 3, Tube.

In connection with the fact that the characteristics of thermocouples may change with time, it is desirable in experiments to determine the divergence in calibration of thermocouples ($\Delta E_0$) periodically, then use these figures to determine the temperature difference between wall and liquid. The value of $\Delta E_0$ can be precisely determined if we know the temperature field between thermocouples measuring the liquid temperature and wall temperature with no heat transfer over the working sector.

A thermocouple grid (Figure 23) and a moving thermocouple may be used to measure the temperature field in the volume of the metal. The measurement of temperature fields by a moving thermocouple provides the most accurate results, since in this case the relative change in temperature is determined by the same thermocouple. Figure 24 shows a moving thermocouple used by the authors for measurement of temperature fields in areas on heat exchange during boiling of sodium, potassium and cesium.

The thermocouple is placed in a tube, the end of which is welded to a tip with a stainless steel capillary 0.8-1 mm in diameter. A chromel-alumel thermocouple (thermal electrode diameter 0.2 mm) is placed in the capillary in an Alundum insulator. The capillary is bent at a right angle to the tube. Displacement of the tube in the vertical direction is achieved by a reversable electric motor. As the tube is displaced the capillary and thermocouple can be brought in close contact with the heating surface. Vertical displacement of the thermocouple (by approximately 300 mm) without /50

disrupting the seal of the insulation is assured by the extension (contraction) of bellows made of stainless steel. The position of the thermocouple with vertical displacement is determined by selsyns with an accuracy of ± 0.1 mm.

Microthermocouples

Problems of the design and technology of manufacture of microthermocouples were analyzed in [59-61]. Here we will touch upon these problems only as concerns microthermocouples for the measurement of high temperatures, since they are used for the measurement of temperatures of the heating surface, the temperature fields in the liquid and in the vapor in experiments with boiling metals.

Usually, microthermocouples are made in a protective cover. In one section there may be one (Figure 25, a) or two (Figure 25, b) thermal electrodes. Thermocouples with one electrode per section are convenient to use for measurement of temperatures of the heat transmitting wall, since with identical diameters of thermal electrodes, their dimensions will be less than those of thermocouples with two electrodes per section. The hot junction of a thermocouple may be non-insulated (Figure 25, d) or insulated (Figure 25, e) from the protective cover. The thermocouples with insulated hot junctions are used for measurement of temperature differences. If the thermocouples, for example in installation into experimental apparatus, must be bent with a small radius (on the order of the diameter of the cover), the envelope of the thermocouple should be tightly pressed against the electrodes in the insulation. In order to do this, the thermocouples containing two electrodes per section should be passed through shaped rollers (Figure 25, c), while thermocouples such as those shown on Figure 25, a are passed through draw plates. Drawn and rolled thermocouples should be annealed [59].

Attention should be turned to the point where the thermal electrode leaves the protective cover, since at this point the insulation can be most easily broken and short circuits occur. When one thermal electrode is brought out, the design shown on Figure 26, a can be used. A bushing turned from an insulating material (for example textolite) is tightly placed over the end of the capillary, and a vinyl chloride tube of the required length is placed over the bushing.

The structure shown on Figure 26, b can be recommended for bringing out two thermal electrodes from one end of the protective cover.

When a thermocouple must be brought out of an installation without disrupting hermetic sealing, the protective cover should be soldered into the wall of the installation (Figure 26, c) or the thermocouple lead should be brought out through a wall insulator (Figure 26, d).

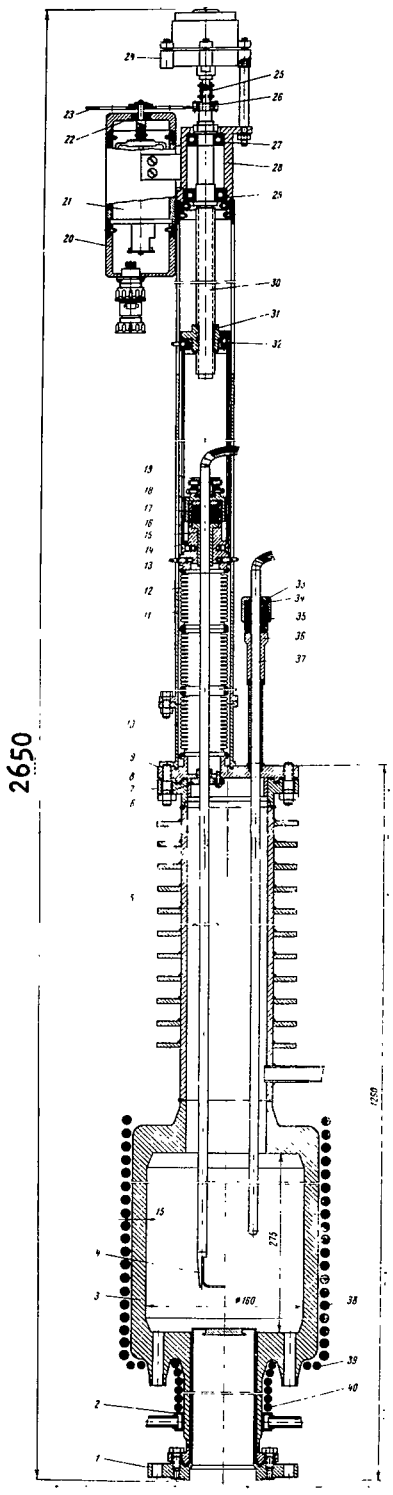


Figure 24. Boiling Tank With Movable Thermocouple Developed By The Authors.
1 - Cup with floor;
2 - Cooling strip;
3 - Working tank;
4 - Moving thermocouple;
5 - Condenser;
6, 32 - Guide bushings;
7, 9 - Flanges;
8 - Insert;
10, 15, 25, 34 - Bushings;
11 - Guide tube;
12 - Bellows;
13 - Guide screw;
14, 36 - Nipples;
16 - Connecting tube;
17, 35 - Seals;
18, 31, 33 - Nuts;
19 - Limb;
20 - Selsyn cover:
21 - Selsyn:
22, 27, 29 - Bearings;
23, 26 - Gears;
24 - Motor;
28 - Body;
30 - Screw;
37 - Thermocouple tube;
38, 39, 40 - Heaters.

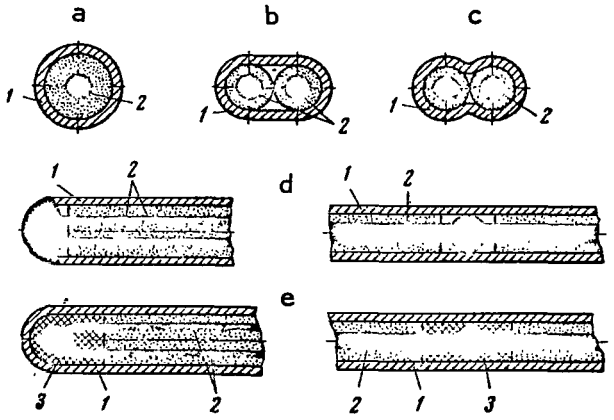


Figure 25. Design of Microthermocouples In Protective Covers. a, Microthermocouple with one thermal electrode in section; b, c, Microthermocouples with two thermal electrodes in cross section; d, Microthermocouple with non-insulated junction; e, Microthermocouples with insulated junction; 1, Capillary; 2, Thermal electrodes in insulation; 3, Insulation ($Al_2O_3$ or MgO).

/52

High temperatures are usually measured using chromel-alumel (up to 900°C), platinum-platinorodium (up to 1,300°C) or tungsten - tungsten-rhenium (up to 2,300°C) thermocouples. The thermal electrodes made of tungsten and the alloy of tungsten with rhenium can operate under vacuum or in an inert gas medium. Microthermocouples are made of wire with diameters from tenths to hundredths of a millimeter. The most common are wires with diameters of 0.08, 0.1, 0.2 and 0.3 mm. The finer the thermal electrode, the less durable the thermocouple, particularly if it operates in an oxidizing medium, for example in air. Therefore, in selecting the diameter of the thermal electrode wire for high temperature thermocouples, one should not strive for extremely fine in diameters. In microthermocouples, the insulation on the thermal electrodes is generally applied in the form of film coverings. In some cases, fine tubes of quartz, porcelain, various ceramics or glass fiber may be used as insulators. Treating of glass fiber insulators with organosilicate material eliminates hygroscopicity and improves the insulating properties.

For high temperature thermocouples, coatings of Alundum, organosilicate materials and combined coatings of Alundum and organosilicate material are used. Depending on the design and operating conditions of the thermocouple, the thickness of the film coating may vary from a few tenths to a few hundredths of a micron. Coatings of organosilicate materials are more elastic and have higher electrical resistance than Alundum. They protect the material of the thermal electrodes from oxidation at temperatures up to 1,000°C [62]. Combined coatings of Alundum and organosilicate materials are similar in mechanical properties to coatings of organosilicate material alone, but have better electrical insulation properties.

Capillaries of stainless steel and alloys based on niobium are used as protective covers for high temperature microthermocouples. The most common dimensions of capillaries of stainless steel are 0.3 × 0.05; 0.5 × 0.1; 0.6 × 0.15; 0.8 × 0.15; and 1.0 × 0.2 mm. In an oxidizing medium, they operate satisfactorily up to 800°C, and in an inert medium or vacuum - up to 1,000°C. Stainless steel covers made of 1Kh18N9T steel can be welded easily

to all thermal electrodes made of chrome-nickel alloys. At temperatures over 1,000°C, capillaries of niobium alloys or other heat resistant material should be used for the manufacture of protective covers.

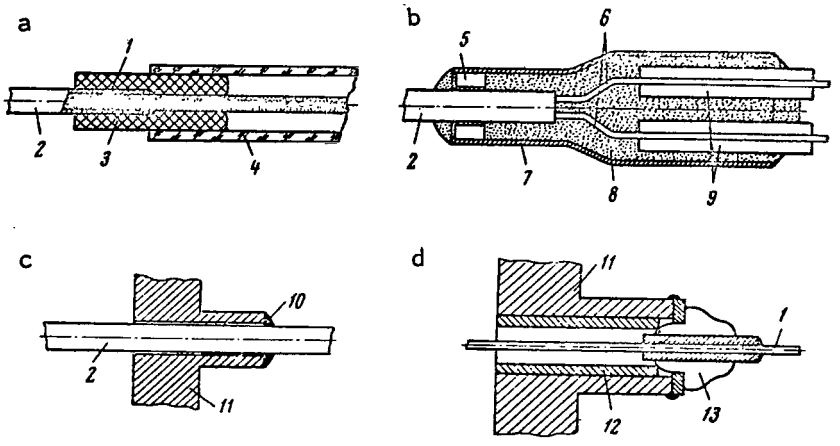


Figure 26. Design of Thermocouple Leads.
a, Lead of thermocouple with single electrode in cross section; b, Lead of thermocouple with two thermal electrodes in cross section; c, Hermetic lead for thermocouple in cover; d, Hermetic lead for microthermocouple without cover; 1, Thermal electrode; 2, Capillary; 3, Insulator (textolite); 4, Vinyl chloride tube; 5, Porcelain lead; 6, Thermal electrode in insulation; 7, Protective cover; 8, Poured insulation ($Al_2O_3$ or MgO); 9, Porcelain stem; 10, Solder (silver or tin); 11, Chamber wall; 12, Porcelain tube; 13, Wall insulator.

The technology of manufacture of microthermocouples is described in [59].

In this section we have analyzed but a few of the specific aspects of the measurement of temperature in experiments on heat exchange in the boiling of metals, and have not touched upon general problems of measurement of temperature, which are discussed, for example, in [63, 64].

## Experimental Installations /53

Figure 27 shows the diagram of an installation used by the authors for the performance of experiments on heat exchange in the boiling of sodium. The installation consists of a working tank, the upper portion of which contains a condenser and moving thermocouple, while the lower portion contains an electron tube. Heating of the working tank is by silit furnace, the power of which is adjusted by an autotransformer. The condenser is air cooled,

with forced air. The air flow rate is adjusted by two valves in the air line, one of which is electrically driven.

At high temperature levels, as occurs in experiments on heat exchange during boiling of metals, cooling of the condenser with a gas (air) is more convenient than cooling with ordinary drop liquids (water). With gas cooling problems of adjustment of the heat flow rate are easier to solve. Cooling with a gas is preferable also from the point of view of safety. Transfer of heat away from a condenser (particularly high power types) can also be performed using a special liquid metal heat transfer agent loop or a heat pipe.

The level of sodium in the working tank is determined by a contact level meter connected with the working tank according to the principle of connecting vessels. In the process of operation, the pipes connecting the level meter and working tank are covered with valves.

A (cold) oxide trap is provided to remove oxides from the sodium [65, 66]. In the purification process, the sodium is pumped through the trap by an electromagnetic pump. The content of oxides in the sodium is tested using a sample collecting distilling device [67].

The principle of operation of the cold trap is based on the decrease in solubility of oxides of sodium in sodium with decreasing temperature. The minimum sodium temperature in the cold trap varies between 120 and 150°C, corresponding to an oxygen concentration in the sodium of (0.5-1) $\cdot 10^{-3}$ weight % [67]. The design of the cold trap is shown on Figure 28. Deeper cleansing of oxygen from sodium can be achieved using hot traps [68]. Purification of sodium to remove oxides in hot traps occurs due to the reduction of the oxides of sodium by certain materials (getters). For example, in hot traps for purification of sodium the getter might be zirconium or its alloy with titanium.

Determination of the content of oxygen in sodium by vacuum distillation is based on the significant difference in the vapor pressure of sodium and its oxides. The content of oxygen in the sodium is determined from the quantity of oxides remaining after evaporation of a known quantity of sodium. /56
The quantity of oxides is studied by titration. The greater the charge of sodium taken and the less the contamination in the process of sampling and preparation for analysis, the higher the accuracy of the results. The distillation method can be used to determine concentrations of oxygen in sodium between $1 \cdot 10^{-4}$ and $5 \cdot 10^{-2}$ weight % [67]. The design of a sampler-distiller is shown on Figure 29. The sampler-distiller may have one or several cups for sampling. The duration of one analysis is approximately 8 hours when a device with one cup is used, or 2-3 hours when a device with four cups is used.

/54

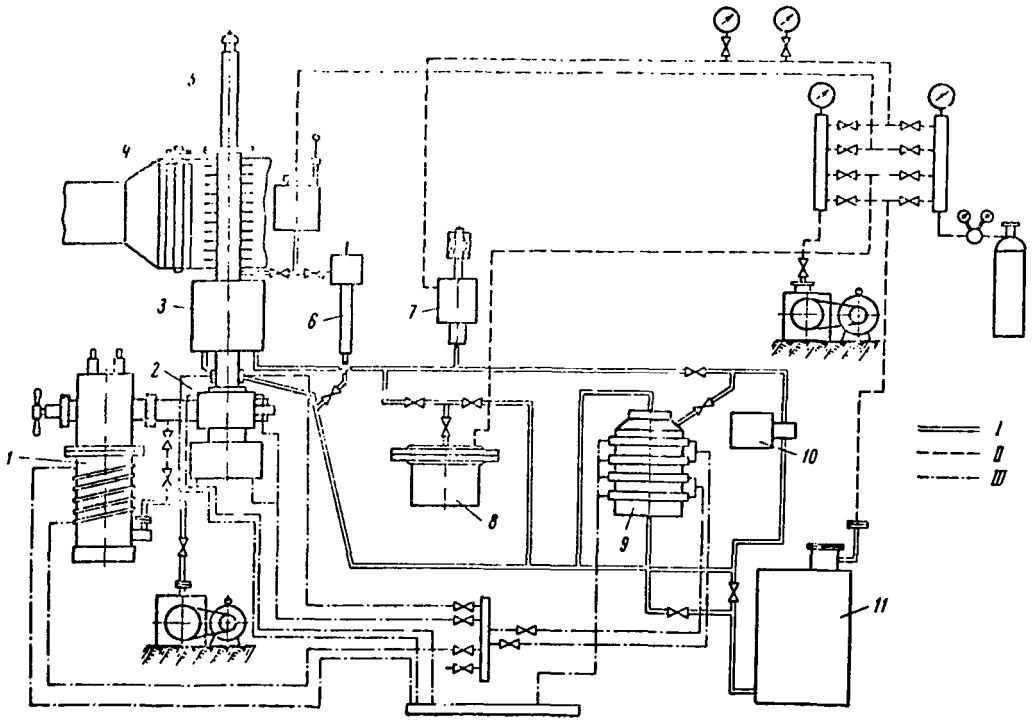


Figure 27. Diagram of Installation For Investigation of Heat Exchange in the Boiling of Alkali Metals.
1, Diffusion pump; 2, Electron tube; 3, Working tank; 4, Valve for smooth regulation of air flow rate; 5, Moving thermocouple; 6, Level measuring tank; 7, Pressure transducer; 8, Sampler-distiller; 9, Oxide cold trap; 10, Electromagnetic pump; 11, Loading tank; I, Main loop; II, Gas-vacuum lines; III, Water lines

The content of oxygen in sodium can be determined using a sample oxygen indicator [69]. This device is less sensitive (to about $10^{-3}$ % oxygen by weight) than the sampler-distiller, however can be used to rapidly (in about 30 minutes) determine the oxygen content at a distance. The principle of operation of the sample oxide indicator is based on the capability of impurities precipitating from a solution to obstruct a cross section. The apparatus includes a special device with a small cross section, a heat exchanger for cooling of the heat transfer medium, an adjusting valve for establishment of the necessary flow rate through the instrument, a flow rate meter and a thermocouple for determination of the temperature of the heat transfer medium. The design of the sample indicator is shown on Figure 30.

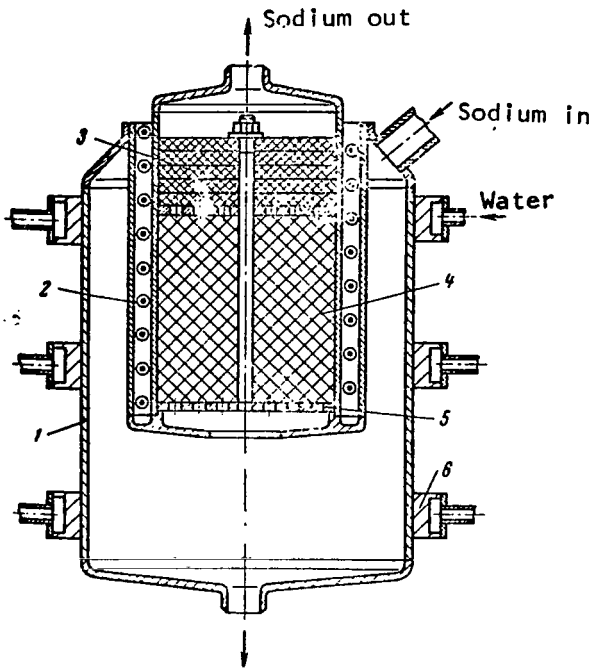


Figure 28. Oxide Cold Trap [66]. 1, Body; 2, Heater; 3, Screen; 4, Chip filler; 5, Grid; 6, Cooling belt.

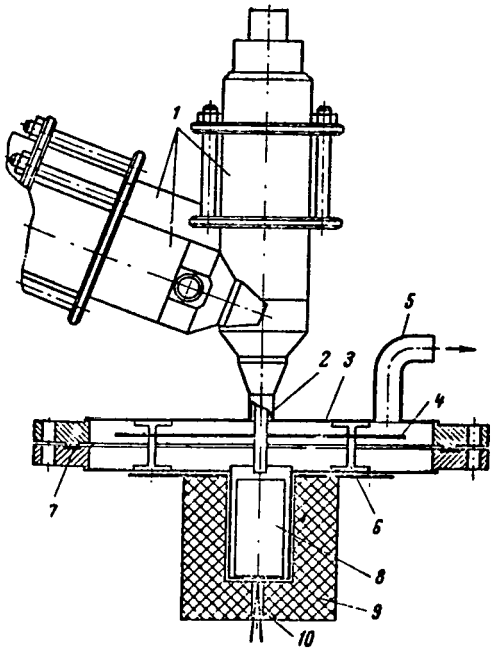


Figure 29. Sampler-Distiller [67]. 1, Valves; 2, Drain tube; 3, Vacuum chamber body; 4, Vapor stop; 5, Vacuum pump line; 6, Strap supports; 7, Insert; 8, Sample cup; 9, Furnace; 10, Thermocouple.

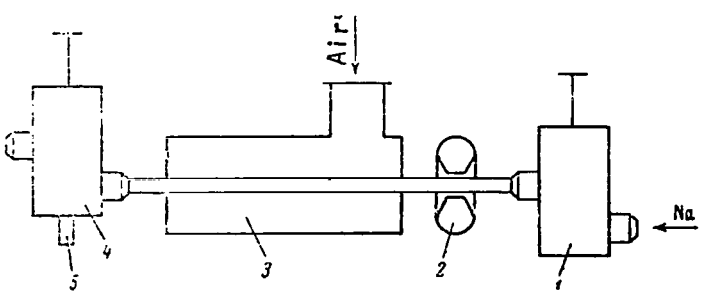


Figure 30. Sample Oxide Indicator [69]. 1, Adjusting valve; 2, Flow rate meter; 3, Heat exchanger; 4, Valve (main) with calibrated cross section; 5, Thermocouple well.

The methods and instruments used for purification and testing of the content of impurities in such alkali metals as potassium and cesium have been developed at the present time to a considerably lesser extent than for sodium.

In order to determine the sodium pressure in an installation, a compensation type pressure transducer has been developed (Figure 31). The sodium pressure within the bellows is balanced by gas pressure. The gas pressure is measured with ordinary instruments. Equality of the pressures can be determined by the position of the bellows, which in turn is determined by an induction method. The sensitivity of this pressure transducer depends on the rigidity of the bellows and the sensitivity of the device determining the position of the bellows. The sensitivity of this transducer is approximately ± 0.5 mm Hg. /57

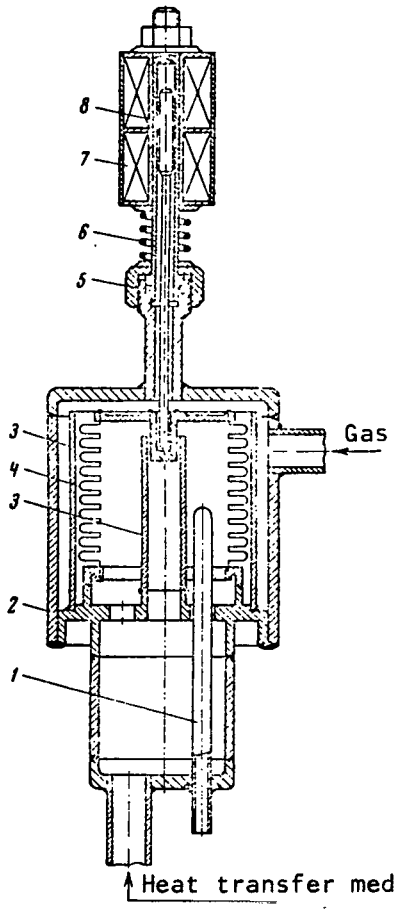


Figure 31. Compensation Type Pressure Transducer. 1, Thermocouple sleeve; 2, Body; 3, Guide; 4, Bellows; 5, Rubber insert; 6, Spring; 7, Induction coil; 8, Plunger.

The accuracy of determination of pressure by the compensation method depends on the sensitivity of the pressure transducer and the class of the manometer used for measurement of the gas pressure.

All units in the installation which are in contact with sodium must be made of 1Kh18N9T stainless steel.

Filling of the working tank with sodium and drainage of sodium, as well as evacuation of gas from the working tank, are performed by a gas vacuum system with the required valves and devices for pressure measurement.

Evacuation of the tube is performed by a type N-5s diffusion pump in combination with a VN-2 prevacuum pump [70]. All valves used on the stand (on gas, vacuum and metal lines) are bellows type.

Figure 32 shows a diagram of an installation used by the authors in experiments on heat exchange in the boiling of sodium, potassium and cesium. Using this device, observations were performed of the process of boiling using x-rays. The tube, together with the

working tank and diffusion pump, was fastened on a plate which can be moved in the vertical direction by an electric motor. The x-rays generated by the tube passed through the working tank and strike the screen of an electronic- /58
optical converter (E.O.C.). Displacement of the installation allows various sectors through the height of the working tank to be irradiated, the E.O.C. screen showing a sector only approximately 70 mm in diameter. The working tank is filled with the heat transfer medium directly from a still, which is then disconnected. The design of the tube and moving thermocouple used in this installation is similar to designs described above.

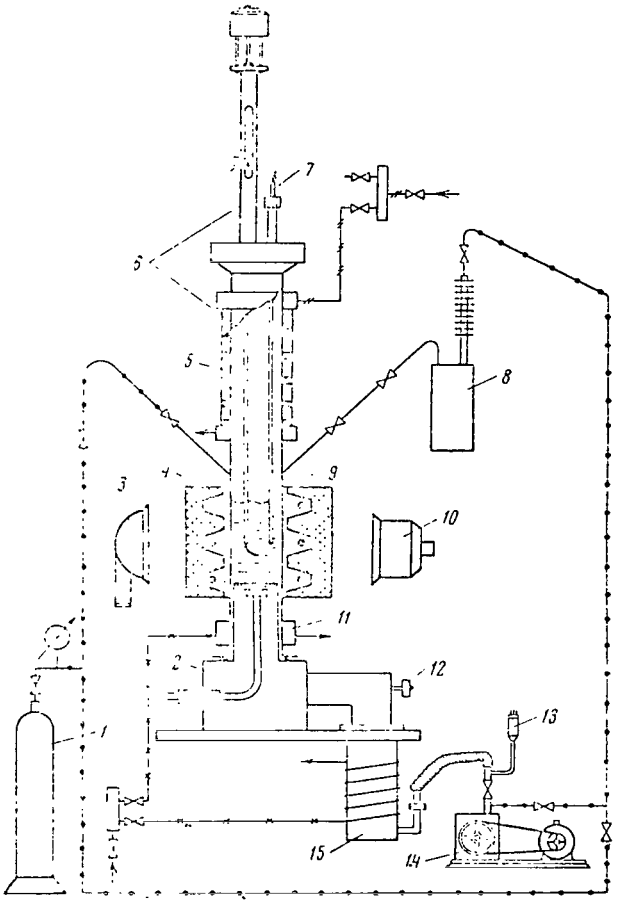


Figure 32. Diagram of Installation for Investigation of Heat Exchange During Boiling of Metals Using X-Rays. 1, Gas tank; 2, Electron tube; 3, X-ray tube; 4, Furnace of working tank; 5, Vapor condenser; 6, Moving thermocouple; 7, Non-moving thermocouple; 8, Evaporation tank; 9, Working tank; 10, Electronic-optical converter (E.O.C.); 11, Cooling belt; 12, 13, Pressure transducers; 14, Prevacuum pump; 15, Diffusion pump.

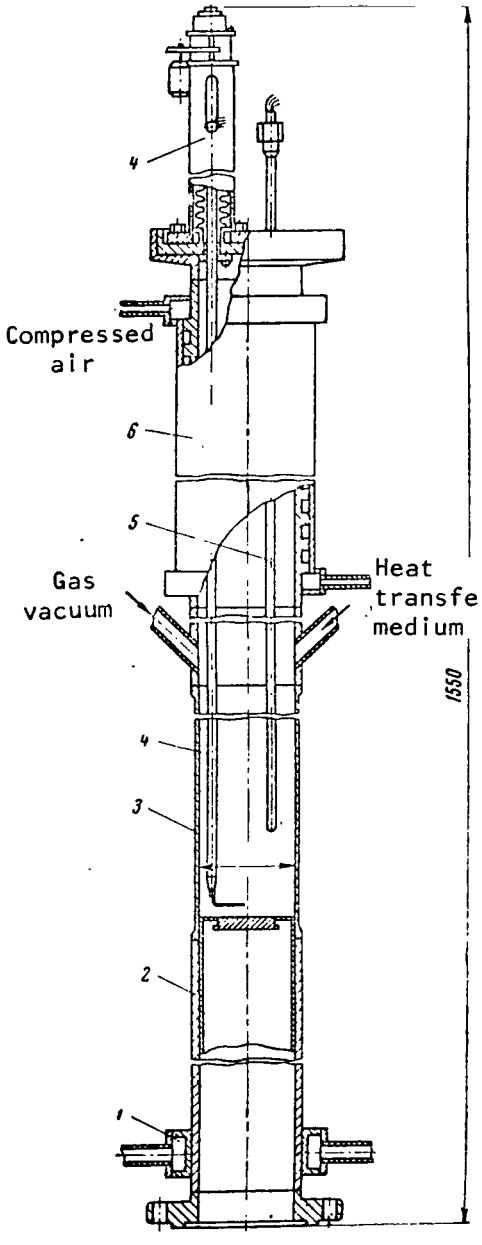


Figure 33 shows the design of the working tank with condenser. The working tank is a thin wall tube (wall thickness 1 mm). The thin wall is required to produce a better image of the boiling. A vapor condenser is fastened above the tank, cooled by compressed air moving through a spiral line. The working tank is surrounded by a furnace with silit heating elements. Type "ultra lightweight" brick is used as the heat insulator, since it has low density and attenuates the x-rays only slightly. /59

As the x-rays pass through the medium, they are attenuated by absorption and scattering [71]. The intensity of the beam of homogeneous x-rays passing through a sector of the medium of thickness $\Delta$ can be calculated from the formula /60

$$I_p = I_{p0} e^{\xi \Delta}, \qquad \text{(I.46)}$$

where $I_{p0}$ is the intensity of the incident ray; $I_p$ is the intensity of the rays passing through the sector of medium of thickness $\Delta$; $\xi$ is the linear attenuation coefficient.

The attenuation coefficient can be related to a unit mass of the material. In this case, it is called the mass attenuation coefficient $\xi_M$. The mass attenuation coefficient depends on the wave length of the x-rays and the atomic number of the material through which the x-rays pass.

Figure 33. Working Tank and Condenser of Installation for Investigation of Heat Exchange by X-Rays During Boiling of Metals. 1, Cooling belt; 2, Cup with floor; 3, Working tank; 4, Moving thermocouple; 5, Non-moving thermocouple; 6, Vapor condenser.

Bremsstrahlung has a continuous spectrum of wave lengths. The spectrum has a sharp boundary on the short end. The minimum wave length of Bremsstrahlung $\lambda_{pmin}$ depends on the voltage accelerating the electrons in the x-ray tube. The value of $\lambda_{p\ min}$ can be determined from the formula

$$\lambda_{p\ min} = \frac{12.35}{U_a}. \qquad (I.47)$$

In formula (I.47), the wave length $\lambda_{p\ min}$ is expressed in angstroms, the anode voltage of the x-ray tube $U_a$ in kilovolts.

The ratio of attenuation of x-rays passing through a liquid and through a vapor for an identical distance will be proportional to the ratio of mass attenuation coefficients for the liquid and vapor, which is equal to $\gamma/\gamma''$.

The quality of the image of the boiling will depend on the following main factors.

1. On changes in the degree of attenuation of the x-rays passing through the medium resulting from the vapor phase. In this case, attenuation occurs in the heat insulation, walls of the tank, liquid and vapor. The less the attenuation of the x-rays by the heat insulation and walls of the tank, the clearer the image will be. Therefore, one should strive for minimum wall thickness of the tank, minimum insulation layer thickness, and the materials for tank and insulation should be selected (from among those materials satisfying the other requirements of the experiment) with minimum value of $\xi$. It is desirable that the thickness of the layer of liquid through which the x-rays pass be comparable to the dimensions of the vapor volumes arising in it.

2. On the hardness of the x-rays. The degree of contrast of an image depends on the ratio of intensities of x-rays in various sectors of the E.O.C. or photographic film. The ratio of intensities of x-rays $I^*_p$ passing through the layer of liquid containing vapor space with a dimension in the direction of movement of the rays of $\Delta^*$, to the intensity of x-rays $I^*_p$ passing through the same layer of liquid but without the vapor space can be approximately expressed as: /61

$$\frac{I^*_p}{I_p} = e^{\xi\Delta^*}. \qquad (I.48)$$

The greater the ratio $I^*_p/I_p$, the more contrast the image will have. The value of $e^{\Delta\xi^*}$ for a given liquid and a given value of $\Delta^*$ depends only (where $\gamma/\gamma'' >> 1$) on the wave length of the x-rays, since $\xi_m \sim \lambda^3_p Z^3$ [71], where Z is the atomic number of the material. Consequently, the softer the x-rays,

the more contrast the image will have. At the same time, the radiation intensity, which is proportional to the anode current and the square of the anode voltage in the x-ray tube, should be sufficient for the production of a good quality image. It is therefore desirable that the anode voltage in the tube be minimal (for considerations of contrast), and that the anode current be maximal. We should also recall that the intensity of x-rays decreases in inverse proportion to the square of the distance from the anode of the tube.

3. On the equipment use. The resolving capacity of the electronic-optical converter should be maximal, and the focus of the x-ray tube should have the minimum dimensions. For example, in our experiments we used an x-ray tube with a focus of 5 mm and a current of 5 ma. The voltage on the tube is continuously adjustable (to 150 kv).

The installations which we have analyzed, with the proper design of individual units and selection of materials, can be used for investigation of heat exchange in the boiling of various metals.

## Preparation of Installations, Performance of Experiments and Initial Processing of Experimental Data

### Safety Techniques

Rooms in which installations containing alkali metals are located, in addition to the usual norms for sanitation and electrical safety, must satisfy certain special requirements. Let us discuss these requirements briefly.

Installations containing alkali metals should be placed in separate rooms - so-called boxes. The heating lines, batteries and water lines in this room should be welded, without fittings. Fittings can be placed in a neighboring room. Air lines, in order to avoid condensation of moisture from the air on them, should be heat insulated. The room should have both intake and exhaust ventilation. The electrical lines, both power and light lines, should be placed in gas pipes or flexible metal hoses. /62

The storage of liquids containing halide substituted hydrocarbons in the room or the washing of alkali metals with these hydrocarbons is categorically forbidden, since powerful explosions may occur. The floor should be metal or tile. Metal bases should be placed beneath the entire installation and all its parts, in case of accidental spillage of the alkali metal.

Rooms in which work is performed with alkali metals should have the following fire extinguishing equipment: dry sand or soda in metal boxes, 1 kg sand per 1 square meter of floor area; asbestos blankets, shovels and scoops. The fire fighting equipment should be located in free, accessible areas.

When working with melted alkali metals, laboratory workers should wear suits made of chrome leather or canvas, caps of chrome leather and gloves

of canvas or chrome leather, safety glasses or protective masks. The clothing should be strong, dry and clean, should be easy to fasten and remove. In case of an accident or fire in the alkali metal, servicing personnel should be provided with gas masks or respirators to protect the respiratory tract.

Work in wet or oily clothing is forbidden.

If the alkali metal leaks from the installation, it will ignite spontaneously. The center or zone of the fire will depend on the quantity of metal spilled. Hot alkali metal with a small burning area can be limited by a sand (or soda) barrier (in case the metal spills on the floor) then covered by pouring sand or soda. In case the metal spills and ignites over a large area, the fire can be put out with an inert gas by spraying it through a flexible hose on to the hot metal. However, this method of fire extinguishing requires that the room be well sealed and requires great amounts of the inert gas. In case of spillage of a small quantity of alkali metal, if the fire center does not threaten the equipment, room, etc., it is best to simply let it burn, taking no measures to put it out. In case of fire, the intake and exhaust ventilation should be turned off, in order to limit the input of fresh air (oxygen) to the room. Extinguishing alkali metal fires with carbon dioxide extinguishers is forbidden, since the high pressure of the carbon dioxide spray may scatter the metal. After the fire has been put out, the room must be cleaned. The room is ventilated, the remains of the alkali metal are picked up and destroyed, the walls, floor and equipment are washed to remove the oxide film.

When a fire is put out or in case the alkali metal is spilled, it is possible that some alkali metal spray may fall on one of the workers. If liquid alkali metal strikes the body, it should be removed as rapidly as possible, for example with a dry piece of cotton. The burned area should be washed with a 5% solution of acetic acid. If the clothing catches fire and liquid alkali metal penetrates to the body, the clothing must be removed as rapidly as possible, then the metal must be carefully removed from the body. The damaged area should be carefully washed with a stream of water, with subsequent neutralization of the alkali with acetic acid. In case the metal, and alkali spray or metal oxides enter the eyes, they must be immediately washed with pure water over a fountain eye washing device, then subsequently neutralized with a 1% solution of boric acid. Vessels containing solutions of acetic and boric acid should be kept handy. The solutions of acetic and boric acid should be replaced each 15 days. /63

When working with mercury, the safety rules must be carefully followed due to its toxicity. The floors of the room in which a mercury installation is located should be covered with plastic with fused seams. At the walls, the edges of the plastic should turn up by approximately 100 mm and be fitted flush to the wall. The floor over which the plastic is laid should be flat and smooth, without cracks. The walls, windows and doors should be painted with an oil base paint. The room should have intake and exhaust ventilation.

The lowest possible temperature should be maintained in the room, since the concentration of mercury vapor in the room can increase sharply with increasing temperatures.

The air in the room should be analyzed for mercury vapor content. To perform this analysis, reactive paper is placed in several areas about the room. If mercury vapor is present, the paper will take on a pink color, the time required for the coloration to begin depends on the concentration of mercury in the room.

In case mercury is spilled or if the concentration of mercury vapor in the room rises above the maximum permissible concentration (norm 0.01 $mg/m^3$), the room must be cleaned. Visible drops of mercury can be collected using amalgamated metal plates (tin plate, copper, etc.) a vacuum cleaner, rubber bulb or water jet pump. After this, the floor of the room is flooded with a 10% solution of ferrous chloride, brushed carefully several times and let stand for 5-6 hours. Then the ferrous chloride solution is removed from the floor and it is washed several times with a soap solution, then with pure water. After completion of the washing cycle, the walls and ceiling are washed with hot soapy water.

Several days after the room is washed, a test analysis of the air must be performed. If mercury concentrations above the limiting permissible are discovered, the room should be cleaned again.

Preparation of Heat Transfer Metal and Its Placement in Installation /64

Such alkali metals as sodium and potassium are received from the chemical plant either in tin, sealed cans or in special containers.

Opening of the cans (their capacity is approximately one liter) should be performed in a specially prepared room. All unnecessary flammable liquids and materials are removed from the room, and the presence of the required fire extinguishing equipment is checked. A metal table or shelf is placed in the room, on which the cans are opened. The room should also contain cans of the wash liquid - kerosene; cans for alkali metal waste; filter paper or dry rags; a chisel, knife, pliers and wire brush. The vessels and tools should be washed and thoroughly dried.

After this, the cans with alkali metals are opened. Before opening, the cans are carefully inspected. Cans with dents and cracks in the walls and seams, with bent walls or bottom and clear traces of corrosion are considered defective. Defective cans are not opened.

A can is placed vertically on the table and a soldering iron is used to unsolder the top cover, the vertical seal is opened with the cutting pliers, usually lubricated with oil. The chunks of metal are removed from the can and the protective lubricant is removed with the wire brush under a layer of kerosene in the prewashing container. Then the metal is wrapped in the filter paper or dry rag. After this, the metal is washed with kerosene in the

secondary washing container, again dried with filter paper or dry rag and placed in the melting tank, into which inert gas flows constantly (argon or nitrogen). After this, the next can with alkali metal can be opened.

Upon completion of washing and placement of the alkali metal in the melting tank, the tank is sealed and the inert gas is placed in it. Tanks with kerosene, empty cans, used filter paper or rags are taken to the area where alkali metal is destroyed and burned. The tanks and tools are carefully washed with steam, then water and dried. The floors of the room in which the alkali metal was cleaned are carefully inspected and washed with a wet mop.

Before transfer of the alkali metal to the loading tank, preliminary purification of the metal must be performed to remove kerosene and the protective lubricant. This purification is performed by distillation of the kerosene and lubricant vapors. The metal is heated to about 150-200°C with continuous evacuation of the melting tank with a vacuum pump for several hours. After this, the metal can be pressed from the melting tank into the loading tank. The pressing should be performed through a filter, which allows insoluble impurities to be removed from the metal. Filter materials used include porous sintered metals and pressed filters made of chips of varying density. Stainless steel is most commonly used for the manufacture of filters. The temperature of the metal during filtration should not be over 120°C. /65

The usage of containers with alkali metals significantly decreases the time required to load the installation with metal in comparison with the usage of metal from cans. In this case, the rather cumbersome operation of preparation of the metal is eliminated. The metal can be easily transferred from the container using an inert gas into the loading tank.

The more expensive alkali metals, cesium and rubidium, are usually delivered in glass sealed ampoules containing from a few tens to a few hundreds of grams of the metal. Removal of the metal from the ampoules and loading of the metal into the tanks of the installation, and hermetic sealing of the tanks should be performed in an atmosphere of purified inert gas (argon or helium) in a sealed chamber equipped with inspecting windows and rubber gloves.

Filling of the installation should be performed with distilled alkali metal. The distillation should be performed at a temperature corresponding to a saturation vapor pressure of not over a few millimeters of mercury.

### Preparation of the Installation and Performance of Experiments

Newly manufactured units of an installation must be washed. If they are made of, for example, 1Kh18N9T steel, washing can be performed as follows.

First the unit is washed with a 0.1% solution of potassium permanganate ($KMnO_4$) and a 1% solution of alkali (NaOH) (held at approximately 90°C for

one hour). Washing with hot water is performed, then a 1% solution of oxalic acid is poured in (and held at a temperature of about 90°C for one hour). After this, it is washed with water and filled with a solution of hydrozene (5 mg in 1 liter water). Then the unit is finally washed with water and dried.

Before performance of experiments, the test stand must be washed (test stands for alkali metals are washed with ethyl alcohol) and checked for good sealing. The working sectors should be checked in experiments with water before experiments with the metal are performed, and the results produced should be compared with those for similar installations. The correspondence of the results is a good guarantee that no errors have been introduced to the method and that the sector is in good working order. /66

Before filling the installation with metal, it is heated (usually to a temperature 200°C higher than the melting point of the heat transfer agent) and evacuated at $10^{-1}$-$10^{-2}$ mm Hg. If the installation calls for purification of the metal of impurities (in particular oxides) and checks of their content, the metal should be purified, while testing the content of impurities. The content of impurities should be determined after performance of the experiments as well.

The required temperature (pressure) of the heat transfer medium is established using the furnace and the temperatures are measured, including measurement of the temperature field using the moving thermocouple with no load on the working sector.

In experiments on heat transfer, the temperature of the liquid and vapor, temperature field, temperature difference between wall and liquid, pressure and power applied to the working sector are measured.

Experiments on heat transfer are usually performed with a constant temperature (pressure) of the liquid, while changing the value of the heat flow. Then the furnace is used to establish a new temperature level, etc.

The critical heat flows are determined from the jump in temperature of the heating wall. Crisis may be produced by increasing the heat load (in small doses - 1-2% with flows near critical) at constant pressure or by smooth decrease in pressure with constant heat load. At the moment of the crisis, the vapor pressure or temperature must be measured in the working tank.

## Initial Processing of Experimental Data

The heat fluxes are usually determined from the power fed to the working sector. In calculating heat flows, one should consider the change in area of the working sector due to thermal expansion. For example, when a stainless steel sector is heated to 800°C, its linear dimensions increase by approximately 1.5%, its area by approximately 2.3% in comparison to the dimensions at room temperature.

The heat transfer coefficient can be determined from the formula

$$\alpha = q/\Delta t_\alpha. \tag{I.49}$$

The temperature head between the surface and liquid $\Delta t_\alpha$ is determined from the wall-liquid temperature differences measured in the experiment considering corrections for the temperature drop in the heat transmitting wall. In this case, when significant pulsations of the temperature difference between wall and liquid occur, $\Delta t_\alpha$ is defined as the mean integral of the temperature /67 head with respect to time

$$\Delta t_\alpha = \frac{1}{\tau}\int_0^\tau \Delta t_\alpha d\tau. \tag{I.50}$$

The time interval $\tau$ during which the determination is performed is usually several minutes.

Conclusions

1. In experiments on heat exchange during boiling, it is necessary to be able to produce great heat flows (on the order to $10^6$ kcal/m$^2$·hr and more) both for investigation of critical heat flows and for investigation of the dependence of heat transfer coefficient on heat flow. Investigation of heat exchange during boiling of metals under conditions of free convection can be performed using heating of the working sector by passage of an electrical current through an insulated conductor or by electronic heating. The usage of refractory metals in combination with electronic heating as the heat wall material makes it possible to expand the range of investigations of heat transfer and the critical heat flows as the metals boil.

2. When liquids boil, including metals, the heat transfer coefficients are high, so that the experiments must be performed with rather high accuracy of determination of the temperature of the heating surface. In experiments on the heat exchange during boiling of metals under free convection conditions the principal method of determining the temperature of the heating surface is measurement of the temperature by thermocouples imbedded in the wall. The greatest accuracy is provided by placement of thermocouples with relatively small dimensions (fractions of a millimeter) in a metal with high heat conductivity (for example, in copper).

3. In order to produce more complete information on the process in installations for the investigation of heat exchange during boiling of metals, it is desirable to provide moving thermocouples for measurement of the temperature field in the liquid and vapor, to make it possible to observe the process of boiling and its photographing, and also to provide systems for purification of the metal of impurities and check the content of impurities.

Installations designed for an investigation of heat exchange during boiling of metals under free convection conditions are simplest and most convenient in operation (from the standpoint of regulation) if constructed with gas (air) cooling of the condenser.

4. In connection with the possibility of existence of various heat removal modes (convection, with developed and unstable boiling), characterized by various pulsations of heating wall temperature, super heating of the liquid, etc., and also in connection with the possibility of transition from one heat removal mode to another at constant pressure and thermal loadings, in experiments on heat exchange during boiling of metals it is expedient to perform continuous recording of the liquid temperature (and vapor temperature) and the temperature difference between the heating wall and the liquid. For this same reason, in order to determine the temperature head between the heating surface and the liquid it is preferable to measure the temperature difference between the wall and the liquid, not the temperature of the heating wall and the liquid separately. In the process of experimentation, at high temperatures, thermocouples may slightly change their calibration curve; therefore, comparison of the indications of thermocouples (calibration) used to determine the temperature head between the heating surface and liquid should be performed periodically. This requires that the field of temperatures in the liquid be known, which can be measured, for example, by a moving thermocouple. /68

Installations with liquid metal heat transfer medium can only be placed in rooms modified for this purpose. When working with liquid metals, the safety rules must be carefully observed both during preparation for and performance of experiments, and during dismounting of the installation or its individual parts.

## CHAPTER 2 /69

## HEAT TRANSFER

Heat removal modes involved in evaporation under conditions of free convection are illustrated on Figure 34. In area of I the heat from the heating surface is removed by convection with slight super heating of the liquid on the heating surface, and is removed by evaporation from the free surface. Subsequently, the curve goes over smoothly into the area of bubble boiling II. The area of bubble boiling can be developed in two sectors. The sector with low density of active centers of vapor formation II, a, where the intensity of heat exchange depends significantly on convection, and the sector of developed boiling II, b, where the intensity of heat exchange is determined by the bubble boiling.

In the area of the transitional mode III, bubble and film boiling occur. Experimentally, area III can be realized under the condition $\Delta t$ = const (for example, when heating is performed by saturated vapor).

The area of stable film boiling IV can be arbitrarily divided into two sectors. Sector IV, a, where the contribution of radiation to heat transfer is negligible, and sector IV, b, where heat transfer by radiation is essential. The position of the boundary area between sectors IV, a and IV, b will depend on the level of the saturation temperature, which differs, for example, for alkali metals and non-metallic liquids, and the temperature head, since the heat flow resulting from radiation is proportional to the absolute temperature in the fourth power.

However, the process of heat removal may occur not only along curve ABCDE. Two other heat removal modes are possible: heat removal by convection with significant overheating of the liquid at the heating surface (area V) and heat removal with unstable boiling (area VI).

Film boiling may begin with small temperature heads and the process of /70
heat removal may correspond to the line B"DE. With small $\Delta t$ (area of point B"), some increase in the intensity of heat removal occurs in comparison to convective heat exchange.

Line BK, corresponding to heat removal by convection with subsequent heat removal by evaporation from the free surface, can be located either closer to the line of bubble boiling or farther from it, depending on the type of the liquid, pressure level and design of the heater. With high temperature heads, transition from convection to boiling occurs not smoothly, as between areas I and II, but suddenly.

Theoretically, the upper boundary of superheating of the liquid (point K on Figure 34) is determined by spontaneous formation of vapor seeds within the volume of the liquid. Usually, with a solid heating surface, the super

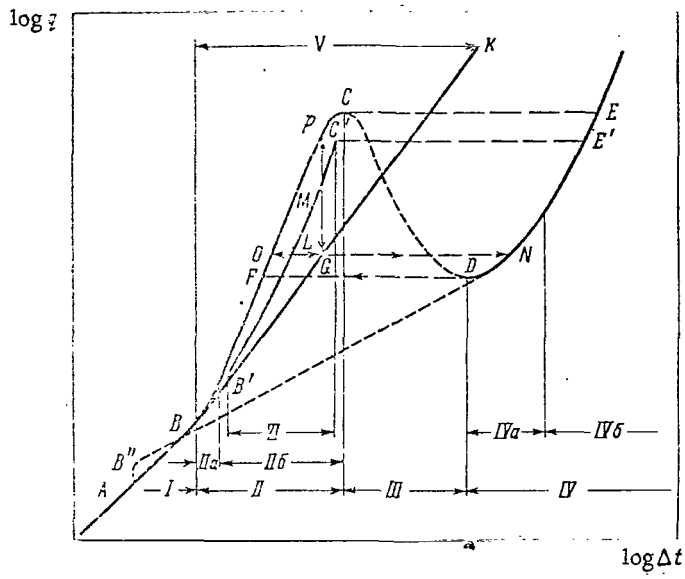


Figure 34. Heat Removal Modes During Vapor Formation Under Conditions of Free Convection.
I, Heat removal by convection with small Δt; II, Heat removal with bubble boiling; II a, With low density of active centers of vapor formation; II b, With high density of active centers of vapor formation (developed boiling); III, Heat removal with transitional boiling; IV, Heat removal with film boiling; IV a, Contribution of heat radiation small; IV b, Contribution of heat radiation large; V, Heat removal by convection with high Δt; VI, Heat removal by unstable boiling. Arrows represent possible sudden transitions from one mode of heat removal to another.

heating of the liquid is considerably less for spontaneous vapor formation. /71
The value of the heat flow at point K depends on the values of the temperature head and coefficient of heat transfer for this point. The heat flow at point K may be either higher or lower than the thermal load corresponding to transition from bubble boiling to film boiling.

The process of unstable boiling corresponds to line B'C', which is located between lines BK and BC. Depending on the concrete conditions, the intensity of heat removal with unstable boiling may approximate the intensity of heat removal with developed boiling or with convection. Transition from one mode of heat removal to another may occur not only smoothly, but suddenly. We will analyze below possible sudden transitions with two boundary conditions q = const and Δt = const.

1. q = const. With a heat flow corresponding to the first critical load (point C on Figure 34), sudden transition occurs from nucleate boiling to

film boiling (transition of type C → E), while with a heat flow corresponding to the second critical load (point D), a transition from film boiling to nucleate boiling occurs (transition type D → F).

Also, transition from unstable boiling to film boiling (transition type C' → E') is possible. If boiling begins along line BK at a certain point G, either developed (transition type G → O) or unstable (transition type G → L) boiling may occur, and film boiling (transition type G → N) is also possible.

If boiling starts with a heat flow above the first critical load, film boiling should occur. The transition to film boiling may also occur with heat flows below the first critical load (up to point J). However, this problem requires experimental checking.

In turn, transitions are possible from developed boiling to unstable boiling (transition type O → L) and to convection (transition type O → G), as well as from unstable boiling to developed boiling (transition type L → O) or to convection (transition type L → G).

Usually, transitions from developed boiling to unstable boiling in convection, as well as from unstable boiling to convection occur when the heat flows decrease, while the transition from unstable boiling to developed boiling occurs when the heat flows increase.

The existence of transitions types C → E and D → F has been well confirmed. Transitions type C' → E', G $\rightleftarrows$ O, L $\rightleftarrows$ G and O $\rightleftarrows$ L have been observed in our experiments on sodium, potassium and cesium, while transitions type G → L and G → O have occurred in experiments with water and organic fluids described, for example, in [72-75]. The transition to film boiling from convection has been achieved in experiments with organic fluids, for example in [97].

2. $\Delta t$ = const. In this case, the transitions from convection to developed boiling (transition type G → P) and unstable boiling (transition type G → M) are possible. We can expect the existence of transitions type P → M, P → G, M → P and M → G as well. The transition boundary from convection to developed boiling with $\Delta t$ = const will be the point corresponding to the temperature head at the crisis. With higher temperature heads, boiling will result in transitional or possibly unstable boiling. The transition from transient boiling to convection is also possible in principle, since a vapor film is unstable during transitional boiling. If transitions of the type C → E, C' → E'; D → F; G $\rightleftarrows$ L; G $\rightleftarrows$ O and O $\rightleftarrows$ L, that is transitions with q = const, are observed experimentally, the possibility of these transitions with $\Delta t$ = const still requires experimental checking. /72

We should note that Figure 34 reflects only the qualitative possibilities of heat removal modes during vapor formation under conditions of free convection. For example, the positions of lines BC and B'C' may change for a given liquid and heater, depending on the state of the surface. Therefore,

upon transitions from point G to point O, for example, point O may not be located precisely on curve BC corresponding to smooth transition from convection to developed boiling, but may be on a slightly different curve, similar in form to BC, but displaced in relation to it. The possibility of realization of any given mode of heat removal depends on the concrete conditions.

Heat exchange has been experimentally investigated on metals under conditions of free convection with developed boiling (area II on Figure 34). With unstable boiling (area VI) and convection with subsequent removal of heat by evaporation from the free surface (area I and V). Investigation of heat exchange with transitional (area III) and film (area IV) boiling, except for mercury in the last case, and also during boiling of an under heated liquid have almost never been performed. Therefore, we analyze below heat exchange only with convection, developed nucleate boiling and unstable boiling, when the temperature of the liquid is higher than the saturation temperature or near it.

## Heat Removal Due to Convection and Subsequent Heat Removal By Evaporation From the Free Surface

The heat flow carried away from the heating surface by convection depends on the super heating of the liquid near the heating wall in relation to the saturation temperature $\Delta t_s$ and the intensity of heat removal.

/73

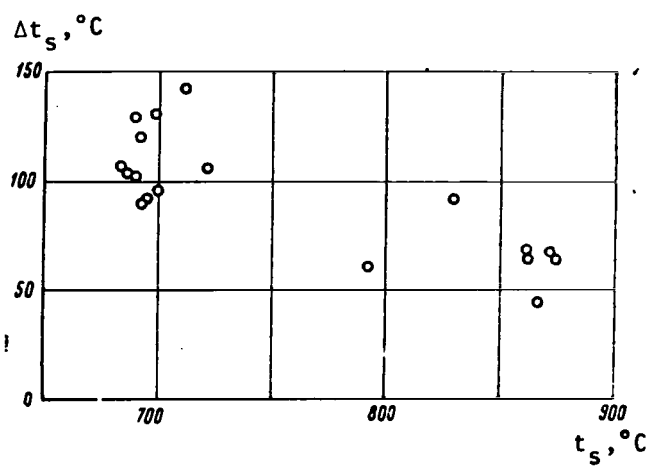


Figure 35. Experimental Data of the Authors on superheating of Sodium $\Delta t_s$ on a Stainless Steel Type 1Kh18N9T Surface.

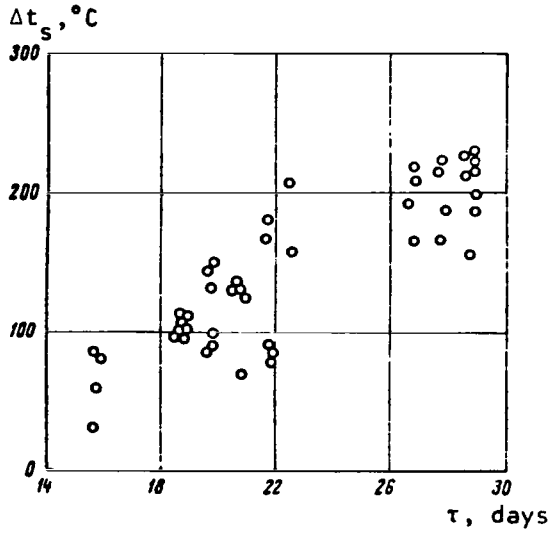


Figure 36. Dependence of Value of Superheating $\Delta t_s$ for Sodium on Contact Time of Sodium with Surface at $t_s$ = 900°C, Produced in [76].

The superheating of water and organic liquids necessary for the beginning of boiling on ordinary metal surfaces, for example at atmospheric pressure, is generally not over a few degrees. The heat flow in this case does not exceed $10^4$ kcal/m$^2$·hr. /74

Figure 35 shows experimental data on superheating of sodium on a stainless steel surface as a function of the saturation temperature, produced by the authors; Figure 36 shows super heating as a function of contact time of sodium with the surface (where $t_s$ = const) produced in [76]. Figures 37 and 38 show data on super heating of potassium produced in [76, 77] respectively. In the experiments, the results of which are shown on Figures 35-38, ordinary metal surfaces were used, not subjected to any special processing. In [17, 19, 35, 78, 79] and other works, rather high super heatings of alkali metals on the heating surfaces were also produced.

For any liquid, the super heating necessary for boiling to start depends on the state of the heating surface, the level of pressure and the temperature field in the liquid near the heating surface. In particular, in experiments on alkali metals, holes in the heating surface, capable of holding gas from vapor [19, 80] and the presence of an inert gas ([80] and the experiments of the authors) lead to a decrease of superheating in alkali metals As the pressure increased and the temperature gradient decreased, superheating in the liquid near the heating surface decreased.

Figure 39 shows the qualitative distribution of temperature in a liquid for conditions of heat removal into a large volume, when $t_l \geqslant t_s$. Superheating on the heating surface

$$\Delta t_s = \Delta t_\alpha + \delta t. \qquad \text{(II.1)}$$

for the case when boiling has not yet started, the equation

$$Q = qF_p + Q_{init} = \alpha_b \delta t F_c, \qquad \text{(II.2)}$$

is correct, where Q is the total quantity of heat applied to the liquid, kcal/hr; $F_p$ is the area of the heated surface of the working sector, $m^2$; $Q_{init}$ is the heat applied to the liquid from the tank heaters, kcal/hr; $F_c$ is the free surface area, $m^2$.

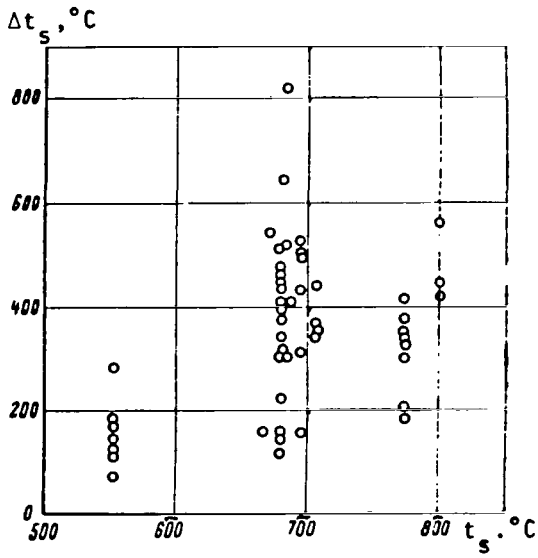


Figure 37. Experimental Data on Superheating of Potassium Produced in [76].

We can easily produce an expression for superheating from equations (II.1) and (II.2):

$$\Delta t_s = \frac{q}{\alpha} + \frac{F_p q + Q_{init}}{F_c \alpha_b} \qquad (II.3)$$

We can see from equation (II.3) that even with fixed pressure and identical surface state, $\Delta t_s$ is not a single valued function of of heat flow q on the heating surface $F_p/F_c$, $Q_{init}$ and $\alpha$ are determined by the conditions of the experiment. The heat transfer coefficient at the phase separation boundary $\alpha_b$ is characterized by the thermal resistance of the boundary layer of liquid near the phase division, the thermal resistance upon phase transition and the thermal resistance of the diffusion layer in the vapor near the division boundary. The thermal resistance in the phase transition depends strongly on the pressure and impurities on the surface of the phase division boundary. The thermal resistance of the diffusion layer as a function of the quantity of non-condensing gases in the vapor can change by more than ten times [81]. Approximate estimates made by the authors on the basis of measurements of the difference in temperatures between liquid and vapor $\delta t$ by a moving thermocouple in experiments on sodium in the pressure range 0.1-1 atm.abs. have shown that in these experiments the value of $\alpha_b$ for the free surface of the phase division boundary was approximately $10^4$ kcal/$m^2$·hr °C.

/76

The heat transfer coefficient $\alpha$ in equation (II.3) characterized convective heat exchange. The authors, using an installation for experiments for heat transfer during boiling of sodium, also performed experiments on heat transfer to sodium under conditions of free convection without boiling (with $t_l < t_s$) [82].

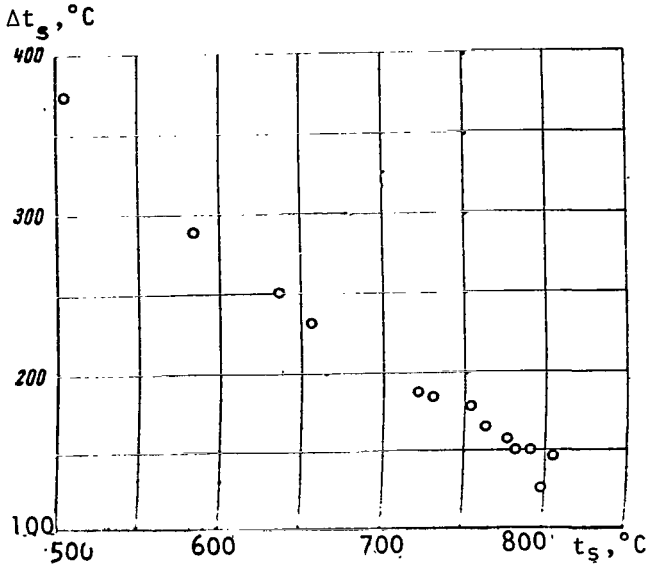


Figure 38. Experimental Data on Super Heating of Potassium Produced in [77].

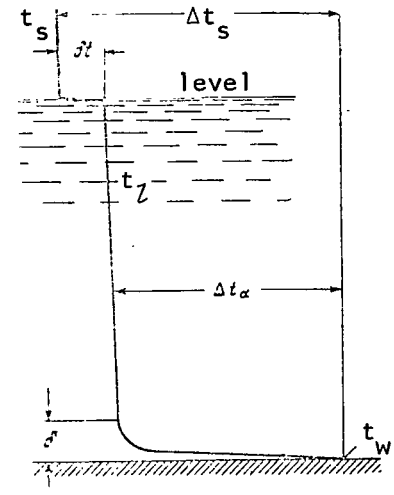


Figure 39. Qualitative Picture of Distribution of Temperature with Saturated Boiling Under Conditions Of Free Convection.

On Figure 40, we show the results of these experiments in coordinates α-q (these coordinates are convenient for comparison with data on heat transfer during boiling. We can see from Figure 40 that the points of practically all four series of experiments lie near the averaging line with a dispersion of not over ± 15%. The averaging line corresponds to the formula

$$\alpha = 95q^{1/3}. \qquad \text{(II.4)}$$

Figure 41 shows temperature profiles in sodium made by measurements using a moving thermocouple for two heat fluxes. With heat fluxes less than about $0.7 \cdot 10^6$ kcal/m$^2$·hr, neither the moving thermocouple near the wall nor thermocouples placed in the wall noted any fluctuations in temperature. With high heat fluxes, both the moving thermocouple and the thermocouples in the wall recorded temperature pulsations at relatively low (about 0.13 Hz) frequency. The formation of pulsations indicates turbulent movement of the fluid near the heating surface. For our working surface with fluxes of $0.7 \cdot 10^6$ kcal/m$^2$·hr, corresponding to the beginning of turbulent movement of the fluid at the wall, the Grashoff number was about $10^8$. This agrees with the conclusions of Fedynskiy [83], who believed that the transition from /77

laminar flow to turbulent flow occurs at Gr about $1.5 \cdot 10^8$ regardless of the Pr number.

The experimental data on heat transfer with free convection of liquid metals are usually processed in the coordinates $Nu\text{-}GrPr^2$. This means that the influence of viscosity on heat transfer is not considered. The data of the authors on heat transfer with free convection for sodium, related to the turbulent area, were constructed in the coordinates $Nu\text{-}GrPr^2$, and are shown on Figure 42. As a defining dimension, we used the diameter of the floor, and as a defining temperature - the temperature of the liquid far from the heating surface. These points are located about the averaging line with a dispersion of ± 15%. The averaging line corresponds to the formula

$$Nu = 0.38(GrPr^2)^{1/4}. \tag{II.5}$$

On Figure 42 we also show the dependence according to the formula of MacDonald and Cannolly

$$Nu = 0.262\,(GrPr^2)^{0.35}, \tag{II.6}$$

produced in [84] as a result of processing of experimental data on heat transfer to sodium on a flat, circular plate 200 mm in diameter. On the basis of the values of the exponent with $GrPr^2$ in formula (II.6), the authors of [84] considered that heat exchange occurred in the turbulent area. In the area of $GrPr^2$ from $2.5 \cdot 10^3$ to $8 \cdot 10^3$, the values of Nu in formula (II.6) are approximately 25% lower than according to formula (II.5). With increasing $GrPr^2$, the difference in the value of Nu calculated using formulas (II.5) and (II.6) decreases. The values of the heat transfer coefficients calculated using formula (II.5) and formula

$$Nu = 0.069\,(Gr\,Pr)^{1/3}\,Pr^{0.074}, \tag{II.7}$$

agree satisfactorily with each other (within 20%). Formula (II.7) was produced on the basis of experimental data on heat transfer with free convection in mercury [85].

For metals, there are no experimentally tested recommendations for calculation of heat transfer from the plane of a horizontal plate in the laminar mode. For horizontal pipes, on the other hand, experiments have been performed primarily in the laminar mode. For example, in [86] for calculation of heat transfer from horizontal cylinders in the laminar area, the following formula is recommended:

$$Nu = 0.53\,(GrPr^2)^{1/4}. \tag{II.8}$$

Formula (II.8) was produced on the basis of experimental data. The experiments were performed on sodium, lead, bismuth, mercury and sodium-potassium and lead-bismuth alloys. The diameter of the cylinders vary from 6.3 to 38 mm. /79

/78

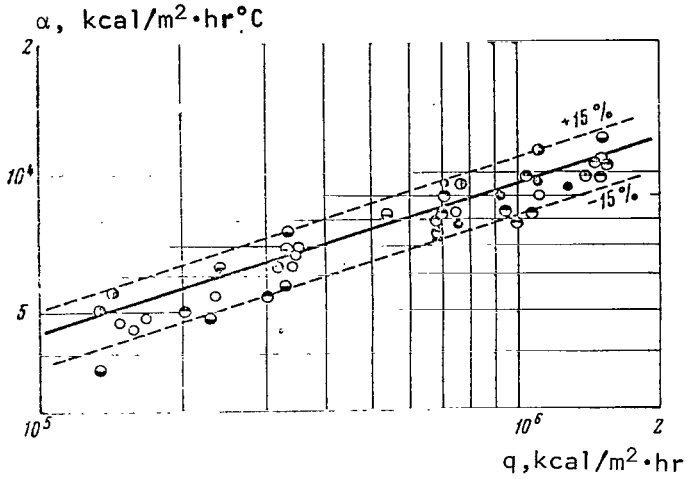


Figure 40. Experimental Data of the Authors on Heat Transfer With Free Convection Produced on Sodium when ($t_l < t_s$) $t_l$, °C: o - 250 ± 50°C; ◑ - 350 ± 50°C; ⊖ - 450 ± 50°C; ● - 550 ± 50°C; ⊖ - 600°C.

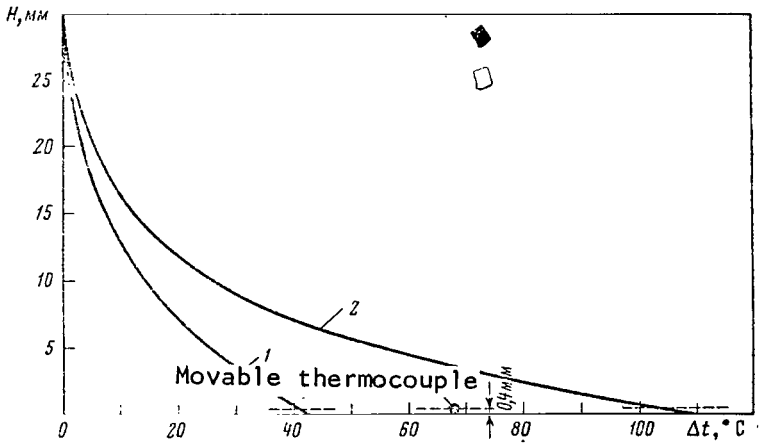


Figure 41. Distribution of Temperature in Liquid Near Heating Wall Produced by Measurement With Moving Thermocouple in Experiments of The Authors on Sodium Under Conditions of Free Convection ($t_l < t_s$). 1, $q = 0.36 \cdot 10^6$ kcal/m²·hr; 2, $q = 0.95 \cdot 10^6$ kcal/m²·hr.

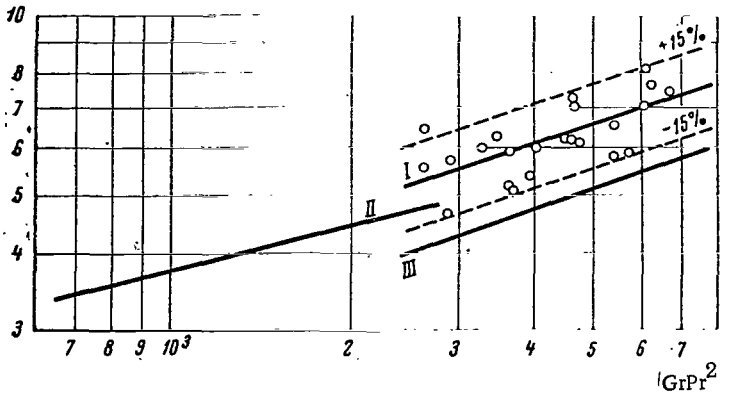


Figure 42. Experimental Data of the Authors on Heat Transfer With Free Convection produced for Sodium in Coordinates Nu-$GrPr^2$.
I, According to formula (II.5); II, According to formula (II.9); III, According to formula (II.6).

The following formulas recommended in [83] for calculation of heat transfer to liquid metals under conditions of free convection:

$$Nu = 0.67\left(\frac{GrPr^2}{1+Pr}\right)^{1/4}. \qquad (II.9)$$

It is easy to see that for liquid metals (Pr << 1) formulas (II.8) and (II.9) are similar.

Dependents (II.9) is constructed on Figure 42. It agrees satisfactorily with dependents (II.5) at the beginning of the turbulent area ($GrPr^2 \sim 2.5 \cdot 10^3$).

Before production of dependences based on experimental data, in order to calculate heat transfer to liquid metals with free convection in the laminar flow mode on a flat horizontal surface we can recommend, as for horizontal cylinders, that formula (II.9) be used, and that calculation of heat transfer in the turbulent area over a horizontal cylinder be calculated using formula (II.5).

Thus, for alkali metals the heat removal of large heat flows by convection and $t_l > t_s$ results from the possibility of achieving significant /84
superheating of the liquid over the heating surface and relatively high values of heat transfer coefficients (for alkali metals $\alpha$ is several times higher than for non-metallic liquids). For example, in our experiments on sodium, convection with subsequent heat transfer by evaporation from the free surface was capable of carrying away fluxes exceeding $10^6$ kcal/$m^2$·hr.

TABLE 11.1

| Authors, year of publication | Heat transfer medium | Range of pressures invest. (atm. abs.) | Range of heat fluxes invest., $10^{-6}$ (kcal/$m^2 \cdot hr$) | Recommd. formulas | Characteristics of working sector | Notes |
|---|---|---|---|---|---|---|
| Lyon, Foust, Katz [9], 1955 | Sodium | 1 | 0.041-0.35 | | Horizontal stainless steel tube 19 mm in diam., 127 mm long. Chromel-alumel thermocouples in drilled apertures 1 mm in diam. Rad. heating from current-heated silit rod, located within tube. Tank 89 mm in diam. | 1. $\alpha$ calculated according to $\Delta t_\alpha$ (see Fig. 39) |
| | Sodium alloy | 1 | 0.041-0.35 | | | |
| Noyes [18], 1963 | Sodium-potassium | 0.07-0.56 | up to 2.17 | $\alpha = 25\, q^{0.58}$ formula (11.10) | Horizontal tubes of molybdenum and stainless steel 9.5 mm in diam., 76 mm long. Thermocouples imbedded in wells soldered or welded on top. Heating by current-heated graphite rod located within tube and insulated with alum. oxide (see Fig. 2). Tank diam. 152 mm. | 1. $\alpha$ calculated from $\Delta t_\alpha$.<br>2. Several values of $q_{cr}$ produced in the interval $P_s \sim$ (0.035-0.105 atm. abs.). |
| Noyes, Lurie [33], 1966 | Sodium | 0.07-0.56 | 0.08-2.5 | | Horizontal tubes of stainless steel and molybdenum, 9.5 mm and 6.4 mm in diam., 76 mm and 51 mm long respectively. Thermocouples placed in wells, welded or soldered at top. Currentheated graphite rod. | 1. $\alpha$ calculated from $\Delta t_\alpha$.<br>2. Data on $q_{cr}$ produced in interval $P_s$ (0.035-0.105) |

TABLE 11.1 (continued)

| Authors, year of publication | Heat trans-medium | Range of pressures invest. (atm.abs.) | Range of heat fluxes invest., $10^{-6}$ (kcal/ $m^2 \cdot hr$) | Recommd. formulas | Characteristics of working sector | Notes |
|---|---|---|---|---|---|---|
| | | | | | Isolated from tube by boron nitride bushing. Tanks 150 mm (9.5 mm heater) and 300 mm (6.4 mm heater) in diam. | |
| Petukhov, Kovalev, Zhukov [17], 1966 | Sodium | 0.011-0.82 | 0.1-1.5 | $\alpha = 0.8 q^{0.7} p_s^{0.25}$ Formula (11.11) | Horizontal tube with surface of stainless steel, 29.6 mm in diam., heated over 85 mm of length. Platinum-platinum/rhodium thermocouples, placed in copper. Electronic heating (see Fig. 15). Tank diam. 172 mm. | 1. $\alpha$ calculated from $\Delta t_\alpha$. |
| Marto, Rohsenow [19], 1965-1966 | Sodium | 0.08; 0.22; 0.55 | 0.10-0.64 | | Flat horizontal plate of nickel and stainless steel, 63 mm in diam. Platinum-platinum/rhodium and chromel-alumel thermocouples located over height of sector in 1.5 mm diam. apertures. Rad. heating (see Fig. 1), tank diam. 63 mm. | 1. $\alpha$ calculated from $\Delta t_\alpha$. (see Fig. 39), $t_s$ determined from measured pressure. 2. Experiments performed on surfaces with various finish. |

TABLE 11.1 (continued)

| Authors, year of publication | Heat trans-medium | Range of pressures invest. (atm.abs.) | Range of heat fluxes invest. $10^{-6}$ (kcal/$m^2 \cdot hr$) | Recommd. formulas | Characteristics of working sector | Notes |
|---|---|---|---|---|---|---|
| Borishanskiy et al., [16], 1965 | Sodium | 0 16-1.25 | 0.014-0.125 | $\alpha = 7_q^{0.7}$ Formula (11.12) | Horizontal and vertical tubes of stainless steel, 20-40 mm in diam., 160-200 mm long. Radiation heating from rod (graphite or silit), located within tube. | |
| | Potassium | 0.04-1.15 | 0.015-0.14 | $\alpha = 3_q^{0.7} P_s^{0.15}$ Formula (11.13) | | |
| Deyev et al., [35], 1967 | Sodium | 0.005-0.75 | 0.08-1.72 | $\alpha = 380 q^{1/3} P_s^{0.1}$ Formula (11.14) | Horizontal flat sector 28 mm in diam. Operating surface made of 1Kh18N9T steel. Electronic heating. Platinum-platinum/rhodium thermocouples in copper. | 1. With $P_s \sim 6 \cdot 10^{-3}$ atm.abs., boiling did not occur with heat fluxes up to $1.1 \cdot 10^6$ kcal/$m^2 \cdot hr$. |
| | | | | In range $q = (8\text{-}78) \cdot 10^4$ kcal/$m^2 \cdot hr$ and with $P_s >$ 0.2 atm. abs. | | 2. With $P_s \sim 4 \cdot 10^{-2}\text{-}2 \cdot 10^{-1}$ atm.abs., boiling was unstable, wall temp. pulsation reaching ± 25°C. |

TABLE 11.1 (continued)

| Authors, year of publication | Heat transmedium | Range of pres. invest. (atm.abs.) | Range of heat flux. invest. $10^{-6}$ (kcal/$m^2 \cdot hr$) | Recommd. formulas | Characteristics of working sector | Notes |
|---|---|---|---|---|---|---|
| Bonilla et al., [20], 1963 | Potassium | 0.003-2 | 0.05-03 | $\alpha = 4.83 \cdot 10^{-2} \times q^{0.885} P_s^{0.293}$ Formula (11.15) | Horizontal nickel plate 78 mm in diam. Chromel-alumel thermocouples in apertures drilled at several cross sections through height of sector. Heat input from plate soldered to sector. Plate heated by resistance heaters wound on insulation (see Fig. 6). Tank diam. 78 mm. | Dependence of $\alpha$ on $P_s$ in formula (11.15) produced on the basis of data at pressures of 0.003 atm.abs. and 1-2 atm.abs. |
| Madsen at al., [22], 1960 | Sodium-potassium alloy | 0.0027-1.04 | 0.054-0.365 | $\alpha = 210 q^{0.2} P_s^{0.2}$ Formula (11.16) | Horizontal nickel plate 78 mm in diam. Thermocouples and heater similar to those used in [20]. Tank diam. 70 mm. | In Formula (11.16), $\alpha$ calculated from $\Delta t_s$. |

## Heat Transfer During Boiling of Alkali Metals

A summary of the experimental works on heat transfer during boiling of alkali metals is presented in Table II.1. This Table shows the ranges of investigations of pressures and heat fluxes, presents empirical formulas suggested by the authors of the works and provides a brief characterization of the working sectors used.

The authors have performed experiments on heat transfer during boiling of alkali metals using sodium, cesium and potassium. The boiling was performed on flat horizontal sectors heated (at 38 mm diameter) by electron bombardment (see Figure 10). The range of investigated heat fluxes for sodium, potassium and cesium varied from approximately $10^5$ kcal/m$^2$·hr right up to the critical loads. In addition to the measurements of liquid temperature, wall-liquid temperature difference, these experiments also included measurement of the temperature field within the liquid and vapor using a moving thermocouple. All indications of these thermocouples were continuously recorded on a high speed (1 sec) type EPP-09 potentiometer and periodically measured on a R 2/1 potentiometer.

Ten series of experiments on sodium were performed in the pressure range from 0.02 to 1.5 atm. abs. By a series, we mean a set of experiments performed using a single working sector without cleaning and replacement of the heat transfer medium.

In nine series of experiments performed on the installation, the diagram and boiling tank of which are shown on Figures 27 and 24 respectively, the sodium boiled under the pressure of its vapors. In one series of experiments performed on an installation similar to the installation shown on Figures 32 and 33, the sodium boiled both under the pressure of its own vapors and under inert gas pressure (argon).

Of the nine series of experiments in which the sodium was boiled under the pressure of its own vapors, two series were performed on copper sectors, the heating surface of which was galvanically covered with a layer of nickel approximately 20 μ thick (see Figure 11), and four series of experiments were performed on the same sectors covered with first a layer of nickel, then a layer of chromium approximately 20 μ thick. In many experiments, the covering was broken and the sodium contacted the copper directly.

In another three series of experiments the surface on which boiling occurred was made of stainless steel (Figure 11). The content of oxygen in the sodium varied between approximately $10^{-1}$-$10^{-3}$% by weight. The experiments were performed both with constant pressure and varying heat flow and with constant heat flow and varying pressure. The maintenance of the experimental regime in time with constant pressure and heat at flow varied from several minutes to several tens of hours. /85

In all series of experiments when boiling occurred under the pressure of the sodium vapors at pressures below 0.1 atm.abs., heat removal was accomplished

only with their own unstable boiling or convection with subsequent liberation of heat by evaporation from the free surface. At pressures above 0.1 atm.abs., three types of heat removal occurred: heat removal with developed and unstable boiling and heat removal by convection with great overheating and subsequently with great heat fluxes.

The experimental data produced with developed boiling of sodium under the pressure of its own vapors on surfaces of stainless steel, nickel, chromium and copper in the pressure range of about 0.1-1 atm. abs. are satisfactorily described by the empirical formula

$$\alpha = 4q^{2/3}. \qquad \text{(II.17)}$$

The values of heat transfer coefficients determined in time with unstable sodium boiling are located between the values of $\alpha$ calculated according to formulas (II.17) and (II.4).

Experiments on the influence of gas on heat exchange during boiling of sodium were performed in the pressure interval approximately 0.015-1.5 atm. abs. Boiling occurred over a stainless steel surface. At first the sodium was held under the pressure of its own vapors. In this case, developed boiling of sodium began only with vapor pressures of about 0.5 atm. abs.and heat fluxes of about $1.1 \cdot 10^6$ kcal/m$^2$·hr. With lower heat fluxes, heat removal was principally by convection, with only periodic boiling of the sodium observed.

Then, experiments were performed under argon. In this case, developed boiling began and was maintained stably at pressures as low as about 0.015 atm. abs. with a heat flux of about $0.5 \cdot 10^6$ kcal/m$^2$·hr. With higher pressures, developed boiling began at lower heat fluxes.

Data produced on heat transfer with developed boiling of sodium under argon can be satisfactorily described by the empirical formula suggested earlier by the authors of [87].

With pressures up to about 0.3 atm. abs.

$$\alpha = 8q^{2/3}p_s^{0.4}. \qquad \text{(II.18)}$$

With pressures of about 0.3-1.5 atm. abs.

$$\alpha = 5.6q^{2/3}p_s^{0.1}. \qquad \text{(II.19)}$$

The values of the heat transfer coefficients with developed boiling of sodium under the pressure of its vapors were somewhat lower than the values of $\alpha$ with boiling of sodium under argon.

Three series of experiments were performed with cesium in the pressure range from 0.02 to 3.2 atm. abs. over surfaces of stainless steel. In these experiments, as in the experiments with sodium, developed and unstable boiling were observed. The values of the heat transfer coefficients produced in two of the series of experiments agree well with each other, while the data of the third series lie as a whole approximately 25% lower. The value of temperature pulsations measured by thermocouples placed in the heat transfer wall in this series of experiments was greater than in the two preceding series. The results produced on heat transfer with developed boiling of cesium can be described by two formulas: /86

$$\alpha = 9.2q^{2/3}p_s^{0.4}, \qquad \text{(II.20)}$$

with $P_s \sim$ 0.02-0.1 atm. abs. and

$$\alpha = 4.6q^{2/3}\ p_s^{0.1} \qquad \text{(II.21)}$$

with $P_s \sim$ 0.1-3.2 atm. abs.

Heat removal from potassium was investigated by the authors over a surface of stainless steel with pressures of about 0.02 to 1 atm. abs. If the potassium was held under the pressure of its vapors, up to a pressure of about 0.1-0.3 atm. abs. the heat removal was primarily by convection, with subsequent heat removal by evaporation from the free surface or with unstable boiling even at high heat fluxes ($0.5\cdot10^6$-$1\cdot10^6$ kcal/m$^2$·hr). With higher pressures, developed boiling began. If argon was added to the boiling tank, developed boiling of potassium began even at pressures of about 0.02 atm. abs. and moderate (about $0.3\cdot10^6$ kcal/m$^2$·hr) heat fluxes.

Heat Removal With Developed Boiling

Many experiments have indicated that with developed nucleate boiling (area II b on Figure 34) of non-metallic liquids, the heat transfer coefficient can be described by formulas such as

$$\alpha = C_\alpha q^n p_s^m, \qquad \text{(II.22)}$$

$$\alpha = C'_\alpha \Delta t^L p_s^m. \qquad \text{(II.23)}$$

The value of the exponent n usually lies between 0.6 and 0.8, and is used as 0.7 or 2/3 in most formulas. The value of coefficient $C_\alpha$ depends on the properties of the boiling liquid and the surface on which boiling occurs. The value of the exponent m depends on the level $P_s$ and type of liquid. There is an unambiguous relationship between $C_\alpha$, n and $C'_\alpha$, L. A broad review of experimental data on heat transfer during boiling of water and organic liquids in the form of (II.22) is presented in [88]. /87

With developed boiling of alkali metals, the heat transfer coefficient can also be described by formulas (II.22), (II.23), the values of the exponent with heat flux, according to the results of most works, lying approximately within the same limits (see Table II.1) as for non-metallic liquids.

The values of the exponent with q in (II.14) and (II.16) differs essentially from those used in other formulas. Possibly in the experiments described in [35] the quantity of active centers of vapor formation was limited, since the area of the working surface was relatively slight (about 6 $cm^2$) and convection had an important influence on the intensity of heat exchange even at high heat fluxes. In [22], in which heat exchange was investigated during boiling of an alloy of sodium and potassium, significant differences were detected both in the temperature between liquid and vapor and in the temperature of the liquid through the height of the boiling tank. However, it is difficult to explain the reason for the existence of significant gradients of temperature through the height of a column of liquid when the saturated liquid is boiled. Possibly errors occurred here in the temperature measurements. The values of the heat transfer coefficients on which formula (II.16) are based are related in [22] to the temperature difference between the heating surface temperature and the temperature above the level of the liquid. The volume over the liquid was filled with inert gas. The values of the heat transfer coefficients related to the difference in temperatures between the heating surface and the liquid near the surface were higher than those calculated from formula (II.16). A further limited quantity of data on heat transfer during boiling of a sodium-potassium alloy was produced in [9]. These data are considerably higher than the values calculated from formula (II.16). We conclude from this that there are not yet sufficient data available to recommend an empirical formula for calculation of heat transfer during boiling of a sodium-potassium alloy.

Figures 43-45 show experimental data of the authors on heat transfer during boiling of sodium and cesium in coordinates $\alpha$-q as an example. The points on Figures 43, 44 (and some subsequent Figures) have numbers which correspond to the order of their production in time.

With developed boiling, the thermocouples placed in the wall recorded temperature pulsations not exceeding a few degrees or showed no pulsations at all, as in experiments with bubble boiling of non-metallic liquids. It is also known that during bubble boiling of non-metallic liquids in the boundary layer and directly on the heating surface significant pulsations of temperature occur [89-92]. With developed boiling of metals, temperature pulsations /89
have also been observed near the heating surface [15]. These temperature pulsations are related to the formation and separation of vapor bubbles. The values of temperature pulsation at distance y from the heating surface can be estimated from the following formula [93]

$$A_\omega = A_{\omega,} e^{-\sqrt{\frac{\pi\omega}{a}}y}, \qquad \text{(II.24)}$$

where $A_{\omega 0}$ is the amplitude of pulsations on the surface, °C; $A_{\omega}$ is the amplitude of pulsations at distance y from the surface, °C; ω is the pulsating frequency, 1/sec.

/88

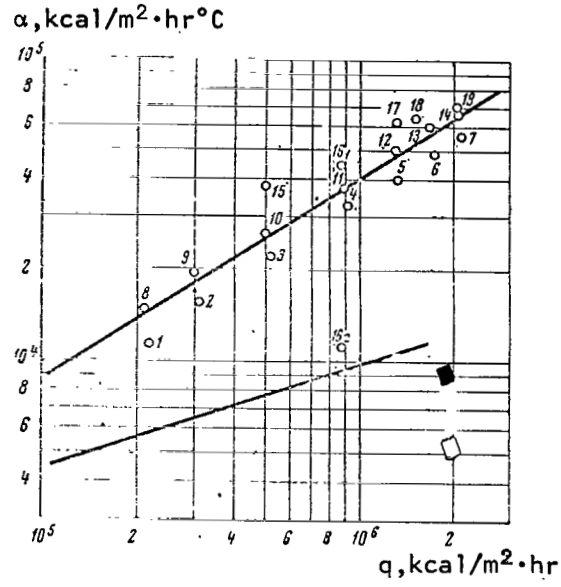


Figure 43. Experimental Data of the Authors on Heat Transfer During Boiling of Sodium ($t_{\gamma}$ = 700°C). Upper line corresponds to formula (II.17), lower - to formula (II.4).

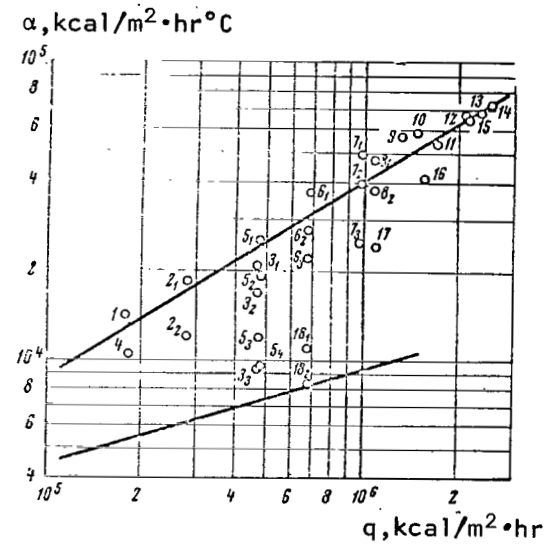


Figure 44. Experimental Data of the Authors on Heat Transfer During Boiling of Sodium ($t_{\gamma}$ = 860°C). Upper line corresponds to formula (II.17), lower - to formula (II.4).

Thus, the difference in the values of temperature pulsations recorded by thermocouples imbedded in the heat transfer wall from the values of pulsations existing on the heating surface depend on the depth of placement of the thermocouples in relation to the surface, the pulsating frequency, the temperature conductivity of the wall material and the quality of the contact of the thermocouple junction to the wall, the inertia of the thermocouple and the secondary device. /90

With ordinary types of thermocouples (placed at some distance from the heating surface), temperature pulsations in the process of developed bubble boiling, for which the frequency of bubble separation is rather high, generally cannot be recorded. Therefore, the indications of developed boiling include observation of dependence (II.22) and absence of high and low frequency pulsations in the indications of the thermocouples measuring the temperature of the heating wall. This last condition doubtless is correct only when satisfactory contact between the thermocouple well and the wall is

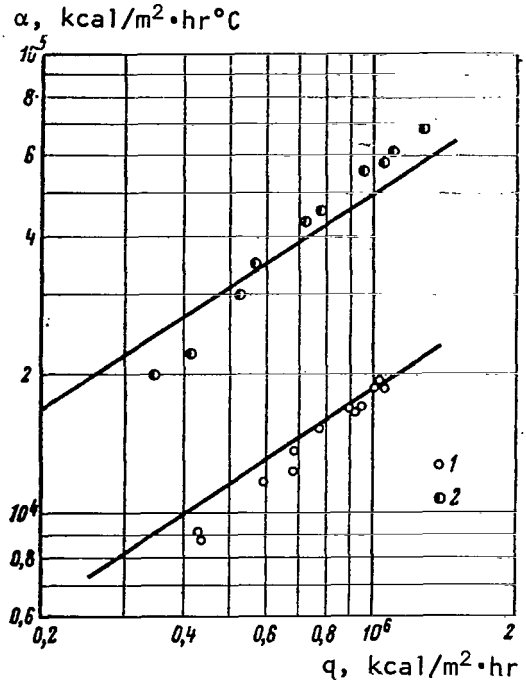


Commas indicate decimal points.

Figure 45. Experimental Data of The Authors on Heat Transfer With Developed Boiling of Cesium. Upper line corresponds to formula (II.21), lower - to formula (II.20). 1, $t_l$ = 380°C; 2, $t_l$ = 720°C.

boiling and heat removal by convection. The less the amplitude of temperature pulsations of the wall and the higher their frequency, the more the values of the heat transfer coefficients approach α with developed boiling.

The data related to unstable boiling cannot be described by a single exponential rule, since the heat removal conditions for individual experiments may differ significantly, approaching heat removal with developed boiling or heat removal with convection without boiling.

Figure 46 shows as an example the experimental data of the authors produced for sodium and related to heat removal with unstable boiling. The upper line corresponds to formula (II.17), describing the data of the authors with developed boiling of sodium, while the lower line corresponds to formula (II.4), describing the experimental data with heat removal by convection, produced on the same installation.

provided, and the secondary device is capable of recording pulsations of the corresponding frequency.

## Heat Removal With Unstable Boiling

The authors were among the first to study heat removal with unstable boiling in experiments on sodium. As the experimental data accumulated to the present time indicate, heat removal with unstable boiling is characteristic for alkali metals over a rather broad range of pressures (from hundredths of an atmosphere to several atmospheres - experiments have not been performed at higher pressures) and heat flows (right up to the critical flows). The characteristic indicator of heat removal with unstable boiling is the existence of significant temperature pulsations of the heating wall at relatively low (fractions of a Hz) frequencies, which are clearly recorded by thermocouples imbedded in the wall.

The time-averaged values of heat transfer coefficients with unstable boiling lie between values of α for heat removal with developed

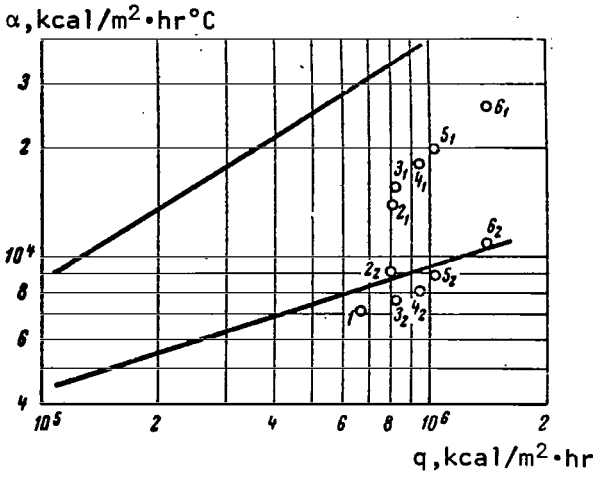


Figure 46. Experimental Data of the Authors on Heat Transfer With Boiling of Sodium ($t_{\gamma}$ = 700°C). Upper line corresponds to formula (II.17), lower- to formula (II.4).

Figure 47 shows a recording of the wall-liquid temperature difference for the time when points 3 and 6 shown on Figure 46 were taken. Points $3_1$ and $6_1$ relate to heat removal with unstable boiling, points $3_2$ and $6_2$ to heat removal by convection. /91 & 92

Figure 48 illustrates the course of the measured surface liquid temperature difference with unstable and developed boiling of cesium from our experiments.

Figure 49 shows the dependence of the temperature heads $\Delta t_{\alpha}$ on heat flux for sodium with heat removal by developed boiling and convection according to formulas (II.17), (II.4) respectively. The maximum value of pulsations $\theta_{max}$ with unstable boiling is equal to the difference between $\Delta t_{\alpha}$ for convection without boiling and with developed boiling.

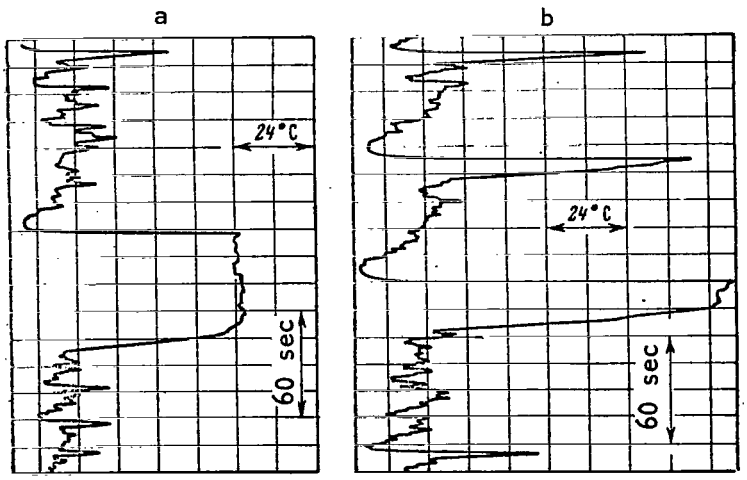


Figure 47. Recording of Wall-Liquid Temperature Differences For Points 3(a) and 6(b) Shown on Figure 46.

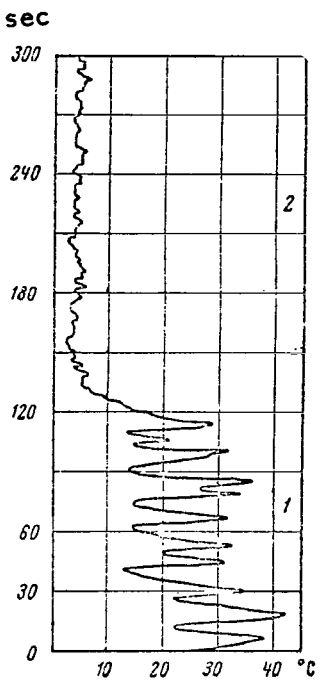


Figure 48. Recording of Temperature Difference Between Wall and Liquid With Developed (2) and Unstable (1) Boiling of Cesium in the Experiments of the Authors ($q = 0.44 \cdot 10^6$ kcal/m$^2$hr; $t_l = 517°C$).

As the heat flux increases, the boiling process becomes more stable, the conditions of heat removal with unstable boiling approach the conditions of heat removal with developed boiling. In this case, the dependence of $\alpha$ on q is quite strong. Let us show this using an example.

Figure 50 shows the data of the authors produced in experiments on sodium. Figure 51 shows a recording of the wall-liquid temperature difference for point 4 and 6 on Figure 50. The pulsations of temperature of the heating wall for point 6 were greater than for point 4. This indicates that the heat removal conditions were different for point 4 and 6.

The question may arise as to whether the dependence constructed on Figure 50 is the only possible dependence of $\alpha$ on q with this sodium saturation pressure in the range of heat fluxes used. We must give a negative answer, since in other experiments at the same sodium temperature and with the same range of heat fluxes, only developed boiling of sodium (see Figure 43) occurred at times. Thus, the dependence of the heat transfer coefficient on the heat flux, as shown on Figure 50, involves differences in the conditions of heat removal with different heat fluxes. /94

Therefore, in analyzing experimental data, particularly in determining the dependence of $\alpha$ on q and $P_s$, for example for developed boiling, in order to avoid errors one should turn attention to the possibility of changing heat removal conditions with increasing heat flux.

Unstable boiling has also been observed in non-metallic liquids [72-75]. However, unstable boiling of non-metallic liquids occurred only at low pressures, generally below 0.1 atm.abs., with low heat fluxes (below about $10^5$ kcal/m$^2$·hr) and over rather smooth surfaces.

Unstable boiling results from the irregularity of the operation of vapor formation centers, the number of which is not great on the heating surface in this case.

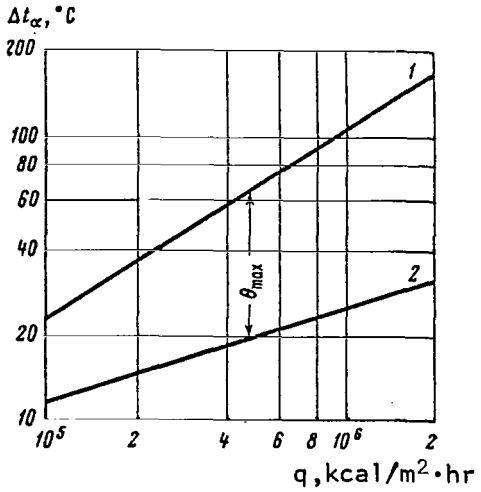


Figure 49. Dependence of Maximum Value of Temperature Pulsation of Surface $\theta_{max}$ With Unstable Boiling of Sodium on Heat Flux. Lines 1 and 2 constructed according to formulas (11.17) and (11.4) respectively.

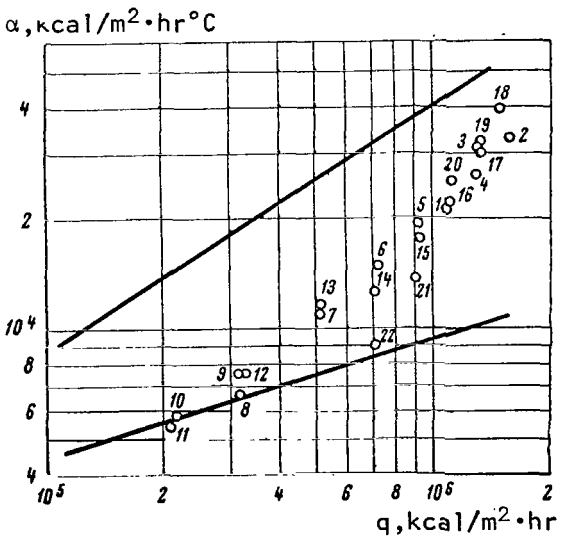


Figure 50. Influence of Heat Flux on Heat Removal Mode With Boiling of Sodium. Data of the Authors ($t_ж$ = 700°C).

## Dependence of Heat Transfer on Pressure

The dependence of the heat transfer coefficient on pressure with bubble boiling of non-metallic liquid has been investigated in the range of corrected pressures of approximately $10^{-3}$ to 1. On Figure 52, borrowed from [94], we show the dependence of the coefficient of heat transfer on the pressure for water and certain organic liquids. We see that in various pressure ranges the dependence of α on $P_s$ differs. At low pressures (in the range $P_s/P_{cr}$ approximately $10^{-3}$-$10^{-1}$) the heat transfer coefficient is proportional to the pressure in the range of approximately 0.2-0.25. In the area of low pressures ($P_s/P_{cr} < 10^{-3}$), insufficient experimental

/95

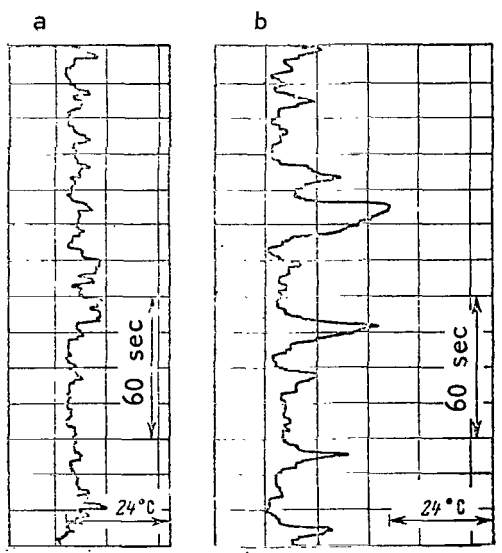


Figure 51. Recording of Temperature Difference Between Wall and Liquid for Point 4(a) and 6(b) Shown on Figure 50.

data are available for establishment of a reliable dependence of $\alpha$ on $P_s$. /95

The dependence of the heat transfer coefficient on pressure with developed boiling of alkali metals has been investigated by the author in experiments on cesium over a rather broad range of pressures. In experiments on other alkali metals, the investigated pressure ranges are more narrow.

On Figure 53 we show the data of the authors on heat transfer with developed boiling of cesium in coordinates $\alpha/q^{2/3} - P_s$. We can see from Figure 53 that with developed boiling of cesium the dependence of the heat transfer coefficient on pressure with $P_s$ of up to approximately 0.1 atm. abs. is stronger than with pressures of higher than 0.1 atm. abs. (within the limits of the pressure range investigated). The data produced are described by the empirical formulas (II.20), (II.21).

For sodium the dependence of heat transfer coefficient on pressure was determined in [16, 17, 19, 33, 35]. In [16] within the pressure range of approximately 0.15-1.25 atm. abs., no noticeable dependence of $\alpha$ on $P_s$ was produced. The dependence of $\alpha$ on $P_s$ based on the results of [35], as we can see from formula (II.14), is also rather weak. In [17], for the pressure interval 0.01-0.8 atm. abs., it was found that $\alpha \sim P_s^{0.25}$. According to the results of our experiments, no clear dependence of heat transfer coefficient on pressure with developed boiling of sodium under the pressure of its own vapors in the interval of $P_s$ of approximately 0.1 to 1 atm. abs. could be determined.

Figure 54 shows experimental data of the authors on heat transfer as a function of pressure produced in experiments with boiling of sodium beneath an inert gas. We can see from Figure 54 that with low pressures, as for cesium, the dependence of $\alpha$ on $P_s$ is stronger.

Figure 55 shows the dependence of the heat transfer coefficient on pressure during boiling of sodium according to the data of the authors (for developed boiling) and the data of [9, 17, 19, 33]. From work [17] we have constructed only points corresponding to the maximum heat flows at each pressure, since in a number of experiments a very steep dependence of $\alpha$ on q is noted, which may be related to transition from unstable boiling to developed boiling with increasing heat flow. The heat transfer coefficients produced in [19] we have related, as for the other data on Figure 55, to the difference of temperatures between the heating surface and the liquid. Figure 55 shows no points from [16, 35], since in [16] the data are constructed only in coordinates $\alpha$-q for a rather narrow range of pressures, and the data produced in [35] show a significantly different dependence of $\alpha$ on q than the other works and of that used on Figure 55. The Figure shows lines /100

corresponding to formulas (II.18) and (II.19). We can see that the experimental points as a whole agree rather well with dependences (II.18 and II.19).

/97

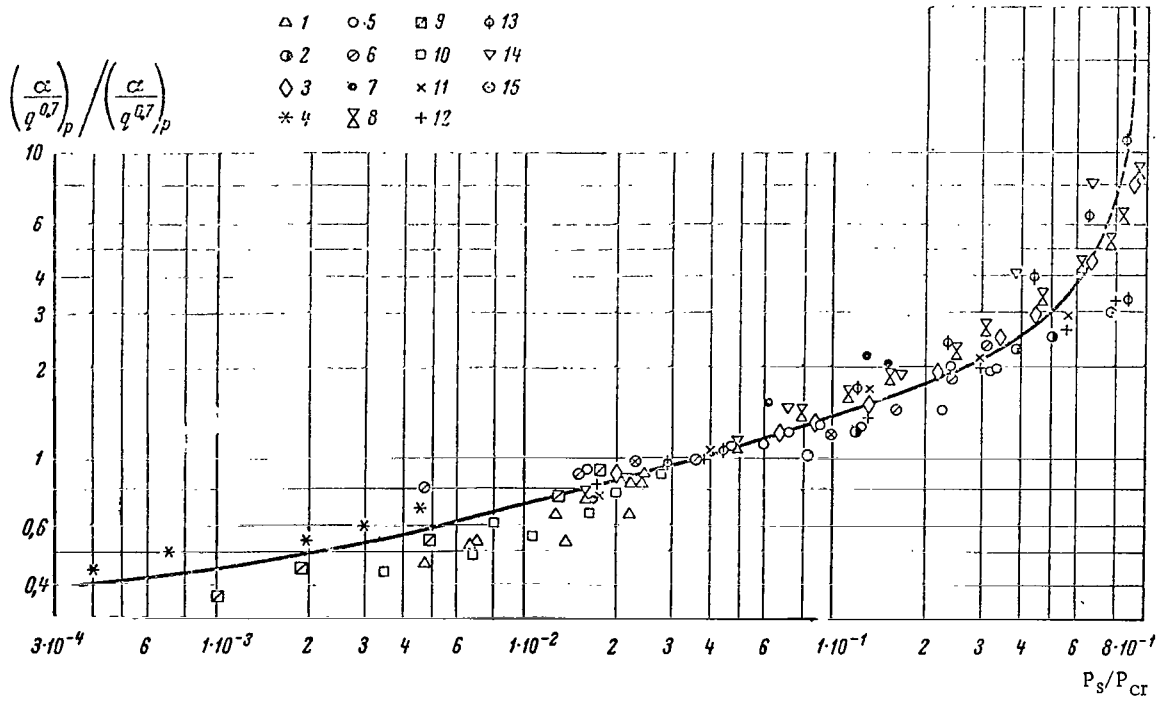


Figure 52. Heat Transfer Coefficient As A Function of Pressure With Bubble Boiling of Non-metallic Liquids [94]. 1-6, Water; 7-8, Ethyl alcohol; 9, Methyl alcohol; 10, Butyl alcohol; 11, 12, Heptane; 13, Pentane; 14, Benzene; 15, Freon. The value of $(\alpha/q^{0.7})p_*$ taken with reference pressure $P_* = 0.0294\ P_{cr}$.

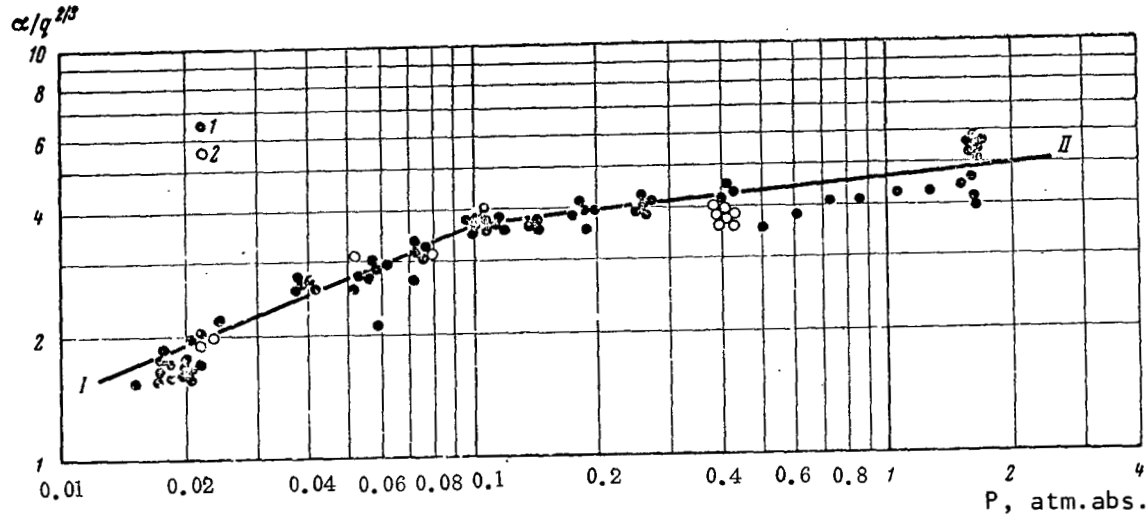


Figure 53. Experimental Data of the Authors on Heat Transfer With Developed Boiling of Cesium. I, According to formula (11.20); II, According to formula (11.21). 1, For a series of experiments; 2, Second series of experiments.

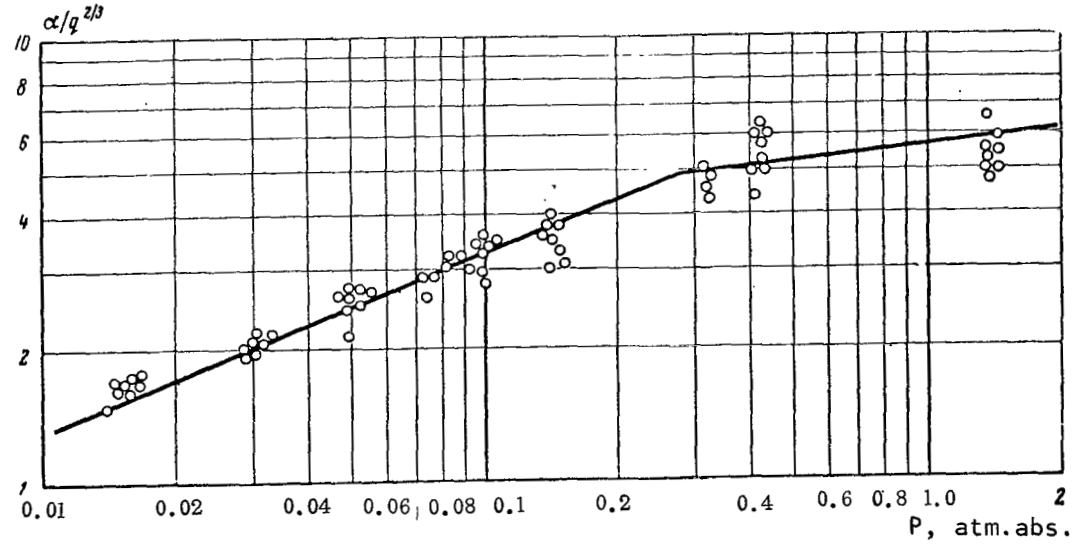


/98

Figure 54. Experimental Data of the Authors on Heat Transfer With Developed Boiling of Sodium Under Argon. Lines Constructed According to Formulas (11.18) and (11.19).

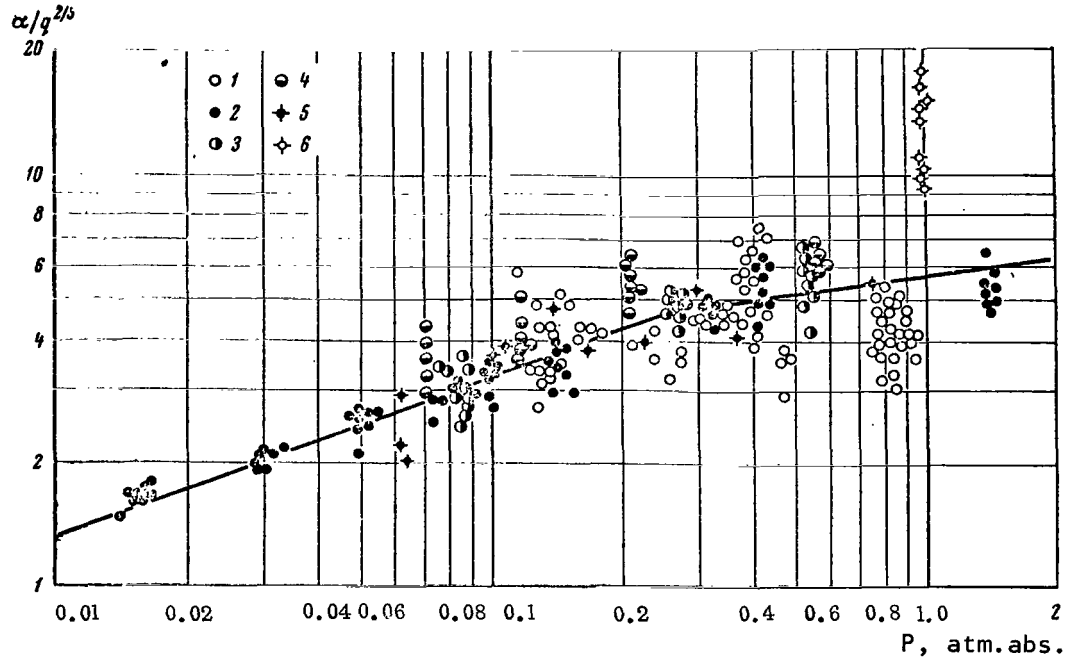


Figure 55. Comparison of Experimental Data of Various Authors On Heat Transfer During Boiling of Sodium Under Conditions of Free Convection. Lines Constructed According to Formulas (II.18) and (II.19).
1, Boiling under pressure of metal vapors; 2, Boiling under argon - data of the authors; 3, Data of Marto and Rohsenow [19]; 4, Data of Noyes [18, 33]; 5, Data of Petukhov et al., [17]; 6, Data of Lyon [9].

The quantity of data on heat transfer during boiling of potassium under conditions of free convection is more limited than that for sodium. In [20], experiments on potassium were performed at very low pressures (several mm of mercury) and at pressures of 1-2 atm. abs. The results of these experiments are shown on Figure 56. The dependence of the heat transfer coefficient on pressure in formula (II.15) was produced on the basis of processing of experimental data from Figure 56. Here also we see the dependence of the coefficient of heat transfer for heat removal by convection according to formula (II.5), since for the installation used in this work the value of $Gr > 10^8$ with $\Delta t_\alpha > 10°C$. As we can see, the value of the heat transfer coefficient produced in [20] at very low pressures does not exceed that calculated by formula (II.5). This, together with the necessity of great super heating to begin boiling at low pressures gives us reason to assume that heat removal here was by convection. Therefore, the dependence of the coefficient of heat transfer on pressure ($\alpha \sim p_s^{0.293}$) calculated in [20] for the boiling of potassium arouses doubt.

Figure 57 shows data on heat transfer with boiling of potassium produced by the authors and in [20]. In the investigated range of pressures, the exponent with $P_s$ can be taken the same for sedium and sodium, equal to 0.1. The averaging line on Figure 57 is described by the formula

$$\alpha = 4.8\, q^{2/3} p_s^{0.1} \qquad \text{(II.25)}$$

with $P_s$ ~0.1-2 atm. abs.

For this pressure range, the values of $\alpha$ calculated from formula (II.13) suggested by V. M. Borishanskiv et al., agrees well with calculation using formula (II.25).

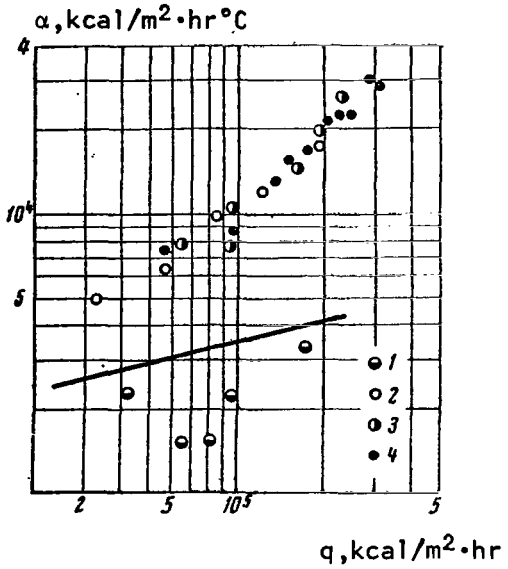


Figure 56. Experimental Data of Bonilla [20] on Heat Transfer During Boiling of Potassium. Line Corresponds to formula (II.5).
1, $P_s$ about 0.003 atm.abs.; 2, $P_s$ about 1 atm. abs.; 3, $P_s$ about 1.6 atm. abs.; 4, $P_s$ about 2.04 atm.abs.

On Figure 58, the experimental data on heat transfer with developed boiling of cesium, sodium and potassium, presented on Figure 53, 54 and 57 respectively, are constructed in the form of dimensionless complexes considering the primary physical properties influencing heat exchange during boiling as a function of the corrected pressure. The values of $P_{cr}$ are taken from [95]. It is easy to see that in the coordinates used, the experimental data for cesium, sodium and potassium agree rather well with each other. The averaging line corresponds to a certain smooth curve which for simplicity can be replaced with two straight lines (in logarithmic coordinates) described by exponential functions.

Thus, the heat transfer coefficient with developed boiling of cesium, sodium and potassium can be described by the generalized empirical formulas /102

$$\alpha = 8q^{2/3}\left(\frac{\lambda r\gamma}{\sigma T_s^2}\right)^{1/3}(P_s/P_{cr})^{0.45} \qquad \text{(II.26)}$$

for $P_s/P_{cr}$ about $4\cdot10^{-5}$ --1 • $10^{-3}$ and

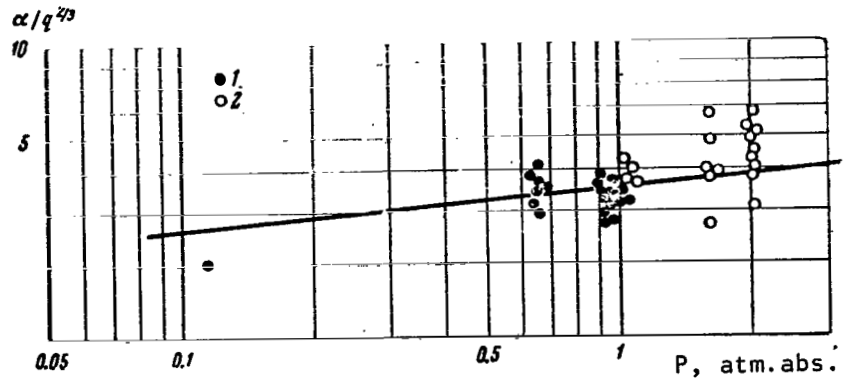


Figure 57. Experimental Data on Heat Transfer With Developed Boiling of Potassium. 1, Data of the Authors; 2, Data of Bonilla, et al., [20] (line corresponds to formula (II.25).

$$\alpha = q^{2/3}\left(\frac{\lambda r\gamma}{\sigma T_s^2}\right)^{1/3}\left(P_s/P_{cr}\right)^{0.15} \qquad \text{(II.27)}$$

for

$$P_s/P_{cr} \sim 1 \cdot 10^{-3}\text{--}2 \cdot 10^{-2}$$

It can be expected that within the range of corrected pressures investigated, dependences (II.26), (II.27) will also be correct for other alkali metals. However, this problem, like the problem of the possibility of using formula (II.27) where $P_s/P_{cr} > 2\cdot10^{-2}$, requires further experimental checking.

For the alkali metals analyzed with $P_s/P_{cr} > 10^{-3}$ (within the investigated range of $P_s/P_{cr}$), $\alpha$ about $P_s^{0.1}$, that is the heat transfer coefficient depends on the pressure somewhat more weakly than for non-metallic liquids, as can be seen by comparison of Figures 53, 54 and 57 with Figure 52. It should be noted that the difference in exponents with $P_s$ in the empirical formulas (II.18)-(II.21), (II.25) and the generalized dependence (II.26), (II.27) results from the fact that the complex $(\lambda r\gamma/\sigma T_s^2)^{1/3}$ is proportional to $P_s$ to approximately the - 0.05 power.

Analysis of experimental data on heat exchange during boiling of sodium and potassium shows that increasing pressure, both the probability of transition from heat removal by convection with subsequent heat removal by

evaporation from the free surface to heat removal by boiling, and the probability of transition from heat removal by unstable boiling to heat removal by developed boiling increase. The same picture is observed qualitatively in experiments on non-metallic liquids [72-75].

The data on Figures 44 and 50 were produced in one series of experiments, but with different pressures. Whereas at the low pressure (Figure 50) unstable boiling of sodium began with heat fluxes only greater than $0.5 \cdot 10^6$ kcal/m$^2$·hr, at the higher pressures (Figure 44) developed boiling occurred with heat fluxes of approximately $0.2 \cdot 10^6$ kcal/m$^2$·hr. However, in all experiments of the authors on cesium at low pressures (about 0.018 atm. abs.) stable, developed boiling was observed. The most unstable boiling of cesium occurred at pressures of 0.06-0.2 atm. abs. This influence of pressure on the nature of heat exchange during boiling of cesium on the surface of stainless steel, as thermodynamic calculations have indicated (see Figure 63) may be related to the fact that as the temperature changes, the cesium wettability of stainless steel changes. /104

It should be emphasized that we cannot note a value of pressure, for example for sodium at which a given heat removal mode will occur, since it is influenced by several other factors which will be analyzed below in addition to pressure.

## Influence of Certain Factors on Heat Transfer During Boiling of Alkali Metals

From the experiments with non-metallic liquids, it is known that heat exchange during boiling, particularly the heat transfer coefficient, may be influenced to some extent by such factors as the material and finish of the heat transfer surface and certain others. The quantity of similar data produced for alkali metals up to the present time is quite limited. In this section, we will analyze the influence of material, finish and geometry of the heating surface, contact time with the metal heat transfer medium, content of impurities in the heat transfer medium and inert gas on heat transfer during boiling of alkali metals.

### Material of heating Surface

The dependence of the heat transfer coefficient during boiling of non-metallic metals on the material of the surface has been studied in [96, 98], etc. For example, in [98] experiments were performed with ethyl alcohol and benzene on pipes of nickelized copper, silver and stainless steel over a broad range of heat flows and pressures. The finish of the surface in all cases was approximately the same. The values of $\alpha$ produced on surfaces of different materials, as the authors note, differ by up to 50%, particularly in the area of small pressures (the experiments were performed with $P_s > 1$ atm. abs.).

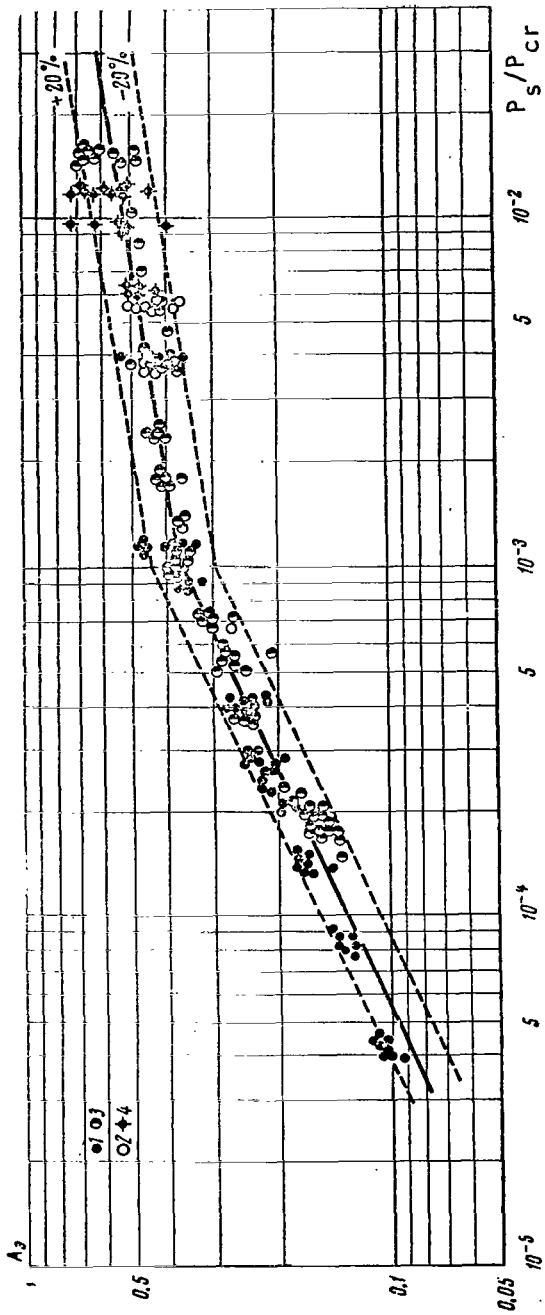


Figure 58. Generalized Dependence of Heat Transfer Coefficient With Developed Boiling of Alkali Metals on Corrected Pressure.

1, Sodium; 2, Potassium; 3, Cesium (data of the Authors); 4, Potassium - data of Bonilla et al., [20]. Averaging line corresponds to dependences (11.26) and (11.27):

$$A_e = \frac{\alpha}{q^{2/3}(\lambda r\gamma/\sigma T_s^2)^{1/3}}$$

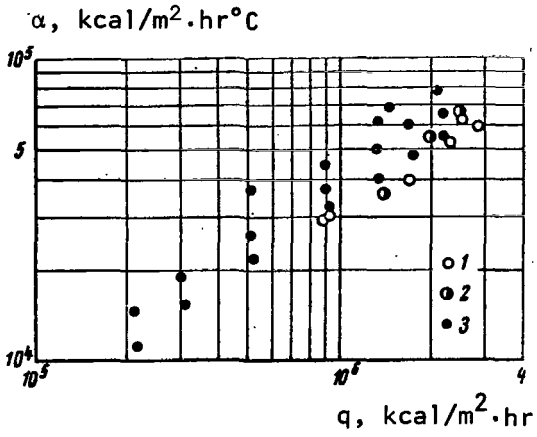


Figure 59. Influence of Heat Transfer Surface Material on Heat Transfer During Boiling of Sodium According to Data of the Authors. 1, Copper; 2, Nickel and chromium; 3, Stainless steel type 1Kh18N9T ($t_z$ = 700°C).

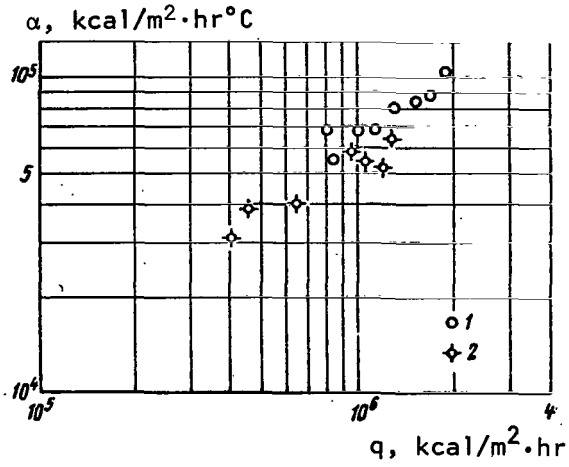


Figure 60. Influence of Surface Material On Heat Transfer During Boiling of Sodium According to Data Of Noyes and Lurie [33]. 1, Stainless steel surface; 2, Molybdenum surface ($P_s$ ~ 0.21 atm. abs.).

/105

No systematic investigation of the influence of the heating surface material on heat exchange during boiling of alkali metals has been performed. Up to the present time, experimental data on heat transfer during boiling of sodium on surfaces of stainless steel (works [9, 16-19, 33, 35] - experiments of the authors), nickel ([19] and experiments of the authors), molybdenum ([33]), chromium and copper (experiments of the authors) have been performed. In the experiments of the authors on surfaces of stainless steel, chromium, nickel and copper (Figure 59) as well as the experiments of Noyes and Lurie [33] on surfaces of stainless steel and molybdenum (Figure 60) no noticeable difference in heat transfer coefficients during developed boiling of sodium have been detected. Values of heat transfer coefficients produced by Marto and Rohsenow [19] on surfaces of nickel and stainless steel agree well with each other.

/106

In the experiments of the authors on sodium boiling over surfaces of stainless steel, chromium, nickel and molybdenum (experiments on the investigation of critical heat flows) various heat removal modes have been noted (heat removal by convection, heat removal by unstable and developed boiling), while over the copper surface, which became rough (eroded) as a result of interactions with the sodium, only developed boiling was noted.

It is noted in [19] that boiling of sodium on a surface of nickel, with otherwise equivalent conditions, is more stable than on a surface of stainless steel. However, we should note that this effect may be related not only with

the influence of the material of the wall, but also with the influence of other factors not considered in [19].

Alkali metals may interact actively with the heating wall. Alkali metals will reduce metal oxides if the free energy of the system is decreased as a result of the reaction [99].

$$M_xO_s + 2sN \rightleftarrows s\,N_2O + xM. \qquad \text{(II.28)}$$

Here M, O, N represent the structural metal, oxygen and the alkali metal respectively. On Figure 61-63 we present diagrams for sodium, potassium and cesium produced by approximate thermodynamic calculations performed at the Physics and Energy Institute by M. N. Arnol'dov on the measurement of the free energy of the system resulting from reaction (II.28). We know of no data concerning the rate of reduction of metal oxide films by alkali metals.

If the oxides of the heat transfer metal are reduced by the heating wall, this may change the wettability and roughness of the heating surface and correspondingly change the heat transfer conditions (level of $\alpha$ with boiling, heat removal mode). Accumulation of oxides on the heating wall also leads to an increase in thermal resistance, causing a decrease in the value of $\alpha$ determined from the indications of thermocouples built into the wall. Therefore, in planning of experiments and analysis of experimental data, the direction of reaction (II.28) should be considered.

Thus, the available relatively sparce data on heat transfer during boiling of sodium over surfaces made of stainless steel, nickel, chromium, molybdenum and copper indicate that the levels of the heat transfer coefficients with developed boiling of sodium on surfaces of these metals is approximately identical. However, further investigations are required to determine the influence of the material of the heating wall on heat exchange /108
during boiling of alkali metals, particularly considering interaction of the heat transfer medium with the heating wall.

Finish of Heating Surface

In [100-102], an essential influence of roughness on the heat transfer coefficient was discovered during boiling of water and certain organic fluids. For example, in the experiments of Berenson [102] with normal pentane at atmospheric pressure, the heat transfer coefficient varied by 5-6 times as a function of the finish of the surface with heat flows right up to the critical values.

Figure 64 shows the data of Marto and Rohsenow [19] on heat transfer during boiling of sodium on surfaces with various finishes, while Figure 65 shows photographs of microscope sections of certain of these surfaces. Analysis of Figure 64 and 65 shows that the specific roughness increases the coefficient of heat transfer. The coefficients of heat transfer change

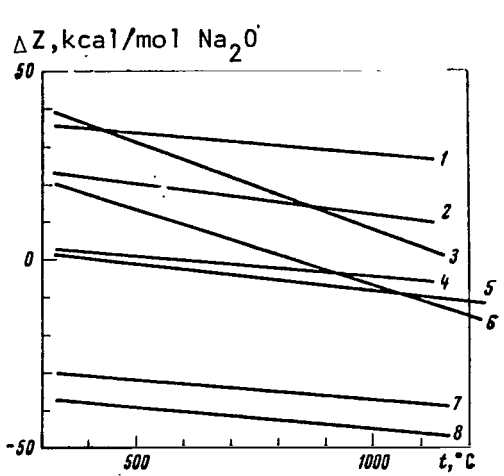


Figure 61. Change in Free Energy of System as a Result of Reaction (11.28) of Metal Oxides With Sodium.

1 — $Na_2O + Ni = NiO + 2Na$;
2 — $Na_2O + {}^1/_2 Mo = {}^1/_2 Mo O_2 + 2Na$;
3 — $Na_2O + {}^3/_4 Fe = {}^1/_4 Fe_3O_4 + 2Na$;
4 — $Na_2O + {}^2/_5 Nb = {}^1/_5 Nb_2O_5 +$ $+ 2 Na$;
5 — $Na_2O + {}^2/_3 Cr = {}^1/_3 Cr_2O_3 {}^1/_4 +$ $+ 2Na$;
6 — $Na_2O + Fe = FeO + 2Na$;
7 — $Na_2O + Ti = TiO + 2Na$;
8 — $Na_2O + Zr = ZrO_2 + 2Na$

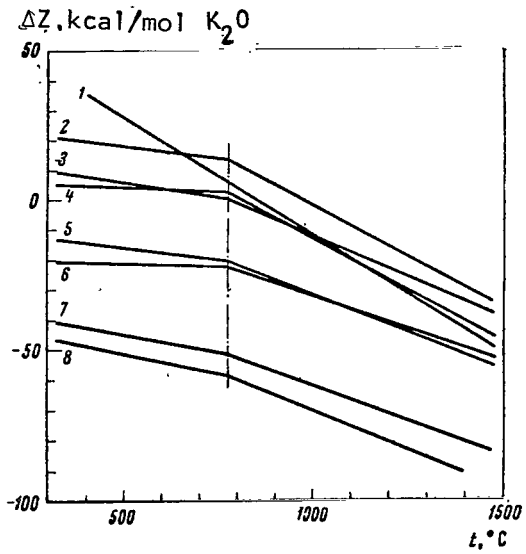


Figure 62. Change in Free Energy of System as a Result of Reaction (11.28) Of Metal Oxides With Potassium.

1 — $K_2O + Fe = FeO + 2K$;
2 — $K_2O + Ni = NiO + 2K$;
3 — $K_2O + {}^1/_2 Mo = {}^1/_2 MoO_2 + 2K$;
4 — $K_2O + {}^3/_4 Fe = {}^1/_4 Fe_3O_4 + 2K$;
5 — $K_2O + {}^2/_5 Nb = {}^1/_5 N_2O_5 + 2K$;
6 — $K_2O + {}^2/_3 Cr = {}^1/_3 Cr_2O_3 + 2K$;
7 — $K_2O + Ti = TiO + 2K$;
8 — $K_2O + {}^1/_2 Zr = {}^1/_2 ZrO_2 + 2K$

/107

particularly strongly in comparison with a smooth surface (both in magnitude and in dependence on heat flow) over a surface with artificial depressions having expansions at their lower ends. The boiling process on surfaces with roughnesses as shown on Figure 65, a, c, d, is more stable than on the smooth surface. On rough surfaces, as the heat flow increases, the values of heat transfer coefficients approach $\alpha$ for the smooth surface. Drilling of /110
cylindrical depressions (Figure 65, b) and etching of the surface with acid did not cause an increase of $\alpha$ in the experiments of Marto and Rohsenow, nor an increase in the stability of heat exchange.

Thus, depending on the finish of the heating surface, as the experiments of Marto and Rohsenow on sodium showed, the value of the heat transfer coefficient with developed boiling of alkali metals may vary just as in non-metallic liquids. The finish of the surface influences the stability of boiling as well. However, only a specific roughness, for example the artificial depressions expanding at the bottom, roughness formed by welding and some others have a noticeable influence on heat exchange during boiling.

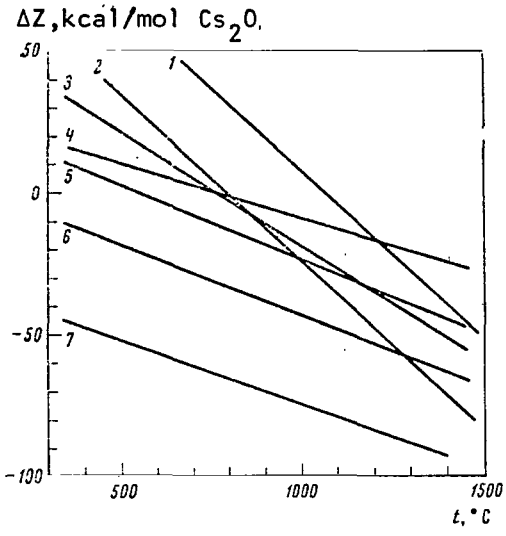


Figure 63. Change in Free Energy of System as a Result of Reaction (II.28) of Metal Oxides With Cesium.

1 — $Cs_2O + {}^1/_3\,Mo = {}^1/_3\,MoO_3 + 2Cs$;
2 — $Cs_2O + {}^2/_5\,Nb = {}^1/_5\,Nb_2O_5 + 2Cs$;
3 — $Cs_2O_2 + {}^1/_3\,Mo = {}^1/_3\,MoO_3 + 2Cs$;
4 — $Cs_2O + Ni = NiO + 2Cs$;
5 — $Cs_2O + {}^3/_4\,Fe = {}^1/_4Fe_3O_4 + 2Cs$;
6 — $Cs_2O + {}^2/_3\,Cr = {}^1/_3\,Cr_2O_3 + 2Cs$;
7 — $Cs_2O + Ti = TiO + 2Cs$

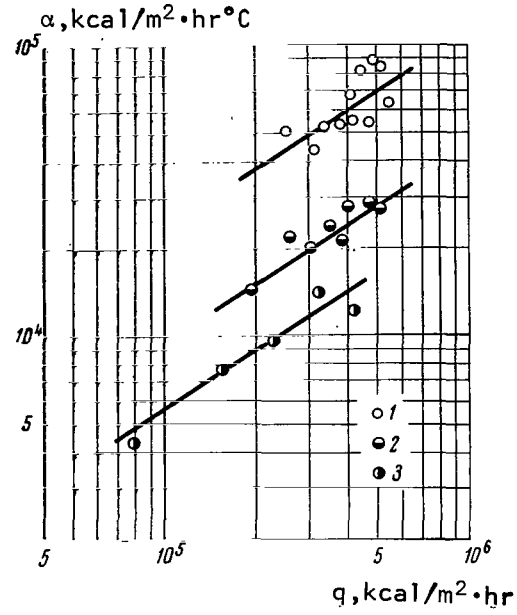


/109

Figure 64. Influence of Roughness on Heat Transfer During Boiling of Sodium According to Data of Marto and Rohsenow [19]. 1, Surface with depressions expanding downward (see Figure 65); 2, Rough surface; 3, Smooth surface.

## Geometry of the Heating Surface

On the basis of experimental data of a number of authors, we can conclude that the dimensions of the heating surface (over a broad range), of the liquid column and orientation of the surface, excluding cases when it is difficult for vapors to leave the surface [103], have no influence on the heat transfer coefficient during bubble boiling of ordinary liquids. The values of the heat transfer coefficients during boiling of sodium produced in experiments on a flat surface as a whole, as we can see from Figure 55, agree satisfactorily with the values of α produced in experiments with boiling of sodium on the surfaces of horizontal tubes.

Figure 66 shows the relative increase in the heat transfer coefficient during boiling in comparison to the heat transfer coefficient during convection for water and sodium as applicable to the design of the installation of the authors (Figure 10, 24). For sodium, the heat transfer coefficients were calculated using formulas (II.4), (II.17), and for water they were calculated using the formulas

/111

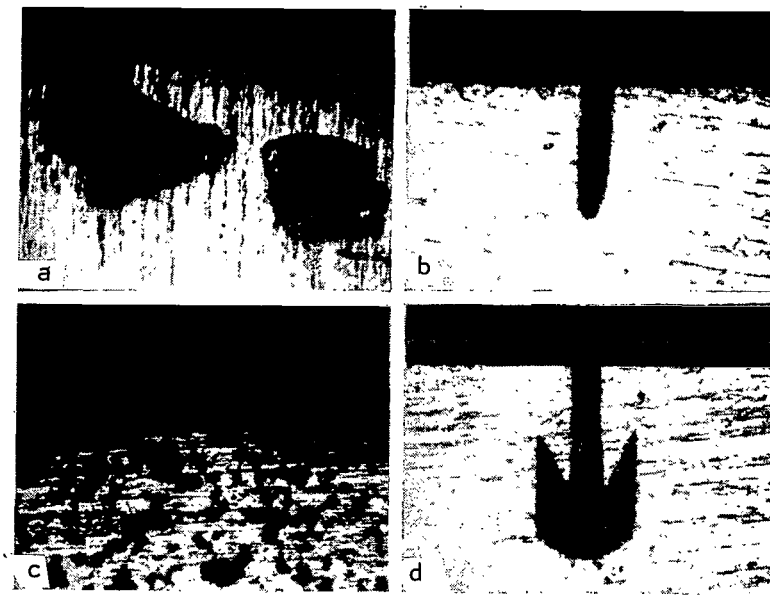


Figure 65. Photographs of Microsections of Working Sectors Used by Marto and Rohsenow [19]; a, Roughness formed by welding; c, Porous nickel; b, Cylindrical depression (diameter 0.1 mm, depth 0.5 mm); d, Depression expanding at the bottom (minimum diameter 0.1 mm, depth 0.6 mm).

$$\alpha = 414\,\Delta t_{\alpha}^{1/3}, \tag{II.29}$$

$$\alpha = 3q^{0.7}, \tag{II.30}$$

which are presented in [88].

We can see from Figure 66 that for water the heat transfer coefficient during boiling increases in comparison with $\alpha$ during convection essentially more rapidly than for sodium. This indicates that the relative contribution of convection to the heat transfer coefficient during boiling of the metals is greater than during boiling of non-metallic liquids. The data produced on various installations for heat transfer during boiling may differ somewhat from each other, particularly at low heat flows (when the number of active centers of vapor formation is small), since the heat transfer coefficient with free convection in the laminar area depends on the geometry of the working sector ($Nu \sim Gr^{1/4}$). With increasing heat flow, this difference should decrease.

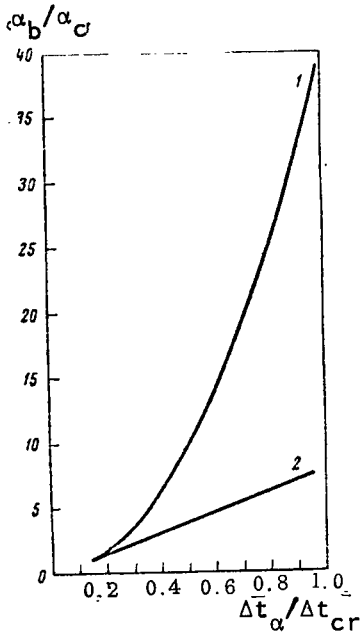


Figure 66. Relative Increase in Heat Transfer Coefficient During Boiling in Comparison to Heat Transfer Coefficient During Convection Under Conditions of Free Convection As A Function of Relative Temperature Head for Water (1) and Sodium (2) at Atmospheric pressure. $\Delta t_{cr}$, temperature head corresponding to $q_{cr}$.

Contact Time of Heating Surface to Heat Transfer Medium

We know from our experiments on non-metallic liquids that the coefficient of heat transfer with bubble boiling may change slightly, particularly in the initial period of operation. This is related to a change in the number of active centers of vapor formation as a result of degassing of the surface and precipitation of impurities on the heating surface.

For alkali metals, a change in heat exchange with time should also be expected, since they may interact with the heating surface.

Let us analyze the change in heat transfer with time in experiments on sodium. Figure 67 shows the dependence of the heat transfer coefficient on time during boiling of sodium on a surface of stainless steel with constant temperature and heat flow, produced in the experiments of the authors. Before the beginning of the experiments, the surface was contacted with liquid sodium for approximately 23 hours. During the first 8 hours of performance of experiments, alternation of convection and unstable boiling occurred (Figure 67, 68), while during the last 9 hours heat removal was exclusively by convection without boiling, with the same q and $t_\zeta$. Then experiments were performed with different heat fluxes (these data are shown on Figure 46). Unstable boiling, replaced with convection, began only at $q = 0.8 \cdot 10^6$ kcal/m$^2$·hr (point 2 on Figure 46). In another series of experiments (Figure 69) for 10 hours (at $q = 1.09 \cdot 10^6$ kcal/m$^2$·hr and $t_\zeta \sim 700°C$) only unstable boiling occurred. /113

In the experiments of the authors whose results are presented on Figure 43, heat removal occurred with developed boiling. Only at the end of the experiments (point 16) did boiling cease for a certain amount of time at $q \sim 0.9 \cdot 10^6$ kcal/m$^2$·hr, whereas at the beginning boiling occurred at lower heat fluxes. The contact time of the heating surface with the sodium before these experiments was approximately one-half that before the experiments whose results are shown on Figure 69.

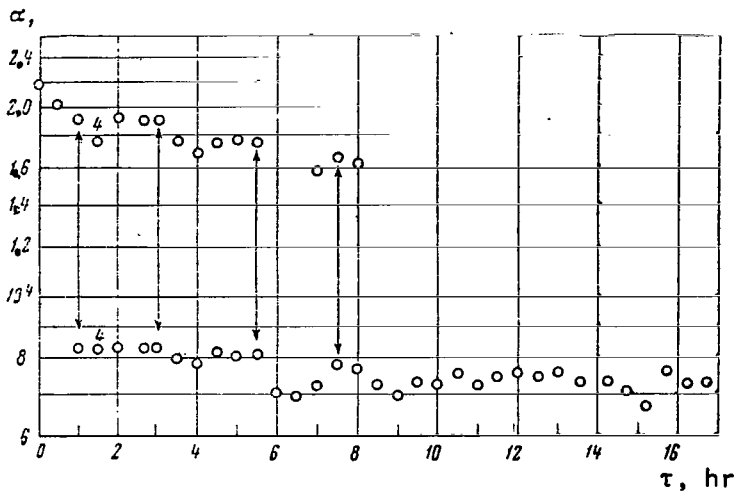


Figure 67. Influence of Contact Time of Heating Surface of Stainless Steel Type 1Kh18N9T With Boiling Sodium on Heat Exchange. (Data of the authors: $q \sim 0.7 \cdot 10^6$ kcal/$m^2 \cdot hr$; $t_l \sim 690°C$; $\alpha \cdot 10^{-4}$ kcal/$m^2 \cdot hr°C$). Top points, unstable boiling; bottom points, convection.

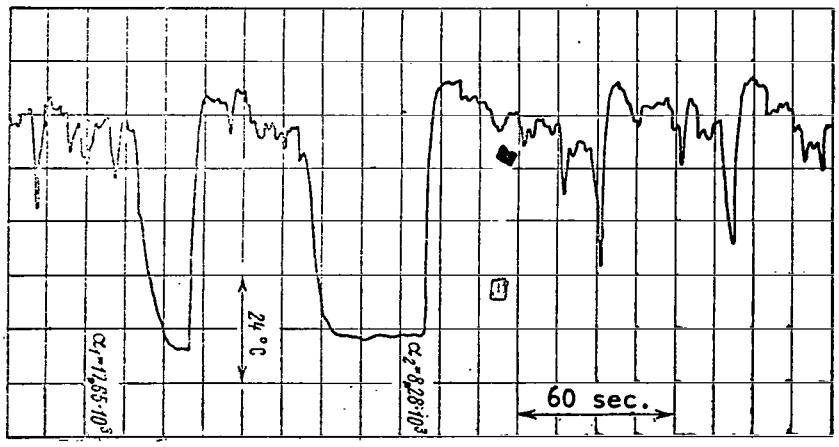


Figure 68. Recording of Temperature Difference Between Wall and Liquid for Point 4 Shown on Figure 67.

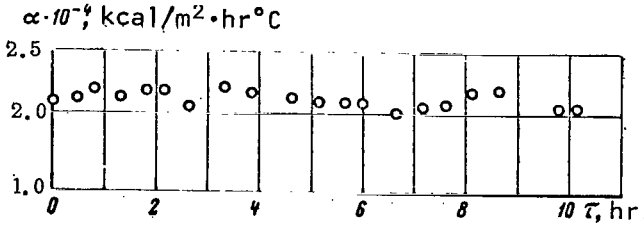


Figure 69. Dependence of Heat Transfer Coefficient During Boiling of Sodium on Time. Data of the authors: $q = 1.09 \cdot 10^6$ kcal/m²·hr, $t_l = 700°C$.

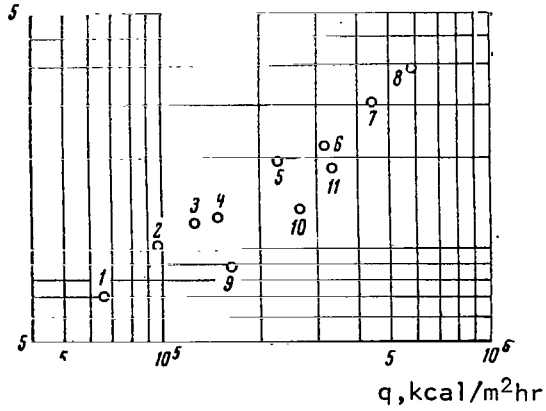


Figure 70. Time Dependence of Heat Transfer Coefficient During Boiling of Sodium ($\alpha \cdot 10^{-4}$ kcal/m²·hr°C). Data of Marto and Rohsenow [19].

Figure 70 shows experimental data on heat transfer during boiling of sodium on a smooth nickel surface, produced by Marto and Rohsenow [19]. We can see that for the first experiments the heat transfer coefficients were higher. The increased superheating of the sodium with time was observed in [76, 79] (see Figure 36).

Thus, these data indicate that an increase (apparently to a certain limit) of the contact time of the heating surface (of stainless steel or nickel) with sodium leads, with otherwise equivalent conditions, to an increase in the instability of heat exchange during boiling and an increase of the heat flow required to maintain boiling. /114

This influence of contact time of the heating surface with sodium may be related to reduction of oxides on the heating surface by the sodium. If this is so, then as time passes stabilization of this process should occur. If the material of the heating surface reduces oxides of the metal being boiled, the influence of contact time should be different than that analyzed above. Furthermore, we should keep in mind that with extended contact (thousands of hours) the roughness of the surface may change markedly as a result of corrosion of the structural material.

## Content of Impurities in the Metal Boiled

The corrosive influence of alkali metals on structural materials depends on the content of such corrosion active impurities as oxygen, nitrogen, carbon and hydrogen [99]. Therefore, the content of these impurities may influence heat exchange during the boiling of alkali metals by changing the state of the surface of the heating wall by corrosion. A typical impurity for alkali metals is their oxides.

The experiments of the authors on sodium have shown that a change in the oxygen content in sodium of $10^{-3}$ to $10^{-1}$ % by weight has no influence on heat transfer during the time of performance of their experiments, which did not exceed 100 hours. The content of oxygen in alkali metals, in addition to corrosion, may also influence heat exchange by boiling as follows.

1. When the content of oxides exceeds the solubility limit at a given temperature, the oxides may precipitate on the heating surface. This may change the properties of the surface (wettability, roughness) and cause additional thermal resistance [104]. Figure 71 shows curves of the solubility for sodium and potassium. In our experiments, the content of oxides in sodium was below their limit of solubility at the experimental temperatures.

2. Depending on the content of oxygen, the thermo-physical properties of the alkali metals, particularly surface tension, may change.

However, as is noted in [106], an increase in the content of oxides in sodium up to the limit of solubility at the temperature used, decreases surface tension by only 8-10%. Other thermo-physical properties of sodium also should not be strongly dependent on the content of oxides in the sodium. Therefore, the change of heat physical properties of alkali metals resulting from changes in the oxide content, within their limits of solubility should not influence heat transfer during boiling. /115

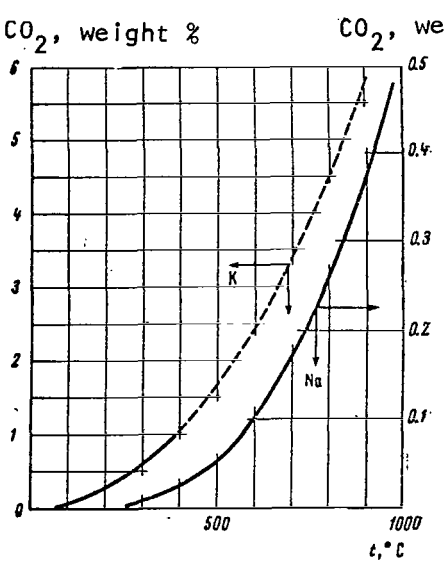


Figure 71. Solubility of Oxygen in Sodium [66] and Potassium [105].

In alkali metals we may also find such impurities as nitrides and hydrides. Experiments performed at the Physics and Energy Institute by M. N. Ivanovskiy et al., have shown that at high temperatures, hydrogen is liberated from hydrides. Due to technological considerations, these gases are usually removed from the system. However, if hydrogen which is liberated remains, it may influence heat exchange during boiling in the same way that an inert gas does.

Influence of an Inert Gas

The experiments of the authors performed on sodium and potassium have shown that the presence of an inert gas (argon was used) stabilizes the boiling process. In experiments when the inert gas was absent and sodium was held under the pressure of its own vapors, developed boiling of sodium began only at pressures over 0.5 atm. abs. with

heat fluxes over $1.1 \cdot 10^6$ kcal/m$^2$·hr. In this series of experiments, the boiling of sodium under the pressure of its own vapors was characterized by instability (spontaneous transition from one mode of heat removal to another) throughout the entire investigated range of pressures (approximately 0.5-1.5 atm. abs.) and heat fluxes (up to $q_{cr}$). Heat removal was achieved primarily by convection with subsequent liberation of heat by evaporation from the free surface or by unstable boiling. When the boiling of the sodium occurred under an inert gas (argon), the pressure of which corresponded approximately to the saturation pressure, developed boiling began at a pressure of approximately 0.015 atm. abs. with a heat flux of about $0.5 \cdot 10^6$ kcal/m$^2$·hr /116
and existed stably throughout the entire investigated range of pressures (approximately 0.015-1.5 atm. abs.). A similar picture was observed in experiments on potassium.

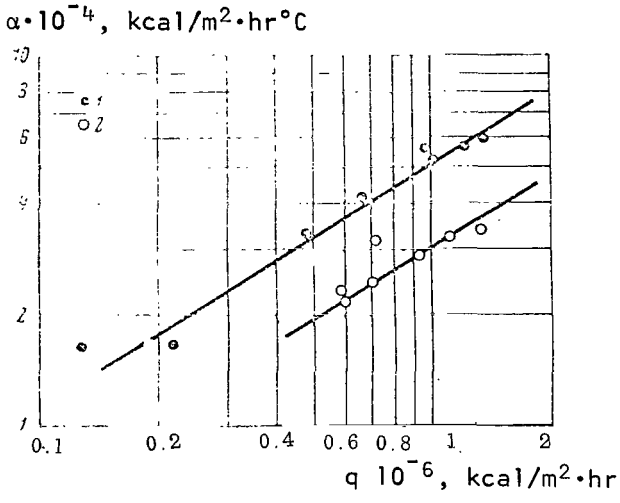


Figure 72. Influence of Gas on Heat Transfer Coefficient With Developed Boiling of Sodium. Data of the authors. 1, Experiments under gas; 2, Experiments under pressure of sodium vapors ($t_l$ = 910 ± 20°C).

The values of heat transfer coefficients produced in experiments with developed boiling of sodium under the pressure of its own vapors were somewhat lower than the values of α produced in experiments under gas (Figure 72). With potassium, we produced values of α only by boiling beneath the pressure of its own vapors.

In the experiments of Bonilla [20], boiling of potassium in the range of pressures of 1-2 atm. abs. occurred under argon and only one experiment was performed with boiling of potassium under the pressure of its own vapors. The value of heat transfer coefficient produced was approximately the same as the value of α produced by boiling potassium under argon. On this basis, it is concluded in [20] that the inert gas has no influence on the value of α during the boiling of potassium. However, we feel that it is a bit early to make this conclusion on the basis of but a single experiment. In other works, experiments on heat transfer during boiling of alkali metals were performed either only under the pressure of the vapors of the boiling metal or only under the pressure of the inert gas. We do not feel that these data can be used to determine the influence of the gas on heat transfer during boiling of alkali metals, since they may be influenced to the same extent by other factors as well.

Thus, this analysis of experimental work indicates that heat exchange during boiling of alkali metals, in addition to pressure, may be influenced by such factors as the material (stability, heat removal mode), finish of the heating surface (stability, heat removal mode, level of $\alpha$), time of contact of heating surface with alkali metal (stability, heat removal mode), impurities (stability, heat removal mode, level of $\alpha$), inert gas (stability, heat removal mode, level of $\alpha$) and to a certain extent by the design (geometry) of the installation. However, quantitative data on the influence of these factors on heat transfer during boiling of metals are as yet sparce. /117

In conclusion we note that with moderate vapor contents, (up to approximately 20%), the values of heat transfer coefficients during boiling of potassium in pipes, according to the data of [23-26, 30] are approximately the same as during boiling in large volumes. It can be expected that a similar picture will be observed for other alkali metals.

## Heat Transfer During Boiling of Mercury and Amalgam

The quantity of data on heat transfer during boiling of mercury is quite limited. The list of works analyzed is presented in Table II.2.

The authors have produced experimental data on heat transfer during boiling of mercury of very flat horizontal surface. The boiling of mercury occurred in a tank with an internal diameter of 45 mm, the lower end of which contains the heating wall, as shown on Figure 11, c. The copper which carried the thermocouples was separated from the mercury by a wall of Armco iron 0.3 mm thick. Film boiling occurred for approximately 40 hours. The temperature of the working sector was maintained between 700 and 970°C, the temperature of the liquid at 360°C. Then, heat exchange improved. However, as was determined upon completion of the experiments, the Armco iron had broken down over a portion of the working surface area and the mercury contacted the copper directly. The rate of solution of iron in mercury depends on the temperature and the content of oxygen [107]. In the experiments in which the heat transfer was studied, the boiling of mercury occurred under the pressure of its own vapors at $P_s$ approximately 5 atm. abs. These data should be looked upon as preliminary.

The boiling of mercury on steel surfaces usually does not involve film boiling. This results from the fact that mercury does not wet oxide films [4, 9]. The formation of oxide films on the steel surface in air occurs in a fraction of a second [4]. However, a fresh steel fracture made beneath a layer of mercury is wet by the mercury [4].

In the work of M. I. Korneyev [6] the following formula is suggested for the heat transfer coefficient with film boiling of mercury at atmospheric pressure for heat fluxes up to approximately $10^5$ kcal/m$^2$·hr: /119

$$\alpha = 2.76\,10^{10}\,q^{-1.58}. \qquad \text{(II.33)}$$

TABLE 11.2

| Authors, reference, year of publication | Range of pressure invest. (atm.abs.) | Range of heat flux-invest., $10^{-6}$ kcal/ $m^2 \cdot hr$. | Recommend. formulas | Characteristics of working sector | Notes |
|---|---|---|---|---|---|
| Lyon, Foust, Katz, [9], 1955 | 1 | 0.011-0.080<br>0.006-0.016<br>0.005-0.27 | | Horizontal stainless steel tube 19 mm in diam., 127 mm long. Chromel-alumel thermocouples in drilled wells 1 mm in diam. Radiation heating by current located within tube. Tank diam. 89 mm. | Mercury. Film boiling.<br>Mercury + 0.1% Na; $q_{cr} = 1.6 \cdot 10^5$ kcal/$m^2 \cdot hr$.<br>Mercury +0.02% Mg + 0.0001% Ti |
| M. I. Korneyev, [6-8], 1955, 1963 | 1-10 | 0.01-0.1<br>0.01-0.35 | $\alpha = 5.25q^{0.67}$ Formula (11.31) | Horizontal and vertical tubes of carbon steel diam. 22 mm, length 190 mm. Chromel-alumel thermocouples. Current heating of graphite rod located within tube. | Merc. Film boil.<br>Mercury + 0.01--0.4% Mg. |
| | | 0.01-0.1 | $\alpha = 0,36q^{0.847}$ Formula (11.32) | Copper tube. | Mercury. |
| Bonilla et al., [10], 1957 | 0.005-3 | 0.016-0.34 | | Horizontal carbon steel plate 76 mm diam. Iron-constantan thermocouples located through height of sector. Heat supplied from plate soldered to sector (see Figure 6). Tank diam. 76 mm. | Mercury. Nucleate boiling began after several weeks operation with film boiling. |
| | 0.113-1.09 | 0.019-0.54 | | | Mercury + 0.02% Mg + 0.0001% Ti. |

Bubble boiling of mercury without addition of surfactants occurred in the experiments of Bonilla [10] on a carbon steel surface, in the experiments of M. I. Korneyev [6] on a copper surface and in the experiments of the authors. In the experiments of Bonilla [10], stable bubble boiling of mercury was observed after extended (several weeks) film boiling. Bubble boiling is possible in addition to film boiling with forced movement of mercury through carbon steel tubes [4, 5]. L. N. Gel'man [5] notes that "good heat exchange could never be achieved immediately after beginning of operation. Only significant over heating of the wall (by about 250 °C leads to partial disruption of continuity and density of the film, and after 60-80 hours operation with considerable velocity of the vapor-mercury mixture (40-60 m/sec) did good heat exchange begin" ($\alpha \sim 10^4$ kcal/m$^2$·hr°C with $q \sim 65 \cdot 10^3$ kcal/m$^2$·hr). The improvement of heat exchange is explained in [4, 5, 10] by removal of the oxide film from the surface. In [12], heat exchange during the boiling of mercury in a stainless steel tube was studied. Upon dismantling of the installation after 100 hours operation in the boiling mode, which was preceded by 100 hours operation without boiling, no traces of wetting of the surface with mercury were observed, although the wall temperature reached 700-760°C. The values of the heat transfer coefficients produced in these experiments were essentially lower than the values of $\alpha$ characteristic for bubble boiling. Hochman [108], on the basis of analysis of data from the literature, concluded that under the proper conditions wetting of the steel surface with mercury can be achieved, but in order for this to occur both the surface and the mercury must be quite pure. However, [108] gives no information on temperature conditions.

In order to improve the wetting of steel surfaces with mercury, small quantities of surfactants are added to the mercury. Magnesium, magnesium plus titanium and less frequently sodium are used for this purpose. During bubble boiling of magnesium amalgams over a copper surface under natural circulation conditions, heat fluxes up to $1.6 \cdot 10^6$ kcal/m$^2$·hr have been achieved [11].

In order to calculate the heat transfer coefficients with bubble boiling of mercury and amalgam under conditions of free convection and with forced circulation (with a vapor content by weight of up to 10%) in the pressure range from 0.07 to 11 atm. abs., the following formula is suggested in [109]:

$$\alpha = 2.8q^{0.7} p_s^{0.3} \qquad \text{(II.34)}$$

This formula was produced by processing experimental data on heat transfer during boiling of mercury under conditions of free convection presented in [10], and experimental data on heat transfer during boiling of amalgams under conditions of free convection and in pipes presented in [6, 8, 11]. /120

Figure 73 shows experimental data of the authors on the heat transfer observed during boiling of mercury and the dependences described by formulas (II.31), (II.32) and (II.34). If dependence (II.32), describing the experimental data of M. I. Korneyev on heat transfer during boiling of mercury on

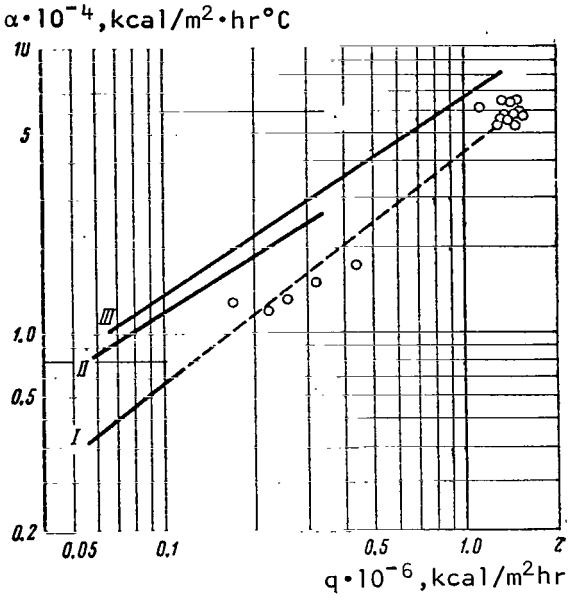


Figure 73. Experimental Data of the Authors on Heat Transfer During Boiling of Mercury Under Conditions of Free Convection ($P_s$ approximately 5 atm. abs.). I, According to Formula (II.32); II, According to Formula (II.31); III, According to Formula (II.34).

the surface of a horizontal copper tube are extrapolated (dotted line) to the area of higher heat flows, it would agree well with our experimental data. The values of heat transfer coefficients calculated from formula (II.31) and the values of α calculated from formula (II.34) for 5 atm. abs. (the mean pressure in the experiments for which the points on Figure 73 are constructed) falls somewhat higher.

A change in the content of magnesium in mercury from $1 \cdot 10^{-2}$ to $4 \cdot 10^{-2}$% by weight, according to the data of M. I. Korneyev [6, 7], leads to no change in the heat transfer coefficients. In experiments [6, 7] on heat transfer during boiling of amalgam on the surface of a horizontal tube, the intensity of heat exchange differed around the perimeter of the tube. The absolute values of heat transfer coefficients on the upper generatrices of the tube were approximately three times the values of α on the lower generatrices. The values of heat transfer coefficients on the upper generatrices of the tube were the same as for a vertically placed tube. /121

Figure 74 shows experimental data on heat transfer during boiling under conditions of free convection of mercury and amalgam as a function of pressure. With pressures approximately up to atmospheric pressure, according to the experimental data of Bonilla both for mercury and for amalgam, the heat transfer coefficient depends on the pressure to approximately the 0.3 power ($\alpha \sim P_s^{0.3}$). With pressures above atmospheric, there are insufficient data available to determine the dependence of α on $P_s$. Possibly at pressures over atmospheric the dependence of the coefficient of heat transfer on pressure during boiling of mercury and amalgam will be weaker than at pressures below atmospheric.

For example, M. I. Korneyev [6-8] notes that as the pressures change from 1 to 10 atm. abs., the coefficient of heat transfer increases by approximately 20%. This increase in α corresponds to the dependence of α on

$P_s$ to approximately the 0.1 power ($\alpha \sim P_s^{0.1}$). For the alkali metals analyzed above at pressures up to approximately $10^{-3}$ $P_{cr}$, the dependence of the heat transfer coefficient on pressure is considerably stronger ($\alpha \sim P_s^{0.4}$) than at higher pressures ($\alpha \sim P_s^{0.1}$) within the limits of the pressure range investigated. For mercury, a corrected pressure of $10^{-3}$ corresponds to an absolute pressure of approximately 1.6 atm. abs. [110].

We can see from Figure 74 that the data of Bonilla and Lyon produced by boiling amalgam are approximately twice as high as the data of Bonilla produced by boiling mercury. Formula (II.34) is produced without considering the data of Bonilla [10] and Lyon [9] on heat transfer during boiling of amalgam. Formula (II.34) essentially describes only the data of Bonilla [10] on heat transfer during boiling of mercury.

Therefore, considering what we have said concerning the dependence of the heat transfer coefficient on pressure at pressures above atmospheric, formula (II.34) cannot be considered sufficiently well founded for calculation of heat transfer coefficients during boiling of mercury and amalgam in the range of pressures indicated in [109].

It is noted in [20] that Averi and Bonilla boiled mercury with the addition of 0.1% sodium at atmospheric pressure on a surface with varying roughness. In spite of attempts of produce reproducible results, significant divergence of data occurred even on two smooth surfaces. An increase in the values of heat transfer coefficient was noted as a result of scratching the heating surface, the optimal distance between parallel scratches /123
being approximately two separation diameters, calculated using the formula of Fritz [111] (see Formula IV.28). Within the range of heat fluxes investigated (up to approximately $2.7 \cdot 10^5$ kcal/m$^2$·hr), the influence of roughness increases with increasing heat flux.

We can make the following conclusions from the works we have analyzed. Film boiling of mercury on steel surfaces is a result, as is noted in the works cited, of the inability of mercury to wet the oxide films covering the surface. Upon contact with mercury, the oxide films on the steel surfaces are disrupted and mercury begins to wet the surface. The time required for disruption of the film depends on the temperature level, mercury velocity (with forced circulation) and surface material (for example carbon or stainless steel). The nature of the dependence of the heat transfer coefficient on the heat flow with bubble boiling of mercury and amalgam is approximately the same as for water. Further investigations on the influence of various factors on heat exchange during boiling of mercury are necessary.

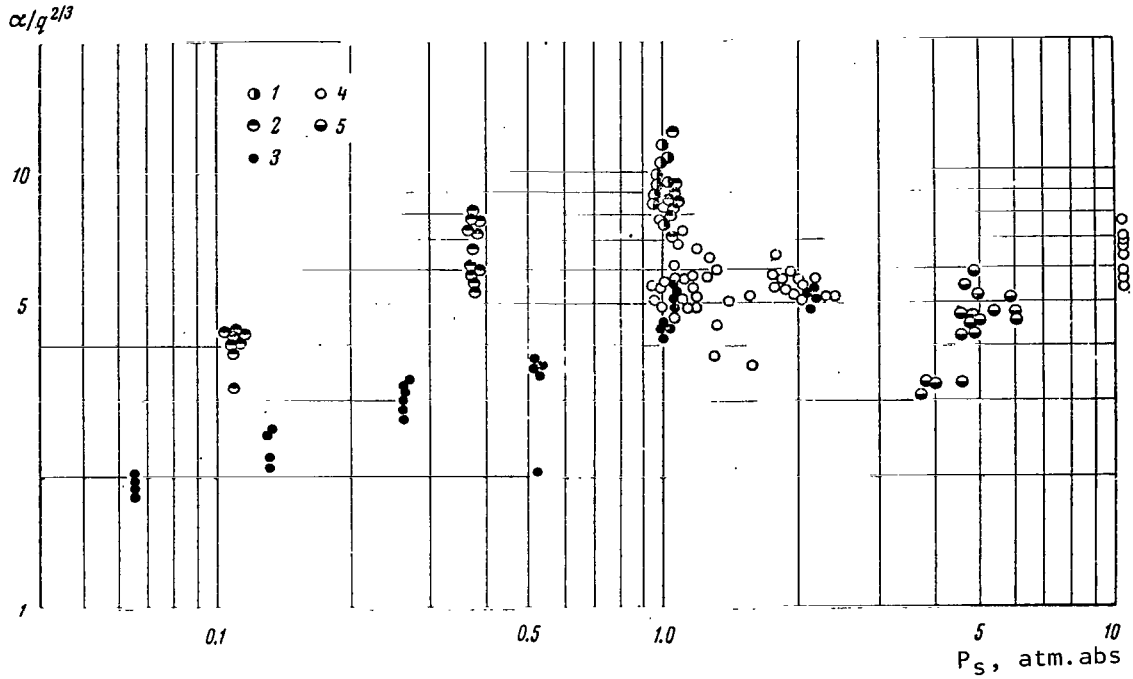


Figure 74. Heat Transfer Coefficient as a Function of Pressure During Boiling of Mercury and Amalgam According to the Data of Various Authors. 1, Amalgam, data of Lyon [9]; 2, Amalgam and 3, Mercury, data of Bonilla [10]; 4, Amalgam, data of Korneyev [6-8]; 5, Mercury (data of the authors).

Comparison of Experimental Data with General Formulas

At the present time, a large number of general formulas have been published for calculation of heat transfer and critical heat fluxes during boiling. From the point of view of methodology of production of these formulas, they can be divided into three groups.

1. Formulas produced using methods from the theory of similarity or the theory of dimensionalities.

2. Formulas produced on the basis of the theory of thermodynamic similarity of materials.

3. Semi-empirical[1] and theoretical formulas.

[1] Some of the formulas which we have placed in the first group are sometimes referred to in the literature as semi-empirical formulas.

General formulas for the calculation of heat transfer coefficients during boiling using the methods of the theories of similarity or dimensionalities have been produced, for example, by
G. N. Kruzhilin [112, 113]

$$\alpha = 6{,}9 \cdot 10^{-3} \frac{\lambda^{0{,}75} q^{0{,}7}}{\mu^{0{,}45} C_p^{0{,}12} T_s^{0{,}37}} \left(\frac{r\gamma''}{\gamma - \gamma''}\right)^{0{,}033} \left(\frac{\gamma}{\sigma}\right)^{0{,}333}, \qquad \text{(II.35)}$$

S. S. Kutateladze [114]

$$\alpha = 7 \cdot 10^{-4} \frac{\lambda}{\sigma^{0{,}5} (\gamma - \gamma'')^{0{,}2}} \left(\frac{P_s q}{r\gamma'' a}\right)^{0{,}7} \mathrm{Pr}^{-0{,}35}, \qquad \text{(II.36)}$$

F. P. Minchenko [115] /124

$$\alpha = 8{,}7 \cdot 10^{-4} \frac{\lambda}{\sigma^{0{,}5} (\gamma - \gamma'')^{0{,}2}} \left(\frac{P_s q}{r\gamma'' a}\right)^{0{,}7}, \qquad \text{(II.37)}$$

I. T. Alad'yev [23, 116]

$$\alpha = 100 \frac{1}{T_s} \left(\frac{A\lambda T_s}{r\, 10^{-6}}\right)^{0{,}3} q^{0{,}7} \qquad \text{(II.38)}$$

and many other authors.

The coefficients in formulas (II.35)-(II.37) were produced on the basis of processing of experimental data on heat transfer during boiling of nonmetallic liquids, while formula (II.38) is recommended for calculation of heat transfer during boiling of metals [23].

Data on heat exchange during boiling can be generalized on the basis of the theory of thermodynamic similarity of materials [94, 117-121]. I. I. Novikov [117] notes that for complete similarity of the processes of heat transfer in various liquids, it is necessary first of all that the liquids be thermodynamically similar, secondly that they be in corresponding states and thirdly that they have equal values of similarity criteria characterizing the conditions that the "liquid-solid" boundary. In practice, these conditions can usually be fulfilled only approximately. V. M. Borishanskiy [94] represented experimental data on heat transfer during boiling of ordinary liquids in the form of the dependence

$$\alpha_p / \alpha_{p^*} = F(P/P_{cr}), \qquad \text{(II.39)}$$

where $\alpha_p = \alpha/q^n$ at pressure P, and $\alpha_{p^*} = \alpha/q^n$ at some standard pressure P*. In order to determine the heat transfer coefficient using (II.39), the value

of α must be known at one pressure. In [120], formula is produced for calculation of heat transfer coefficients during boiling using the critical parameters

$$\alpha = 384 \frac{P_{cr}^{1/3}}{T_{cr}^{5/6} M^{1/6}} \left(\frac{P}{P_{cr}}\right)^{0.1} \left[1 + 4.64 \left(\frac{P}{P_{cr}}\right)^{1.16}\right] q^{2/3}. \qquad \text{(II.40)}$$

The values of constants and exponents in formula (II.40) have been found by comparison with experimental data on heat transfer during boiling of nonmetallic liquids.

The third group includes formulas produced, for example, in [122-129]. In particular, D. A. Labuntsov [122, 129] suggested a formula for calculation of heat transfer during boiling of metals which for pressures considerably below the critical pressure has the form

$$\alpha = 0.1 \left(\frac{\lambda C_p \gamma}{A\sigma T_s}\right)^{1/3} q^{2/3}. \qquad \text{(II.41)}$$

Comparison of experimental data on heat transfer during boiling of water and organic liquids with the calculated values of heat transfer coefficients from the general formulas produced by the methods of the theory of similarity and dimensionalities indicates that they can be significantly different from each other [116, 130, 131]. The dependences produced on the basis of the theory of approximate thermodynamic similarity of materials, for example (II.39), (II.40) describe the experimental data for non-metallic liquids which their authors present satisfactorily. The formulas which we have related to the third group provide no advantage as to accuracy of calculation of heat exchange in comparison with formulas produced by other methods. However, they are of doubtless interest in the methodological respect. /127

The work of Hygmark [132], who performed (computerized) statistical processing of data on heat transfer during boiling of 25 different liquids, for many of them the data of different authors, cannot be related to any of these groups. The formula which he produced, as Hygmark notes, considers only the heat physical properties of the liquid and vapor. The formula is not theoretically well founded, but agrees satisfactorily with experimental data.

The experimental data on heat transfer with developed boiling of sodium, potassium and cesium are described by the general formulas (II.26), (II.27). Therefore, a comparison of the results of calculations using these general formulas with experimental data can be performed by comparing them with calculations by formulas (II.26), (II.27). Comparison of the results of calculations using the general formulas of G. N. Kruzhilin (II.35), S. S. Kutateladze (II.36), F. P. Minchenko (II.37), I. T. Alad'yev (II.38), V. M. Borishanskiy (II.40) and D. A. Labuntsov (II.41) with calculations using the general formulas (II.26), and (II.27) has been performed for sodium

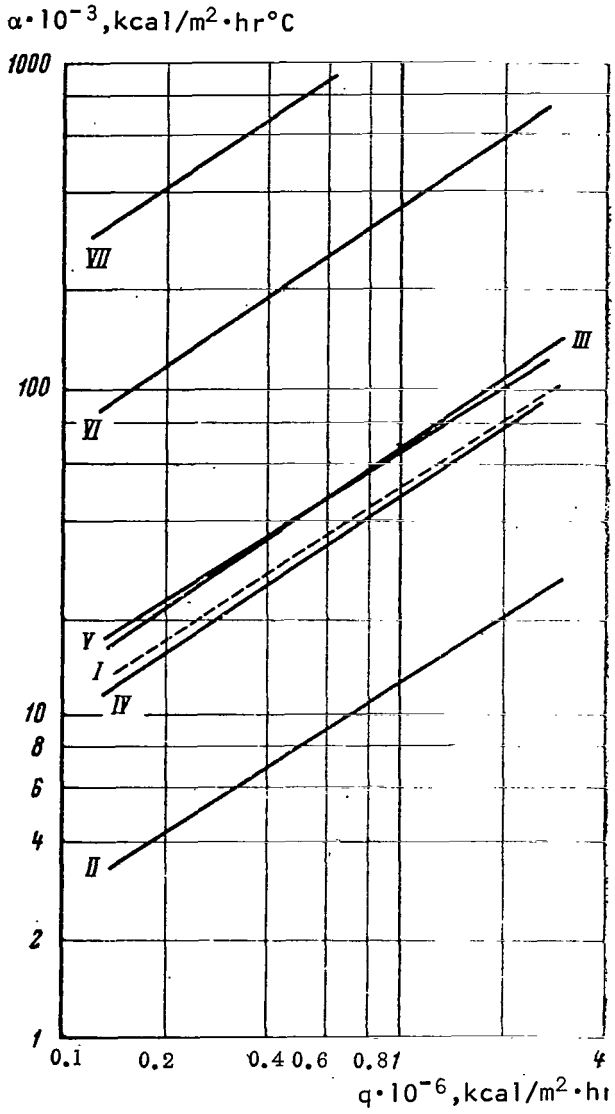


Figure 75. Dependence of Heat Transfer Coefficient on Heat Flux During Boiling of Sodium Calculated by Various Formulas ($P_s$ = 1 atm.abs.). I, Formula (II.27); II, Formula (II.40); III, Formula (II.37); IV, Formula (II.38); V, Formula (II.41); VI, Formula (II.36); VII, Formula (II.35).

(Figure 75, 78), potassium (Figure 76, 79) and cesium (Figure 77, 80). We can see from Figure 75 and 76 that for sodium and potassium the formulas of D. A. Labuntsov and I. T. Alad'yev, recommended for calculation of heat transfer during the boiling of metals agree rather well with the experimental data for these metals at atmospheric pressure. However for cesium (Figure 77) the difference in the values of heat transfer coefficients calculated using the formulas of D. A. Labuntsov and I. T. Alad'yev at atmospheric pressure from the values of α calculated using the empirical formula (II.27) is significant. The values of the heat transfer coefficients calculated using the formulas of G. N. Kruzhilin and S. S. Kutateladze whose empirical coefficients were produced by processing experimental data on heat transfer during boiling of nonmetallic liquids, are much higher than the experimental data for sodium, potassium and cesium. The formula of F. P. Minchenko (II.37), in which the empirical coefficients were produced also on the basis of processing of experimental data for heat transfer during boiling of ordinary liquids at atmospheric pressure agree with dependence (II.27) for all three alkali metals better than the others. The formula of V. F. Borishanskiy (II.40), which includes critical parameters of the heat transfer medium, produces much lower results than the experimental data for sodium, potassium and cesium, as we can see from Figures 75-77.

/129

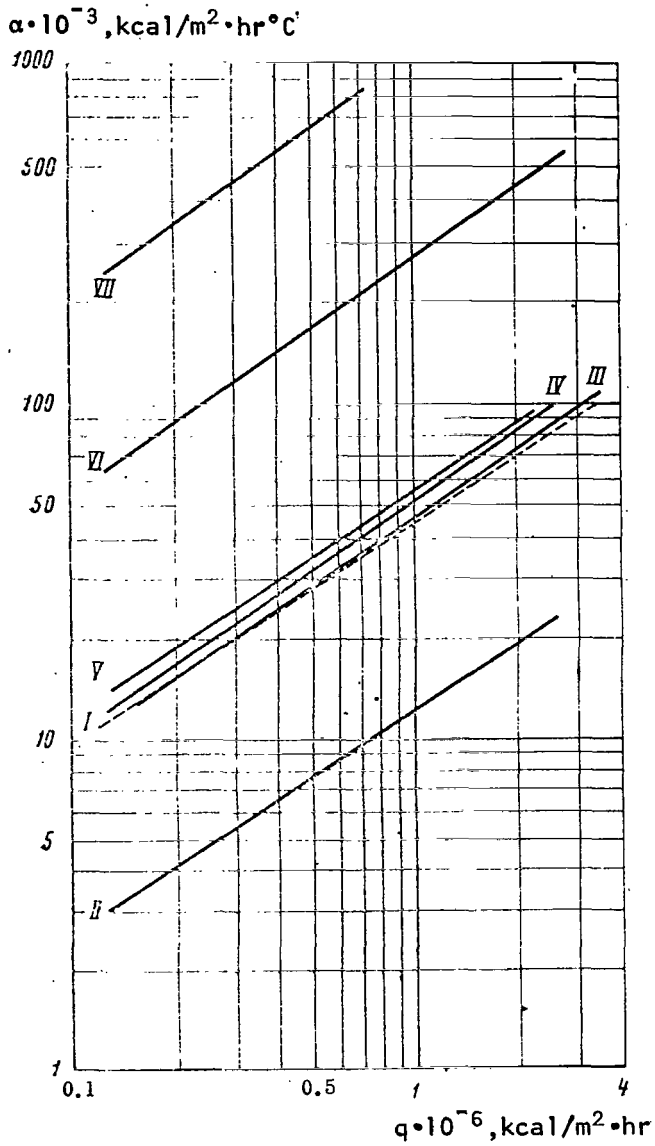


Figure 76. Dependence of Heat Transfer Coefficients on Heat Flux During Boiling of Potassium Calculated by Various Formulas ($P_s$ = 1 atm. abs.). I, Formula (II.27); II, Formula (II.40); III, Formula (II.37); IV, Formula (II.38); V, Formula (II.41); VI, Formula (II.36); VII, Formula (II.35).

Analysis of Figures 78-80 shows that the dependence of α on pressure (with pressures above approximately 0.3 atm. abs. for sodium, 0.1 atm. abs. for cesium and 0.16 atm. abs. for potassium) according to the general formulas of G. N. Kruzhilin (II.35), S. S. Kutateladze (II.36), F. P. Minchenko (II.37) and V. M. Borishanskiy (II.40) is approximately the same as those produced by experiments. With pressures below 0.3 atm. abs. for sodium and 0.1 atm. abs. for cesium according to the experimental data α depends on pressure more strongly than is indicated by the general formulas.

Thus, with developed boiling of sodium, potassium and cesium within the pressure ranges in which experiments have been performed, the heat transfer coefficients can be calculated by either using the empirical formulas or the general formulas (II.26) and (II.27). The possibility of using formulas (II.26) and (II.27) for the calculation of the heat transfer coefficients during boiling of sodium, potassium and cesium at higher pressures, or during boiling of other alkali metals requires experimental testing. /130

It must be emphasized that for alkali metals under conditions of free convection, in addition to heat removal by developed boiling, other heat removal regimes are possible: heat removal by unstable boiling and heat removal by /131

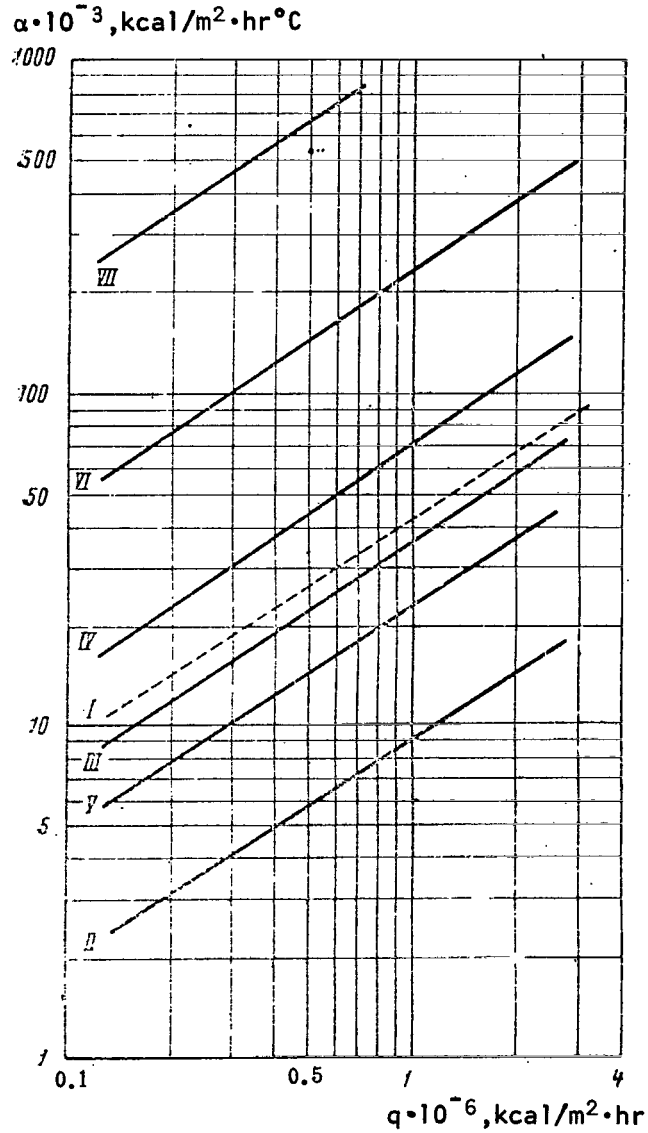


Figure 77. Dependence of Heat Transfer Coefficient on Heat Flux According to Various Formulas During Boiling of Cesium ($P_s$ = 1 atm.abs.). I, Formula (II.27); II, Formula (II.40); III, Formula (II.37); IV, Formula (II.38); V, Formula (II.41); VI, Formula (II.36); VII, Formula (II.35).

convection with subsequent liberation by evaporation from the free surface. For this last mode of heat removal, the heat transfer coefficients can be calculated using the formulas for convective heat exchange under conditions of free convection. With unstable boiling, the time-averaged values of heat exchange coefficients are located between the values of α with developed boiling and with convection.

Figure 81 shows the dependence of the heat transfer coefficient on pressure for mercury according to various general formulas recommended for calculation of heat transfer coefficients during boiling of liquids. Comparison of Figure 81 with Figure 74 shows that neither of the formulas analyzed above can be recommended for calculation of the heat transfer during boiling of mercury or amalgam. For convenience of comparison, Figure 81 shows the dependence of α on $P_s$ according to formula (II.34), which describes the experimental data of Bonilla [10] for mercury at pressures below 1 atm. abs. quite well. /132

## Conclusions

1. Heat exchange has been experimentally investigated for alkali metals under free convection conditions with sodium, potassium and cesium with developed boiling, with unstable boiling and with convection. When the liquid is heated to the saturation

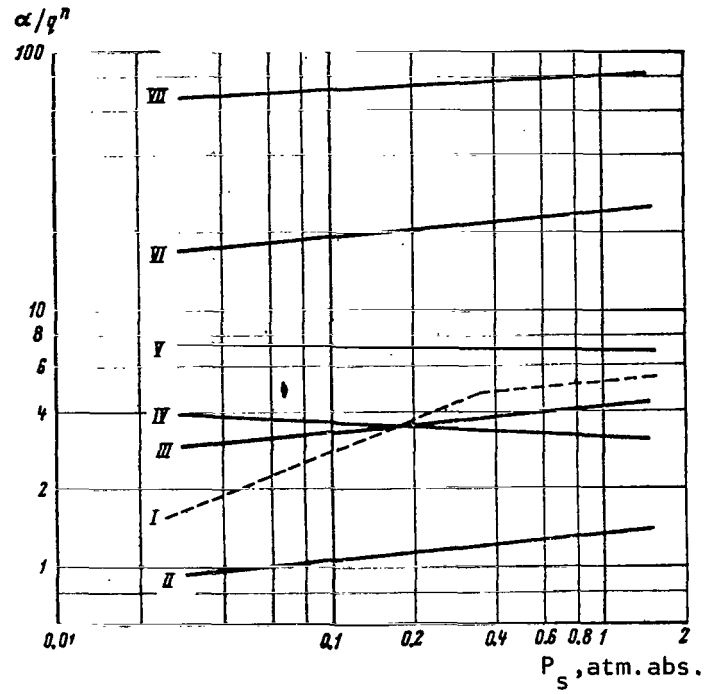


Figure 78. Comparison of Dependence of Coefficients of Heat Transfer During Boiling of Sodium on Pressure According to Various Formulas. I, Formula (11.26), (11.27); II, Formula (11.40); III, Formula (11.37); IV, Formula (11.38); V, Formula (11.41); VI, Formula (11.36); VII, Formula (11.35).

temperature, the existence of a given heat removal mode depends on the heat flux and pressure, material and finish of the heating surface, contact time of the heating surface with the heat transfer medium and the presence of inert gases, and also possibly on other factors.

2. Heat removal of high heat flows by convection with subsequent liberation of heat by evaporation from the free surface results from the possiblity of significant super heating of the liquid on the heating surface /133
(up to 100°C and more) and the relatively high values of heat transfer coefficient for alkali metals for convective heat removal. In this case, the calculation of the heat transfer coefficients can be performed using formulas for convective heat exchange, in particular (II.9) for the laminar are ($Gr < 10^8$) and formula (II.5) for the turbulent area.

3. With developed boiling of alkali metals, the heat transfer coefficient, as is the case for boiling of non-metallic liquids, can be described by the dependence of the type $\alpha = C_\alpha q^n p^m$. For calculation of heat transfer

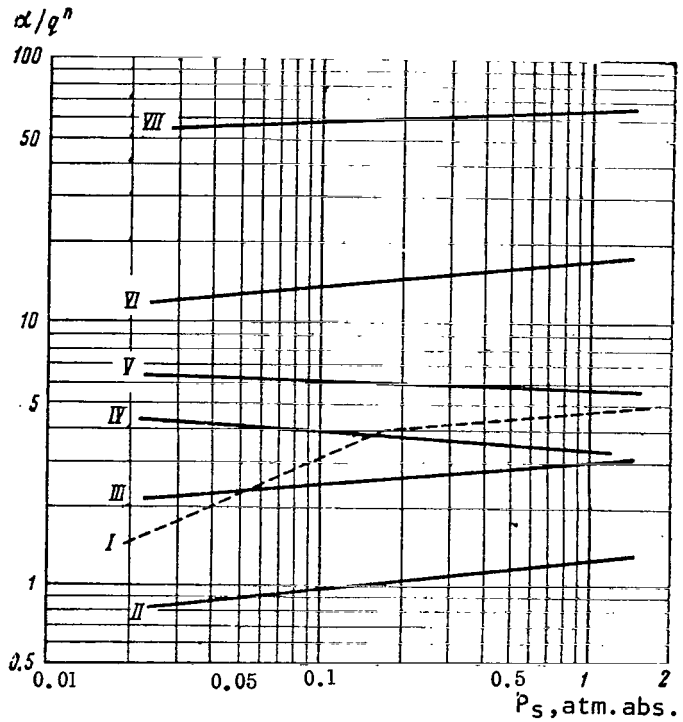


Figure 79. Comparison of Dependence of Heat Transfer Coefficients During Boiling of Potassium on Pressure According to Various Formulas. I, Formula (II.26), (II.27); II, Formula (II.40); III, Formula (II.37); IV, Formula (II.38); V, Formula (II.41); VI, Formula (II.36); VII, Formula (II.35).

coefficients during developed boiling of sodium, potassium and cesium within the pressure ranges in which experiments with these metals were performed, we can recommend both the empirical formulas (II.18), (II.19), (II.25) and (II.20), (II.21), respectively, and the general dependences (II.26), (II.27). The possiblity of using formula (II.27) for calculation of heat transfer coefficients during boiling of sodium, potassium and cesium at pressures above about $2 \cdot 10^{-2}\ P_s/P_{cr}$, and during boiling of other alkali metals requires experimental testing.

4. Heat removal during unstable boiling is characterized by significant pulsations of temperature of the heating wall at relatively low frequency (a fraction of one Hz). The time-averaged values of heat transfer coefficient with unstable boiling lie between the values of $\alpha$ for heat removal with developed boiling and heat removal by convection. The less the amplitude of the low frequency pulsations in wall temperature, the more the values of heat transfer coefficient approach $\alpha$ with developed boiling. The maximum

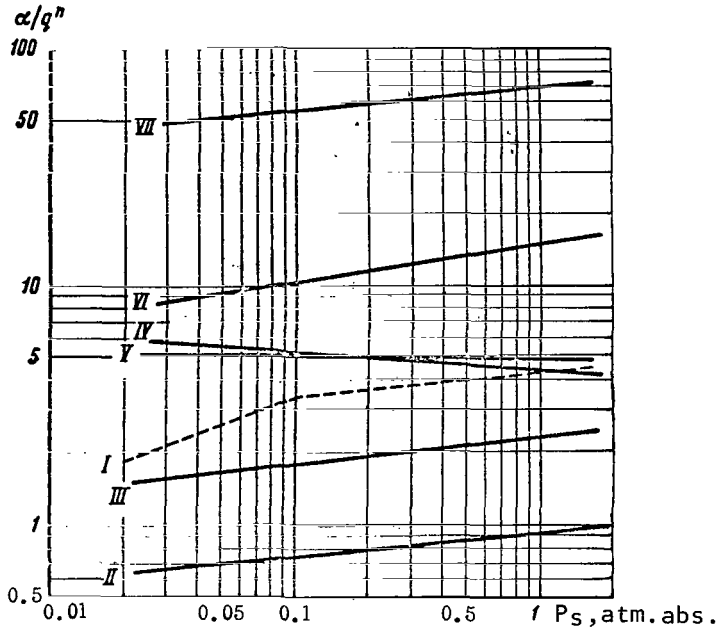


Figure 80. Comparison of Dependences of Heat Transfer Coefficients During Boiling of Cesium on Pressure According to Various Formulas. I, Formula (11.26), (11.27); II, Formula (11.40); III, Formula (11.37); IV, Formula (11.38); V, Formula (11.41); VI, Formula (11.36); VII, Formula (11.35).

value of temperature pulsations of the heating wall with unstable boiling is equal to the difference in temperature heads during heat removal by convection without boiling and with developed boiling.

5. On steel surfaces, high values of heat transfer coefficients during boiling of mercury, characteristic for bubble boiling, can be achieved by reduction of oxide films on the heating surface by the mercury, and by addition of surfactants to the mercury. The possibility and time of reduction of oxide films by the mercury depend on the temperature, surface material, degree of purity of the mercury and other factors. The nature of the dependence of heat transfer coefficients on heat flux during boiling of mercury and amalgam are approximately the same as during boiling of alkali metals.

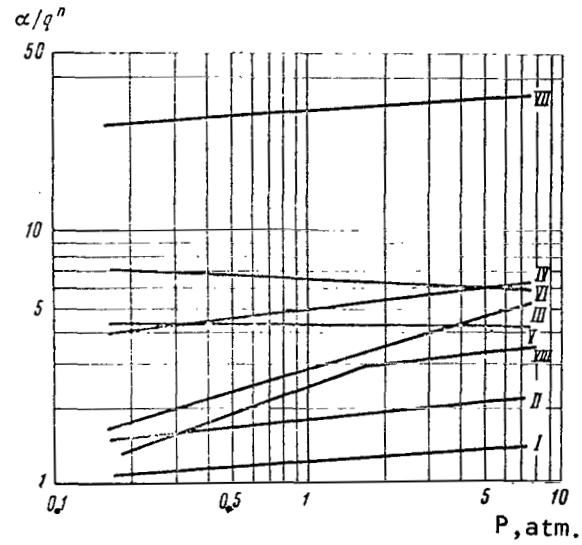


Figure 81. Comparison of Dependence of Heat Transfer Coefficients During Boiling of Mercury on Pressure According to Various Formulas. I, Formula (11.34); II, Formula (11.40); III, Formula (11.37); IV, Formula (11.38); V, Formula (11.41); VI, Formula (11.36); VII, Formula (11.35); VIII, Formulas (11.26), (11.27).

## CHAPTER 3 /134

## CRITICAL HEAT FLOWS

Usually, the critical heat flow under free convection conditions means the amount of heat flow corresponding to the transition from developed nucleate boiling to film boiling (with q = const). The main quantity of experimental works has been dedicated to the determination of this quantity. However, as was noted in the second Chapter, film boiling (under the condition q = const) may also be preceded by heat removal with unstable boiling or heat removal by convection (see Figure 34).

The transition to film boiling from unstable boiling, characteristic for alkali metals, has been investigated experimentally by the authors. The transition to film boiling from heat removal by convection has been observed only in experiments on non-metallic liquids so far. There is reason to believe that, for example, in alkali metals, the transition from convection to film boiling may also be achieved experimentally, since for these metals great superheating of the liquid on the heat transmitting surface and relatively high values of heat transfer coefficients under free convection conditions are typical.

We will use the term "critical heat flow" to refer to the heat flow at which the transition to film boiling either from developed or from unstable boiling occurs, without making special distinctions, for example the delineation between the first critical load (transition from nucleate boiling to film boiling) and the second critical load (transition from film boiling to nucleate boiling).

At the present time, a small number of experiments have been performed on critical heat flows during boiling of metals under free convection conditions. However, these limited experimental data do make it possible to /135
determine some regularities, for example the dependence of critical heat flow on pressure over the investigated pressure range.

In order to compare the dependences on critical heat flow during boiling of metals with dependences for critical heat flows during boiling of non-metallic liquids, in this Chapter we will briefly analyze the principal regularities of the formation of the crisis, produced in experiments with water and organic liquids. Problems relating to critical heat flows during boiling of under heated liquids and solutions, as well as to the transition from film boiling to bubble boiling, will not be touched upon, since these data have not yet been produced for metals.

## Principal Regularities in Formation of Boiling Crisis in Non-metallic Liquids Under Free Convection Conditions

Most experimental works on the investigation of critical heat flows during boiling of non-metallic liquids have been performed at atmospheric pressure or higher. In this pressure range, the dependence of $q_{cr}$ on pressure for water and many organic liquids is shown on Figure 82, borrowed from [94].

A limited number of works have been performed on the influence of pressure on $q_{cr}$ at low pressures. Figure 83 shows the experimental data of the authors and data from [97] on the dependence of $q_{cr}$ on pressure for water boiling at low pressures. A comparison of Figure 83 with Figure 82 shows that the dependence of critical heat flow on pressure at low (down to approximately $10^{-3}$ $P_{cr}$) pressures is weaker than with pressures on the order of ($10^{-3}$-0.2) $P_{cr}$. The weaker dependence of $q_{cr}$ on $P_s$ at low pressures is also indicated by the results of [133, 134].

The state of the heating surface has a significant influence on the critical heat flow. Many experiments by the authors, performed in water at atmospheric pressure, boiling on flat horizontal surfaces of copper and stainless steel, have shown that the values of $q_{cr}$ tend to change significantly (up to 100%) with sequential experiments performed on the same surface without cleaning and without changing the water (both increasing and decreasing) in comparison to the value of critical heat flow in the first experiment. This difference in values of $q_{cr}$, probably, can only be related to a change in the state of the surface as a result, for example, of increased temperature at the moment of the crisis, since the other conditions /137
in all experiments remained unchanged. A smaller scattering of points (approximately ± 15%) relative to the mean value of $q_{cr}$ was produced in experiments using newly, approximately identically prepared surfaces and water with identical salt contents.

In a work by V. I. Yashnov [135] performed using water at atmospheric pressure it was demonstrated that the value of $q_{cr}$ depends on the method of cleaning the heating surface, the heat flow and the time of preliminary boiling, the salt content of the boiling water, the roughness of the surface and chemical etching, high temperature calcination of grease films and the surface material of the heating surface. The value of $q_{cr}$ changed as a function of the state of the surface alone with otherwise equal conditions between $95 \cdot 10^3$ kcal/m$^2$·hr and $1625 \cdot 10^3$ kcal/m$^2$·hr. In the works of Gambill [136] using distilled water at atmospheric pressure, the values of $q_{cr}$ varied from about $0.55 \cdot 10^6$ kcal/m$^2$·hr to $1.6 \cdot 10^6$ kcal/m$^2$·hr as a result of changes of the state of the surface. V. I. Yashnov [135] believes that the principal

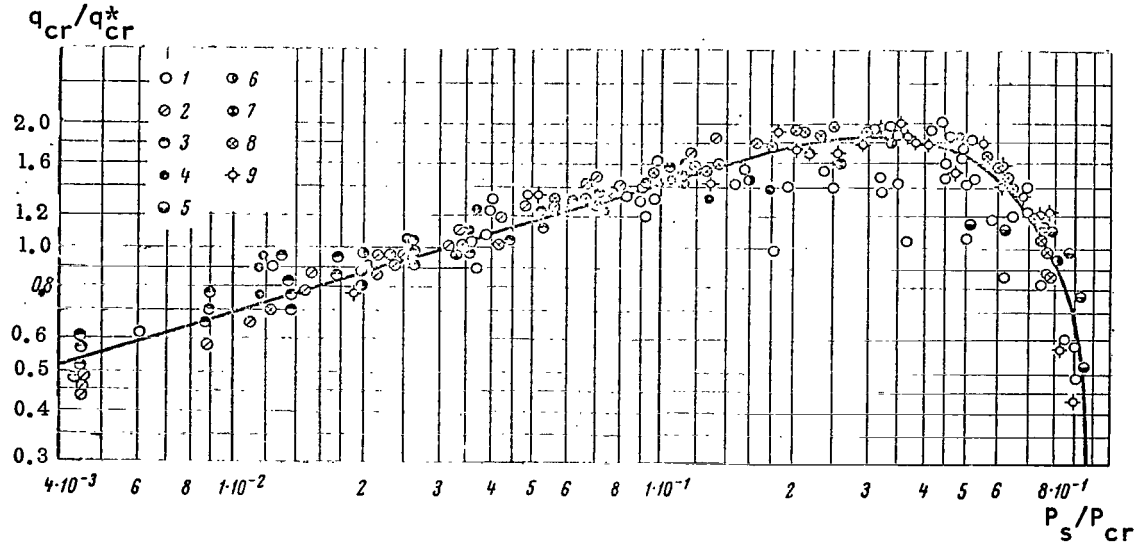


Figure 82. Dependence of Critical Heat Flows on Pressure for Water and Organic Liquids [94]. Value of $q^*_{cr}$ taken with reference pressure 0.3 $P_{cr}$. 1-3, Water; 4-5, Ethyl alcohol; 6, Benzene; 7, Heptane; 8, Methyl alcohol; 9, Propyl alcohol.

factor influencing the critical heat flow during boiling of liquids under conditions of free convection is the wettability (contact wetting angle) of the surface, which may vary significantly as a function of preparation of the surface.

The value of the critical heat flow is influenced by the geometry [137] and the dimensions [138-144] of the heating surface, the position of the heater in space [138] and the degree of screening from the main mass of the liquid [145]. The dependence of $q_{cr}$ on heater diameter between a few microns and a few millimeters during boiling of water and other organic materials over a broad pressure range was investigated in [74, 138, 144]. A typical dependence of critical heat flow on diameter of the horizontally placed heater, produced in these works, is presented for ethyl alcohol on Figure 84. A similar nature of the dependence of $q_{cr}$ on diameter of a horizontally placed heater was produced in [139, 142, 143]. On vertically placed heaters, the maximum value of $q_{cr}$, which is clearly seen on Figure 84, was not noted [138].

Processing of the results of experiments on the influence of the diameter of a horizontally placed heater on the critical heat flow, performed for various fluids over a broad range of pressures (up to about 0.8 $P_{cr}$) showed that these data can be generalized in the coordinates B-We [144], where

$$B = \frac{q_{cr}}{r(g\gamma'')^{1/2}[\sigma(\gamma-\gamma'')]^{1/4}}, \qquad \text{(III.1)}$$

$$We = d\left[\frac{\gamma-\gamma''}{\sigma}\right]^{1/2}, \qquad \text{(III.2)}$$

d is the diameter of the heater. This is illustrated by Figure 85, taken from [144]. With a value of the criterion We > 2, self modeling of the quanity B occurs, and consequently of the quanity $q_{cr}$ relative to the heater diameter. The value of b where 0.2 < We < 1 has a maximum and where 0.03 < We < 0.1 has a minimum. With lower values of the We number, the value of B increases again. For a small heater diameter, the role of convection in the removal of heat is great. For example, in ethyl alcohol at atmospheric pressure, the transition from heat removal by convection to heat removal by boiling on a wire 25 μ in diameter occurs with a heat flux of about 0.7 $q_{cr}$, while on a wire 8 μ in diameter it occurs with q at approximately 0.9 $q_{cr}$ [144]. Therefore the conclusion that the increase in values of critical heat flux in the area of very small diameters of the heater results from a significant contribution by convection, made by the authors of [144], seems rather logical. However, the results of the experiments of S. P. Kaznovskiy and V. G. Sviridenko, performed at the Physics and Energy Institute on pure (dry residue less than 1 mg/l) distilled water, boiled at atmospheric pressure on horizontal wires with diameters from 5 μ to 1.8 mm, do not confirm this conclusion and do not agree with the data presented on Figures 84 and 85. The value of critical heat flow produced in these experiments for all diameters of heaters used was on the average $10^6$ kcal/$m^2$·hr, and the deviation of individual points from the mean value did not exceed ± 5%. As the wire diameter decreased, the beginning of bubble boiling, as in [144], was delayed. Thus, on wires with 100, 50 and 20 μ diameters, boiling began at heat fluxes of $1.0\cdot10^5$, $3.5\cdot10^5$and $8.0\cdot10^5$ kcal/$m^2$·hr respectively. On wires with diameters from 20 to 58 μ, when only 1-3 vapor formation centers were formed (over a length of 50 mm), super heating occurred in all experiments at the points where the centers of vapor formation did not form right up to the crisis. On wires 5-7 μ in diameter, bubble boiling was not noted, and superheating occurred at a heat flux of $10^6$ kcal/$m^2$·hr. No explanation of the divergence of the results of these experiments with the data on Figures 84 and 85 has been found.

/139

/140

Many investigators have determined the influence of the material of the heating wall on the critical heat flux. In [139, 140], experiments on critical heat fluxes during boiling of water at atmospheric pressure were performed on heaters made of four and seven different materials respectively. No essential influence of the heating surface material on $q_{cr}$ was detected. In [146], critical heat fluxes were studied during boiling of water, alcohol and benzene on surfaces of various materials with varying pressures from atmospheric to near critical. The difference in the values of $q_{cr}$ for

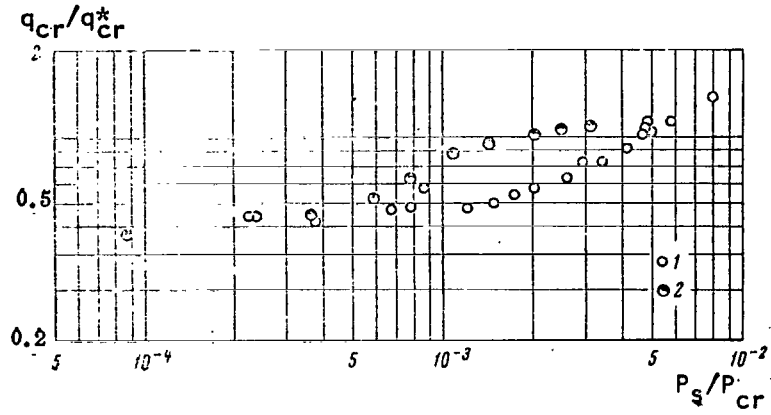


Figure 83. Critical Heat Fluxes as Functions of Pressure For Water Boiling at Low Pressures. 1, Data of the Authors; 2, Data from [97] (values of $q^*_{cr}$ taken at $P_s$ = 1 atm. abs.).

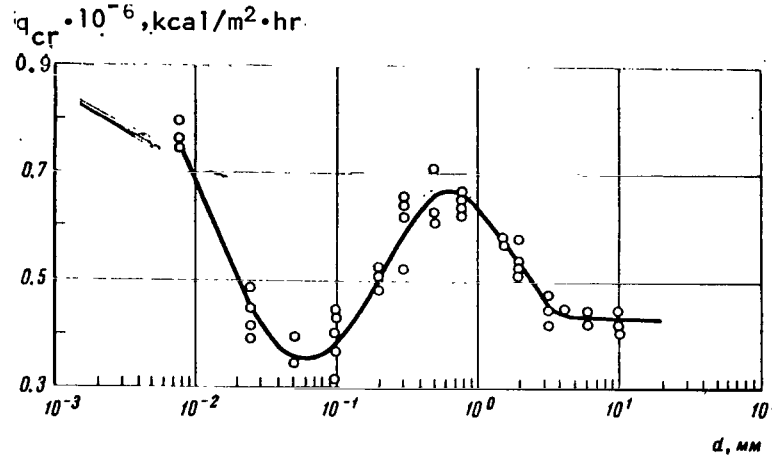


Figure 84. Critical Heat Flux During Boiling of Ethyl Alcohol By Horizontal Heater As a Function of Heater Diameter [144] ($P_s$ = 1 atm. abs.)

different surfaces reached approximately 50%; beginning at pressures of about 0.3 $P_{cr}$ it began to decrease and that pressures near the critical pressure it disappeared entirely. The influence of the material of the heating wall on the critical heat flux in [146] as in [135] is explained by variations in surface conditions. However, the reason for the influence of heating surface material on critical heat flux may be not only differences in surface conditions for various materials, but differences in the physical properties (particular temperature conductivity) and dimensions (thickness) of the

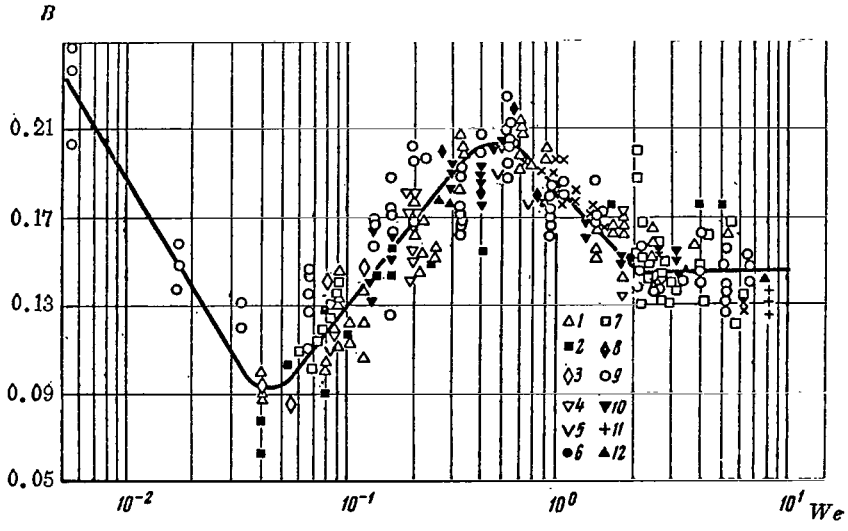


Figure 85. Generalization of Dependence of Critical Heat Flow On Diameter of Horizontal Heater [144]. 1-8, Water; 9, Ethyl Alcohol; 10, Benzene; 11, Carbon tetrachloride; 12, Methanol, butanol, propanol.

heating wall. This is indicated by the results of experiments [74, 139-141, 147], in which for thin (beginning at tenths of a millimeter or less) heating walls, the dependence of $q_{cr}$ on material and wall thickness is found. With decreasing thickness and heat conductivity of the wall, the value of heat flow decreases. For example, when the product of heat conductivity times effective wall thickness is changed from its minimum to its maximum value (approximately 370 times) in [147], the value of $q_{cr}$ is doubled. This effect is explained by the increase in the degree of irregularity of distribution of local heat flows with decreasing heat conductivity and thickness of the heating wall heated by electric current [147].

Since the value of critical heat flow is influenced not only by pressure, /141 but also significantly by the state of the surface (which also depends on impurities in the boiling liquid), position, geometry and dimensions of the heater, and in some cases the thickness and heat conductivity of the heating wall, during a strict comparison of the data of various authors and the determination of the dependence of $q_{cr}$ on various factors in the process of experiments, we must consider the degree of influence of other factors as well. Unfortunately, in many works this is done insufficiently. Furthermore, many published data do not include an indication of all the conditions of the experiments, for example the results of chemical analyses for impurities, description of the conditions of preparation of the heating surface,

etc. are eliminated, which naturally hinders comparison of these data with the results of other works.

Critical Heat Flows During Boiling of Metals Under Conditions of Free Convection

The critical heat flows during boiling of metals under free convection conditions have been experimentally studied for sodium (by Kebon; in [18, 33, 37] and by the authors), potassium (in [39] and by the authors), cesium (by the authors), rhubidium (in [37]), mercury (by the authors) and magnesium amalgams (in [8]).

In our experiments, the boiling of metals for which the critical heat flows were investigated was performed on flat horizontal surfaces heated by electron bombardment over a diameter of 38 mm, (Figure 10, 11). In all experiments, the heat exchange surface was treated approximately identically (smoothness corresponding to class 6-7) and distilled metals were used. However, the content of impurities in the heat transfer media was not checked. In experiments on sodium, boiling tanks with internal diameters of 165 and 45 mm were used (see Figure 24), while in the experiments on potassium and cesium tanks 70 mm in diameter were used (see Figure 33) and in the experiments on mercury tanks of 45 mm diameter were used.

In all experiments, except for one series on sodium, the boiling of the metals occurred under the pressure of their own vapors.

The experiments were primarily performed with $P_s$ = const and increasing heat flow. Individual experiments on the attainment of crisis (with q = const) by decreasing pressure gave good agreement with results produced by the first method. The crisis was fixed by the sharp increase in wall temperature. On sodium, eight series of experiments were performed in the pressure range of approximately 0.015 to 1.2 atm. abs. Of these, five series were performed on a surface of VZH-98 alloy, two on a surface of stainless steel and one on a surface of molybdenum.

In the first seven series of experiments (a boiling tank with an internal diameter of 165 mm was used), in which the sodium was boiled under the pressure of its own vapors, heat removal occurred primarily with unstable boiling even with heat flows corresponding to the critical values. Depending on the value of low frequency pulsations of temperature of the heating wall, the values of critical heat flows varied. Great temperature fluctuations of the heating wall corresponded to smaller values of $q_{cr}$. Figure 86 shows a recording of the wall-liquid temperature difference before crisis and at the moment of crisis with a pressure of about 0.35 atm. abs. for two points in the same series of experiments. Before crisis occurred in the first experiment the pulsations of heating wall temperature were considerably greater (Figure 86, a) than the pulsations before crisis in the second experiment (Figure 86, b). The value of critical heat flow in the first case was $1.5 \cdot 10^6$ kcal/m$^2$·hr, in the second case - $2.5 \cdot 10^6$.

/142

/143

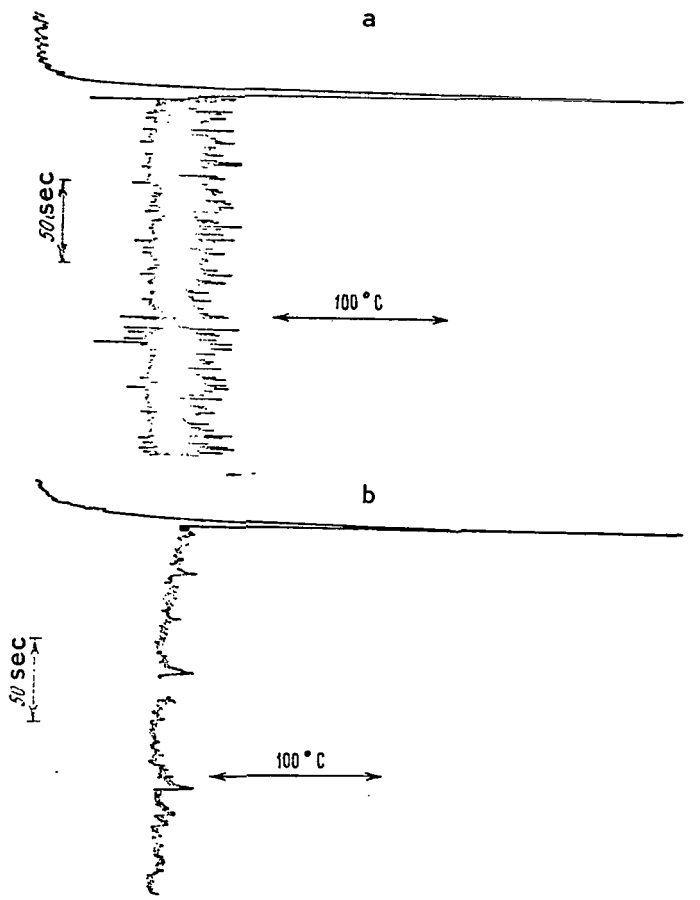


Figure 86. Recording of Wall-Liquid Temperature Difference Before Crisis and At Moment of Crisis in Experiments of the Authors on Sodium ($P_s \sim 0.36$ atm. abs.). a, $q_{cr} = 1.5 \cdot 10^6$ kcal/m$^2$hr; b, $q_{cr} = 2.5 \cdot 10^6$ kcal/m$^2$·hr.

Thus, the value of $q_{cr}$ in the first experiment was about 60% lower than in the second experiment. In the eighth series of experiments (using the 45 mm diameter boiling tank), the sodium boiled over a surface of stainless steel under the pressure of its own vapors and under the pressure of an inert gas (argon). In the first case, the crisis occurred with unstable boiling, whereas when the sodium was boiled beneath argon the crisis occurred after only developed boiling. The value of critical heat fluxes produced in the experiments with developed boiling of sodium under the inert gas were higher than the values of $q_{cr}$ produced with instable boiling beneath the pressure of the sodium vapors, which agree well with the values of critical heat fluxes

measured in the preceding series of experiments, where the boiling of sodium was unstable.

Noyes and Lurie [18, 33] investigated critical heat flows during boiling of sodium over horizontal tubes of stainless steel and molybdenum 6.35 and 9.53 mm in diameter, located in boiling tanks with internal diameters of 300 and 150 mm respectively. The pressure range covered was approximately 0.04-0.6 atm. abs.

In [33], experimental data are presented on the critical heat flows during boiling of sodium over a horizontal tube 11.2 mm in diameter, produced by Kebon in the pressure interval 0.03-1.5 atm. abs. Unfortunately, the information presented in [18, 33] do not allow us to establish the heat removal modes which preceded the onset of crisis.

In [37], in which two experiments on $q_{cr}$ during boiling of sodium were performed (over a horizontal tube 9.53 mm in diameter of "Haynes-25" alloy, contained in a tank 55 mm in diameter), it is reported that the temperature pulsations of the heating wall before the onset of crisis reached 110°C. This indicates that the transition to film boiling was proceded by unstable boiling.

On Figure 87 we have constructed experimental data on critical heat fluxes for sodium as a function of pressure. Analysis of Figure 87 indicates that with developed boiling of sodium, the value of $q_{cr}$ are approximately twice as high as with unstable boiling, when large fluctuations in the temperature of the heating surface occur (for example, point a). As the value of the low frequency pulsations of heating wall temperature decrease, that is as developed boiling is approached, the values of $q_{cr}$ increase (for /145 example, see Figure 86, b and Figure 87, point b). Comparison of the experimental data of Noyes and Lurie with our data and the data of [37] produced upon transition to crisis from unstable boiling gives us reason to believe that most of the experiments of Noyes and Lurie as well as Kebon were performed with unstable boiling, since these data agree rather well in magnitude with the similar data from our works and [37].

The critical heat fluxes during boiling of potassium were studied by the authors on a flat stainless steel surface (two series of experiments) and by Balzhiser [39] on horizontal tubes of "Haynes-25" alloy 9.53 mm in diameter located in a tank 35 mm in diameter. Our experiments involved variation of the pressure from about 0.03 to 1.5 atm. abs., the experiments of Balzhiser from about 0.01 to 1.5 atm. abs. The results of the experiments are shown on Figure 88, from which we can see that the data in question agrees satisfactorily with each other.

Upon transition to film boiling from unstable boiling, the value of $q_{cr}$ was lower than upon transition from developed boiling.

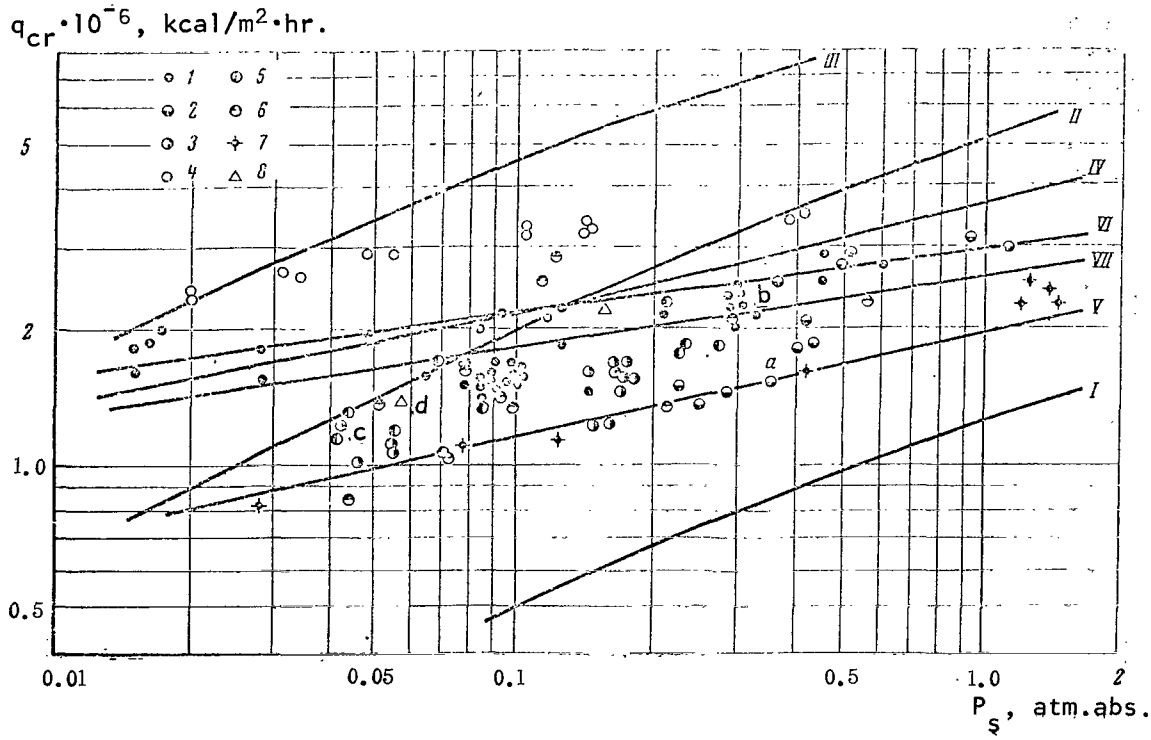


Figure 87. Experimental Data on Critical Heat Fluxes During Boiling of Sodium. Flat horizontal surface, heated over 38 mm diameter. 1, VZH-98 alloy; 2, Molybdenum; 3, Stainless steel; 4, Stainless steel, boiling (developed) under argon (data of the authors); 5, 6, Horizontal tubes (diameter 6.36 and 9.53 mm) of stainless steel and molybdenum [33]; 7, Horizontal tube (diameter 11.2 mm) [33]; 8, Horizontal tube (diameter 9.53 mm) of Haynes-25 alloy [37]. For points a and b, recording of temperature difference shown on Figure 86. Point c produced with unstable boiling. For point d, value of pulsation of wall temperature before crisis reached 110°C. I, Formula (III.1); II, Formula (III.5); III, Formula (III.4); IV, Formula (III.6); and Formula (III.11); V, C = 18; VI, C = 45; VII, Formula (III.7).

Here, the values of critical heat fluxes produced in the experiments differed by more than two times. The lower points of Figure 88 correspond to the critical heat fluxes with unstable boiling, the upper points - with developed boiling.

The authors performed four series of experiments on cesium over a horizontal surface of stainless steel in the pressure range of about 0.018 to 3.5 atm. abs. The results of the experiments are shown on Figure 89. In the first series of experiments, the value of measured temperature pulsations

of the heating wall with all heat flows did not exceed 5°C. In experiments of the second through fourth series, the temperature pulsations of the heating wall in the period preceding crisis were generally greater than in the experiments of the first series. With increasing value of pulsations, the value of critical heat flows decreases as in the experiments on sodium and potassium.

Figure 90 shows a record of the wall-liquid temperature difference before crisis and at the moment of crisis typical for these experiments. The lowest values of critical heat flows were produced in the second and third series of experiments with pressures of 0.06-0.2 atm. abs., where the boiling process was most unstable. /147

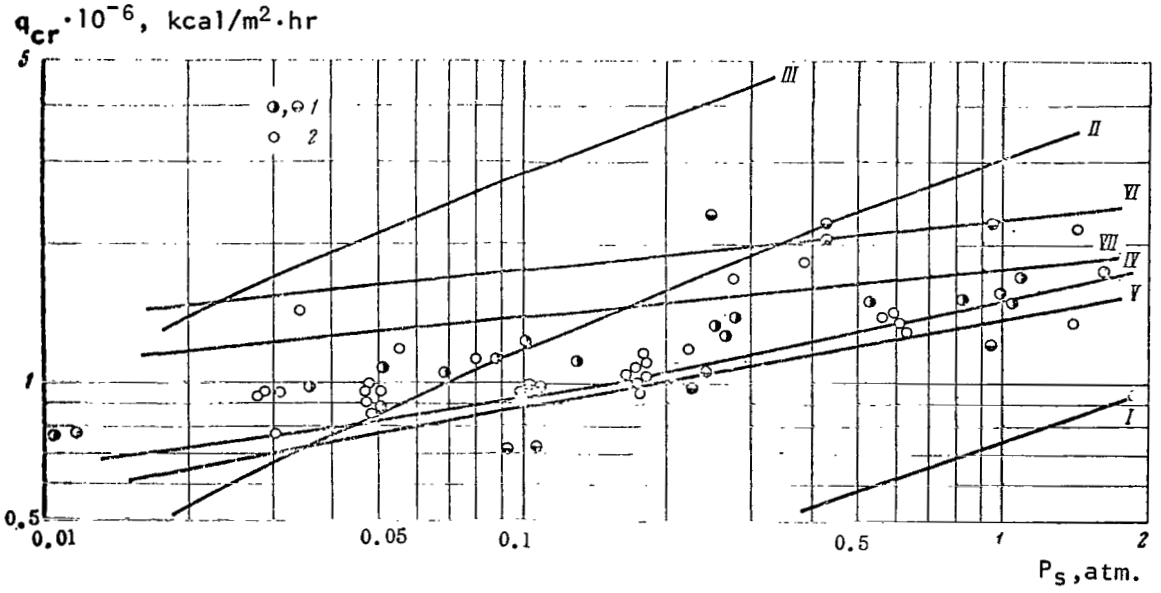


Figure 88. Experimental Data on Critical Heat Flows During Boiling of Potassium. 1, Flat horizontal stainless steel surface (data of the authors - two series); 2, Horizontal tube of "Haynes-25" alloy 9.63 mm in diameter. Data of Balzhiser [39]. I, According to Formula (III.1); II, Formula (III.5); III, Formula (III.4); IV, Formula (III.6); Formula (III.11); V, C = 18; VI, C = 45; VII, Formula (III.7).

In all experiments the boiling tank was filled by evaporating cesium from a supplementary evaporating tank, from which it was separated by a system of valves. Upon completion of the experiments, the cesium was evaporated back into the supplementary tank. Before each new series of experiments, the boiling tank, valves and lines were carefully washed. However, a slight quantity of cesium oxide could remain in the valve on the side of the evaporating tank, in spite of the measures taken. Therefore, the

content of oxygen in the seizium in the second through fourth series of experiments could have been somewhat higher than in the first series, when all valves were clean. In the first series of experiments, for which the points have slight dispersion (Figure 89) we see a weaker dependence of $q_{cr}$ on pressure with $P_s \sim 0.02\text{-}0.2$ atm. abs. ($q_{cr} \sim P_s^{0.08}$) than with $P_s \sim 0.2\text{-}3$ atm. abs. ($q_{cr} \sim P_s^{0.15}$). According to the data of the second through fourth series of experiments, for which the difference between points is significantly greater, this change in the dependence of $q_{cr}$ on $P_s$ cannot be traced.

Caswell and Balzhiser [37] performed experiments on critical heat flows during boiling of rhubidium over a horizontal tube 9.53 mm in diameter of "Haynes-25" alloy, located in a tank 55 mm in diameter, over the pressure range 0.035-1.93 atm. abs. The results of these experiments are shown on Figure 91. The temperature of the heating wall is shown for individual points in [37]. The value of low frequency pulsations of temperature before onset of crisis was approximately 25°C. Therefore, we can consider that the transition to film boiling occurred from unstable boiling. Judging from the mutual placement of points on Figure 91, all remaining experiments also relate to unstable boiling.

M. I. Korneyev [6, 7] investigated the dependence of critical heat flux during boiling of magnesium amalgam on magnesium concentration in the mercury. The experiments were performed on horizontal tubes of carbon steel 22 mm in diameter. We can see from Figure 92 that with increasing concentration of magnesium in the mercury, the critical heat flux increases and reaches a maximum with a magnesium content of about 0.03% by weight. In the pressure range investigated (1-10 atm. abs.), the dependence of $q_{cr}$ on pressure was not noted by M. I. Korneyev.

The authors have produced some data on critical heat flows during boiling of mercury over a flat horizontal surface (see Figure 93).

The working sector was made of copper, which was separated from the mercury by a wall of Armco iron 0.3 mm thick. However, as an inspection of the sector after the experiments showed, the Armco iron wall was disrupted over a portion of the surface and the mercury contacted the copper. Therefore, the data produced can only be looked upon as preliminary. /149

Let us analyze the results of these experimental works on the critical heat flows during boiling of metals. First of all, we should note a decrease (in certain individual cases, by more than two times) in the value of critical heat flow with unstable boiling, which is characteristic for alkali metals within the range of pressures investigated in comparison with $q_{cr}$ with developed boiling (see Figure 87-90). We have received no information concerning experiments on the transition to film boiling from unstable boiling on non-metallic liquids. It might be expected that for non-metallic liquids

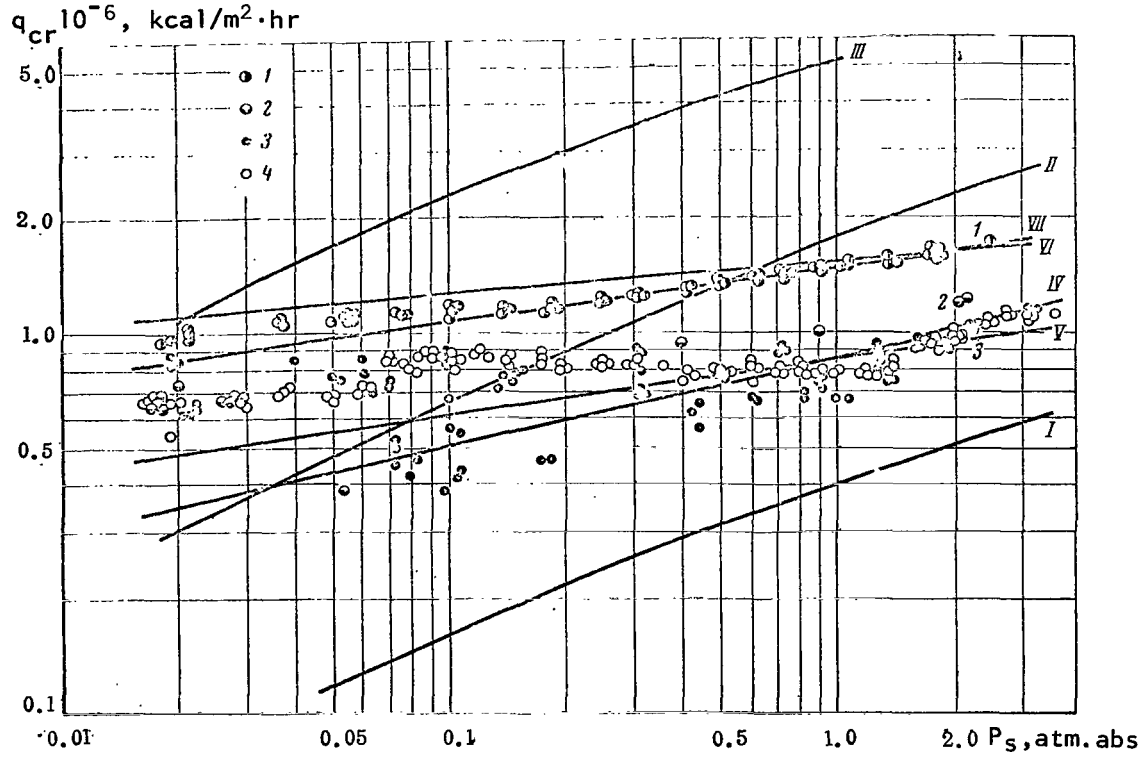


Figure 89. Experimental Data of the Authors on Critical Heat Fluxes During Boiling of Cesium over Flat Horizontal Surface of 1 Kh18N9T Steel. 1-4, Data of first, second, third and fourth series of experiments respectively. I, According to Formula (III.1); II, Formula (III.5); III, Formula (III.4); IV, Formula (III.6); Formula (III.11); V, C = 18; VI, C = 45; VII, Formula (III.7)

with transitions of this type the value of $q_{cr}$ would be lower than with transitions to film boiling from developed boiling.

The decrease in $q_{cr}$ from unstable boiling is probably related to the fact that the liquid is rather strongly superheated over relatively large areas of the surface. As a result of this, when boiling starts a significant quantity of vapor is formed, isolating those sectors for a certain period of time, which increases the probability of formation of stable vapor films over the heating surface.

Figure 94 shows experimental data on critical heat fluxes during boiling of sodium, potassium, cesium and rhubidium in the form of the dependence

$$\frac{q_{cr}}{q^{*}_{cr}} = F\left(\frac{P_s}{P_{cr}}\right), \qquad \text{(III.3)}$$

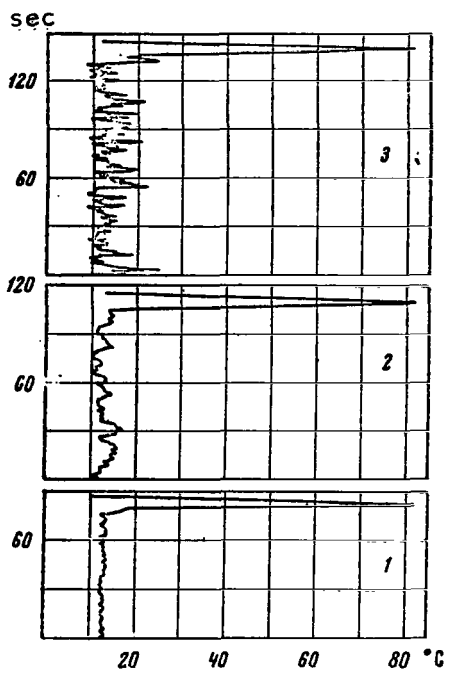


Figure 90. Recording of Wall-Liquid Temperature Difference in Experiments on $q_{cr}$ During Boiling of Cesium for Points 1, 2 and 3 of First, Second and Third Series of Experiments Respectively Shown on Figure 89.

suggested by V. M. Borishanskiy [94]. Here $q^*_{cr}$ is the critical heat flow at the standard reference pressure $(P/P_{cr})^*$. Figure 94 shows points produced for each metal under identical conditions. Thus, for sodium and cesium only data relating to developed boiling are taken; for potassium the data of Balzhiser are used, since they encompass a broader range of pressures than our experiments. The usage of only a portion of the available data on Figure 94, which reflects the dependence of critical heat fluxes on pressure during boiling of alkali metals in the range of pressures of approximately $4 \cdot 10^{-5}$ to $3 \cdot 10^{-2}$, is justifiable, since the nature of the dependence of $q_{cr}$ on pressure, as we can see from Figures 87 and 89, is approximately the same for all experimental data. There is only a difference in the levels of $q_{cr}$. During processing of the data shown on Figure 94, the reference pressure was the pressure $(P_s/P_{cr})^* = 3 \cdot 10^{-3}$. It is easy to see that the dependence of critical heat fluxes on pressure for all four alkali metals is practically identical within the range of pressures studied. The tangent of the inclination angle of the averaging line was approximately 0.12.

The range of relative pressures in which critical heat fluxes have been studied for both metals and non-metallic liquids lies within the limits of approximately $2 \cdot 10^{-4}$ to $3 \cdot 10^{-2}$. Data were also produced for metals at lower reduced pressures, whereas for ordinary liquids $q_{cr}$ was investigated up to pressures close to critical values.

Comparison of Figure 94 with Figures 82 and 83 indicates that with identical reduced pressures for non-metallic liquids the dependence of $q_{cr}$ on pressure is generally considerably stronger than for metals. The tangent of the angle of inclination of the averaging line on Figures 82 and 83 (within the limits $P_s/P_{cr}$ approximately $10^{-3}$-$2 \cdot 10^{-1}$) is approximately 0.3; whereas for alkali metals (within the limits $P_s/P_{cr}$ approximately $4 \cdot 10^{-5}$- $3 \cdot 10^{-2}$) it is approximately 0.12. We can see from Figure 83 that with low pressures (below

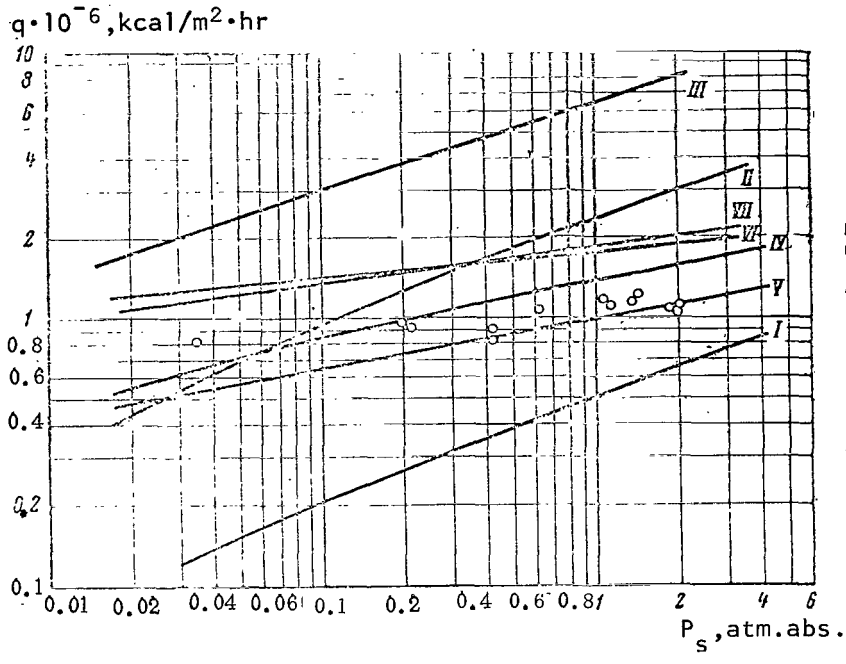


Figure 91. Experimental Data of Caswell and Balzhiser [37] on Critical Heat Fluxes During Boiling of Rubidium over a Horizontal Tube 9.63 mm in Diameter Made of "Haynes-25" Alloy. I, According to Formula (III.1); II, Formula (III.5); III, Formula (III.4); IV, Formula (III.6); Formula (III.11); V, C = 18; VI, C = 45; VII, Formula (III.7).

$10^{-3}$ $P_{cr}$) the dependence of $q_{cr}$ on $P_s$ becomes weaker and approaches the dependence produced for alkali metals. Possibly, at higher pressures (on the order of $10^{-1}$ $P_{cr}$ and higher) the nature of the dependence of critical heat flux on pressure during boiling of metals will approximate the nature of the dependence of $q_{cr}$ on pressure during boiling of non-metallic liquids.

Due to the limited nature of the experimental data, we cannot as yet draw conclusion concerning the nature of the dependence of critical heat fluxes during boiling of mercury. We can only assume that for mercury the dependence of $q_{cr}$ on pressure with reduced pressures such as those for which at the present time data have been produced on the critical heat flows during boiling of alkali metals will be weaker than for non-metallic liquids.

Depending on the state of the heating surface, as was indicated in the second Chapter, heat removal may occur either with unstable or with developed boiling. For example, with an increase in contact time between a stainless steel surface and sodium, the probability of existence of unstable boiling increases, while the application of specific roughness on a heating wall causes developed boiling. Therefore, the state of the heating surface can /153

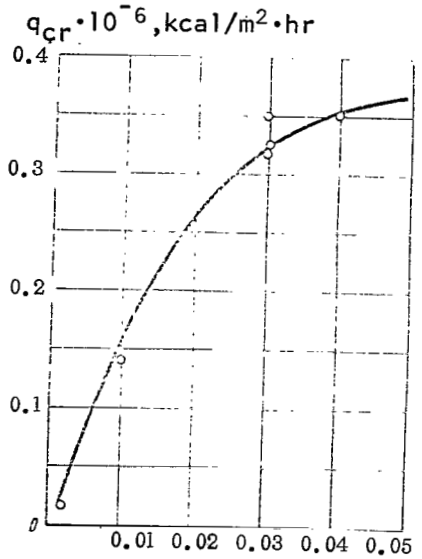


Figure 92. Experimental Data of Korneyev [6, 7] on Critical Heat Flows During Boiling of Magnesium Amalgam as a Function of Magnesium Concentration.

influence the value of critical heat flow significantly, since depending on the heat removal mode preceding the crisis the value of $q_{cr}$ differs. Data on the influence of the state of surface on the value of critical heat flux during boiling of metals with identical heat removal modes (for example, developed boiling and identical dependence of $\alpha$ on q) are as yet insufficient.

It can be assumed that the reduction of the values of $q_{cr}$ in the second through fourth series of our experiments on cesium (Figure 89) is related to an increase in the content of oxygen in the cesium, since all four series of experiments were performed over identically prepared surfaces of stainless steel. In particular, the decrease (drop) in critical heat flux at pressures of about 0.06-0.2 atm. abs. in the second and third series of experiments may be related to redistribution of oxygen between the cesium and the heating surface, which leads to a change in wettability of the surface.

As can be seen from Figure 63 iron, the principal component of 1Kh18N9T steel, should take up oxygen from cesium at temperatures beginning at about 500°C (the temperature of 500°C corresponds to a cesium vapor pressure of about 0.14 atm. abs.). The surface of the experimental sector should begin to operate as a getter first, since its temperature is highest. With a further increase in temperature, the surface of the tank will also act as a getter, which may lead to a change in the wettability of the heating surface as a result of redistribution of oxygen between the surface and the cesium.

If the heat transfer metal acts as a getter in relation to the heating surface, the content of oxygen (within the limits of solubility of oxides) should not have an essential influence on $q_{cr}$. Data on critical heat flows during unstable boiling of sodium produced on surfaces of VZH-98 alloy, stainless steel (our data), "Haynes-25" alloy, agree quite satisfactorily with each other, as well as with the data of Noyes and Lurie, produced over surfaces of stainless steel and molybdenum.

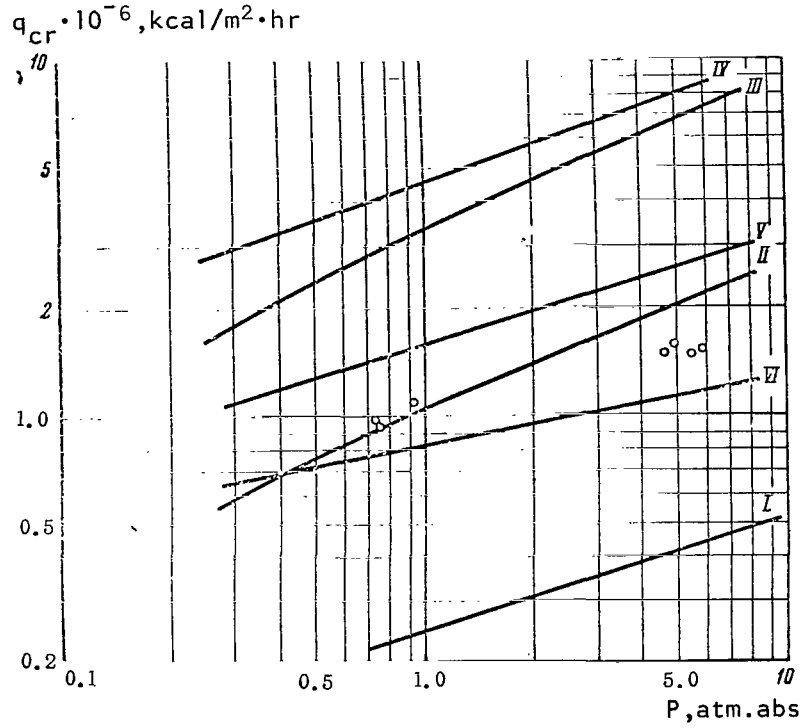


Figure 93. Experimental Data of the Authors on Critical Heat Fluxes During Boiling of Mercury I, According to Formula (III.6); II, Formula (III.1); III, Formula (III.5); IV, Formula (III.4); Formula (III.11); V, C = 45; VI, Formula (III.7).

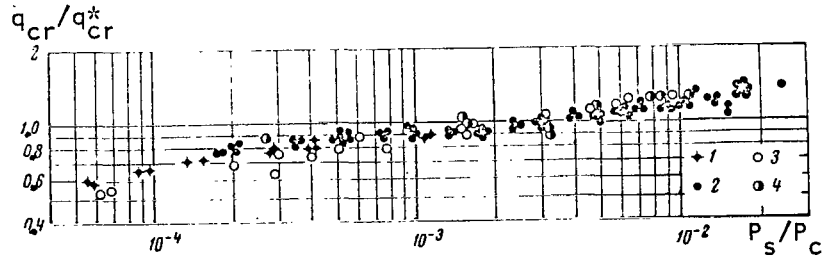


Figure 94. Dependence of Critical Heat Fluxes For Alkali Metals on Reduced Pressure. Value of $q^*_{cr}$ Taken at Reference Pressure $P_* = 0.003\ P_{cr}$. 1, Sodium; 2, Cesium (Data of the Authors); 3, Potassium [39]; 4, Rubidium [37].

With alkali metals (when the heat removal mode does not change in the process of the experiments), good reproducibility is achieved in experiments on $q_{cr}$ performed in series over the same surface. For example, the data produced in our experiments with developed boiling of cesium (first series on Figure 89), performed twice in series from minimum to maximum pressure values, agree quite well with each other. Rather good agreement within each series of experiments was produced for other alkali metals as well. /154

This fact is quite important in a study of the influence of various factors on the critical heat fluxes, for example in investigations of the dependence of $q_{cr}$ on $P_s$, for any liquids and particularly for alkali metals, since in this case changing of the working sector is a rather difficult operation, for obvious reasons. Whereas in experiments with non-metallic liquids, the working sectors may be replaced after every single experiment, for alkali metals, where dozens or hundreds of experimental points must be produced, this would be rather difficult.

The good reproducibility of results in experiments on critical heat fluxes during boiling of alkali metals over the same working sector can be explained by the slight changes in the state of the surface with sudden changes in temperature at the moment of crisis, by values up to several hundred degrees. This change in surface temperature at the moment of crisis, for example in experiments on water, as was noted above, can lead to a change in the value of $q_{cr}$ by more than double. Probably, since it is in contact with the vapors of the alkali metals and water at a temperature exceeding the saturation temperature by several hundred degrees for only a short time (on the order of one second), the surface in the latter case undergoes a greater change, for example a change in the contact wetting angle, which influences the value of critical heat flux.

The critical heat fluxes during boiling of alkali metals have been investigated only over flat surfaces heated to a diameter of 38 mm and horizontal tubes 9.53 and 6.35 mm in diameter, the 6.35 mm diameter tube being used only for a small number of points in experiments on sodium [33]. Data produced during boiling of sodium and potassium (see Figures 87, 88) over flat horizontal surfaces and horizontal tubes agree satisfactorily with each other. However, obviously, we cannot use the available experimental data as a basis for conclusions concerning the influence of dimensions and geometry of the working sector on the value of $q_{cr}$ during boiling of metals. We can only note that in most experiments on metals the value of the criterion We calculated according to (III.2) exceeded 2. Only in some individual experiments on sodium (6.35 mm tube) was the value of We somewhat less than 2. With $We > 2$, according to the results of [144], the value of $q_{cr}$ during boiling on horizontal cylindrical heaters (in [144], data were processed only for non-metallic liquids) is independent of the heater diameter.

Figures 87-89, 91, 93 show lines constructed according to the generalizing formula of S. S. Kutateladze (III.1) and G. N. Kruzhilin [113] /155

$$q_{cr} = 4700 \frac{T_s^{0.32}\sigma^{0.21}\lambda^{0.4}(r\gamma'')^{0.36}(\gamma-\gamma'')^{0.48}}{\gamma^{0.31}C_p^{0.08}\mu^{0.14}}, \quad \text{(III.4)}$$

describing the dependence of critical heat fluxes on pressure during boiling of non-metallic liquids at pressures over $10^{-3}P_{cr}$. We can see that these formulas do not agree with the experimental data on critical heat flows during boiling of alkali metals in magnitude or in nature of the dependence of $q_{cr}$ on pressure.

Generalized formulas for the calculation of critical heat flows during boiling of metals under conditions of free convection have been suggested by Noyes [18]

$$q_{cr} = 0.144 r\gamma''\left(\frac{\gamma-\gamma''}{\gamma}\right)^{1/3}\left(\frac{g^2\sigma}{\gamma}\right)^{1/4}\mathrm{Pr}^{-0.245}, \quad \text{(III.5)}$$

Caswell and Balzhiser [37]

$$q_{cr} = 5.038\cdot10^{-6}\frac{\gamma''\lambda r^2}{C_p\sigma}\left(\frac{\gamma}{\gamma''}\right)^{0.71} \quad \text{(III.6)}$$

and P. L. Kirillov [148]

$$q_{cr} = 0.666\cdot10^{6}\lambda^{0.6}\left(\frac{P}{P_{cr}}\right)^{1/4}. \quad \text{(III.7)}$$

On Figures 87-89, 91, 93 we see the dependence of critical heat fluxes calculated according to formulas (III.5)-(III.7). Analysis of these figures indicates that the formula of Noyes (III.5) does not agree with the experimental data for alkali metals and mercury either in magnitude or in the nature of the dependence of $q_{cr}$ on pressure. The formula of Caswell and Balzhiser (III.6) agrees rather well with the lower values of critical heat fluxes for potassium and cesium produced in experiments with unstable boiling and with data for rhubidium, which also relate to unstable boiling. For sodium, however, the lower values of $q_{cr}$ produced in the experiments differ from those calculated according to formula (III.6) by approximately two times. For mercury, the experimental values of $q_{cr}$ are considerably higher than those calculated from formula (III.6). The dependence of critical heat flows on pressure according to the Caswell-Balzhiser formula is somewhat stronger than that produced in the experiments on alkali metals the results of which are summarized on Figures 87-89, 91. The formula of P. L. Kirillov (III.7) agrees satisfactorily with the higher values of $q_{cr}$ produced in experiments on alkali metals, while the dependence of critical heat flows on pressure

according to this formula corresponds approximately to the dependence of $q_{cr}$ on $P_s$ produced experimentally. Satisfactory agreement of formula (III.7) /156 is observed with the experiments on mercury.

At the present time, the hydrodynamic theory of the boiling crisis under conditions of free convection is one of the most widely used theories. In the hydrodynamic theory of the boiling crisis it is assumed that the crisis is determined by the vapor content near the heating wall, which is proportional to the heat flux. Zuber [123] theoretically produced a value of constant B in the formula of Kutateladze (III.1), based on the hydrodynamic model of the boiling crisis, assuming that all the heat from the heating wall is carried off with the vapor. Works on bubbling [149, 150] also agree with the hydrodynamic conception of the boiling crisis. However, the hydrodynamic theory does not explain the essential influence of the state of the heating surface on the value of critical heat flows.

It is possible that the onset of crisis is related to the attainment on the heating surface of a temperature corresponding to the temperature of the spheroidal state of the liquid.

From this point of view, we can explain the influence on the critical heat flow of the state of the surface, thickness and material of the heating wall. Actually, the thinner the heating wall (beginning at a certain thickness) and the lower the value of temperature conductivity coefficient of the wall material, the higher can be the values of local temperature with $q = \text{const}$ and $p^s = \text{const}$. However, in order to confirm or negate this hypothesis, we require more data.

The weakening of the dependence of $q_{cr}$ on pressure, which is equivalent to an increase in the value of B in formula (III.1), at low pressures for non-metallic liquids is explained in [133] by an increase in the rate of growth of vapor bubbles as the pressure is decreased. P. L. Kirillov [148] also relates the onset of crisis at low pressures to the rate of growth of vapor bubbles. Here, in order to calculate the rate of increase of vapor bubbles in metals, dependences are used (as for non-metallic liquids), based on limitation of the rate of bubble growth by thermal resistance of the boundary layer of the liquid around the bubble. However, these dependences, as will be shown in the next Chapter, cannot be used for calculation of the rate of growth of vapor bubbles of metals, at least at low pressures.

On Figure 95 we show the results of experiments on the transfer of heat from the heating surface with vapor performed on water by A. A. Tsyganok at the Physics and Energy Institute.

We can see from Figure 95 that during boiling of water as the heat flow increase, $q_v$ increases, and at over about 0.5 $q_{cr}$, the rate of this increase is decreased. As the pressure decreases, the share of heat carried away with the vapor decreases and the role of convective heat liberation increases. /157

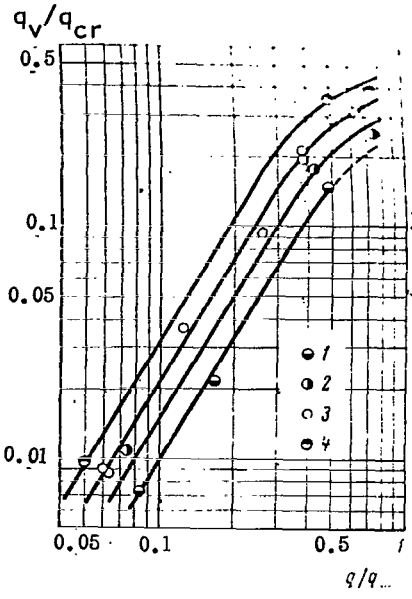


Figure 95. Dependence of Share of Heat $q_v/q$, Transferred by Vapor on Relative Heat Flow $q/q_{cr}$ During Boiling of Water Over Wire 1.8 mm in Diameter.
1, P = 0.13 atm.abs.;
2, P = 0.29 atm.abs.;
3, P = 0.68 atm.abs.;
4, P = 1.24 atm. abs.

Therefore, the weakening of the dependence of critical heat flows on pressure at reduced pressures may be related to the increased contribution of convective heat transfer.

The difference in the nature of the dependence of $q_{cr}$ on pressure during boiling of alkali metals and non-metallic liquids over a broad range of pressures and the difference in the formula of S. S. Kutateladze from experimental data on critical heat flows during boiling of sodium, potassium, cesium and rubidium can be explained by the fact that during boiling of alkali metals with high heat conductivity, even at heat flows near the critical values, it is possible for a significant portion of the heat in the investigated pressure range to be transmitted from the heating surface by way of the liquid, and the dependence of vapor content in the layer near the wall on heat flow is different than for non-metallic liquids. The critical heat flow can be written as the sum of two flows

$$q_{cr} = q_{\zeta} + q_v, \qquad \text{(III.8)}$$

where $q_{\zeta}$ is the heat flow carried away from the surface by the liquid; $q_v$ is the heat flux carried away from the heating surface by vapor bubbles.

We must emphasize that we are not analyzing the mechanism of heat transfer directly from the heating surface to the bubble growing on its surface, but rather are discussing only the quantity of heat carried through the boundary layer by bubbles ($q_v$) and by liquid ($q_{\zeta}$).

If we assume that $q_v$ can be calculated using the formula of S. S. Kutateladze (III.1), then from (III.8) is easy to produce

$$q_{cr} = \left[1 + \frac{q_{\zeta}}{q_v}\right] Br\,(g\gamma'')^{1/4}\,[\sigma(\gamma - \gamma'')]^{1/4}. \qquad \text{(III.9)}$$

Processing of data on critical heat flows during boiling of sodium, potassium, cesium and rubidium, presented on Figures 87-89, 91, has indicated that $q_ж/q_v$ can be expressed in the form of the dependence

/158

$$\frac{q_ж}{q_v} = \frac{C}{P_{cr}}\left(\frac{P_s}{P_{cr}}\right)^{-m}. \qquad \text{(III.10)}$$

During processing of experimental data, the heat flow $q_ж$ was found as the difference $q_{cr} - q_v$, while the heat flow $q_v$ was calculated using the formula of S. S. Kutateladze (III.1). The values of critical pressures were taken from [95] and were 357, 169, 103 and 130 atm. abs. for sodium, potassium, cesium and rubidium respectively. We can see from (III.10) that with increasing pressure the share of heat transferred by the liquid $(q_ж/q_v)$ should drop. Formula (III.9), considering (III.10), can be written in the form

$$q_{cr} = \left[1 + \frac{C}{P_{cr}}\left(\frac{P_s}{P_{cr}}\right)^{-m}\right] Br\,[g\gamma'']^{1/2}[\sigma(\gamma-\gamma'')]^{1/4}. \qquad \text{(III.11)}$$

The coefficients C, B and possibly the exponent m in formula (III.11) can take on various values, like the coefficient B in the formula of S. S. Kutateladze, depending on the conditions of performance of the experiments. The values of coefficients may also change somewhat in relation to more precise determination of the values of critical pressures for alkali metals. Comparison of formulas (III.10) and (III.11) with experimental data indicates that the values of coefficients can be assumed as follows: C = 45 for developed boiling; C = 18 for unstable boiling; B = 0.14; the exponent m = 0.4. Coefficient C has the dimensionality of pressure.

On Figures 87-89, 91, 93, the dependence of $q_{cr}$, calculated according to formula (III.11) (with the values of C, B and m assumed above) for sodium, potassium, cesium, rhubidium and mercury respectively is compared with experimental data on critical heat flows for these metals. We can see that the formula quite satisfactorily agrees with the experimental data both as to value of critical heat flows and as to the nature of the dependence of $q_{cr}$ on pressure for alkali metals in the investigated pressure range. Formula (III.11), better than the other formulas analyzed, describes the experimental data produced on critical heat flows during the boiling of alkali metals. In particular, it considers the difference in values of $q_{cr}$ with developed and unstable boiling. However, formula (III.11) cannot be recommended for calculation of critical heat flows during boiling under natural convection conditions except for sodium, potassium, cesium and rubidium at pressures from a few hundredths of an atmosphere to a few atmospheres. The possibility of using formula (III.11) for calculation of $q_{cr}$ during boiling

of these metals in the area of higher pressures, as well as during boiling of other metals requires further experimental testing.

Formula (III.11), the formula of S. S. Kutateladze (III.I) and that of P. L. Kirillov (III.7), agree satisfactorily with the experimental data for mercury presented in Figure 93, but due to the limited nature of the experimental material it is as yet difficult to give preference to any one of these formulas. /159

## Conclusions

1. The critical heat flows during boiling of alkali metals under conditions of free convection has been experimentally investigated for sodium (0.015-1.5 atm. abs.), potassium (0.01-1.5 atm. abs.), cesium (0.018-3.5 atm. abs.) and rubidium (0.35-1.9 atm. abs.). The experiments have encompassed a range of reduced pressures of approximately $4 \cdot 10^{-5}$ to $3 \cdot 10^{-2}$.

2. With increasing values of low frequency pulsations of the temperature of the heating wall, that is instability of the boiling process, the values of critical heat flows for the alkali metals decrease. The difference between the values of critical heat flows with developed and unstable boiling may reach over 100%.

3. Within the investigated range of pressures, the dependence of critical heat flows on reduced pressure for sodium, potassium, cesium and rubidium is identical and considerably weaker than for water and organic liquids.

4. Generalized formulas for the calculation of critical heat flows during boiling of liquids under conditions of free convection, describing the experimental data for water and organic liquids, do not agree with the experimental data on critical heat flows during boiling of alkali metals within the range of pressures, either in magnitude, or in nature of the dependence of $q_{cr}$ on pressure. For the calculation of critical heat flows during boiling of sodium, potassium, cesium and rubidium at pressures from a few hundredths of an atmosphere to several atmospheres, formula (III.11) can be recommended, in which the difference in values of $q_{cr}$ during developed and unstable boiling is considered, and which satisfactorily reflects the nature of the dependence of critical heat flows on pressure produced in the experiments for these alkali metals within the pressure range investigated.

5. Some data have been produced on critical heat flows during boiling under conditions of free convection for mercury (0.7 and 5 atm. abs.) and magnesium amalgam (1-10 atm. abs.). The experimental data on critical heat fluxes for mercury agree satisfactorily with the calculated values of $q_{cr}$ from formulas (III.1), (III.7) and (III.11). Due to the limited nature of the experimental data, we can not as yet conclude the influence of pressure and other factors on critical heat flows during boiling of mercury.

# CHAPTER 4 /160

## CERTAIN PROBLEMS IN THE PHYSICS OF BOILING OF METALS

In order to achieve an understanding and construct a well founded model of the process of heat exchange during boiling, it is necessary to know the elementary processes determining heat exchange under these conditions. During bubble boiling, heat from the surface is carried away with the vapor ($q_v$) and with the liquid ($q_\ell$). For metals boiling at high temperatures, heat radiation should also make a slight concentration to the transfer of heat.

The relationship between the components of the heat flow depends on the nature of the liquid, distribution of temperatures, velocities and phases at the heating wall, which in turn are determined by the distribution of the active centers of vapor formation, rate of growth, frequency of separation and separation volumes of the vapor bubbles, as well as the geometry, dimensions and materials of the heater.

For non-metallic liquids, problems of the growth and separation of vapor bubbles have been the subject of a significant number of experimental and theoretical works. In some works, the temperature field in the liquid has been measured (in the volume, at the heating surface and in the boundary layer of a vapor bubble) as well as in the vapor (over the level of the liquid and in the vapor bubbles).

The conditions of seeding of vapor bubbles and the stability of operation of centers of vapor formation are of great significance for heat exchange during boiling.

In metals, direct experimental determination of such quantities as the distribution of vapor formation centers, growth rate, frequency of separation and separation diameter of vapor bubbles involves, for obvious reasons, considerable experimental difficulties. However, the individual elementary processes involved in the boiling of metals can be judged to some extent, /161
primarily on the basis of indirect observations and comparison with similar elementary processes studied for non-metallic liquids considering the physical properties of these two classes of liquids.

### Distibution of Temperature in Boiling Liquid and Vapor

On Figure 39 we show the qualitative distribution of temperature during boiling of a liquid in a large volume at the saturation temperature. The principal drop in temperature occurs at the wall in boundary layer $\delta$, and further through the height the temperature of the liquid remains approximately constant, while there is a certain temperature jump $\delta t$ between the free level of the liquid and vapor.

The profiles of temperatures during boiling of water at atmospheric pressure and at heat fluxes up to approximately $10^5$ kcal/m$^2$·hr were measured in [92, 151]. The principal drop in temperature occurs over a distance of several tenths of a millimeter (about 0.3 mm) from the heating surface.

It is found in [92] that $\delta \sim \alpha^u$ $(u < 0)$, and formulas are recommended for calculation of the temperature field in the boundary layer describing the experimental data

$$\frac{\Delta t_y}{\Delta t} = 1 - \frac{y}{\delta} \tag{IV.1}$$

where $y < 0.57\delta$ and

$$\frac{\Delta t_y}{\Delta t} = A_\delta \left(\frac{y}{\delta}\right)^{-k} \tag{IV.2}$$

where $y > 0.57\delta$, where $A_\delta$ is a constant determined by simultaneous solution of equations (IV.1) and (IV.2) where $y = 0.57\ \delta$.

In the boundary layer, the value of pulsations of the temperature reached about 0.6 $\Delta t_a$. Pulsations of temperature of the heating wall, the values of which are comparable to the temperature head $\Delta t_\alpha$, and a frequency approximately the same as the frequency of separation of vapor bubbles were measured in experiments on water in [89-91, 152].

Figure 96 shows a record of the pulsations of temperature of the heating wall during boiling of water from [90]. The slow rise in temperature corresponds to the period of heating of the liquid after separation of a vapor bubble, and the sharp drop in temperature corresponds to the period of bubble growth. This conclusion was drawn on the basis of comparison of recordings of wall temperature and results of synchronized high speed cinamatography [91, 152].

On Figure 97 we show a typical temperature profile for developed boiling of metals, measured by a moving thermocouple (see Figure 24) in experiments of the authors on sodium, while Figure 98 shows a typical temperature profile for heat removal by convection without boiling, produced in the same series of experiments. The thickness of the thermal boundary layer $\delta$ with developed boiling of sodium is several millimeters, whereas with heat removal by convection without boiling $\delta$ is considerably greater. Further through the height of the liquid, the temperature remains approximately constant. Located next to the heating wall, a thermocouple records temperature pulsations at a frequency on the order of one Hz. The measured value of pulsations is approximately 50% of the temperature head $\Delta t_\alpha$. Noyes and Lurie [33] measured the temperature pulsations of a heating wall during boiling of sodium using a thermocouple fixed (welded) near the heating surface. The

/162

processing of this data indicates that the resonant frequency of pulsations is about 1.7 Hz. with a sodium pressure of about 0.1 atm. abs.

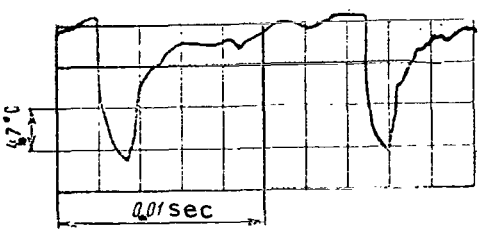


Figure 96. Change in Temperature of Heating Surface During Boiling of Water at Atmospheric Pressure [90]. = $547 \cdot 10^3$ kcal/m$^2$·hr.

A comparison of the results of measurements of temperature at the heating surface on the side of the liquid and the side of the wall during boiling of water and sodium indicates that in both cases there are temperature pulsations, the values of which are comparable with mean temperature head $\Delta t_\alpha$. With identical pressures and heat fluxes, the frequency of temperature pulsations of the heating surface for water is greater than for sodium. Just as with convective heat exchange, during developed boiling of sodium the thickness of the thermal boundary layer is considerably greater than during boiling of water.

According to the data of [151] during boiling of water at atmospheric pressure the heating of the liquid in the volume in relation to the vapor amounts to some tenths of a degree, whereas the temperature heat $\Delta t_\alpha$ is about 10°C. In this case, in order to calculate the coefficient of heat transfer we can use both $\Delta t_\alpha$ and $\Delta t_s$. Usually, the coefficient of heat transfer is related to $\Delta t_s$, although in many experiments $\Delta t_\alpha$ is measured, and no corrections to $\delta t$ are entered during processing of experimental data. Analysis of experimental data of the authors and from [17, 19] indicates that super heating of the liquid $\delta t$ during boiling of metals in the range of pressures investigated may be greater than some tenths of a degree. Super heating of the liquid during boiling results from the fact that a portion of the heat liberated by the heating surface is transmitted to the liquid, then within the volume from the liquid to the vapor. The quantity of heat Q transmitted from liquid to vapor can be expressed as: /164

$$Q = \int_{F\phi} \alpha_b \, \delta t \, dF_\phi, \qquad \text{(IV.3)}$$

where $dF_\phi$ is the elementary surface area of the phase separation boundary; $\delta t$ is the super heating of the liquid in the zone $dF_\phi$. Where Q = const and $P_s$ = const, $\delta t$ will be greater, the less the area of the surface of the phase separation boundary $F_\phi$ and the value of $\alpha_b$. In this case, when there is no boiling, the phase separation boundary is the free surface, the value of superheating $\delta t$ should be maximal. With unstable boiling, superheating $\delta t$ should also be greater than with developed boiling, since $F_\phi$ is greater with developed boiling. This has been confirmed by the experimental data of the authors. Actually, super heating of a liquid in relation to the vapor,

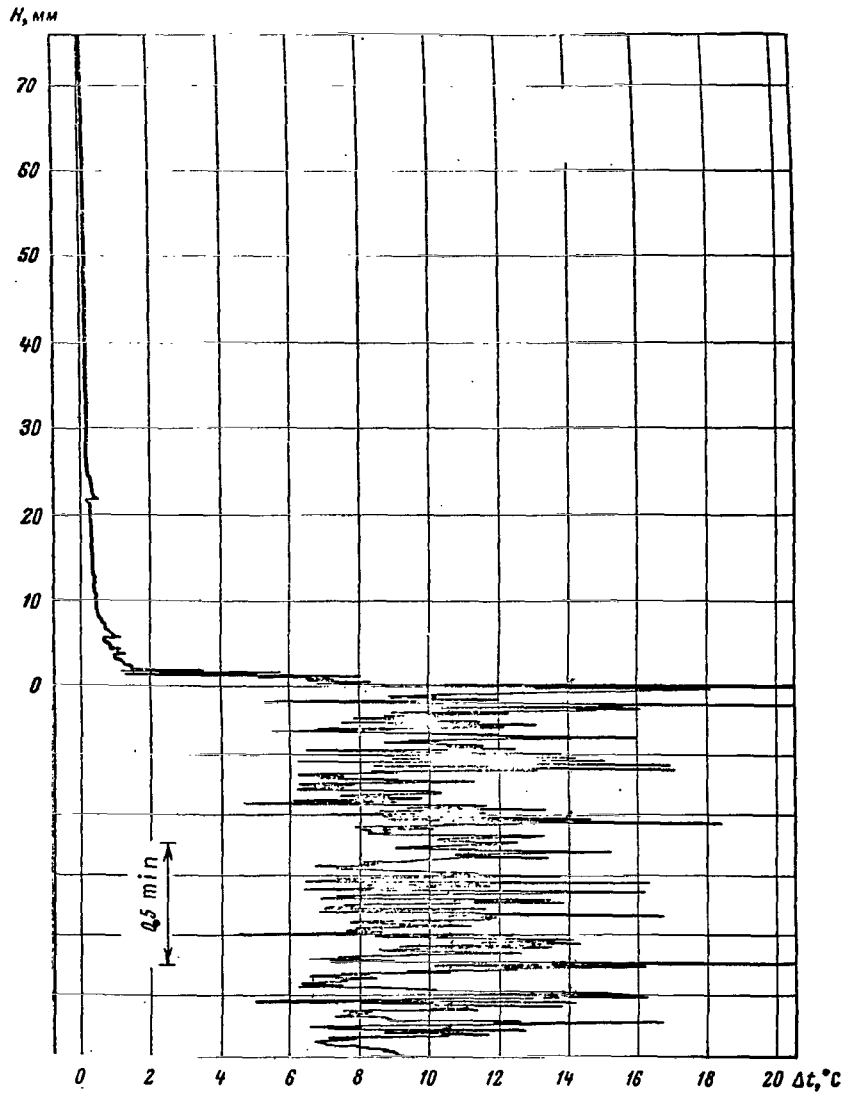


Figure 97. Distribution of Temperatures in Sodium During Developed Boiling (Data of the Authors). $q = 0.7 \cdot 10^6$ kcal/m$^2$·hr; $t_z = 785°C$, H is the Distance From The Heating Surface.

as measured by a moving thermocouple, during heat removal by convection with subsequent liberation of heat by evaporation from the free surface was greater than with unstable boiling with comparable heat flows and pressures, and was greater with unstable boiling than with developed boiling. These discussions are also confirmed by experiments on water [153]. For surfaces with great roughness, having a large number of centers of vapor formation and consequently a large area of the phase separation boundary $F_\phi$, lower values of super heating $\delta t$ and higher values of heat transfer coefficients are produced.

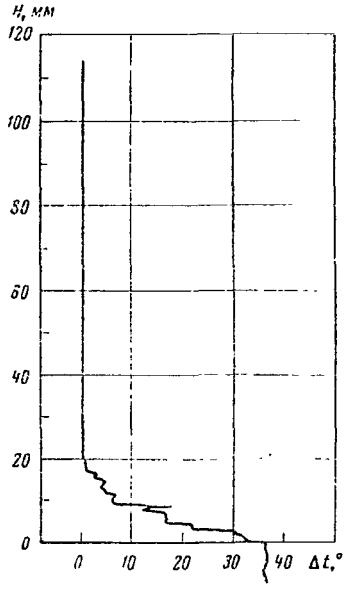


Figure 98. Distribution of Temperature in Sodium During Heat Removal by Convection Without Boiling (Data of the Authors) $q = 0.2 \cdot 10^6$ kcal/$m^2 \cdot hr$, $t_l = 789°C$; H is the Distance From the Heating Surface.

## Conditions of Seeding of Vapor Bubbles

The problem of seeding of the vapor phase in a liquid has been studied theoretically on a number of works, for example [154-159], and has been investigated experimentally [78, 100, 160-166].

If the dimension of a new phase center, including the vapor phase, is less than a certain critical dimension $\rho^*$, the center is unstable and will disappear after a certain time interval following its formation. Centers of a new phase having dimensions equal to $\rho^*$ are called seeds. In order to form the new phase, its seeds must be formed in the old phase. The probability of formation of a new phase in an old phase $\psi$ is determined by the work W required for formation of the new phase

/165

$$\psi \sim e^{-\frac{W}{KT}}. \qquad \text{(IV.4)}$$

It follows from this dependence that the less W, the greater $\psi$. Homogeneous formation of vapor seeds (within the volume of a super heated liquid) and heterogeneous formation (in the presence of a separating surface) are distinguished. The problems have been analyzed in detail in [154, 159].

V. P. Skripov [160], for example, superheated water at atmospheric pressure (in another liquid having a higher boiling point and forming mutually insoluble vapors with water) to about 300°C. The results produced by V. P. Skripov [160, 161] agree well with the calculated values of superheating according to the formula of Dering-Fol'mer for volumetric boiling with homogeneous seed formation, presented in [161]

$$J_z = \tau z \left[\frac{6\sigma}{(3-\chi)\pi m^*}\right]^{1/2} e^{-\frac{r^*}{KT}} e^{-\frac{16\pi\sigma^3}{3KT(P_s-P)^2(1-\gamma''/\gamma)^2}}, \qquad \text{(IV.5)}$$

where $J_z$ is the number of vapor seeds formed over time $\tau$ in a liquid containing z molecules; m* is the mass of a molecule; $\chi = 1 - P/P_s$; r* is the heat of vapor formation per molecule; P is the pressure in the liquid; $\sigma$ and $P_s$ are taken at the super heating temperature. The boundary of super heating is considered the temperature at which one seed arises in one second per 1 $cm^3$. It should be noted that at temperatures near the temperature of volumetric boiling, $J_z$ depends very strongly on temperature. For example, at atmospheric pressure, according to the calculations using formula (IV.5) performed in [161], for ethyl alcohol $J_z = 1$ $cm^{-3}$ $sec^{-1}$ and $J_z = 10^{20}$ $cm^{-3}$ $sec^{-1}$ at 188 and 198°C respectively. An estimate of the temperature of the beginning of volumetric boiling of sodium at atmospheric pressure using formula (IV.5) gives the value t ~1800°C.

The relatively slight super heating of liquids required for boiling to start usually encountered in practice result from factors which facilitate the beginning of boiling. Let us analyze in greater detail the conditions of formation of the vapor phase on the surfaces of solid bodies. Ye. I. Nesis [156], on the basis of analysis of work W related to the formation of a vapor seed, has shown that W will be minimal, with otherwise equivalent conditions, if the liquid does not wet the surface. In his work he concludes that the centers of vapor formation are "active pores" in the walls of the vessel. These pores are active if their dimensions lie within certain limits, dependent on the contact wetting angle $\theta$, the degree of superheating of the liquid $\Delta t_s$, and for the surfaces being wet, on the length of preliminary /166 contact of the liquid with the wall. This latter condition is related to the solution of gas in the liquid located in the pores. Bankoff [157] analyzed the conditions of seeding of the vapor phase in the volume of a homogeneous liquid, on a flat surface, on steps and depressions in the surface. He showed that for boiling to start under these conditions with the contact wetting angles usually encountered in practice, great superheating of the liquid is required. The centers of vapor formation, Bankoff concludes, might be non-wet depressions or wet depressions filled with gas or vapor. Similar conclusions are drawn in a number of other works. The thermodynamic approach to the analysis of conditions of seeding of the vapor phase used in [154-159] is general in nature and is valid both for non-metallic liquids and for liquid metals.

The conclusions of the theoretical works are confirmed by a number of experiments. In [163, 166], it is reported that water at atmospheric pressure was heated in clean glass to 200-270°C. The contact wetting angle of clean glass by water is near 0° [164].

Sabersky [165] succeeded in superheating water at atmospheric pressure on very clean wires to 150-160°C, after first subjecting the entire system to the effects of high pressure (up to 1,000 atm. abs.) or careful degassing. Under the influence of the high pressure, the gas located in the scratches and the depressions is dissolved in the liquid [163].

According to the data of [17] for sodium on stainless steel surfaces, the contact wetting angles at 120°C are 100-110°. As the temperature is increased, the wetting angle decreases continually. At temperatures over 350°C, complete wetting occurs, that is the contact angles are near 0°.

In [167, 168], the wettability of pure metal surfaces by sodium was studied. It was discovered that the wettability ($\theta < 90°$) of surfaces of such metals as, for example, molybdenum, tungsten, chromium begins at temperatures over 160°C, and the time required for wetting decreases with increasing temperature. The onset of wetting is explained in [17, 167, 168] by the reduction of sodium on the surfaces of the oxide films.

It was noted in the second Chapter that as the contact time with the heating surface increases, for example for stainless steel surfaces and sodium, the superheating of the liquid $\Delta t_s$ required for boiling to begin decreases. This can be explained by the fact that as time passes the area of the heating surface covered with the oxide films is decreased. Probably the oxide films are reduced in depressions with minimum dimensions last, and these depressions begin to be wet by the sodium. This should also be true /167
in relation to other liquid metal heat transfer media which are getters (reducing oxide films) in relationship to the structural metal.

The seeding of bubbles only in depressions or scratches on the heating surface was observed directly in experiments with ordinary liquids described in [100, 169-171]. Corty and Foust [100], in experiments with a number of organic liquids, discovered that the superheating required to stop boiling depends on the time which has passed after boiling has stopped. This can be explained by the fact that the greater the time passed since the moment a bubble has separated, the less vapor remains in the depression due to its condensation. As the contact wetting angle decreases the penetration of liquid into depressions filled with gas or vapor is facilitated [157].

When the heating surface is not wet by the liquid, boiling begins at temperatures on the heating surface near the saturation temperature. This has been observed in experiments with water [96, 172] and mercury [1-10].

It was experimentally demonstrated in [169] that under isothermal conditions, the radius of the mouth of a depression acting as a center of vapor formation agrees satisfactorily with the radius of a vapor seed $\rho^*$ calculated according to the formula

$$\rho^* = \frac{2A\sigma T_s}{r\gamma''\Delta t_s}. \qquad \text{(IV.6)}$$

However, with an uneven temperature field at the heating wall activization of the same vapor formation centers requires more intensive superheating $\Delta t_s$ than that corresponding to formula (IV.6). Hsu [173], on the basis of the assumption that a bubble in a depression of radius $\rho$ can arise only if superheating of the liquid $\Delta t_s$ calculated according to formula (IV.6) is reached for distance $\rho^*$ from the heating surface, produced in expression for estimation of the maximum $\rho_{max}$ and minimum $\rho_{min}$ radii of depressions on the heating surface which can act as vapor formations centers with $t_w$ = const or q = const. For the case of $t_w$ = const with the liquid heated to $t_s$

$$\rho_{\substack{max\\min}} = \frac{\delta^*}{2C_1}\left[1 \pm \left(1 - \frac{8A\sigma T_s C_2}{r\gamma''\delta^*\Delta t_s}\right)^{1/2}\right], \qquad \text{(IV.7)}$$

where $\delta^*$ is a certain thickness of the boundary layer; $C_1$, $C_2$ are constants defined by experiment. The comparison of formula (IV.7) with available sparce experimental data on water, pentane and ether performed by Hsu, has shown that the experimental values of $\rho$ lie between $\rho_{max}$ and $\rho_{min}$ calculated /168
according to formula (IV.7). It is not yet possible to use formula (IV.7) for metals, since as yet there are no experimental data for determination of $C_1$, $C_2$ and $\delta^*$, which are essentially determined on the basis of experimentation by determining the dependence of $\rho$ on $\Delta t$. However, as was shown in [173], the dependence of $\rho^*$ on $\Delta t_s$ according to formula (IV.6) passes approximately equidistantly from the dependence of $\rho_{min}$ on $\Delta t_s$, differing, for example, for water (where $\Delta t_s > 5°C$ and $P_s$ = 1 atm. abs.) by only two times. This gives us some basis for estimation of the minimum value of the radius of a depression (filled with a vapor or gas) which can act as a vapor formation center by using formula (IV.6).

Figure 99 shows the dependence of $\rho^*$ according to formula (IV.6) on pressure for sodium, potassium, cesium, mercury, water and ethyl alcohol with a liquid superheating $\Delta t_s$ of 1°C. We can see that with identical absolute pressures, the value of $\rho^*$ for metals is greater than for water and ethyl alcohol.

Figure 100 shows the dependence of $\rho^*$ on reduced pressure for $\Delta t_s$ = 1°C for the same materials as on Figure 99. With identical reduced pressures, the difference between values of $\rho^*$ for these liquids is even less than with identical absolute pressures, and for the alkali metals analyzed the dependence of $\rho^*$ on $P/P_{cr}$ is practically identical. Figures 99 and 100 indicate that the dimensions of depressions acting as centers of vapor formation for alkali metals and mercury should be larger than for water and ethyl alcohol

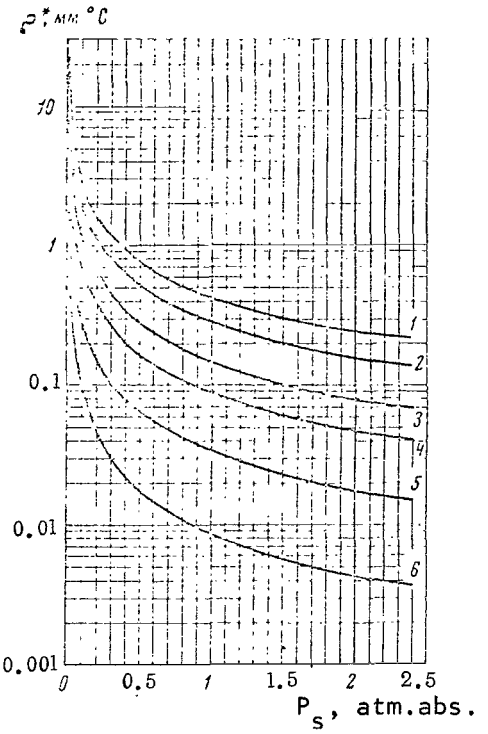


Figure 99. Dependence of Vapor Seed Radius ρ* on Absolute Pressure for Certain Metals and Nonmetallic Liquids, Calculated According to Formula (IV.6) (Superheating 1°C). 1, Mercury; 2, Sodium; 3, Potassium; 4, Cesium; 5, Water; 6, Ethyl alcohol.

with comparable $P_s$ and $\Delta t_s$. For example, ρ* for sodium should be approximately ten times as large as for water. Most experiments with sodium have been performed on surfaces with ordinary finishing, on which water (without degassing of the vapor formation centers) at atmospheric pressure boils at $\Delta t_s$ usually not over 5°C. If we consider that the same depressions, filled with gas or vapor, act as vapor formation centers for sodium, then $\Delta t_s$ for sodium, calculated according to formula (IV.6) on the assumption of ρ = idem, will be approximately 225°C and 80°C with $t_s$ 700 and 800°C respectively. However, this comparison does not consider the differences in contact wetting angles, which may be quite essential, for water and sodium on the metal surfaces. /169

As the contact wetting angle is decreased, the superheating required for boiling of a liquid on the heating surface to begin, increases both due to an increase in the work required for formation of a vapor seed (with ρ* = const) and due to the reduction in dimensions of vapor or gas phase in the depression as a result of facilitation of filling of the depression with liquid with decreasing θ.

Thus, high superheating of alkali metals, particularly sodium and potassium, produced in experiments using a number of structural materials as heating surfaces, can be explained by the large dimensions of vapor seeds (calculated for $\Delta t_s$ = 1°C) and the good wetting of these structural materials with the alkali metals. /170

A number of authors [100, 101, 170, 174-177] have performed experimental investigations into the number of vapor formation centers N per unit area of the heating surface during boiling of water, organic liquids and aqueous salt solutions. In all these works, a strong increase of N has been noted with increasing $\Delta t_s$. For example, according to [176], the density of vapor formation centers is 176 $cm^{-2}$ with a heat flux of $860 \cdot 10^3$ kcal/$m^2$·hr. For rough surfaces, with otherwise equivalent conditions, N is greater than for smooth surfaces [100, 101, 174]. With increasing pressure (with q = const)

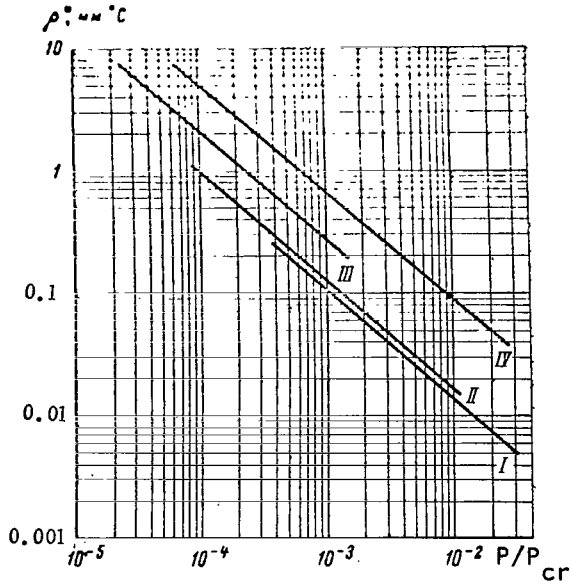


Figure 100. Radius of Vapor Seed Formation ρ* For Certain Metals and Non-metallic Liquids Calculated According to Formula (IV.6) (Superheating of 1°C) As A Function of Reduced Pressure. I, Ethyl alcohol; II, Water; III, Mercury; IV, Sodium, potassium, cesium.

the number of active vapor formation centers increases [174, 175]. With increasing degree of roughness of the heating surface and with increasing pressure, the number of active vapor formation centers should also increase during boiling of metals. Experimental data on the number of active centers of vapor formation during boiling of metals have not yet been produced.

## Stability of Operation of Vapor Formation Centers

The most probable vapor formation centers during boiling of liquid, as has been noted, are depressions on the surface of the heating wall, filled with gas or vapor. The stability of operation of vapor formation centers is quite significant for the process of heat exchange during boiling, particularly when the number of active centers of vapor formation is not great. For example, during developed boiling of sodium in the pressure range of approximately 0.1-1 atm. abs., the temperature heats are approximately the same as during boiling of water at atmospheric pressure. This gives us reason to assume that during developed boiling of sodium, primarily large depressions act as vapor formation centers. On surfaces not subjected to special working, the distribution of depressions by dimensions should be near normal. Therefore, the number of "large" depressions, which primarily act as vapor formation centers for the boiling of sodium, will be relatively small. Obviously, the less the number of active centers of vapor formation on the heating surface, the higher the probability that boiling will stop on this surface or over individual sectors of the surface. As the pressure is reduced, the number of active centers of vapor formation decreases. The operation of individual vapor formation centers has been seen to stop (with q = const) in experiments with non-metallic liquids [73, 114]. The transition from heat removal with developed boiling to heat removal with unstable boiling and from heat removal with boiling to heat removal by convection with unchanging values of q and $P_s$, characteristic for alkali metals in the pressure range investigated, indicate that the operation of some or all of the vapor formation centers have stopped operating. If after a bubble is separated, a depression is fully or even partially filled with liquid, this vapor formation center will cease to function. The probability of filling of a depression with liquid, as

/171

Bankoff has noted [157, 178, 179], is greater, the less the contact wetting angle $\theta$ and the greater the absolute geometric dimensions of the depressions. For example, for a conical depression with a solid angle $\beta$, the condition of retention of the vapor (gas) Bankoff considers to $\theta > \beta$. According to Griffith [169], "the most stable depressions are those for which the contact wetting angles are greatest." Depressions with parafinned surfaces in experiments described in [169] operated more stably as vapor formation centers than depressions of the same geometry and dimensions with clean surfaces. It was shown in [169] that if a depression expands downward, it should be stable (as a center of vapor formation) in all cases. Obviously, the greater the contact time of the liquid with the surface in the area of the depression, the higher the probability of filling of this depression with liquid. Due to the high temperature conductivity involved in the boiling of metals, both the thickness of the boundary layer and the heating time of the liquid after separation of a bubble required to reach the temperature necessary for seeding a new bubble are considerably greater than, for example, in the boiling of water.

In order for a new vapor bubble to arise on a vapor formation center after separation of an old vapor bubble, the liquid in the area of the vapor formation center should be heated to a certain temperature. If we consider that the liquid is heated only by input of heat through heat conductivity, we can use the solution of the univariate equation of heat conductivity in a semi-limited body for second order boundary conditions

$$\frac{\partial t}{\partial \tau} = a \frac{\partial^2 t}{\partial x^2}, \tag{IV.8}$$

$$t = t_l \text{ where } \tau = 0, \tag{IV.9}$$

$$\left(\frac{\partial t}{\partial x}\right)_{x=0} = -\frac{q}{\lambda} \text{where } \tau > 0, \tag{IV.10}$$

where x is the distance from the heating surface. The solution of equation (IV.8) under conditions (IV.9), (IV.10) is given in [180] /172

$$\frac{\Delta t}{\frac{q x}{\lambda}} = \frac{1}{\pi} \frac{2\sqrt{a\tau}}{x} e^{-\frac{x^2}{4a\tau}} + erf\left(\frac{x}{2\sqrt{a\tau}}\right), \tag{IV.11}$$

If we calculate the heating time of the liquid at the heating surface according to formula (IV.11), which where x = 0 can be converted to the form

$$\tau = \frac{\pi^2}{4}\left(\frac{\Delta t}{q}\right)^2 \lambda C_p \gamma \tag{IV.12}$$

for water and sodium at $P_s$ = 1 atm. abs. and identical q and $\Delta t_s$, then $\tau$ for sodium will be approximately 20 times greater than $\tau$ for water.

Marto and Rohsenow [181] have produced an expression for the criterion characterizing the stability of boiling, using the following simplified model of the process of formation of a bubble in a depression. After separation of the bubble, the cold liquid tends to flow into the mouth of the depression. At the same time, the wall surrounding the depression is cooled to a temperature equal to the temperature of the liquid. It is assumed that the liquid is somewhat superheated in relationship to the saturation temperature at the pressure of the liquid, but the temperature of the liquid is below the saturation temperature at the pressure of the vapor in the depression. The temperature of the liquid depends on the specific heat flow, wall material and bubble separation frequency. It is considered that the forces of inertia can be ignored, since the liquid flows relatively small distances into the depth of the depression, since the dimensions of the depression itself are small. As a result of curvature of the division surface between vapor and liquid, the vapor included within the depression is at higher pressure than the liquid. Since the temperature of the liquid is below the saturation temperature of the vapor, the vapor condenses. The vapor-liquid division boundary descends into the depression, the rate of descent being limited by the rate at which the heat carried to the separation surface by condensation of the vapor can be carried away by the liquid due to its heat conductivity. The liquid in the depression receives heat both from the condensing vapor and from the walls of the depression. As the temperature of the liquid increases, the rate of descent of the phase division boundary decreases and at a certain point, when the temperature of the liquid is comparable with the temperature of the vapor, the condensation stops and the bubble begins to grow again. If the temperature of the liquid never reaches the temperature of the vapor, all of the vapor is condensed and the depression will no longer serve as an active vapor formation center. Using a number of simplifying assumptions, Marto and Rohsenow produced an expression[1] for the relationship of the maximum penetration of the phase division boundary in the depression x* during the time after separation of a bubble to depth of the depression L* /173

$$\eta^* = \frac{x^*}{L^*} = \frac{4}{\pi} \frac{t_s^2 \sqrt{\lambda C_p \gamma}}{(r\gamma'')^3} \left(\frac{2\sigma}{AR^*}\right)^2 \times \qquad \text{(IV.13)}$$

$$\times \frac{\left(1+\frac{\varepsilon^*}{2}\right)^2 C_*^2}{b^* q^{2n_*-1} f^{n_*} a_w^{1-a_*} \sqrt{\lambda_w \gamma_w C_{p_w}}} \frac{1}{L(1+\sin\theta)},$$

[1]Empirical coefficients in formula (IV.13) selected for physical properties of heat transfer medium and wall expressed in English units.

where R* is the radium of curvature of the liquid-vapor phase division boundary (for a cylindrical depression $R^* = R_{depr}/\cos\theta$); $\varepsilon^*$ is an empirical coefficient ($\varepsilon^* < 1$); $C_*$ is an empirical coefficient changing as a function of the state of the surface; $a_*$ is the empirical value of the exponent, changing as a function of the state of the surface.

The authors of [181] note that "due to the simplifying assumptions in the analytical expression here presented and the necessity of fixing the diameter and depth of the depression, we cannot affirm that the precise requirement of stability is $\eta^* < 1$, but can assume that the value of $\eta^*$ is a comparative index: the operating conditions for which $\eta^*$ is great are less stable than conditions for which $\eta^*$ is small."

In Table IV.1, we present values of $\eta^*$ calculated by Marto and Rohsenow for the case of boiling of various liquids on a surface of stainless steel (type 316) at atmospheric pressure.

In calculating the values of $\eta^*$ presented in Table IV.1, we used the following values of quantities: $q = 136 \cdot 10^3$ kcal/m$^2$·hr; radius of cylindrical depression $R^* = 0.03$ mm, depth of depression $L^* = 0.3$ mm ($L^*/d_{depr} = 5$), $b^* = 20$; $a_* = 0.92$; $C_* = 486.5$; $\varepsilon^* = 0.3$. The value of the contact angle for sodium is taken by estimation, and the frequency on the basis of estimates resulting from recording of noises made during boiling of sodium [19]. The values of $\theta$ and f for other liquids are taken from the literature.

We can see from the Table that for sodium $\eta^*$ is essentially greater (although $\eta^* > 1$ has no physical sense) than $\eta^*$ for other liquids, for which stable boiling is observed. The factors considered by equation (IV.13) are divided by Marto and Rohsenow into the following groups: physical properties of liquid and vapor, properties of surface material, heat flow and depression geometry. Let us analyze the effects of each of these factors individually.

The physical properties of the liquid and vapor are considered in (IV.13) by the term $t_s^2\sqrt{\lambda C_p \gamma}/(r\gamma'')^3$. As this term increases, the instability should increase. For alkali metals the value of $t_s^2\sqrt{\lambda C_p \gamma}/(r\gamma'')^3$ is great, since /174
alkali metals have high boiling point $t_s$, high heat conductivity $\lambda$ and low specific gravity of the vapor $\gamma''$ at the pressures which have been studied to date. Furthermore, alkali metals should wet a number of metal surfaces well (for example, for sodium and stainless steel, as was noted, at $t > 350$°C, $\theta$ is near 0°), and the frequency of separation of vapor bubbles during boiling of alkali metals, in any case with $p \ll P_{cr}$ should be low. This leads to relatively high values of the terms $\frac{1}{1+\sin\theta}$ and $\frac{1}{f^{\alpha_*}}$ ($\alpha_* > 0$). With increasing pressure, the value of $t_s^2\sqrt{\lambda C_p \gamma}/(r\gamma'')^3$ decreases and the value of

$\frac{1}{f^{\alpha_*}}$ should increase due to an increase in the frequency of bubble separation; Consequently, the stability of boiling should increase. Actually, as the pressure increases, the boiling of sodium becomes more stable. With increasing pressure, the number of active vapor formation centers increases, which doubtless has a stabilizing effect on the process of boiling. Therefore, on the basis of the available experimental data, it is difficult to judge the role of the complex $t_s^2 \sqrt{\lambda C_p \gamma}/(r\gamma'')^3$ in stabilization of the boiling process with increasing $P_s$, according to equation (IV.13).

TABLE IV.1

| Liquid | Dynamic contact angle $\theta°$ | Bubble separation frequency f, 1/sec | Value of $\eta^*$ |
|---|---|---|---|
| Methyl alcohol | 46 | 27 | $1.37 \cdot 10^{-5}$ |
| Liquid nitrogen | 0 | 95 | $3.30 \cdot 10^{-5}$ |
| Water | 80 | 32 | $1.7 \cdot 10^{-5}$ |
| Water | 60 | 32 | $15.4 \cdot 10^{-5}$ |
| Water | 0 | 32 | $116 \cdot 10^{-5}$ |
| Sodium | 0 | 1.3 | 6.23 |

The properties of the surface material in formula (IV.13) are considered by the term $\frac{1}{a_w^{1-a_*}\sqrt{\lambda_w \gamma_w C_{p_w}}}$. For metals with high values of heat conductivity and temperature conductivity (exponent $a_*$ in formula (IV.13) is less than 1), for example for molybdenum and nickel, expression $\frac{1}{a_w^{1-a_*}\sqrt{\lambda_w \gamma_w C_{p_w}}}$ is less than for metals with lower values of these quantities, for example, for stainless steel. Consequently, with identical distribution of vapor formation centers, boiling of alkali metals over a surface of stainless steel should be less stable than over a surface of molybdenum or nickel. However, as yet there are no reliable experimental data which could confirm this dependence. /175

With increasing heat flow, the stability of boiling should increase, since $\eta^*$ depends on the heat flow to the $(2a_* - 1)$ power, and the value of $a_* > 0.6$ [181]. Experiments have shown (see Chapter 2) that with increasing heat flow, boiling becomes more stable. The geometry of the depression also has an essential role in the stability of boiling. The greater L*, that is

the deeper the depression and the less $2\sigma/AR^*$, the more stable boiling should be. If the wetting angle $\theta$ reaches 90° or if the form of the depression is such that the radius of curvature increases with depth, the stability of boiling should also increase. Therefore, the operation of cylindrical and conical depressions for centers of vapor formation should be less stable than, for example, mushroom shaped depressions (expanding downward).

Thus, theoretical works in experiments show that the stability of operation of a depression as a center of vapor formation, with otherwise equivalent conditions, depends on the dimensions and geometry of the depression, its wettability by the liquid and the contact time of the depression with the liquid after separation of a vapor bubble.

## Growth of Vapor Bubbles

Experimental data on the rate of growth of vapor bubbles during boiling of metals have not as yet been produced. In [182], some experimental data are presented on the separation diameters of vapor bubbles during boiling of potassium, produced using x-ray cinamatography. For five bubbles, in addition to the dimensions of the separation diameters and the growth time of the bubbles to the separation diameters, the temperature heats were also produced. In the first approximation, these data might indicate a certain average rate of growth of vapor bubbles during boiling of potassium under the conditions under which the experiments were performed. The results of [182] can be looked upon only as preliminary.

Investigation of the rate of growth of vapor bubbles during boiling of non-metallic liquids has been the subject of a number of experimental works. The growth of vapor bubbles over the heat transmitting surface has been studied experimentally, for example, in [151, 171, 183, 184]. Dergarabedian [185] produced experimental data on the growth of vapor bubbles in the volume of an evenly superheated liquid. In a number of works, the problem of the growth of vapor bubbles in the volume of an evenly superheated nonmoving liquid [186-189] and over a heated wall [123, 189-191] has been studied theoretically.

In [186, 187, 189], identical equations have been produced (with an accuracy to a constant) for the asymptotic ($R \gg \rho^*$) growth of a vapor bubble in the volume of an evenly superheated liquid /176

$$R = b_r \frac{2C_p \gamma \delta t (\pi a \tau)^{1/2}}{\pi r \gamma''}. \qquad \text{(IV.14)}$$

The value of coefficient $b_r$ is $\sqrt{3}; \pi/2; \sqrt{\pi}$ according to Plesset and Zwick [186], Forster and Zuber [187] and D. A. Labuntsov [189] respectively. The equation (IV.14) was produced under the following principal assumptions: 1) a bubble has spherical form during growth; 2) the temperature of the vapor in the bubble is equal to the temperature of the liquid at the wall of the

bubble. This means that the rate of evaporation is great in comparison to the rate of bubble growth; 3) the ratio of enthalpy of superheating of the liquid per unit volume to enthalpy of latent heat of evaporation per unit volume of the vapor

$$\frac{C_p\gamma\delta t}{r\gamma''} \gg 1. \qquad \text{(IV.15)}$$

Condition (IV.15) is fulfilled at relatively low pressures ($\gamma >> \gamma''$) and means physically that the thermal boundary layer of the bubble during the process of its growth changes insignificantly; 4) the inertial effects resulting from the growth of the bubble are slight and have no influence on bubble growth.

When the temperature on the surface of the bubble and the thickness of the boundary layer are analyzed as functions of time, the equation for bubble growth becomes more complex. Considering these factors, the following equation is produced in [189] for bubble growth:

$$R = 2\frac{C_p\gamma\delta t}{r\gamma''}\left[1 + \frac{1}{\sqrt[3]{10}}\left(\frac{C_p\gamma\delta t}{r\gamma''}\right)^{-2/3}\right]^{1/2}(a\tau)^{1/2}. \qquad \text{(IV.16)}$$

In [183], on the basis of processing of tabular data from Scriven [188] on the growth of bubbles in the volume of a superheated liquid, produced by analytic calculation, the following dependence is suggested:

$$R = 2\sqrt{\frac{3}{\pi}}\frac{C_p\gamma\delta t}{r\gamma''}\left[1 + \frac{1}{2}\left(\frac{\pi}{6\frac{C_p\gamma\delta t}{r\gamma''}}\right)^{2/3} + \frac{\pi}{6\frac{C_p\gamma\delta t}{r\gamma''}}\right]^{1/2}(a\tau)^{1/2}. \qquad \text{(IV.17)}$$

When conditions (IV.15) are fulfilled, formulas (IV.16) and (IV.17) become formula (IV.14).

The equation for growth of a vapor bubble over the heating surface has been suggested by Zuber [123] and D. A. Labuntsov [189] in the following forms respectively /177

$$R = \frac{C_p\gamma\Delta t}{r\gamma''}s\left(1 - \frac{q(\pi a\tau)^{1/2}}{2\lambda\Delta t_s}\right)(\pi a\tau)^{1/2}, \qquad \text{(IV.18)}$$

$$R = \left(2\beta_L\frac{\lambda\Delta t_s\tau}{r\gamma''}\right)^{1/2}. \qquad \text{(IV.19)}$$

The values of $\beta_L$ in formula (IV.19) is taken as 6 in [183] on the basis of experimental data.

Equation (IV.18) was produced on the basis of the assumption that the principal quantity of heat is supplied to the bubble from the surrounding layer of superheated liquid, and that heat transfer from the wall to the base of the bubble is slight. Labuntsov produced equation (IV.19) by considering that the main supply of heat to the bubble is directly from the wall through the adjacent thin liquid layer. The fact that the zone of intensive evaporation is located near the base of the bubble is indicated by the results of [90, 91, 152]. In order to solve the problem of the relationship between the quantity of heat supplied to a vapor bubble at the zone of its base (zone of evaporation of microlayer) and the quantity of heat supplied to the remaining portion of the surface of the vapor bubble, further experimental investigations must be performed.

Equation (IV.14) describes the experimental data on the growth of a bubble in the volume of superheated water well [185], and agrees satisfactorily (with an accuracy of 40-50%) with data on the growth of bubbles on a heating wall (ether, pentane, water) at atmospheric pressure [171, 183]. Equation (IV.18) describes the experimental data in water at atmospheric pressure. Equation (IV.19) satisfactorily agrees with experimental data on the growth of a vapor bubble on a heating wall, produced in [183] for a broad interval of pressures (1-100 atm. abs.) and heat fluxes ($35 \cdot 10^3$-$1300 \cdot 10^3$ kcal/m$^2$·hr).

These works show that for ordinary liquids in most cases the principal factor determining the growth of the vapor bubble is the input of heat to the bubble. Only with small values of R (on the order of $\rho^*$) or large values of $C_p \gamma \delta t / r \gamma''$ (low pressure, high super heating) can inertial effects influence the rate of growth of the vapor bubble [186, 187, 195].

One of the principal distinguishing properties differentiating the rate of growth of a vapor bubble in metals from the rate of growth in ordinary liquids is the high heat conductivity of the metals. Whereas in concluding equation (IV.14), describing experimental data for water on the growth of a vapor bubble in the volume of the super heated liquid, it was assumed that the rate of evaporation was great, in comparison with the growth of the vapor bubble (which is defined by the rate of input of heat through the boundary layer) this assumption cannot be made for liquid metals in a number of cases, since with comparable pressures $(\alpha_\phi/\lambda)_{met} << (\alpha_\phi/\lambda)_{H_2O}$. Using the same assumptions which were used in concluding equation (IV.14), except for the second assumption, we can write the heat balance equation for the bubble

/178

$$4\pi R^2 dR r\gamma'' = 4\pi R^2 \alpha_\phi (t_1 - t_s)\, d\tau = 4R^2 b_r \lambda \frac{t_1 - t_1}{(\pi a \tau)^{1/2}} d\tau, \qquad \text{(IV.20)}$$

where $t_1$ is the temperature on the division boundary of the bubble phase, °C; $t_\zeta$ is the temperature of the superheated liquid, °C; $b_r$ is the same coefficient as in formula (IV.14); $\alpha_\phi$ is the heat transfer coefficient during the phase transition, kcal/m²·hr °C.

From equation (IV.20) we obtain

$$\frac{dR}{d\tau} = \frac{b_r\lambda}{r\gamma''} \frac{t_\zeta - t_s}{\frac{b_r\lambda}{\alpha_\phi} + (\pi a\tau)^{1/2}}. \qquad \text{(IV.21)}$$

Replacing $\tau$ by $z^2$, we obtain

$$dR = \frac{2b_r\lambda\delta t z dz}{r\gamma''\left[\frac{b_r\lambda}{\alpha_\phi} + (\pi a z^2)^{1/2}\right]}, \qquad \text{(IV.22)}$$

where $\delta t = t_\zeta - t_s$. Let us represent for convenience the expression $r\gamma''/2\alpha_\phi\delta t$ as $A_z$, and the expression $(\pi a)^{1/2}r\gamma''/2b_\gamma\lambda\delta t$ as $B_z$; then equation (IV.22) takes on the form

$$dR = \frac{z dz}{A_z + B_z z}. \qquad \text{(IV.22a)}$$

Integrating equation (IV.22), we obtain

$$R = \frac{1}{B_z^2}[A_z + zB_z - A_z \ln(A_z + zB_z)] + C_z. \qquad \text{(IV.23)}$$

After finding the values of constant $C_z$ from condition R = 0 where z = 0 and going over to our initial symbols, we obtain

$$R = b_r \frac{2}{\pi} \frac{C_p\gamma\delta t}{r\gamma''}\left[(\pi a\tau)^{1/2} + \frac{b_r\lambda}{\alpha_\phi} \ln \frac{\frac{b_r\lambda}{\alpha_\phi}}{\frac{b_r\lambda}{\alpha_\phi} + (\pi a\tau)^{1/2}}\right] \qquad \text{(IV.24)}$$

In [49, 50], $\alpha_\phi$ was experimentally determined for condensation of potassium and sodium vapors over a continually renewed surface of liquid metal. The experimental data agree well with the formula /179

$$\alpha_\phi = \frac{2f_\kappa}{2 - f_\kappa}\left(\frac{r^4 P_s^2 M^3}{2\pi g B_g^3 T_s^5}\right)^{1/2} \qquad \text{(IV.25)}$$

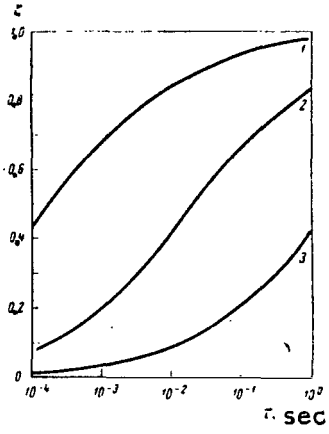


Figure 101. Ratio of Radii of Vapor Bubbles $\xi$, Calculated From Formulas (IV.24) and (IV.14), As a Function of Time For Sodium at $t_s$ = 800°C With Various Values of $\alpha_\phi$.
1, $\alpha_\phi = 10^6$ kcal/m$^2$·hr°C;
2, $\alpha_\phi = 10^5$ kcal/m$^2$·hr°C;
3, $\alpha_\phi = 10^4$ kcal/m$^2$·hr°C.

with a value of the condensation coefficient f = 1. However, the problem of how the values of $\alpha_\phi$ will change in the process of bubble growth in metals in various cases can be solved only on the basis of measurement of the temperature fields within the vapor bubble and indirectly on the basis of experimental data on the rate of growth of vapor bubbles, since $\alpha_\phi$ is significantly influenced by impurities on the phase division boundary, which may accumulate in the process of bubble growth.

Figure 101 shows the ratio of radii of bubbles for sodium calculated according to formulas (IV.24) and (IV.14), as a function of time with three values of $\alpha_\phi$. The values of $\lambda$ and a are taken at a temperature of 800°C, $b_r$ is taken after Forster-Zuber equal to $\pi/2$. The heat conductivity and temperature conductivity of sodium do not change strongly with temperature; therefore, the ratio between the radii of the bubbles calculated according to formulas (IV.24) and (IV.14) for other temperatures will be approximately the same.

Equations (IV.14) and (IV.24) are produced on the assumption that the growth of a vapor bubble is determined by the input of heat, and that inertial effects are slight. If we consider that pressure remains constant in the process of bubble growth and that the pressure drop $\delta P$ corresponds to super heating of the liquid $\delta t$, in this case the growth of the bubble will be determined by the inertia of the liquid and described by the Rayleigh equation: /180

$$R\frac{\partial^2 R}{\partial \tau^2}+\frac{3}{2}\left(\frac{\partial R}{\partial \tau}\right)^2=\frac{\delta P-\frac{2\sigma}{R}}{\frac{\gamma}{g}}. \qquad \text{(IV.26)}$$

With relatively large R (about 1 mm) the dependence of R on $\tau$ can be expressed by using equation (IV.26), as shown in [185], as follows:

$$R=\left(\frac{2}{3}\frac{g\delta P}{\gamma}\right)^{1/2}\tau. \qquad \text{(IV.27)}$$

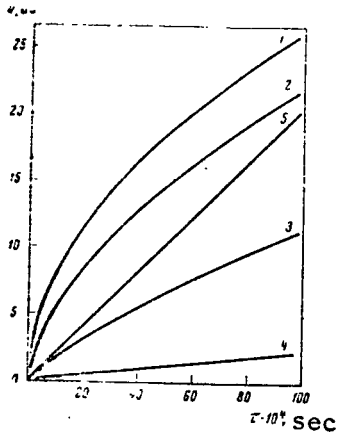


**Figure 102.** Dependence of Radius of Vapor Bubble for Sodium with $t_s$ = 800°C and $\delta t$ = 10°C. 1, According to Forster-Zuber (IV.14); 2, $\alpha_\phi = 10^6$ kcal/m²·hr °C; 3, $\alpha_\phi = 10^5$ kcal/m²·hr °C; 4, $\alpha_\phi = 10^4$ kcal/m²·hr °C; According to equation of the authors (IV.24); 5, According to Rayleigh equation (IV.27).

Figure 102 shows the dependence of the radius of a vapor bubble on time for sodium with $t_l$ = 800°C, $\delta t$ = 10°C according to formulas (IV.14), (IV.24) and (IV.27). We can see that when $\alpha_\phi$ are great (curve 1, $\alpha_\phi \to \infty$; curve 2, $\alpha_\phi = 10^6$ kcal/m²·hr °C), the rate of growth of the sodium bubble will be determined by inertial forces (curve 5), while for low values of $\alpha_\phi$ (curve 4, $\alpha_\phi = 10^4$ kcal/m²·hr °C), the determining factor will be the input of heat to the bubble.

Table IV.2 presents a comparison of values of diameters of vapor bubbles of potassium measured in [182] with values of diameters calculated according to formulas (IV.14), (IV.24) and (IV.27) for temperature heats and time sectors corresponding to the experimental data.

We can see from the table that low pressures, the values of diameters (which is equivalent to the averaged rate of growth of vapor bubbles) calculated according to Rayleigh's formula (IV.27) are closest to the experimental values, while at higher pressures, the values of diameters calculated according to formula (IV.24) with $\alpha_\phi = 10^4$ kcal/m²·hr °C are closest. However, as was noted above, the results of [182] can be looked upon only as preliminary; in addition to the calculations such as those shown in graphic form on Figures 101 and 102, they show that formulas (IV.14), (IV.16)-(IV.19) cannot be used for calculation of the growth of metal vapor bubbles, at least at low pressures (below about $10^{-2}$ $P_{cr}$). /181

In conclusion, we should note that the models of the process of vapor bubble growth analyzed here and in other works are idealized to a significant extent. Actually, the process is more complex. In particular, during the process of growth of a vapor bubble, its surface undergoes oscillations [171]; bubbles may not have spherical form, as is assumed in all models; bubbles may interact with each other etc.

TABLE IV.2

| Experimental data | | | | | Calculated data of diameters (with Δt and τ corresponding to experimental) according to formulas | | | | |
|---|---|---|---|---|---|---|---|---|---|
| | | | | | (IV.14) | (IV.24) | | | (IV.27) |
| $P_s$, atm.abs. | $P_s/P_{cr}$ | τ, sec. | Δt, °C | $d_0$, mm | $b_r = \frac{\pi}{2}$ | $\alpha_\Phi = 10^3$ kcal/m²hr °C | $\alpha_\Phi = 10^5$ kcal/m²hr °C | $\alpha_\Phi = 10^4$ kcal/m²hr °C | |
| 0,047 | $0,278 \cdot 10^{-3}$ | $6,5 \cdot 10^{-2}$ | 9,0 | 41 | 680 | 620 | 480 | 174 | 100 |
| 0,058 | $0,343 \cdot 10^{-3}$ | $7,7 \cdot 10^{-2}$ | 14,0 | 61 | 854 | 784 | 712 | 236 | 171 |
| 0,152 | $0,9 \cdot 10^{-3}$ | $8,6 \cdot 10^{-2}$ | 12,5 | 52 | 300 | 284 | 224 | 88 | 234 |
| 0,22 | $1,3 \cdot 10^{-3}$ | $6,2 \cdot 10^{-2}$ | 13,0 | 46 | 184 | 180 | 134 | 50 | 121 |
| 0,27 | $1,6 \cdot 10^{-3}$ | $7,0 \cdot 10^{-2}$ | 12,5 | 42 | 158 | 148 | 116 | 44 | 288 |

Commas indicate decimal points.

## Frequency of Separation and Separation Diameters of Vapor Bubbles

The visual observations of the authors of the process of boiling of water and alkali metals (sodium, potassium and cesium) by x-rays have made possible a qualitative comparison of separation diameters of vapor bubbles for these materials. Some experimental data on the separation diameters during the boiling of potassium, as was noted above, were produced in [182]. Here also are presented several values of separation frequencies of vapor bubbles, defined, like the separation diameters, using x-ray cinamatography.

The investigation of separation frequencies f and separation diameters $d_0$ of vapor bubbles during boiling of non-metallic liquids has been the subject of a large number of experimental works. For example, experiments on /182
water were performed in [74, 151, 183, 193-196], and in organic fluids in [74, 151, 171, 194, 196-198]. The frequency of separation and the separation diameters of vapor bubbles are distributed statistically, their distribution being near normal.

The mean frequency of separation of vapor bubbles for water at atmospheric pressure is approximately 40-50 Hz. [183, 194-196]. The results of [195], performed on water over a broad range of heat flows at pressures of 1-52 atm. abs., indicate that the separation frequency of vapor bubbles does not change with the heat flow, and is only slightly dependent on pressure. For example, at $P_s$ = 1-20 atm. abs., the mean value of F was approximately 35 1/sec, and at $P_s$ = 52 atm. abs., approximately 45 1/sec. At

reduced pressures, the separation frequency of vapor bubbles during boiling of water and organic fluids is noticeably decreased, and depends on the heat flow [73, 74].

Table IV.3 presents experimental data from [73, 74] on the frequencies of separation and separation diameters of vapor bubbles for water boiling at reduced pressure.

We can see from Table IV.3 that under reduced pressure conditions, as the heat flow increases (where $P_s$ = const) the separation frequency of vapor bubbles increases strongly.

TABLE IV.3

| $P_s$, atm.abs. | $P/P_{cr}$ | $q \cdot 10^{-6}$ $\frac{kcal}{m^2hr}$ | f, $sec^{-1}$ | $d_0$, mm | Source |
|---|---|---|---|---|---|
| 0,122 | $0,544 \cdot 10^{-3}$ | 0,241 | 9,0 | 27,0 | |
| 0,153 | $0,68 \cdot 10^{-3}$ | 0,086 | 1,5 | 26,0 | |
| 0,153 | $0,68 \cdot 10^{-3}$ | 0,172 | 4,0 | 22,5 | |
| 0,153 | $0,68 \cdot 10^{-3}$ | 0,331 | 13,5 | 25,0 | |
| 0,184 | $0,816 \cdot 10^{-3}$ | 0,069 | 4,0 | 18,0 | |
| 0,184 | $0,816 \cdot 10^{-3}$ | 0,138 | 11,0 | 18,5 | [74] |
| 0,184 | $0,816 \cdot 10^{-3}$ | 0,284 | 22,0 | 20,5 | |
| 0,306 | $1,358 \cdot 10^{-3}$ | 0,069 | 6,0 | 15,0 | |
| 0,306 | $1,358 \cdot 10^{-3}$ | 0,138 | 15,0 | 19,0 | |
| 0,510 | $2,26 \cdot 10^{-3}$ | 0,069 | 15,0 | 6,80 | |
| 0,510 | $2,26 \cdot 10^{-3}$ | 0,138 | 20,0 | 10,0 | |
| 0,193 | $0,856 \cdot 10^{-3}$ | 0,150 | 2,4 | 35,7 | |
| 0,193 | $0,856 \cdot 10^{-3}$ | 0,296 | 10,7 | 23,2 | [73] |
| 0,418 | $1,85 \cdot 10^{-3}$ | 0,070 | 12,6 | 11,3 | |
| 0,418 | $1,85 \cdot 10^{-3}$ | 0,098 | 25 | 7,7 | |

Commas indicate decimal points.

The period between formation of two bubbles consists of two parts: the time required for bubble growth on the surface $\tau_1$ and the time required for heating of the liquid next to the surface $\tau_2$, after the liquid replaces the separated bubble. The increase in frequency noted with increasing heat flow results primarily from a reduction in $\tau_2$, the bubble growth time $\tau_1$ being almost independent of q [73, 74]. /183

The growth period of a vapor bubble, as was noted above, corresponds to a sharp drop in temperature of the heating surface in the area of the vapor formation center, while the time of heating of the liquid corresponds to a relatively smooth increase in temperature (see Figure 96). The local

temperature of the heating surface, particularly with high densities of active centers of vapor formation, will depend on the process of vapor bubble formation at neighboring vapor formation centers, which is individual for each center, that is will depend on differences in the phases of formation of the bubbles. This is reflected particularly in local values of temperature. However, experiments on non-metallic liquids [89-91, 152] have shown that the mean frequency of pulsations of temperatures measured at the heating surface on the side of the wall and on the side of the liquid are approximately the same as the mean frequency of separation of vapor bubbles. Therefore, on the basis of measurements of pulsation frequencies of the heating surface we can, with some approximation, judge the frequency of separation of vapor bubbles.

The frequency of temperature pulsations during boiling of alkali metals was measured (using a movable thermocouple) in our experiments (with heat flows from approximately $10^5$ kcal/m$^2$·hr to near the critical and pressures of up to approximately 1 atm. abs.), and usually did not exceed a few Hz. According to the results of the experiments of Noyes and Lurie [33], the resonant frequency of pulsations during boiling of sodium was about 1.7 Hz. ($P_s$ = 0.1 atm. abs.).

TABLE IV.4

| P, atm. abs. | $P/P_{cr}$ | $q \cdot 10^{-6}$, kcal/m$^2$·hr | f, sec$^{-1}$ | $d_0$, mm |
|---|---|---|---|---|
| 0,171 | 1,01·10$^{-3}$ | 0,57 | 4,0 | 43 |
| 0,175 | 1,035·10$^{-3}$ | 0,57 | 6,5 | 29 |
| 0,562 | 3,32·10$^{-3}$ | 0,58 | 2,0 | 32 |
| 0,248 | 1,467·10$^{-3}$ | 0,43 | 2,0 | 33 |
| 0,755 | 4,46·10$^{-3}$ | 0,55 | 7,0 | 22 |

Commas indicate decimal points.

Table IV.4 presents experimental data from [182] on frequencies of separation of vapor bubbles during boiling of potassium.

A comparison of the data in Tables IV.3 and IV.4 indicates that with comparable pressures and heat flows (experiments on potassium performed at higher q than experiments on water) the frequency of separation of vapor bubbles for potassium is much less than for water. /184

Estimates of the time required for heating the liquid on the heating surface for sodium in water (with q = const), performed above, indicate that $\tau_2$ for sodium should be considerably greater than for water. The same relationship is qualitatively true for $\tau_3$ for water and other metals.

Thus, the available experimental data on temperature pulsations near the heating surface during boiling of alkali metals, preliminary data on separation frequencies of vapor bubbles during boiling of potassium, as well as estimates of the heating time of the liquid at the heating surface indicate that the frequency of separation of vapor bubbles during boiling of metals, particularly alkali metals, is essentially less than during boiling of water under comparable conditions (identical q and $P/P_{cr}$).

Experiments with non-metallic liquids have indicated that at low heat flows, individual isolated bubbles separate from the heating surface. As the heat flow increases, the number of active centers of vapor formation increases. With increasing heat flow (at atmospheric and higher pressures with $q > 0.1\ q_{cr}$) vapor bubbles formed at neighboring vapor formation centers merge, so that the separating diameter is increased [74, 193, 195, 199]. As the pressure increases, the separation diameter of vapor bubbles decreases [73, 74, 183, 193-196].

Visual observations of the authors using x-rays of the process of boiling of alkali metals (sodium, potassium and cesium) and water indicate that for alkali metals the separation diameters of vapor bubbles are greater than for water. The same conclusion follows from comparison of the dimensions of separating vapor bubbles for potassium and water presented in Tables IV.2-IV.4. The well known formula of Fritz for the most probable value of separating diameter of a bubble

$$\overline{d_0} = 20 \cdot \theta \left(\frac{\sigma}{\gamma - \gamma''}\right)^{1/2} \qquad \text{(IV.28)}$$

describes the experimental data well only at low heat flows and atmospheric pressures. At high pressures [193] and at pressures below atmospheric [73, 74], and also at atmospheric pressure but with high heat flows [199], formula (IV.28) gives values of $\overline{d}_0$ differing essentially from the experimental values.

Cole [199], in contrast to Fritz, considered the drag on the bubble in addition to the lifting force and force of surface tension; the drag should be significant for bubbles of large diameters. He suggested the following formula for calculation of the separation diameter of a bubble: /185

$$\frac{d_0}{\theta\left(\frac{\sigma}{\gamma - \gamma''}\right)^{1/2}} = 0.4\left[\frac{g^2\sigma}{W''^2(\gamma - \gamma'')}\right]^{-0.22}, \qquad \text{(IV.29)}$$

where W'' is the rate of bubble growth at the moment of separation. The numerical values of the coefficient (0.4) and exponent (- 0.22) he found on the basis of processing of his own experimental data on separation diameters of vapor bubbles at high heat flows and the data of Jacob for low q. Mamontova [74] processed her experimental data on separation diameters of

vapor bubbles for water, ethyl alcohol and benzene boiling at pressures below atmospheric in the coordinates

$$\frac{d_0}{\left(\frac{\sigma}{\gamma-\gamma''}\right)^{1/2}} - \left[\frac{g^2\sigma}{W''^4(\gamma-\gamma'')}\right]^{1/3}, \qquad \text{(IV.30)}$$

that is essentially in the same coordinates used by Cole [199], but without considering the contact wetting angle. The results are shown on Figure 103. We can see that the points are well located with respect to the averaging line. Figure 103 shows points for potassium from [182], which are higher than the data for non-metallic liquids. /186

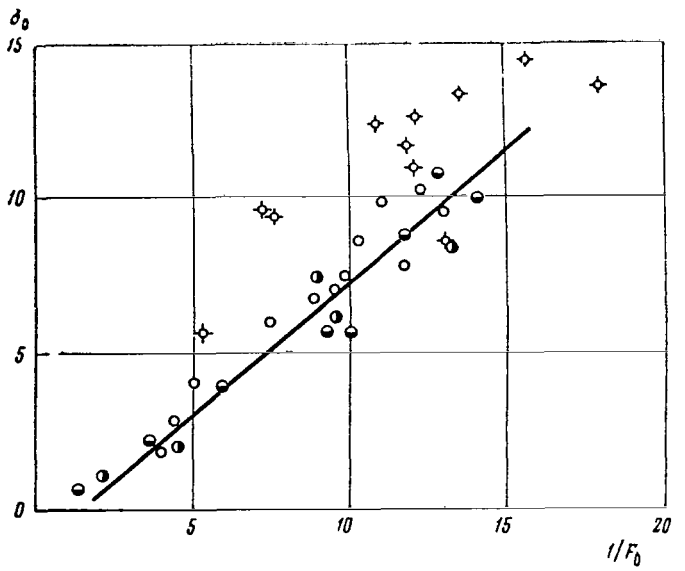


Figure 103. Experimental Data on Separation Diameters of Vapor Bubbles at Low Pressures. o, water; ●, ethyl alcohol; ◐ benzene [74]; ⊗, potassium [182]:

$$\frac{d_0}{\theta\left(\frac{\sigma}{\gamma-\gamma''}\right)^{1/2}} = 0.4\left[\frac{g^2\sigma}{W''^2(\gamma-\gamma'')}\right]^{-0.22}$$

where $W_0'' = d_0/\tau''$.

According to the estimates made in [200] on the assumption that only the lifting force and the drag act on a bubble, the separation diameter for a sodium bubble should be several centimeters with $P_s$ = 0.15 atm. abs. and $\Delta t$ = 4°C.

Recently, interesting data were produced on the separation of vapor bubbles, which are reported in detail in [201]. The experiments were performed at atmospheric pressure on water boiling over wires 0.2 mm in diameter. The separation of vapor bubbles from the surface of horizontally and vertically placed heaters occurs in all directions (including in the direction opposite to the influence of the lifting force), strictly perpendicular to the surface. The distribution of active centers of vapor formation in the direction of initial movement of the bubbles are random in nature. The bubbles separate at an initial rate of 0.5-0.6 m/sec (which cannot be related to the effect of lifting force alone) and move in a straight line for 3-4 mm from the heating surface. Over this distance, their movement is slow: if they are moving downward, it slows to zero; if they are moving upward, it

slows to a rate corresponding to the equilibrium movement under the influence of the lifting force and the force of resistance.

Calculation of the energy required for movement of vapor bubbles over the distances and speeds produced in the experiments indicates that this energy is approximately $10^6$ times less than the total energy of the vapor bubble after it has reached the separation diameter. In other words, from the energetic point of view the movement of the bubbles observed in the experiments is quite possible.

In [201], several hypotheses are stated concerning the nature of the forces causing the bubbles to move in this manner after separation from the wall.

1. The vapor bubbles move the surrounding liquid during the process of growth. The liquid, set in motion, draws the bubble along with it when the bubble reaches a certain diameter.

2. The jump of the vapor bubble away from the wall is related to the effects of the forces of surface tension.

3. As the vapor bubble grows, a reactive force arises, which repels it from the wall.

At the present, it is difficult to give preference to any one of these hypotheses.

Possibly, for large vapor bubbles, which separate from the heating surface during boiling of non-metallic liquids at reduced pressures and during boiling of metals, the trajectory of the bubbles, like those described in [201], will be less remarkable, since drag forces have a significant /187
influence on the bubble in this case. In order to clarify this question and check the hypotheses stated in [201] and other hypotheses on the nature of the forces determining the conditions of separation of vapor bubbles in various cases, further experimental and theoretical investigations are required. We can assume that the factors determining the separation of vapor bubbles during boiling of metals and non-metallic liquids are the same.

## General Characterization of Process of Heat Exchange During Nucleate Boiling Under Conditions of Free Convection

During nucleate boiling, heat from the heating surface is carried with the vapor bubbles ($q_v$) and with the liquid ($q_l$). During the process of growth of a vapor bubble on the wall, the heat enters the bubble from the surrounding liquid and directly from the heating surface. However, as investigations performed in [152] on water at atmospheric pressure have shown, the share of the surface contacting the vapor directly is slight. The quantity of heat supplied directly from the heating wall to the vapor (by convection, and at high temperatures by radiation) is also slightly due to the

small area of contact of the surface with the vapor and the low intensity of heat transfer by the vapor. The results of works on water [90, 91, 152] show that the area of intensive heat input to the vapor bubble is concentrated in the zone of the microlayer of liquid separating the bubble from the wall. A certain share of heat should be supplied to the vapor bubble from the remaining phase separation boundary surface as well, since the bubble is surrounded by a superheated liquid layer [192]. The problem of the relationship of the quantities of heat supplied to various sectors of the vapor bubble can be solved on the basis of measurements of temperature fields in the boundary layer of the liquid with the vapor bubble and in the bubble itself. It can be assumed that in metals, due to the high temperature conductivity, the share of heat supplied to the bubble outside the microlayer will be higher (with comparable conditions) than in non-metallic liquids.

With increasing pressure and heat flow, the quantity of heat $q_v/q$ transferred by the vapor increases (see Figure 95). The relative share of heat $q_v/q$ transferred with the vapor increases at first more rapidly with increasing heat flow than at heat flows near critical. With identical reduced pressures and heat flows for metals $q_v/q$ should be less than for non-metallic liquids, due to the high heat conductivity of metals and, possibly, due to the smaller number of active centers of vapor formation during boiling of the metals. This should be analyzed in each concrete case of comparison of heat exchange during boiling considering such quantities as the separation volumes, separation frequency of vapor bubbles and product $r\gamma''$. /188

Heat transfer by the liquid results from molecular heat conductivity, turbulent vortices arising as a result of the dynamic influence of bubbles on the liquid, mixing of the liquid in the boundary layer due to the difference in densities, and also to a significant extent due to mixing of super heated liquid layers surrounding the moving vapor bubbles.

The measurement of temperature fields using microthermocouples performed at the Physics and Energy Institute by A. A. Tsyganok [192] and at the Atomic Center in Grenoble under the leadership of Semeria[1] have indicated that a bubble growing on the heating surface is surrounded by a layer of rather highly superheated liquid. For example, A. A. Tsyganok measured the temperature field in a vapor bubble and its boundary layer using a copper-constantan thermocouple drawn between two spring plates. The diameter of the thermal electrodes of the thermocouple was 50 μ. The superheating of the liquid surrounding the vapor bubble measured in these experiments reached 12°C with $P_s$ about 0.1 atm. abs. and $q = 150 \cdot 10^3$ kcal/m$^2$·hr.

[1] Personal communication.

The heat transfer coefficient with nucleate boiling

$$\alpha \sim A_N \cdot N^L. \qquad \text{(IV.31)}$$

According to the data of [101], L = 1/3 (experiments with water and organic liquids at atmospheric pressure and heat flows up to $200 \cdot 10^3$ kcal/m$^2$·hr), while the data of [176] indicate L = 0.43 (experiments with aqueous solution of nickel salts with q up to $1.4 \cdot 10^6$ kcal/m$^2$·hr). It can be assumed that for metals the coefficient of proportionality $A_N$ in function (IV.31) will be essentially higher than for ordinary liquids. With increasing pressure, the number of active centers of vapor formation increases. Judging from the dependence of $\rho^*$ on pressure, constructed on Figures 99, 100, the strongest increase in the number of active centers of vapor formation with increasing pressure will occur at low pressures, since at these pressures $d\rho^*/dP$ is considerably greater. For example, for alkali metals $d\rho^*/dP$ reaches its highest values at pressures of approximately $10^{-3}$ $P_{cr}$ and less. This may explain the different inclination of the averaging line drawn through the experimental data on heat transfer with developed boiling of sodium and cesium (Figure 53, 54).

With bubble boiling, as has been established in experiments on ordinary liquids, after separation of a vapor bubble and following a relatively short /189
period of time (from tenths to thousandths of a second) a new vapor bubble arises at the same vapor formation center, as a rule. It is probable that during the developed boiling of metals the boiling process is similar in this respect.

During the process of growth of vapor bubbles on the heating surface, oscillations of the bubble surfaces occur at frequencies reaching the order of 1,000 Hz [171]. The boiling of a liquid is accompanied by a high frequency noise which is probably related to oscillations and interactions of vapor bubbles during the process of their growth [171, 202]. The noise spectrum and level of acoustical pressure depend on the type of liquid, saturation pressure and heat flow. In particular, as the crisis is approached, the spectrogram of the noise sharply changes in nature [203]. Recordings of noise during boiling of sodium were performed by Marto and Rohsenow [19].

The nature of the process of heat exchange during unstable boiling differs from the process of heat exchange during developed boiling. Analysis of recordings of temperature pulsations of the heating wall and visual observations by x-rays of the process of unstable boiling of alkali metals performed by the authors have indicated that over the entire surface or its individual parts, temporary cessation of boiling occurs with subsequent restarting of boiling. After boiling is started, large vapor bubbles travel through the volume. The liquid in the volume is more superheated during unstable boiling than during developed boiling. In [73, 74], on the basis of visual observations and photographic investigations of the boiling

process of water and organic liquids at reduced pressures, it is noted that the unstable boiling regime is characterized by a replacement of vapor formation centers and irregularity of their action. When boiling starts, several bubbles are formed simultaneously, then a long period follows when vapor formation over this portion of the surface does not occur.

The great pulsations in temperature at relatively low frequency (fractions of a Hz), characteristic for unstable boiling, are related to the cessation and restarting of boiling over individual sectors of the surface. Actually, there is a certain probability that the formation of a vapor bubble at one of the vapor formation centers or even simultaneously at several neighboring vapor formation centers requires higher superheating of the liquid $\Delta t_s$ than during developed boiling. The greater the number of neighboring vapor formation centers which cease to operate with fixed $\Delta t_s$ and the higher the superheating required for restoration of their operation, the greater the superheating of the heating surface in this area and the greater the pulsations of the temperature. Unstable boiling results from insufficient numbers and instability of vapor formation centers.

For alkali metals, instability of the operation of vapor formation centers is related to the following factors: /190

1) the relatively large dimensions of vapor formation centers (large $\Delta t_s$ are required, the larger depressions are more easily filled with liquid); 2) good wettability of a number of structural metals with alkali metals (requiring higher $\Delta t_s$, depressions more easily filled with liquid); 3) the high temperature conductivity (increasing the heating time of the liquid near the wall after separation of a bubble and thereby increasing the probability of filling of the depression with liquid).

The relatively low values of boundary heat transfer coefficients $\alpha_b$ on the free surface also facilitate the existence of unstable boiling, particularly at low heat flows. When boiling starts, $\Delta t_s$ is decreased due to a decrease in $\Delta t_\alpha$ and $\delta t$ (see Figure 39). The difference in the values of $\Delta t_s$ during heat removal without boiling and under conditions of boiling (with $q$ = const) depend essentially on $\Delta t$ which, in turn, is determined by the design of the installation and $\alpha_b$. The greater the ratio $\delta t/\Delta t_s$, the higher the probability that boiling will stop.

The pressure pulse accompanying the start of boiling may have some influence on the suppression of operation of vapor formation centers and, consequently, stopping of boiling. However, the time of action of the pressure pulse, measured in the experiments of the authors, as alkali metals started boiling was considerably less than the time of boiling, which can be determined from recordings of the temperature difference between wall and liquid and observations by x-rays.

With unstable boiling, the quantity of heat liberated from the heating surface with the vapor $q_v$ is less than with developed boiling. This is particularly indicated by the higher super heating of the liquid in its volume $\delta t$ with unstable boiling in comparison to $\delta t$ with developed boiling.

Analysis of the integral characteristics of the process of heat exchange (heat removal regimes, values of heat transfer coefficients and critical heat flows and their dependence on various factors) as well as the local characteristics (distribution of temperature fields, dimensions and stability of operation of vapor formation centers, rate of growth, frequency of separation and separation volumes of vapor bubbles, etc.) during boiling of metals and non-metallic liquids shows that in addition to their common features, there are differences in heat exchange during boiling of these classes of liquids. Although the fundamental rules which determine heat exchange during boiling are common for all liquids, individual local processes (due to differences in physical and chemical properties) during boiling of metals and non-metallic liquids may differ significantly both quantitatively and qualitatively (for example, wettability of the surface by the heat transfer medium), leading to differences in the integral characteristics as well.

Thus, as a difference in integral characteristics of heat exchange /191
during vapor formation under conditions of free convection for metals and non-metallic liquids (on surfaces of most construction materials with ordinary finish) we can note (for alkali metals):

1) the possibility of heat removal of large heat flows by convection with subsequent liberation of heat by evaporation from the free surface (due to the high $\Delta t_s$ and $\alpha$ with free convection);

2) unstable boiling, which for non-metallic liquids is achieved only at very low pressures (tenths or hundredths of an atmosphere) and relatively low heat flows (not over several hundred thousand kcal/$m^2 \cdot hr$), while for alkali metals unstable boiling (due to the small number and instability of vapor formation centers) is characteristic over a broad range of pressures (experiments performed in the range of $P_s$ from hundredths of an atmosphere to several atmospheres) and heat flows (q from tens of thousands of kcal/$m^2 \cdot hr$ to q near critical);

3) dependence of critical heat flows on pressure in the investigated range of pressures (about $5 \cdot 10^{-5}$-$2 \cdot 10^{-2}$ $P/P_{cr}$) is generally considerably weaker than for non-metallic liquids. It can be assumed that one reason for this is the lower values of $q_v/q$ for metals than for non-metallic liquids.

For mercury, film boiling is characteristic (due to the inability of mercury to wet the surface) at low temperature heats, whereas with the same $\Delta t_\alpha$ for non-metallic liquids, nucleate boiling usually occurs.

Possible differences in local characteristics of the process of boiling for metals and non-metallic liquids were analyzed in this Chapter.

The study of the physics of boiling at critical and near critical heat flows is of greatest interest.

However, the investigation of local characteristics of the boiling process has been performed primarily at low and moderate heat flows. The correctness of extending the data produced under these conditions to the process of heat exchange at heat flows near critical requires further study.

Conclusions

1. For comparable conditions with developed boiling of alkali metals: a) the thickness of the thermal boundary layer is significantly greater; b) the frequency of separation of vapor bubbles is less; c) the separation diameters of vapor bubbles are greater, than for nucleate boiling of non-metallic liquids.

With developed boiling of metals, as with nucleate boiling of non-metallic liquids, temperature pulsations occur in the heating surface and in the /192
liquid near the heating surface, the magnitude of which is comparable to the mean temperature head $\Delta t_\alpha$, and the frequency of which is on the same order as the frequency of bubble separation.

2. The significant superheating of the heating surface observed in experiments with alkali metals, required for boiling to start, unstable boiling and transition from one mode of heat removal to another with unchanged values of pressure and heat flow can be explained on the basis of the conditions of seeding of vapor bubbles and the stability of operation of vapor formation centers, which are common as concerns thermodynamics for non-metallic liquids and for metals. The principal factors determining the possibility of high superheating of liquids over the heating surface can be considered the relatively large dimensions of vapor nuclei with identical superheating and the good wettability of the heating surface by the liquid. The instability of boiling is influenced by these factors and also by the high temperature conductivity of alkali metals.

3. Usually, the growth of vapor bubbles for non-metallic liquids is described by formulas in which the rate of bubble growth is determined by the input of heat through the boundary layer. For metals, at least at low pressures (up to several atmospheres), these formulas are not suitable.

4. The difference in local characteristics of the heat exchange process (distribution of temperature fields and vapor formation centers, dimensions and stability of operation of vapor formation centers, rate of growth, separation frequency and separation volumes of vapor bubbles, etc.) for metals and non-metallic liquids due to differences in their physical and

chemical properties leads to differences in the integral characteristics (establishment of heat removal mode, values of heat transfer coefficients and critical heat flows and their dependence on various factors), although the fundamental rules determining heat exchange during boiling are common for all liquids.

Heat exchange during the boiling of water and organic liquids, as we know, has been studied for a long time. However, it is basically only in recent years that works on the physics of boiling have been performed. These works have allowed a deeper understanding of the process, and have upset a number of earlier accepted hypotheses. However, today's knowledge is still quite insufficient for any sort of complete description of the process of heat exchange during boiling. The authors hope to continue their study of the physical regularities of boiling in the future.

## REFERENCES


1. Styrikovich, M. A., I. Ye. Semenovker, and A. R. Sorin, *Sovetskoye kotloturbostroyeniye*, No. 9, 1940. /193
2. Styrikovich, M. A. and I. Ye. Semenovker, *Zh. tekhn. fiz.*, Vol. 10, No. 16, 1940.
3. Siriy, I. O., A. A. Kanayev, and A. N. Lozhin, *Sovetskoye kotloturbostroyeniye*, No. 8-9, 1938.
4. Lozhkin, A. N. and A. A. Kanayev, *Binarnyye ustanovki* [Binary Installations], Mashgiz Press, 1946.
5. Gel'man, L. N., "Intensification of Heat Transfer to Boiling Mercury," *Zhidkiye metally* [Liquid Metals], Atomizdat, 1963.
6. Korneyev, M. I., "Heat Exchange during Boiling of Mercury and Amalgam," *Zhidkiye metally* [Liquid Metals], Atomizdat Press, 1963.
7. Korneyev, M. I., "Heat Transfer to Mercury and Amalgam of Magnesium during Boiling Under Free Convection Conditions," *Teploenergetika*, No. 4, 1955.
8. Korneyev, M. I., "Investigation of Heat Exchange to Mercury and Magnesium Amalgam Under Natural Circulation Conditions," *Teploenergetika*, No. 7, 1955.
9. Lyon, R. E., A. S. Foust, and D. L. Katz, "Boiling Heat Transfer with Liquid Metals," *Chem. Engng. Progr. Sympos. Series*, Vol. 15, No. 17, 1955.
10. Bonilla, C. F., I. S. Busch, A. Stalder, N. S. Shaikhmanmud, and A. Ramachandran, "Pool-boiling Heat Transfer with Mercury," *Chem. Engng. Progr. Sympos. Series*, Vol. 53, No. 20, 1957.
11. Romie, F. E., I. W. Brovarney, and W. H. Giedt, "Heat Transfer to Boiling Mercury," *Trans. A.S.M.E. Ser. C*, Vol. 82, No. 4, 1960.
12. Smith, C. R., Y. S. Tang, and P. T. Ross, "Potassium-Mercury Amalgam Heat Transfer and Two-Phase Flow Investigation," Proc. 2nd Annual High-Temp. Liquid-Metal Heat-Transfer Technol. Meet., Brookhaven Lab., 1962.
13. Tang, Y. S., P. T. Ross, R. Nicholson, and C. R. Smith., "Forced Convection Boiling of Potassium-Mercury Systems," *J. A. I. Ch. E.*, Vol. 10, No. 5, 1964.

14. Subbotin, V. I., P. A. Ushakov, P. L. Kipillov, M. K. Ibragimov, M. N. Ivanovskiy, Ye. V. Nomofilov, D. M. Ovechkin, D. N. Sorokin, and V. P. Sorokin, "Heat Exchange in Elements of Reactors with Liquid Metal Cooling," Report No. P/328, Proc. 3rd Internat. Conf. Peacefule Uses Atom. Energy. Geneva, 1964. Reactor Engineering and Equipment, Vol. 8, N. Y., 1965.
15. Kudryavtsev, A. P., D. M. Ovechkin, D. N. Sorokin, V. I. Subbotin, and A. A. Tsyganok, "Heat Transfer during Boiling of Sodium in Large Volumes," *Zhidkiye metally* [Liquid Metals], Atomizdat Press, 1967.
16. Borishanskiy, V. M., K. A. Zhokhov, and A. A. Andriyevskiy, "Heat Transfer during Boiling of Alkali Metals," *Atomnaya energiya*, Vol. 19, No. 2, 1965.
17. Petukhov, B. S., S. A. Kovalev, V. M. Zhukov, "Study of Sodium Boiling Heat Transfer," *Proc. 3rd Internat. Heat Transfer Conf.*, Chicago, August, Vol. 5, 1966.
18. Noyes, R. C., "An Experimental Study of Sodium Pool Boiling Heat Transfer," *Trans. A. S. M. E., Ser. C.*, Vol. 85, No. 2, 1963.
19a. Marto, P. I. and W. M. Rohsenow, "Effect of Surface Conditions on Nucleate Pool Boiling Heat Transfer to Sodium," Mass. Inst. Technol. Rep., pp. 5219-33, 1965.
19b. Marto, P. I. and W. M. Rohsenow, "The Effect of Surface Conditions on Nucleate Pool Boiling Heat Transfer to Sodium," *Trans. A. S. M. E., Ser. C.*, Vol. 88, No. 2, 1966.
20. Bonilla, C. F., M. Wiener, and H. Bilfinger, "Pool Boiling of Potassium" - /194 Proc. High-Temp. Liquid-Metal Heat-Transfer Technol. Meet. Vol. 1, (O.R.N.L.-3605), Sept., 1963.
21. Subbotin, V. I., D. M. Ovechkin, D. N. Sorokin, and A. P. Kudryavtsev, "Heat Transfer during Boiling of Cesium Under Free Convection Conditions," *Teploenergetika*, No. 6, 1968.
22. Madsen, N. and C. F. Bonilla, "Heat Transfer to Sodium-Potassium Alloy in Pool Boiling," Chem. Engng. Progr. Sympos. Series, Vol. 56, No. 30, 1960.
23. Aladyev, I. T., I. G. Gorlov, L. D. Dodonov, R. I. Sevastyanov, and O. S. Fedynsky, "Heat Transfer to Boiling Potassium in Tubes," Proc. 3rd Internat. Heat Transfer Conf., Chicago, Vol. 5, August, 1966.
24. Borishanskiy, V. M., A. A. Andriyevskiy, K. A. Zhokhov, G. S. Bykov, and L. S. Svetlova, "Heat Transfer during Boiling of Potassium in a Tube in the Area of Moderate Vapor Content," *Atomnaya energiya*, Vol. 21, No. 1, 1966.
25. Brooks, R. D., "Alkali Metals Boiling and Condensing Investigations," Proc. 2nd Annual High-Temp. Liquid-Metals Heat-Transfer Technol. Meet., Brookhaven Nat. Lab., 1962.
26. Hoffman, H. W., "Recent Experimental Results in O.R.N.L. Studies with Boiling Potassium," Proc. High-Temp. Liquid-Metals Heat-Transfer Technol. Meet., Vol. 2 (O.R.N.L.-3605), Sept., 1963.
27. Killakey, I. I., "Liquid Metal Heat Transfer Test Programs," Proc. 2nd Annual High-Tempr. Liquid-Metal Heat Transfer Technol. Meet., Brookhaven Nat. Lab., 1962.
28. Longo, I., R. D. Brooks, "Alkali Metals Boiling and Condensing Investigation,: Proc. High-Temp. Liquid-Metal Heat Transfer Technol. Meet., Vol. 2 (O.R.N.L.-3605), Sept., 1963.

29. Berenson, P. I. and I. I. Killakey, "Experimental Investigation of Forced-Convection Vaporization of Potassium," Proc. High-Temp. Liquid-Metal Heat Transfer Technol. Meet., Vol. 2 (O.R.N.L.-3605), Sept., 1963.
30. Grachev, N. S., V. N. Zelenskiy, P. L. Kirillov, V. I. Subbotin, and N. M. Turchin, "Heat Exchange and Hydrodynamics during Boiling of Potassium in Tubes," *Teplofizika vysokikh temperatur*, Vol. 6, No. 4, 1968.
31. Fischer, C. R., "Heat Transfer and Pressure Dro0 Characteristics for Boiling Rubidium in Forced Convection," Proc. High-Temp. Liquid-Metal Heat Transfer Technol. Meet., Vol. 2 (O.R.N.L.-3605), Sept., 1963.
32. Fischer, C. R., "Heat Transfer and Pressure Drop Characteristics for Boiling Rubidium and Cesium in Forced Convection," Proc. 2nd Joint USAEC-EURATOM Two-Phase Flow Meet., Apr. 29-30, Germantown, Maryland, 1964.
33. Noyes, R. C. and H. Lurie, "Boiling Sodium Heat Transfer," Proc. 3rd Internat. Heat Transfer Conf., Chicago, Vol. 5, August, 1966.
34. Lottes, P. A., "Applying High-Temperature Instrumentation in Liquid Metal Experiments," *Power Reactor Technol.*, Vol. 9, No. 3, 1966.
35. Deyev, V. I., G. P. Dubrovskiy, L. S. Kokarev, I. I. Novikov, and V. I. Petrovichev, "Investigation of Heat Transfer during Boiling of Sodium under Free Convection Conditions," *Atomnaya energiya*, Vol. 22, No. 1, 1967.
36. Subbotin, V. I., D. M. Ovechkin, D. N. Sorokin, A. P. Kudryavtsev, and A. A. Tsyganok, "Experimental Investigation of Critical Heat Flows during Boiling of Sodium in Large Volumes," *Zhidkiye metally* [Liquid Metals], Atomizdat Press, 1967.
37. Caswell, B. F. and R. E. Balzhiser, "The Critical Heat Flow for Boiling Liquid-Metal Systems," *Chem. Engng. Progr. Sympos. Series*, Vol. 62, No. 64, 1966.
38. Subbotin, V. I., D. M. Ovechkin, D. N. Sorokin, and A. P. Kudryavtsev, "Critical Heat Flows during Boiling of Cesium under Free Convection Conditions," *Teploenergetika*, No. 10, 1968.
39. Balzhiser, R. E., "Boiling Studies with Potassium," Proc. 3rd Annual Conf. High-Temp. Liquid-Metal Heat Transfer Technol., (O.R.N.L.-3605), September, 1963. /195
40. Gyunter, F., "The State of Investigations of Nuclear Engines and Nuclear Power Sources for Space Craft," *Voprosy raketnoy tekhniki*, No. 9, 1962.
41. Croke, E. J., "Key to Rankine Cycle Space Applications," *Power Reactor Technol.*, Vol. 9, No. 4, 1967.
42. Petrick, M., "Performance Characteristics of a Liquid-Metal MHD-Generator, Proc. MHD-Internat. Sympos. Magnetohydrohynamic Electrical Power Generation, Paris, July, 1964.
43. Shpil'rayn, E. E. and K. A. Kol'chugin, "The Thermodynamics of MHD Power Plants with Vapor-Liquid Injector," *Teplofizika vysokikh temperatur*, Vol. 3, No. 5, 1965.
44. MacFarlane, D. R. and R. O. Brittant, "Transaction Sodium Boiling Calculations," *Nucl. Engng. and Design.*, Vol. 4, No. 4, 1966.
45. Pruschek, R., M. Schindler and K. Moritz, "The Heat Pipe," *Chem. Ingr.-Techn.*, No. 1, 1967.

46. Zotov, V. V., B. A. Nevzorov, and Ye. V. Umnyashkin, "Corrosion Resistance of Construction Materials to Sodium," *Zhidkiye metally* [Liquid Metals], Atomizdat Press, 1967.
47. Kol', V., *Tekhnologiya materialov dlya elektrovakuumnykh priborov* [Technology of Materials for Electric-Vacuum Devices], Gosenergoizdat Press, 1957.
48. Tsarev, B. M., *Raschet i konstruirovaniye elektronnykh lamp.*, [Calculation and Design of Electron Tubes], Gosenergoizdat Press, 1961.
49. Subbotin, V. I., M. N. Ivanovskiy, V. P. Sorokin, and B. A. Chulkov, "Heat Transfer during Condensation of Potassium Vapors," *Teplofizika vysokikh temperatur*, Vol. 2, No. 4, 1964.
50. Bakulin, N. V., M. N. Ivanovskiy, V. P. Sorokin, V. I. Subbotin, and B. A. Chulkov, "Investigation of Phase and Diffusion Resistance during Condensation of Alkali Metals," *Atomnaya energiya*, Vol. 22, No. 5, 1967.
51. *Teplofizicheskiye svoystva veshchestv*, [Heat Physical Properties of Materials], Handbook edited by Prof. I. B. Vargaftik, Gosenergoizdat Press, 1956.
52. Povarnin, P. I. and I. G. Kulakov, "Heating by Electron Bombardment for Boiling Crisis Studies," *Inzhenerno-fizicheskiy zhurnal*, Vol. 1, No. 3, 1958.
53. Hickey, I. S., "Heat-Transfer at High-Power Densities," *J. Appl. Phys.*, Vol. 24, No. 10, 1953.
54. Ivashkevich, A. A., A. P. Kudryavtsev, D. M. Ovechkin, D. N. Sorokin, V. I. Subbotin, and A. A. Tsyganok, "Electron Heating Device for Investigation of Heat Exchange during Boiling of Metals under Free Convection Conditions," *Zhidkiye metally* [Liquid Metals], Atomizdat Press, 1967.
55. Schindler, M. and G. Woner, "Theoretical Model of Heat Transfer in Heat Pipes," *Atomkernenergie*, No. 9-10, 1965.
56. Minashin, V. Ye., V. I. Subbotin, P. A. Ushakov, and A. A. Sholokhov, "Error in Measurement Related to Distortion of Isotherms in the Region of Thermocouples," *Konvektivny i luchistyy teploobmen* [Convective and Radiant Heat Exchange], Academy of Sciences, USSR Press, 1960.
57. Popov, V. N., "The Distortion of the Temperature Field in the Area of Implantation of Thermocouples," *Teplofizika vysokikh temperatur*, Vol. 4, No. 2, 1966.
58. Sorokin, D. N., A. A. Ivashkevich, and A. P. Kydryabtsev, "Method of Placing Thermocouples in the Surface of Metal Products," *Byulleten' izobreteniy*, No. 18, 1962.
59. Krivtsov, V. A. and N. P. Kharitonov, *Mikrotermopary dlya tochnykh izmereniy temperatury* [Microthermocouples for Precise Temperature Measurement], Leningrad Scientific and Technical Propaganda Press, 1966.
60. Minashin, V. Ye., V. I. Subbotin, P. A. Ushakov, and A. A. Sholokhov, "Usage of Microthermocouples in the Investigation of Heat Transfer," *Voprosy teploobmena* [Problems of Heat Transfer], Academy of Sciences, USSR Press, 1959. /196
61. Subbotin, V. I., V. A. Krivtsov, Yu. N. Pokrovckiy, M. Kh. Ibragimov, and N. P. Kharitonov, "Small Thermocouples for Measurement of Temperature in the Reactor of the First Atomic Power Station," *Teplonergetika*, No. 5, 1965.

62. Belinskaya, G. V., N. B. Peshkov, and N. P. Khaptitonov, *Zharostoykaya izolyatsiya obmotochnykh provodov* [Heat Resistant Insulation for Wire Windings], Nauka Press, 1965.
63. Preobrazhenskiy, V. P., *Teplotekhnicheskiye izmereniya i pribory*, [Heat Engineering Measurements and Devices], Gosenergoizdat Press, 1953.
64. *Metody izmereniya temperatury* [Methods of Temperature Measurement], Collection of Articles edited by V. A. Sokolov, Part II, Foreign Literature Press, 1954.
65. Kirillov, P. L., F. A. Kozlov, V. I. Subbotin, and N. M. Turchin, "Purification of Sodium Through Oxides and Tests for their Content," *Atomnaya emergiya*, Vol. 8, No. 1, 1960.
66. Kozlov, F. A., V. I. Subbotin, and P. L. Kirillov, "Purification of Sodium to Remove Oxygen and Tests for Oxygen Content in Sodium," *Teplofizika vysokikh temperatur*, Vol. 3, No. 1, 1965.
67. Dmitriyeva, I. B., F. A. Kozlov, and E. K. Kuznetsov, "Determination of the Oxygen Content in Sodium and Sodium-Potassium Alloys by Vacuum Distillation," *Zhidkiye metally* [Liquid Metals], Atomizdat Press, 1967.
68. Kozlov, F. A. and E. K. Kuznetsov, "Purification of Sodium to Remove Oxygen by Hot Traps," *Zhidkiye metally* [Liquid Metals], Atomizdat Press, 1967.
69. Kozlov, F. A., E. K. Kuznetsov, and V. I. Subbotin, "The Plug Indicator - A Device for Detecting Impurities in Sodium," *Zhidkiye metally* [Liquid Metals], Atomizdat Press, 1967.
70. Korolev, B. I., *Osnovy vakuumnoy tekhniki* [Principles of Vacuum Technology], Gosenergoizdat Press, 1957.
71. Kharadzha, F. N., *Obshchiy kurs rentgenotekhniki* [General Course in X-Ray Technology], Energiya Press, 1966.
72. Rallis, C. and H. Iawurak, "The Mechanism of Nucleate Boiling," Proc. 3rd Internat. Conf. Peaceful Uses Atom. Energy, Geneva, 1964. Reactor Engineering and Equipment, Vol. 8, New York, 1965.
73. Deyev, V. I., V. V. Gusev and G. P. Dubpovskiy, "Investigation of the Mechanism of Boiling of Water at Reduced Pressures," *Teploenergetika*, No. 8, 1965.
74. Mamontova, N. N., "Boiling of Certain Liquids at Reduced Pressures," *Prikl. mekh. i teoret. fiz.*, No. 3, 1966.
75. Raben, I. A., R. T. Beaubouef, and G. E. Commerford, "A Study of Heat Transfer in Nucleate Pool Boiling of Water at Low Pressure," *Chem. Engng. Progr. Sympos. Series*, Vol. 61, No. 57, 1965.
76. Grass, G., H. Kottowski, and K. H. Spiller, "Measurements of the Superheating and Studies about Boiling Phenomena in Liquid-Metals," Conf. Internat. surete reacteurs a neutrons rapides. Aix-en-Provence, (II-B/4), September, 1967.
77. Edwards, I. E. and H. W. Hoffman, "Superheat with Boiling Alkali Metals," Proc. Conf. Application High Temp. Instrum. Liquid-Metal Experim., (N.N.L.-7100), 1965.
78. Krakoviak, A. I., "Superheat Requirements with Boiling Liquid Metals," Proc. High-Temp. Liquid-Metal Heat Transfer Technol. Mett., Vol. 2, September, 1963.
79. Conidee, La., Rouvillois, R. Semeria, N. Lions, M. Robin, and Simon,

"Experimental Studies on Sodium Boiling," Conf. Internat. Surete reacteurs a neutrons rapides. Aix-en-Provence, (II-B/5), Septermber, 1967.
80. MacPherson, R. E., "Techniques for Stabilizing Liquid Metal Pool Boiling," Conf. Internat. Surete reacteurs a neutrons rapides. Aix-en-Provence, (II-B/11), September, 1967.
81. Ivanovskiy, M. N., Yu. V. Milovanov, V. P. Sorokin, V. I. Subbotin, and B. A. Chulkov, "Heat Exchange during Film and Drop Condensation," Report at Symposium at Grenoble (France), November, 1966. /197
82. Kudryavtsev, A. P., D. M. Ovechkin, D. N. Sorokin, V. I. Subbotin, and A. A. Tsyganok, "Experimental Investigation of Heat Transfer from Horizontal Flat Surface to Sodium with Free Convection," *Zhidkiye metally* [Liquid Metals], Atomizdat Press, 1967.
83. Kutateladze, S. S. V. M. Borishanskiy, I. I. Novikov, and O. S. Fedynskiy, *Zhidkometallicheskiye teplonositeli* [Liquid Metal Heat Transfer Media], Atomizdat Press, 1958.
84. MacDonald, I. C. and T. I. Cannolly, "Investigation of Natural Convection Heat Transfer in Liquid Sodium," *Nucl. Sci. and Engng.*, Vol. 8, No. 5, 1960.
85. Globe, S. and D. Dropkin, Trans. A.S.M.E. Ser. C., No. 1, 1959.
86. *Zhidkometallicheskiye teplonositeli* [Liquid Metal Heat Transfer Media], Collection of articles edited by A. Ye. Sheyndlin, Foreign literature Press, 1958.
87. Subbotin, V. I., D. M. Ovechkin, D. N. Sorokin, and A. P. Kudryavtsev, "Heat Transfer during Boiling of Sodium under Free Convection Conditions," *Atomnaya energiya*, Vol. 24, No. 5, 1968.
88. Kutateladze, S. S. and V. M. Borishanskiy, *Spravochnik po teploperedache* [Handbook on Heat Transfer], Gosenergoizdat Press, 1961.
89. Hsu, S. T. and F. W. Schmidt, "Measured Variations in Local Surface Temperature in Pool Boiling of Water," Trans. A.S.M.E., Ser. C., No. 3, 1961.
90. Moore, F. D. and R. B. Mesler, "The Measurement of Rapid Surface Temperature Fluctuations during Nucleate Boiling of Water," *J.A.I. Ch. E.*, Vol. 7, No. 4, 1961.
91. Rogers, T. F. and R. B. Mesler, "Experimental Study of Surface Cooling by Bubbles during Nucleate Boiling Water," *J.A.I. Ch. E.*, Vol. 10, No. 5, 1964.
92. Markus, B. D. and D. Droplin, "Measured Temperature Profiles within the Superheated Boundary Layer above a Horizontal Surface in Saturated Nucleate Pool Boiling of Water," Trans. A.S.M.E., Ser. C., No. 3, 1965.
93. Lykov, A. V., *Teoriya teploprovodnostic* [The Theory of Heat Conductivity], GITL Press, 1952.
94. Borishanskiy, V. M., "Consideration of the Influence of Pressure on Heat Transfer at Critical Heat Loads during Boiling on the Basis of the Theory of Thermodynamic Similarity," *Voprosy teplootdachi i gidravliki dvukhfaznykh sred* [Problems of Heat Transfer and Hydraulics of Two-Phase Media], Gosenergoizdat Press, 1961.
95. Kirillov, P. L., "Critical Parameters of Alkali Metals," FEI Preprint, No. 52, 1966.

96. Averin, K. Ye., "Influence of Materials on Mechanical Finish of Surface on Heat Transfer during Boiling of Water," *AN SSSR OTN*, No. 3, 1954.
97. Shrok, L., "Influence of Pressure, Geometric Factors and Equation of State on Maximum and Minimum Heat Flows during Boiling," *Teploperedacha, Series C*, No. 3, 1963.
98. Golovin, V. S., B. A. Kol'chugin, and D. A. Labuntsov, "Investigation of Heat Exchange during Boiling of Ethyl Alcohol and Benzene on Surfaces of Various Materials," *Inzh.-fiz. zhurnal*, No. 6, 1964.
99. Leypunskiy, A. I., V. I. Subbotin, and M. N. Ivanovskiy, "State and Distribution of Impurities, Their Detection and Removal in Circulating Alkali Metal Heat Transfer Media," Report at MAGATE Conference, Austria, November, 1966.
100. Corty, C. and A. S. Foust, "Surface Variables in Nucleate Boiling," *Chem. Engng. Progr. Sympos. Series*, Vol. 51, No. 17, 1955.
101. Kurihara, H. M. and J. E. Myers, "The Effect of Superheat and Surface Roughness on Boiling Coefficients," *J.A.I. Ch. E.*, Vol. 6, No. 1, 1960.
102. Berenson, P. I., "Experiments on Pool Boiling Heat Transfer," *Internat. J. Heat and Mass Transfer*, Vol. 5, No. 6, 1962.
103. Githiyi, P. M. and R. H. Sabersky, "Some Effects of the Orientation of the Heating Surface in Nucleate Boiling," Trans. A.S.M.E., Ser. C., Vol. 85, No. 4, 1963. /198
104. Subbotin, V. I., M. N. Ivanovskiy, and Yu. I. Orlov, "Contact Thermal Resistance during Cooling of Channels with Liquid Metals," *Teplofizika vysokikh temperatur*, Vol. 5, No. 6, 1967.
105. Willions, D. D., J. A. Grand, and R. R. Miller, "Determination of the Solubility of Oxygen Bearing Impurities in Sodium, Potassium, and their Alloys," *J. Phys. Chem.*, Vol. 63, No. 1, 1959.
106. Solov'yev, A. N., "Development of Methods and Investigation of Properties of Melted Alkaline Metals," Moscow, Dr. Dissertation, 1966.
107. Gudtsov, N. G. and M. N. Gavze, "Influence of Mercury as Heat Transfer Medium on Steel in Power Plants," *AN SSSR*, 1956.
108. Hochman, J. M., "Mercury Wetting and Its Effect on Heat Transfer," Nucl. Sci. Abstrs., Vol. 19, No. 11, 1965.
109. Borishanskiy, V. M., A. A. Kanayev, A. A. Andriyevskiy, and K. A. Zhokhov, "Heat Transfer during Nucleate Boiling of Mercury and Amalgam," *Energomashinostroyeniye*, No. 7, 1966.
110. Birch, F., "Electrical Resistance and Critical Points of Mercury," *Phys. Rev., Ser. 2*, Vol. 41, 1932.
111. Fritz, W., "Calculation of Maximum Volumes of Vapor Streams," *Phys. Z.*, No. 11, 1935.
112. Kruzhilin, G. N., "Heat Transfer from Heating Surface to Boiling Single Component Liquid with Free Convection," *AN SSSR, OTN*, No. 7, 1948.
113. Kruzhilin, G. N. and V. I. Subbotin, "Cooling of Water-Water Reactors," Works of Second Geneva Conference on Peaceful Usage of Atomic Energy. *Nuclear Reactors and Nuclear Power (Geneva, 1958)*, Atomizdat Press, 1959.
114. Kutateladze, S. S., *Osnovy teorii teploobmena* [Principles of the Theory of Heat Exchange], Mashgiz Press, 1962.
115. Minchenko, F. P., "The Problem of Heat Exchange during Nucleate Boiling," *Energomashinostroyeniye*, No. 6, 1960.

116. Alad'yev, I. T., "Heat Transfer during Nucleate Boiling," *Konvektivnyy i luchistyy teploobmen* [Convective and Radiant Heat Exchange], Academy of Sciences USSR Press, 1960.
117. Novikov, I. I., "Conditions of Similarity of Processes of Heat Transfer with Variable Properties of Liquids," *Voprosy teplootdachi i gidravliki dvukfaznykh sred* [Problems of Heat Transfer and Hydraulics of Two-Phase Media], Gosenergoizdat Press, 1961.
118. Borishanskiy, V. M., "Heat Transfer Coefficient to Boiling Water with Super High Pressures," *Energomashinostroyeniye*, No. 7, 1958.
119. Mostinskiy, I. L., "Usage of the Law of Corresponding State for Calculation of Heat Transfer and Critical Heat Flows during Boiling of Liquids," *Teploenergetika*, No. 4, 1963.
120. Borishanskiy, V. M., A. P. Kozyrev, and A. S. Svetlova, "Heat Transfer during Boiling of Water Over a Broad Range of Changes of Saturation Pressures," *Konvektivnaya teploperedacha v dvukjfaznom i odnofaznom potokakh* [Convective Heat Transfer in Two-Phase and Single Phase Flows], Energiya Press, 1964.
121. Borishanskiy, V. M. and K. A. Zhokhov, "Consideration of Influence of Pressure on Heat Transfer during Nucleate Boiling of Liquid Metals," *Atomnaya energiya Press*, Vol. 18, No. 3, 1965.
122. Labuntsov, D. A., "Approximate Theory of Heat Exchange with Developed Nucleate Boiling," *Energetika i transport, OTN*, No. 1, 1963.
123. Zuber, N., "Hydrodynamic Aspects of Boiling Heat Transfer," (Thesis), A.E.C.U., 1959.
124. Rohsenow, W. M., "A Method of Correlating Heat-Transfer Data for Surface Boiling of Liquids," *Trans. A.S.M.E.*, Ser. C., Vol. 74, No. 6, 1952.
125. Levy, S., "Generalized Correlation of Boiling Heat Transfer," *Trans. A.S.M.E.*, Ser. C., Vol. 81, No. 2, 1959.
126. Tien, C. L., "A Hydrodynamic Model for Nucleate Pool Boiling," *Internat. J. Heat and Mass Transfer*, Vol. 5, No. 6, 1962.
127. Hara, T., "The Mechanism of Nucleate Boiling Heat Transfer," *Internat. J. Heat and Mass Transfer*, Vol. 6, No. 11, 1963. /199
128. Kotake, S., "On the Mechanism of Nucleate Boiling," *Internat. J. Heat and Mass Transfer*, Vol. 9, No. 8, 1966.
129. Labuntsov, D. A., Ye. M. Shevchuk, and P. A. Pazyuk, "Limiting Levels of Heat Exchange during Boiling of Liquid Metals," *Teplofizika vysokikh temperatur*, Vol. 3, No. 2, 1965.
130. Borishanskiy, V. M., A. P. Kozyrev, and L. S. Svetlova, "Investigation of Heat Exchange during Developed Nucleate Boiling of Liquids," *Trudy TSKTI*, No. 57, 1965.
131. Mitsyul', Ya. A. and T. G. Fillipova, "Results of Composition of Calculation Dependences during Boiling," *Trudy TSKTI*, No. 57, 1965.
132. Hygmark, C., "A Statistical Analysis of Nucleate Pool-Boiling Data," *Internat. J. Heat and Mass Transfer*, Vol. 5, No. 7, 1962.
133. Kutateladze, S. S. and N. N. Mamontova, "Investigation of Critical Heat Flows during Boiling of Liquids in Large Volumes under Reduced Pressure Conditions," *Inzh.-fiz. Zhurnal*, Vol. 12, No. 2, 1967.
134. Ornats'kiy, A. P. A. M. Kichigin, and M. Stochniy, "Investigation of the Dependence of the Critical Density of Thermal Flow on Vacuum Pressure under High Volume Conditions," No. 3, 1967.

135. Yashnov, V. I., "Influence of Wettability of Heating Surface on Boiling Crisis," *Trudy TSKTI*, No. 58, 1965.
136. Gambill, W. R., "Experimental Investigation of the Inherent Uncertainty in Pool Boiling Critical Heat Flowed to Saturated Water," *J.A.I. Ch. E.*, Vol. 10, No. 4, 1964.
137. Morozov, V. G., "Investigation of Cessation of Nucleate Boiling on Submerged Surface," *Trudy TSKTI*, No. 58, 1965.
138. Bobrovich, G. I., I. I. Gogonin, and S. S. Kutateladze, "Influence of Heating Surface Size on Critical Heat Flow during Boiling in Large Volumes," *Prikl. mekh. i teoret. fiz.*, No. 4, 1964.
139. Pitts, C. C. and G. Leppert, "The Critical Heat Flow for Electrically Heated Wires in Saturated Pool Boiling," *Internat. J. Heat and Mass Transfer*, Vol. 9, No. 4, 1966.
140. Ivey, H. I. and D. L. Morries, "The Effect of Test Section Parameters on Saturation Pool Boiling Burnout at Atmospheric Pressure," *Chem. Engng. Progr. Sympos.*, Series, Vol. 61, No. 60, 1965.
141. Bernath, L., "A Theory of Local-Boiling Burnout and Its Application to Existing Data," *Chem. Engng. Progr. Sympos. Series*, Vol. 56, No. 30, 1960.
142. Lienhard, J. and K. Watanable, "On Correlating the Peak and Minimum Boiling Heat Flows with Pressure and Heater Configuration," *Trans. A.S.M.E., Ser. C.*, Vol. 88, No. 1, 1966.
143. Gaydarov., Sh. A., P. A. Grigor'yev, and A. G. Ustmanov, "Influence of Heater Diameter on Critical Heat Flow during Boiling," *Prikl. mekh. i teoret. fiz.*, No. 3, 1966.
144. Kutateladze, S. S., N. V. Valukina, and I. I. Gogonin, "Dependence of Critical Heat Flow on Heater Dimensions during Boiling of Saturated Liquid under Free Convection Conditions," *Inzh.-fiz. zhurnal*, Vol. 12, No. 5, 1967.
145. Costello, C. P., C. O. Bock, and C. C. Nichols, "A Study of Induced Convective Effect on Saturated Pool Boiling Burnout," *Chem. Engng. Progr., Sympos. Series*, Vol. 61, No. 59, 1965.
146. Golovin, V. S., B. A. Kol'chugin, and D. A. Labuntsov, "Investigation of Heat Exchange and Critical Heat Loads during Boiling of Liquids under Conditions of Free Movement on Surfaces of Various Materials," *Trudy TSKTI*, No. 58, 1965.
147. Maleom, C. and D. Charlesworth, "Thermal Conduction Effect on the Critical Heat Flow in Pool Boiling," *Chem. Engng. Progr., Sympos. Series*, Vol. 62, No. 64, 1966.
148. Kirillov, P. L., "Generalized Dependence for Critical Heat Flow on Pressure during Boiling of Metals in Large Volumes," *Atomnaya energiya*, Vol. 24, No. 2, 1968. /200
149. Malenkov, I. G., "Critical Phenomena in Nuclaeate and Boiling Processes," *Prikl. mekh. i teoret. fiz.*, No. 6, 1963.
150. Kutateladze, S. S. and I. G. Malenkov, "Experimental Investigation of Analogy in Processes of Boiling and Bubbling," *Prikl. mekh. i teoret. fiz.*, No. 2, 1966.
151. Fritz, W. and W. Ende, "On the Front Evaporations of Kinematic Graphs Taken on Steam Bubbles," *Phys. Z.*, No. 11, 1936.

152. Torikai, K., M. Hori, A. Akiyama, T. Kobori, and H. Adachi, "Boiling Heat Transfer and Burnout Mechanism in Boiling-Water Cooled Reactors," Proc. Internat. Conf. Peaceful Uses Atom. Energy, Geneva, 1964, *Reactor Engineering and Equipment*, Vol. 8, N. Y., 1965.
153. MacAdams, William H., *Teploperedacha* [Heat Transfer] Metallurgizdat Press, 1961.
154. Frenkel', Ya. M., *Kineticheskaya teoriya zhidkostey* [Kinetic Theory of Liquids], Academy of Sciences, USSR Press, 1945.
155. Levich, V. G., *Vvedeniye v statisticheskuyu fiziku* [Introduction to Statistical Physics], GITTL, 1954.
156. Nesis, Ye. I., "Boiling under Actual Conditions," *Zh. tekhn. fiz.*, Vol. 22, No. 9, 1952.
157. Bankoff, S. G., "Ebullition from Solid Surfaces in the Absence of Pre-existing Gaseous Phase," *Trans. A.S.M.E.*, Vol. 79, No. 4, 1957.
158. Labuntsov, D. A., "Heat Exchange during Nucleate Boiling of Liquids," *Teploenergetika*, No. 12, 1959.
159. Herst, D. and G. Paund, *Isparenive i kondensatsiya* [Evaporation and Condensation], Metallurgiya Press, 1966.
160. Skripov, V. P., "The Boiling Crisis and Thermodynamic Stability of Liquids," *Teplo-massoperenos* [Heat and Mass Transfer], II, Minsk, Academy of Sci. VSSR Press, 1962.
161. Pavlov, P. A. and V. P. Skripov, "Boiling of Liquids with Pulsed Heating," *Teplofizika vysokikh temperatur*, Vol. 3, No. 1, 1965.
162. Skripov, V. P., P. A. Pavlov, and Ye. N. Sinitsyn, "Beginning of Boiling with Pulsed Heating," *Teplofizika vysokikh temperatur*, Vol. 3, No. 5, 1965.
163. Piz and Blins, "Cavitation Over Solid Surfaces with No Gas Seeds," *Voprosy fiziki kipeniya* [Problems of the Physics of Boiling], Mir Press, 1964.
164. Harvey, MacElroy and Whitley, "The Formation of Cavities in Water," *Voprosy fiziki kipeniya* [Problems of the Physics of Boiling], Mir Press, 1964.
165. Sabersky, R. H. and C. W. Gates, "On the Start of Nucleation in Boiling Heat Transfer," *Jet. Propuls.*, Vol. 25, No. 2, 1955.
166. Din, "The Formation of Bubbles," *Voprosy fiziki kipeniya* [Problems of the Physic of Boiling], Mir Press, 1964.
167. Addision, C. C. and E. Iberson, "The Wetting of Chromium, Molybdenum and Tungsten by Liquid Sodium," *J. Chem. Soc.*, No. 2, 1965.
168. Addision, C. C., E. Iberson, and I. A. Manning, "The Role of Oxide Films in the Wetting of Iron, Cobalt, Nickel by Liquid Sodium and by Solutions of Barium and Calcium in Liquid Sodium," *J. Chem. Soc.*, No. 7, 1962.
169. Griffith, P. and J. Wallis, "The Role of Surface Conditions in Nucleate Boiling," *Chem. Engng. Progr. Sympos. Series*, Vol. 56, No. 30, 1960.
170. Clark, H. B., P. S. Strenge, and J. W. Westwater, "Active Sites for Nucleate Boiling," *Chem. Engng. Progr. Sympos. Series*, Vol. 55, No. 29, 1959.
171. Strenge, P. S., A. Orell, and J. W. Westwater, "Microscopic Study of Bubble Growth during Nucleate Boiling," *J. A. I. Ch. E.*, Vol. 7, No. 4, 1961.

172. Young, R. And R. Hymmel, "Improved Nucleate Boiling Heat Transfer," *Chem. Engng. Progr.*, No. 7, 1964.
173. Hsu, Y. Y., "On the Size Range of Active Nucleation Cavities on a Heating Surface," *Trans. A.S.M.E., Ser. C.*, Vol. 84, No. 3, 1962.
174. Zysina-Molozhen, A. M., "Some Data on the Numbers of Vapor Formation Centers during Boiling over Technical Heating Surfaces," *Voprosy teploobmena pri izmenenii agregatnogo sostoyaniya veshchestva*, [Problems of Heat Exchange during Changes of State of Matter], Gosenergoizdat Press, 1953. /201
175. Treshchev, G. G., "Experimental Investigation of the Mechanism of Surface Boiling," *Teploobmen pri vysokikh teplovykh nagruzkakh i drugikh spetsial'nykh usloviyakh* [Heat Exchange under High Heat Loads and Other Special Conditions], Gosenergoizdat Press, 1959.
176. Gaertner, R. F. and J. W. Westwater, "Population of Active Sites in Nucleate Boiling Heat Transfer," *Chem. Engng. Progr. Sympos. Series*, Vol. 56, No. 30, 1960.
177. Heled, Y. and A. Orell, "Characteristics of Active Nucleation Sites in Pool Boiling," *Internat. J. Heat and Mass Transfer*, Vol. 10, No. 4, 1967.
178. Bankoff, S. G., "Entrapment of Gas in the Spreading of a Liquid over A Rough Surface," *J. A. I. Ch. E.*, Vol. 4, No. 1, 1958.
179. Bankoff, S. G., "The Predictions of Surface Temperatures at Incipient Boiling," *Chem. Engng. Progr. Sympos. Series*, Vol. 55, No. 29, 1959.
180. Voskresenskiy, K. D., *Sbornik raschetov i zadach po teploperedache*, [Collection of Calculations and Problems on Heat Transfer], Gosenergoizdat Press, 1959.
181. Marto, P. I. and W. M. Rohsenow, "Nucleate Boiling Instability of Alkali Metals," *Transactions A.S.M.E.*, Vol. 88, No. 2, 1966.
182a. Bobrovich, G. I., B. P. Avksentyuk, and N. N. Mamontova, "On the Mechanism of Boiling of Liquid Metals," *Papers J.S.M.E., Genic*, International Symposium, Tokyo, Vol. 2, 1967.
182b. Avksentyuk, B. P., G. I. Bobrovich, V. I. Moskvicheva, and N. N. Mamontova, "Investigation of Mechanism of Boiling of Liquid Metals," Report at 3rd All-Union Conf. on Heat Exchange and Hydraulic Resistance to Movement of Two-Phase Flow in Elements of Power Machines and Apparatus, Leningrad, April, 1967.
183. Labuntsov, D. A., B. A. Kol'chugin, B. S. Golovin, E. A. Zakharova, and L. N. Vladimirova, "Investigation of Bubble Growth during Boiling of Saturated Water by High Speed Cinematography over a Broad Range of Pressures," *Teplofizika vysokikh temperatur*, No. 3, 1964.
184. Cole, R. and H. Schuman, "Bubble Growth Rates at High Jacob Numbers," *Internat. J. Heat and Mass Transfer*, Vol. 9, No. 12, 1966.
185. Dergarabedian, P., "The Rate of Growth of Vapor Bubbles in Superheated Liquid," *J. Appl. Mech.*, Vol. 20, No. 4, 1953.
186. Plesset, M. S. and S. A. Zwick, "The Growth of Vapor Bubbles in Superheated Liquid," *J. Appl. Phys.*, Vol. 25, No. 4, 1954.
187. Forster, H. K. and N. Zuber, "Growth of a Vapor Bubble in Superheated Liquid," *J. Appl. Phys.*, Vol. 25, No. 4, 1954.
188. Scriven, L. E., "On the Dynamics of Phase Growth," *Chem. Engng. Sci.*, Vol. 10, No. 1, 1959.

189. Labuntsov, D. A., "Mechanism of Growth of Vapor Bubbles on Heating Surface during Boiling," *Inzh.-fiz. zhurnal.*, No. 4, 1963.
190. Forster, H. K., "On the Conduction of Heat Into a Growing Vapor Bubble," *J. Appl. Phys.*, Vol. 25, No. 8, 1954.
191. Griffith, P., "Bubble Growth Rates in Boiling," *Trans. A.S.M.E.*, Vol. 80, No. 3, 1958.
192. Gard, S. O. and T. D. Patten, "Temperature and Pressure Transients Near the Heating Surface during Nucleate Pool Boiling of Saturated Water," Proc. 3rd Internat. Heat Transfer Conf., Chicago, August, Vol, 3, 1966.
193. Mondin, H., P. Lavique, and R. Semeria, "Some Fundamental Aspects of Boiling in Nuclear Reactors," Report No. P/55, Proc. 3rd Internat. Conf. Peaceful Uses Atom. Energy., Geneva, 1964, Reactor Engineering and Equipment, Vol. 8, N. Y., 1965.
194. Zysina, L. M . and S. S. Kutateladze, "The Problem of the Influence of Pressure on the Mechanism of Vapor Formation in Boiling Liquids," *Zh. tekhn. fiz.*, Vol. 20, No. 1, 1950.
195. Mamontova, N. N., "Study of the Mechanism of Boiling at High Heat Flows by Cinematography," *Prikl. mekh. i teoret. fiz.*, No. 3, 1963. /202
196. Tolubinsky, V. I. and I. N. Ostrowsky, "On the Mechanism of Boiling Heat Transfer," *Internat.. J. Heat and Mass Transfer*, Vol. 9, No. 12, 1966.
197. MacFadden, P. W. and P. Grossman, "The Relation Between Bubble Frequency and Diameter during Nucleate Pool Boiling," *Internat. J. Heat and Mass Transfer*, Vol. 5, No. 5, 1962.
198. Danilova, G. N., V. K. Bel'skiy, and A. V. Kupriyanova, "Investigation of the Process of Boiling of Freon-12 by Cinematography," *Kholodil'naya tekhnika*, No. 2, 1964.
199. Cole, R., "A Photographic Study of Pool Boiling in the Region of the Region of the Critical Heat Flow," *J. A. I. Ch. E.*, Vol. 6, No. 4, 1960.
200. Deyev, V. I. and A. N. Solov'yev, "The Mechanism of Boiling of Liquid Sodium on Heating Surfaces with Free Convection," *Inzh.-fiz. zhurnal*, No. 6, 1964.
201. Subbotin, V. I., S. P. Kaznovskiy, S. K. Karatayev, V. Ye. Sviridenko, and Yu. F. Selivanov, "Investigation of Dynamics of Vapor Bubbles Separation during Boiling of Water under Natural Convection Conditions," *Atomnaya energiya*, Vol. 27, No. 9, 1969.
202. Nesis, Ye. N., "Boiling of Liquids," *Uspekhi fiz. nauk*, Vol. 87, No. 4, 1965.
203. Lykov, Ye. V. and L. I. Cherednichenko, "investigation of Ultrasonic Oscillations in the Critical Area of Liquid Boiling," Report of 3rd All-Union Conference on Heat Exchange and Hydraulic Resistance in Elements of Power Machines and Apparatus. April, 1967, Leningrad.
204. Gol'tsova, Ye. I., "The Density of Lithium, Sodium and Potassium up to 1500-1600°C," *Teplofizika vysokikh temperatur*, Vol. 4, No. 3, 1966.
205. Shpil'rayn, E. E., "Experimental Investigation of Thermophysical and Electrophysical Properties of Liquid Alkali Metals at High Temperatures," *Teplofizika vysokikh temperatur*, No. 6, 1965.
206. Vukalovich, M. P., V. I. Zubarev, and L. R. Fokin, "Calculation of

Thermodynamic Properties of Potassium Vapors at Temperatures up to 1300°C and Pressures up to 25 kg/cm$^2$," *Teploenergetika*, No. 8, 1962.
207. Volyak, P. D., "Phenomenon of Dimerization in Vapors of Alkali Metals and Calculation of Their Heat Physical Properties up to 1500°C, *Inzh.-fiz. zhurnal*, No. 3, 1962.
208. Nikol'skiy, A., A. Kalakutskaya, I. M. Pchelkin, T. V. Klassen, and A. A. Vel'tishcheva, *Voprosy teploobmena* [Problems of Heat Exchange], Academy of Science, USSR Press, 1959.
209. Os'minin, Yu. P., "Heat Capacity of Liquid Alkali Metals," *Inzh.-fiz. zhurnal*, No. 4, 1963.
210. Vargaftik, N. B., *Spravochink po teplofizicheskim svoystvam gazov i zhidkostey*, [Handbook on Heat Physical Properties of Gases and Liquids], Fizmatgiz Press, 1963.
211. Makansi, M. H., C. H. Muendel, and W. A. Selke, *J. Phys. Chem.*, Vol. 50, No. 40, 1955.
212. Achener, P. Y., "The Determination of the Latent Heat of Vaporization, Vapor Pressure, Enthalpy and Density of Liquid Rubidium and Cesium up to 1800°F," Proc. High-Temp. Liquid-Metal Heat Transfer Technol. Meet., (O.R.N.L.-3605), Sept., Vol. 1, 1963.
213. Bonilla, C. F., D. L. Sawhney, and M. H. Makensi, "Vapor Pressure of Alkali Metals Rubidium, Cesium and Sodium - Potassium Alloy (NaK) up to 100 psi," *Trans. Amer. Soc. Metals*, Vol. 55, No. 1, 1962.
214. Clearly, R. E. and S. M. Kapelner, "Alkali Metal Properties Program at Pratt and Whitney Aircraft - CANEL., Proc. High-Temp. Liquid Metal Heat Transfer Technol. Meet., (BNL-756), May, 1962.
215. Hochman, I. and C. F. Bonilla, "The Electrical and Thermal Conductivity of Liquid Cesium to 1650°C and Critical Point of Cesium," *Nucl. Sci. and Engng.*, Vol. 22, No. 4, 1965.

## TABLE 1. PROPERTIES OF METALS

Sodium ($T_{cr}$ = 2530°K; $P_{cr}$ = 357 atm.abs.; $\rho_{cr}$ = 0.027 g/cm$^3$ [95])

| Parameter | $t_s$, °C | | | | | | Source |
|---|---|---|---|---|---|---|---|
| | 400 | 500 | 600 | 700 | 800 | 900 | |
| $\gamma$, kg/m$^3$ . . . | 856 | 832 | 808 | 784 | 760 | 737 | [204] |
| $\gamma''$, kg/m$^3$ . . . | $2{,}1\cdot10^{-4}$ | $2{,}02\cdot10^{-3}$ | $1{,}13\cdot10^{-3}$ | $4{,}45\cdot10^{-2}$ | $1{,}33\cdot10^{-1}$ | $3{,}27\cdot10^{-1}$ | [207] |
| $\lambda$, kcal/m·hr °C . . . | 59,1 | 54,9 | 52,1 | 50,8 | 50,1* | 49,8* | [208] |
| r, kcal/kg . . . | 1026 | 998 | 969 | 941 | 916 | 893 | [210] |
| $C_p$, kcal/kg °C . . . | 0,306 | 0,302 | 0,300 | 0,300 | 0,303 | 0,308 | [207] |
| $\sigma\cdot10^3$, kg/m . . . | 17,75 | 16,8 | 15,9 | 14,9 | 14,0 | 13,1 | [106] |
| $\nu\cdot10^8$, m$^2$/sec . . . | 33,0 | 28,9 | 25,7 | 23,2 | 21,4* | 20,3* | [208] |
| $\mu\cdot10^5$, kg·sec/m$^2$ . . . | 2,88 | 2,45 | 2,12 | 1,85 | 1,66 | 1,53 | ** |
| $\alpha\cdot10^5$, m$^2$/sec . . . | 6,27 | 6,07 | 5,97 | 5,99 | 6,04 | 6,09 | ** |
| $Pr\cdot10^3$ . . . | 5,27 | 4,76 | 4,30 | 3,87 | 3,54 | 3,33 | ** |
| $P_s$, kg/cm$^2$ . . . | $5{,}8\cdot10^{-4}$ | $5{,}95\cdot10^{-3}$ | $3{,}58\cdot10^{-2}$ | $1{,}47\cdot10^{-1}$ | $4{,}72\cdot10^{-1}$ | 1,22 | [211] |

*Produced by extrapolation. **Values of Pr, a, $\mu$ calculated from data of $\gamma$, $\lambda$, $C_p$, $\nu$, presented in the table.

Commas indicate decimal points.

TABLE 2

Potassium ($T_{cr}$ = 2125°K; $P_{cr}$ = 169 atm. abs; $\rho_{cr}$ = 0.202 g/cm$^3$ [95])

| Parameter | $t_s$, °C | | | | | | |
|---|---|---|---|---|---|---|---|
| | 400 | 500 | 600 | 700 | 800 | 900 | Source |
| $\gamma$, kg/m$^3$ | 748 | 724 | 700 | 676 | 652 | 629 | [204] |
| $\gamma''$, kg/m$^3$ | $3,5\cdot10^{-3}$ | $2,39\cdot10^{-2}$ | $9,4\cdot10^{-2}$ | $2,9\cdot10^{-1}$ | $6,9\cdot10^{-1}$ | 1,4 | [206] |
| $\lambda$, kcal/m·hr °C | 34,0 | 30,0 | 26,6 | 24,3 | 22,5 | 21,5 | [208] |
| r, kcal/kg | 507,5 | 497 | 486 | 474 | 462 | 450 | [210] |
| $C_p$, kcal/kg °C | 0,183 | 0,182 | 0,183 | 0,185 | 0,189 | 0,194 | [210] |
| $\sigma\cdot10^3$, kg/m | 9,65 | 8,98 | 8,35 | 7,65 | 6,76 | 6,3 | [106] |
| $\nu\cdot10^8$, m$^2$/sec | 29,8 | 25,7 | 22,1 | 20,5 | 19,9 * | 19,5 * | [208] |
| $\mu\cdot10^5$, kg·sec/m$^2$ | 2,27 | 1,89 | 1,58 | 1,42 | 1,33 | 1,22 | ** |
| $a\cdot10^5$, m$^2$/sec | 6,90 | 6,33 | 5,77 | 5,37 | 5,07 | 4,89 | ** |
| $Pr\cdot10^3$ | 4,32 | 4,06 | 3,83 | 3,81 | 3,93 | 3,99 | ** |
| $P_s$, kg/cm$^2$ | $5,67\cdot10^{-3}$ | $3,93\cdot10^{-2}$ | $1,73\cdot10^{-1}$ | $5,58\cdot10^{-1}$ | 1,44 | 3,14 | [206] |

* Produced by extrapolation.

**Values of Pr, a, $\mu$, produced by calculation from data of $\gamma$, $C_p$, $\lambda$, $\nu$, presented in the table.

Commas indicate decimal points.

TABLE 3

Rubidium ($T_{cr}$ = 1980°K; $P_{cr}$ = 130 atm.abs; $\rho_{cr}$ = 0.352 g/cm$^3$ [95])

| Parameter | $t_s$, °C | | | | | Source |
|---|---|---|---|---|---|---|
| | 400 | 500 | 600 | 700 | 800 | |
| $\gamma$, kg/m$^3$ . . . | 1301 | 1255 | 1210 | 1165 | 1120 | [205] |
| $\gamma$, kg/m$^3$ . . . | 0,029 | 0,145 | 0,49 | 1,29 | 2,79 | ** |
| $\lambda$, kcal/m·hr °C . . . | 25,4 | 24,1 | 22,3 | 20,6 | 18,7* | [214] |
| r, kcal/kg . . . | 209* | 203,8* | 198,7 | 193,6 | 188,4 | [212] |
| $\sigma \cdot 10^3$ kg/m . . . | 7,05 | 6,45 | 5,85 | 5,16 | 4,47 | [106] |
| $C_p$, kcal/kg °C . . . | 0,084 | 0,0839 | 0,0844 | 0,086 | 0,0884 | [209] |
| $\nu \cdot 10^8$, m$^2$/sec . . . | 16,5 | 14,8 | 13,6 | 12,6 | 12,1 | *** |
| $\mu \cdot 10^5$, kg·sec/m$^2$ . . . | 2,18 | 1,89 | 1,67 | 1,5 | 1,38 | [205] |
| $\alpha \cdot 10^5$, m$^2$/sec . . . | 6,46 | 6,36 | 6,07 | 5,71 | 5,25 | *** |
| $Pr \cdot 10^3$ . . . | 2,55 | 2,33 | 2,24 | 2,21 | 2,3 | *** |
| $P_s$, kg/cm$^2$ . . . | 0,019 | 0,107 | 0,4 | 1,15 | 2,7 | [213] |

* Produced by extrapolation.

**Values of $\gamma''$ calculated by formula PV = RT considering dimerization [95].

***Values of Pr, a, $\nu$, produced by calculation from data of $\gamma$, $\lambda$, $C_p$, $\mu$, presented in the table.

Commas indicate decimal points

/205

TABLE 4

Cesium ($T_{cr}$ = 1900°K; $P_{cr}$ = 103 atm.abs; $\rho_{cr}$ = 0.456 g/cm$^3$ [95])

| Parameter | $t_s$, °C | | | | | |
|---|---|---|---|---|---|---|
| | 400 | 500 | 600 | 700 | 800 | Source |
| $\gamma$, kg/m$^3$ | 1625 | 1567 | 1510 | 1453 | 1397 | [205] |
| $\gamma''$, kg/m$^3$ | $6{,}5\cdot10^{-2}$ | $2{,}92\cdot10^{-1}$ | $9{,}27\cdot10^{-1}$ | 2,3 | 4,97 | * |
| $\lambda$, kcal/m·hr °C | 16,2 | 15,5 | 14,6 | 13,8 | 13,0 | [215] |
| r, kcal/kg | 128 | 124 | 121 | 117 | 113 | [212] |
| $C_p$, kcal/kg °C | 0,054 | 0,054 | 0,055 | 0,056 | 0,058 | [209] |
| $\sigma\cdot10^3$, kg/m | 5,65 | 5,14 | 4,62 | 4,10 | 3,58 | [106] |
| $\nu\cdot10^8$, m$^2$/sec | 21,4 | 17,6 | 14,4 | 11,5 | 10,3 | ** |
| $\mu\cdot10^5$, kg·sec/m$^2$ | 3,52 | 2,8 | 2,2 | 1,7 | 1,5 | [205] |
| $\alpha\cdot10^5$, m$^2$/sec | 5,13 | 5,08 | 4,88 | 4,71 | 4,46 | ** |
| $Pr\cdot10^3$ | 4,17 | 3,47 | 2,95 | 2,44 | 2,30 | ** |
| $P_s$, kg/cm$^2$ | $2{,}8\cdot10^{-3}$ | $1{,}42\cdot10^{-1}$ | $5{,}01\cdot10^{-1}$ | 1,37 | 3,2 | [213] |

* Values of $\gamma''$ calculated by formula PV = RT considering dimerization [95].
**Values of Pr, a, $\nu$, produced by calculation from data of $\gamma$, $\lambda$, $C_p$, $\mu$, presented in the table.

Commas indicate decimal points

TABLE 5

Mercury ($T_{cr}$ = 1460°K; $P_{cr}$ = 1640 atm.abs [110])

| Parameter | $P_s$, kg/cm$^2$ | | | | | |
|---|---|---|---|---|---|---|
| | 0,6 | 1,0 | 2,0 | 4,0 | 10,0 | Source |
| $\gamma$, kg/m$^3$ | 12804 | 12739 | 12642 | 12531 | 12361 | [210] |
| $\gamma''$, kg/m$^3$ | 2,26 | 3,77 | 7,07 | 13,23 | 29,56 | [210] |
| $\lambda$, kcal/m·hr °C | 10,25 | 10,50 | 10,83 | 11,15 | 11,53 * | [210] |
| r, kcal/kg | 70,88 | 70,68 | 70,4 | 70,06 | 69,45 | [210] |
| $C_p$, kcal/kg °C | 0,0328 | 0,0328 | 0,0329 | 0,0329 | 0,0330 | [210] |
| $\sigma \cdot 10^2$, kg/m | 4,08 | 4,01 | 3,90 * | 3,78 * | 3,60 * | [51] |
| $\nu \cdot 10^8$, m$^2$/sec | 6,92 | 6,77 | 6,60 | 6,41 | 6,14 * | [210] |
| $\mu \cdot 10^3$, kg·sec/m$^2$ | 9,03 | 8,79 | 8,50 | 8,19 | 7,74 | ** |
| $\alpha \cdot 10^2$, m$^2$/hr | 2,43 | 2,50 | 2,59 | 2,68 | 2,80 * | [210] |
| $Pr \cdot 10^3$ | 10,2 | 9,68 | 9,07 | 8,57 | 7,90 * | [210] |
| $t_s$, °C | 328 | 355,9 | 395,8 | 442,4 | 515,5 | [210] |

* Produced by extrapolation.
** Values of $\mu$ calculated from values of $\nu$ presented in table.

Commas indicate decimal points.

NASA-Langley, 1971 - 33
Coml., Phila., Penn.

*"The aeronautical and space activities of the United States shall be conducted so as to contribute . . . to the expansion of human knowledge of phenomena in the atmosphere and space. The Administration shall provide for the widest practicable and appropriate dissemination of information concerning its activities and the results thereof."*

—NATIONAL AERONAUTICS AND SPACE ACT OF 1958

# NASA SCIENTIFIC AND TECHNICAL PUBLICATIONS

TECHNICAL REPORTS: Scientific and technical information considered important, complete, and a lasting contribution to existing knowledge.

TECHNICAL NOTES: Information less broad in scope but nevertheless of importance as a contribution to existing knowledge.

TECHNICAL MEMORANDUMS: Information receiving limited distribution because of preliminary data, security classification, or other reasons.

CONTRACTOR REPORTS: Scientific and technical information generated under a NASA contract or grant and considered an important contribution to existing knowledge.

TECHNICAL TRANSLATIONS: Information published in a foreign language considered to merit NASA distribution in English.

SPECIAL PUBLICATIONS: Information derived from or of value to NASA activities. Publications include conference proceedings, monographs, data compilations, handbooks, sourcebooks, and special bibliographies.

TECHNOLOGY UTILIZATION PUBLICATIONS: Information on technology used by NASA that may be of particular interest in commercial and other non-aerospace applications. Publications include Tech Briefs, Technology Utilization Reports and Technology Surveys.

*Details on the availability of these publications may be obtained from:*

**SCIENTIFIC AND TECHNICAL INFORMATION OFFICE**

**NATIONAL AERONAUTICS AND SPACE ADMINISTRATION**

**Washington, D.C. 20546**